

A new European species of *Ceratophysella* (Collembola, Hypogastruridae) revealed by morphological data and DNA barcodes

Dariusz Skarżyński¹, Adrian Smolis¹, Lubomír Kováč², David Porco³

1 Institute of Environmental Biology, Department of Invertebrate Biology, Evolution and Conservation, University of Wrocław, Przybyszewskiego 65, 51-148, Wrocław, Poland **2** Department of Zoology, Institute of Biology and Ecology, Faculty of Science, Pavol Jozef Šafárik University, Moyzesova 11, 041 54, Košice, Slovakia **3** Musée National d'Histoire Naturelle, 25 rue Munster, 2160, Luxembourg, Luxembourg

Corresponding author: Dariusz Skarżyński (dariusz.skarzynski@uwr.edu.pl)

Academic editor: W.M. Weiner | Received 14 January 2021 | Accepted 26 January 2021 | Published 1 March 2021

<http://zoobank.org/E2418295-8A9F-425D-8728-5686C41FF59B>

Citation: Skarżyński D, Smolis A, Kováč L, Porco D (2021) A new European species of *Ceratophysella* (Collembola, Hypogastruridae) revealed by morphological data and DNA barcodes. ZooKeys 1021: 1–18. <https://doi.org/10.3897/zookeys.1021.63147>

Abstract

A new species, *Ceratophysella stachi*, from Denmark, Germany, Luxembourg, Norway, Poland, and Ukraine is described based on morphological data and DNA barcodes. It belongs to a small European group of species with type B chaetotaxy and strong tegumentary granulation with distinct fields of coarse granules: *C. granulata* Stach, 1949, *C. laurencei* (Gisin, 1963), *C. neomeridionalis* (Nosek & Červek, 1970), *C. scotica* (Carpenter & Evans, 1899), and *C. silvatica* Rusek, 1964. It differs from all of them in the chaetotaxy of lateral parts of thoracic terga II–III (setae m_6 present and one additional seta outside lateral sensillum m_6 , present or absent) that is exceptional within the whole *C. armata*-group. Notes on closely related species *C. granulata* are also given.

Keywords

Springtails, integrative taxonomy, COI sequences, *Ceratophysella stachi* sp. nov., *Ceratophysella granulata*

Introduction

Ceratophysella Börner, 1932, comprising 140 species (Bellinger et al. 1996–2021), is one of the largest collembolan genera within the family Hypogastruridae. Although the genus is considered cosmopolitan, the vast majority of species live in the temperate climatic zone of the northern hemisphere. Unfortunately, some of these species are insufficiently known, and there are doubts concerning their taxonomic status. One of these is *Ceratophysella granulata* Stach, 1949. This species was described from the Tatra Mountains (Polish Carpathians) by Stach (1949) and also reported by him from Slovakia, Ukraine, the former Yugoslavia (Slovenia), and France. Then, it has been frequently recorded from various European countries: Austria (Christian 1987), Bosnia and Herzegovina (Bogojevič 1968), Denmark (Fjellberg 1998), Germany (Eckert and Palissa 1999), Great Britain (Goto 1955a, b), Hungary (Danyi and Traser 2008), Norway (Fjellberg 1998), Poland (Stach 1949, 1964, Weiner 1981, Sterzyńska and Kaprus' 2000, Smolis and Skarżyński 2003, 2006), Romania (Danyi et al. 2006, Popa 2012), Slovakia (Nosek 1958, 1969, Kováč et al. 2016), the former Soviet Union (Grinbergs 1960), Switzerland (Gisin 1949), and Ukraine (Kaprus' et al. 2006). However, the reliability of these data is questioned. For example, Hopkin (2007) found that British specimens from the collection of Natural History Museum in London refer to *Ceratophysella denticulata* (Bagnall, 1941). Babenko et al. (1994) came to a similar conclusion after examination of specimens identified as *C. granulata* from the area of the former Soviet Union. They found that most of them referred to other species, usually of the *C. denticulata* group. Moreover, the comparison of the morphology of the topotypic population (Skarżyński 2004a) and the populations from Denmark and Norway (Fjellberg 1998) showed subtle differences in chaetotaxy, which indicates that *C. granulata* may be a complex of species. In order to establish the taxonomic status of the forms included in this complex, a classical taxonomic analysis of materials identified as *C. granulata* from several European scientific collections and DNA barcoding were performed.

Material and methods

Species/populations studied

Morphological analysis of available specimens designated as *C. granulata* (*C. cf. granulata*, *Hypogastrura granulata*) from Denmark, Germany, Hungary, Luxembourg, Norway, Poland (including syntypes and topotypes), Romania, Slovakia, Switzerland, and Ukraine from the collections of eight institutions (Table 1) was performed. Unfortunately, specimens of *C. granulata* mentioned in the original description (Stach 1949) from Slovakia (Podlužany, orig. “Dobó–Berekalja”), West Ukraine (Czarnohora Range: Zaroślak and Breskuł), former Yugoslavia (Slovenia, Škocjan Caves, orig. “St. Canzian cave”), and France (Arles) could not be found in the ISEZ collection (*in litt.* Wanda

Table 1. A list of institutions and countries in which specimens are deposited, with abbreviations.

Abbreviation	Depository	Country
AF	Collection of Dr Arne Fjellberg	Norway
DIBEC	Department of Invertebrate Biology, Evolution and Conservation, University of Wrocław	Poland
PJSU	Department of Zoology, Institute of Biology and Ecology, Faculty of Science, Pavol Jozef Šafárik University, Košice	Slovakia
HNHM	Hungarian Natural History Museum, Budapest	Hungary
ISEZ	Institute of Systematics and Evolution of Animals, Polish Academy of Sciences, Cracow	Poland
MHNG	Muséum d'histoire naturelle, Geneva	Switzerland
SMNG	Senckenberg Museum of Natural History, Görlitz	Germany
SMNHL	State Museum of Natural History, Ukrainian National Academy of Sciences, Lviv	Ukraine

Table 2. List of barcoded species. *N* = number of sequences available.

Species	Collecting data (all from Poland)	<i>N</i>	Published sequences
<i>Ceratophysella granulata</i> (= <i>C. stachi</i> sp. nov.)	Beskid Niski Mountains, Carpathians, litter of the Carpathian beech forest on the slopes of Ostra Góra near village Tylawa, at an altitude of 500 m a.s.l., 20.X.2009, leg. M. Furgol	2	–
<i>Ceratophysella granulata</i>	Tatra Mountains, Carpathians, litter of dwarf mountain pine shrubs on the slopes of the Gładkie Uplaziańskie, at an altitude of 1600 m a.s.l., 14.VIII.2009, leg. D. Skarżyński	5	Porco et al. (2012)
<i>Ceratophysella denticulata</i>	Nizina Śląska Lowland, oak-hornbeam forest in Wrocław, 10.X.2009, leg. D. Skarżyński	5	–
<i>Ceratophysella cavicola</i>	Karkonosze Mountains, Sudetes, old adit Krucze Skaly near Karpacz, 650 m a.s.l., 6.VI.2009, leg. D. Skarżyński	4	Porco et al. (2012)
<i>Ceratophysella engadinensis</i>	Wzgórze Trzebnickie Hills, peat bog near Twardogóra, 11.X.2009, leg. D. Skarżyński	5	–

M. Weiner); therefore, they were not examined. The search for materials of this species mentioned in the “Catalogus faunae Austriae” (Christian 1987) in the collection of Natural History Museum Vienna also did not bring any results (*in litt.* Harald Bruckner). In addition, the sequences from 21 specimens from five species were analysed to assess the status of *C. granulata* forms in the context of the genetic divergence within the genus (Table 2).

Morphology

Specimens stored in alcohol were cleared in Nesbitt’s fluid (chloral hydrate, concentrated hydrochloric acid, distilled water), slide-mounted in a mixed medium (distilled water, gum arabic, glycerol, chloral hydrate), and studied using a Nikon Eclipse E600 phase contrast microscope. Figures were drawn using a camera lucida. A set of characters commonly used in the taxonomy of the genus (Fjellberg 1984, 1998, 1999; Babenko et al. 1994; Thibaud et al. 2004) was analysed.

DNA barcoding

Lysis of the tissues was carried out in 50 µl volume of lysis buffer and proteinase K incubated at 56 °C overnight. DNA extraction followed a standard automated protocol on 96-well glass fibre plates (Ivanova et al. 2006), and during this DNA extraction, a voucher recovery specially designed for high-throughput workflow (Porco et al. 2010)

was used. The 5' region of COI used as a standard DNA barcode was amplified using M13 tailed primers LCO1490 and HCO2198 (Folmer et al. 1994). A standard PCR reaction protocol was used for PCR amplifications and products were checked on a 2% E-gel 96Agarose (Invitrogen). Unpurified PCR amplicons were sequenced in both directions using M13 tails as primers. The sequencing reactions followed standard protocols of the Canadian Centre for DNA Barcoding (Hajibabaei et al. 2005), with products subsequently purified using Agencourt CleanSEQ protocol (Agencourt) and processed using BigDye v. 3.1 on an ABI 3730 DNA Analyzer (Applied Biosystems). Sequences were assembled with Sequencer v. 4.5 (GeneCode Corporation, Ann Arbor, MI, USA) and aligned by eye using BIOEDIT v. 7.0.5.3 (Hall 1999); we observed no indels in this coding region of the mitochondrial genome, and therefore, all base positions were aligned with confidence in positional homology. Sequences are publicly available on BOLD (Ratnasingham and Hebert 2007; <http://www.barcodinglife.org>) within the public dataset NCERAT and in GenBank (HM398990–HM399010, JX261875, MW471668). Distance analyses were conducted with MEGA7 (Tamura et al. 2007) using a Neighbor-Joining (Saitou and Nei 1987) algorithm and distances corrected with the Kimura-2 parameter (Kimura 1980). Kimura-2 parameter is the best metric when distances are low (Nei and Kumar 2000). The robustness of nodes was evaluated through bootstrap re-analysis of 1000 pseudoreplicates.

Results

Morphology

The material under study appeared to be taxonomically heterogeneous. Hungarian specimens (HNHM, “*Hypogastrura granulata*” det. Loksa: 27 spp., Sz(N.) 1975/76, Szentbékka, 1975.05.09, leg. Loksa, coll-1868 and 2 spp., Bátorliget, 1989-90, coll-1008) were identified as *C. denticulata* and *C. silvatica* (Rusek, 1964). Most of the specimens from Ukraine (SMNHL, “*Ceratophysella granulata*”, Carpathians: 5 spp., Perkalab river, litter of spruce forest, 1.VIII.1991, leg. I. Kaprus', 2.2.4.5; 2 spp., Skole, litter of beech forest, 3.IV.2004, leg. Javornitsskij, 2.2.4.4; 2 spp., Vorokhta, litter of spruce forest, 5.IX.1999, leg. Javornitsskij, 2.2.4.7; 2 spp., Borzhava, 1200 m a.s.l, soil and turf, 5.XI.1996, leg. L. Sukovata, 2.2.4.6) appeared to be the epitokous form of *C. silvatica*, while Swiss specimens suitable for examination (MHNG, Gisin's collection, “*Hypogastrura cf. granulata*”: 2 spp., Neuchâtel, Forêt de Chuffort, Mont Chaumont, 8 km from Neuchâtel; ca 1170 m, X.1963, Fn 51; 14 spp., Genève, Vessy, forest, ca 400 m, samples from an ecological study in 1946–1948, Ga57) were assigned to *C. armata* (Nicolet, 1842) and *C. attenuata* Cassagnau, 1959. The original designations of some specimens from Luxembourg also proved to be erroneous, six specimens from Obereisenbach (5 juv., Holzbichsbaach, oaks, litter and mosses, 5.VII.1991, leg. Tommasi-Ursone, L-91-51 and 1 juv., Husterbaach, beeches, in nettles, *Geranium*, *Digitalis*, etc., 5.VII, 1991, leg. M. Ursone, L-91-53, ISEZ) actually belong to

C. denticulata. An unambiguous determination of species status of juvenile individuals with type B chaetotaxy and integument with fields of especially coarse granules from three samples (1 juv., Poland, Puszcza Zgorzelecka, Ruzsów, temperate thickets and scrub, *Spiraea* site, mowed, 16.X.2013, leg. U. Burkhardt, 882-01; 5 juv., Germany, Saxony, Zittau, Roschertal, Mandau river valley near Hainewalde, sample 27, mosses on meadow, 10 m above Mandau, 3.V.1972, leg. W. Dunger, 8825-8827, SMNG and 1 juv.; Romania, Carpathians, Maramureş District, Rodnei Mts, Borşa, N slope of Pietrosul Rodnei, ca 1700 m a.s.l., 27.VII.2004, leg. J. Radwański, RU/04/1/70, ISEZ) was unsuccessful due to the lack of useful features distinguishing immature stages.

Among the examined specimens that can be referred to *C. granulata*, two morphotypes were found, differing in the chaetotaxy of the lateral part of thoracic terga II–III, the size and shape of accessory boss near the postantennal organ, and the shape of mucro. Considering their clear morphological differentiation, both forms are treated as separate species. Thus, the form from the northwestern part of the Carpathians (Poland and Slovakia) was recognized (based on syntypes and topotypes) as *C. granulata*, whereas the form distributed in Norway through Denmark, Germany, Luxembourg, and the eastern part of Polish Carpathians to Ukraine (Fig. 1) was considered to be a species new to science—*C. stachi* sp. nov. Notes on the former and description of the later are given below.

DNA barcoding

The mean genetic divergence among the four *Ceratophysella* species included into the analysis was 24.2% (ranging from 19% to 28.2%), and their mean intraspecific variation was 0.5% (ranging from 0% to 0.6%). Similar values were found for both inter-specific (mean 23% ranging from 21% to 24.4%) and intraspecific (1%) in *C. stachi* sp. nov., thus supporting the status of the new species (Table 3, Fig. 2). Moreover, these values are in line with the usual ‘barcoding gap’ described so far in the family Hypogastruridae (e.g. Nakamori 2013; Skarżyński et al. 2018) but also more generally in Collembola (e.g. Porco et al. 2014; Nilsai et al. 2017).

Taxonomy

Ceratophysella stachi Skarżyński, Smolis & Porco, sp. nov.

<http://zoobank.org/40BF0CC2-AF12-43DB-9F35-368E6EC004F8>

Figures 3–9

Ceratophysella granulata: Fjellberg, 1998: 41.

Type material. *Holotype* (DIBEC): female, POLAND, Carpathians, Beskid Niski Mts, litter of the Carpathian beech forest on the slopes of Ostra Góra near Tylawa village, 500 m a.s.l., 20.X.2009, leg. M. Furgoł. *Paratypes* (DIBEC): 2 males, same data as holotype; male, juv., 14.V.2001, leg. A. Smolis, D. Skarżyński, other data same as



Figure 1. Distribution of *Ceratophysella stachi* sp. nov. (black circles) and *C. granulata* (empty circles). Abbreviations: AKE – Akershus, B – Bieszczady Mts, BM – Beskid Mały Mts, BN – Beskid Niski Mts, BRA – Brandenburg, BS – Beskid Sądecki Mts, BW – Beskid Wyspowy Mts, BZ – Beskid Żywiecki Mts, CH - Čierna hora Mts, FUN – Funen, HES – Hesse, JUT – Jutland, L - Levočské vrchy Mts, LD – Lviv District, LT – Low Tatra Mts, LUX – Luxembourg, M – Muránska planina Plateau, MEC – Mecklenburg-West Pomerania, P – Pieniny Mts, S – Slovak Paradise, SAX – Saxony, SK – Slovak Karst, T – Tatra Mts, VES – Vestfold, VF – Veľká Fatra Mts.

Table 3. Intraspecific and interspecific % of K2P distances in the targeted *Ceratophysella* species.

#	Species	Intraspecific distances	Interspecific distances				
			1	2	3	4	5
1	<i>C. cavicola</i>	0.2					
2	<i>C. denticulata</i>	0.6	26.6				
3	<i>C. engadinensis</i>	0.0	28.2	19.0			
4	<i>C. granulata</i>	1.1	21.3	24.3	25.9		
5	<i>C. stachi</i> sp. nov.	1.0	24.4	23.6	22.9	21.0	–

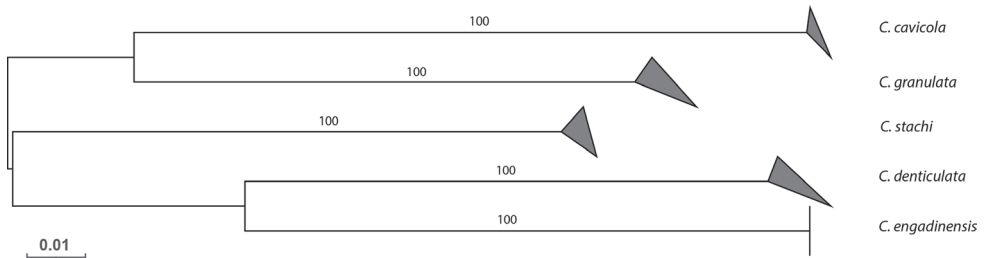
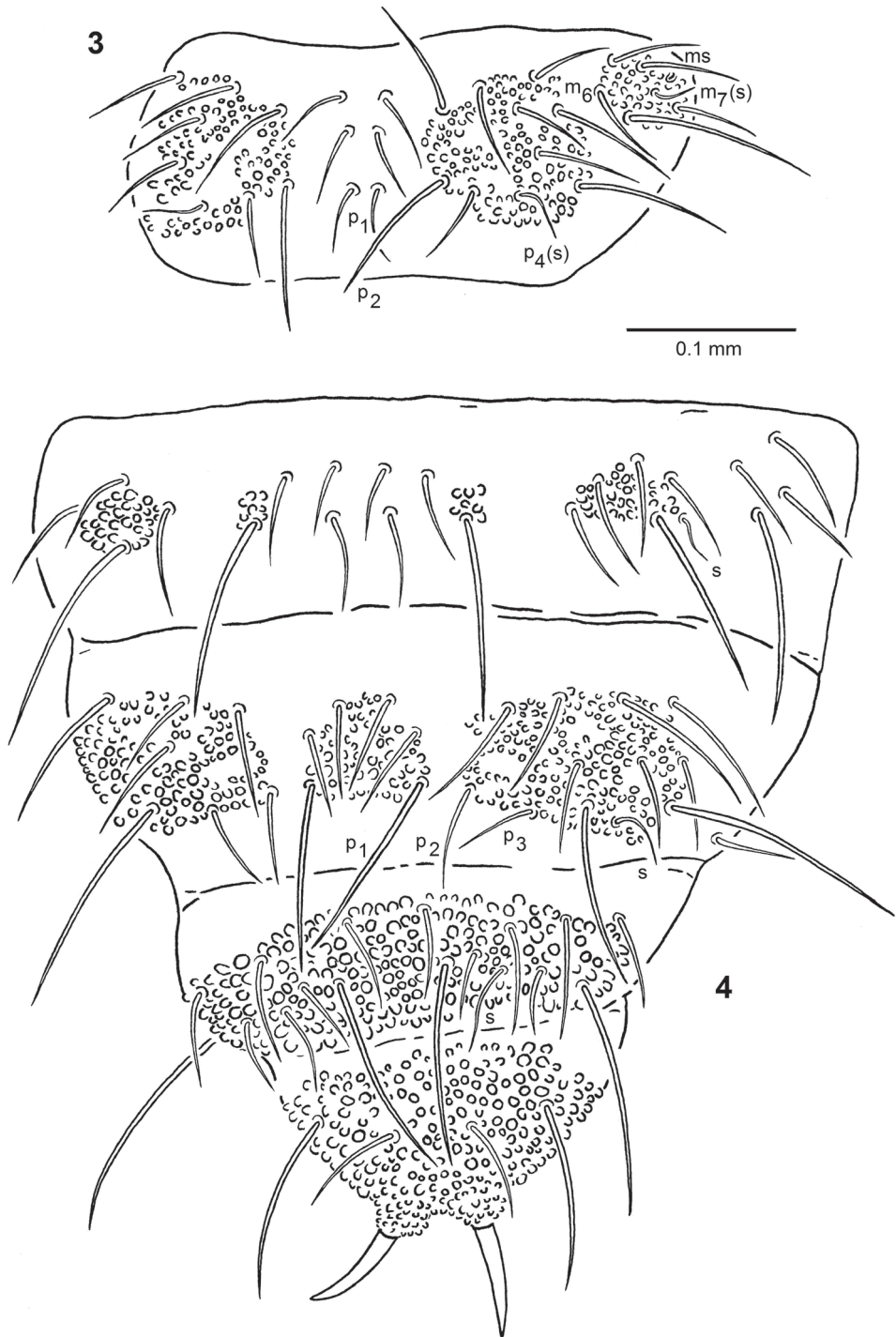


Figure 2. Neighbor joining tree (K2P) of the five *Ceratophysella* species targeted (based on the 5' end of COI). Bootstrap supports showed on the branches. The upper and lower side of the triangle represent respectively the maximum and minimum of genetic distances within the species.

holotype; 3 females, 5 males, juv., 14.V.2002, leg. A. Smolis, D. Skarżyński, other data same as holotype.

Other material. DENMARK (AF, leg. A. Fjellberg): female, Jutland, Himmerland, Rold Skov, *Fagus* litter, 20.III.1994, 94.024; Funen: 6 females, 2 males, Fiskerup Skov, forest stream, 24.III.1994, 94.076; female, Syltemade Adal, *Fraxinus/Ulmus/Viburnum* litter, 23.III.1994, 94.070. GERMANY (SMNG): Brandenburg: 6 females, 3 males, 3 juv., “Wanninchen” nature reserve, bog, 1.V.1972, leg. Hiebsch, 11911; 9 females, male, “Wanninchen” nature reserve, wet heather, 1972, leg. Hiebsch, 11911; male, 2 juv., “Bergener Moor” nature reserve, moor, *Sphagnum*, heather, pine forest, 1.V.1972, leg. Hiebsch, 11912. Hesse: 5 females, Vogelsberg, 1985–1995, leg. W. Böhle. Mecklenburg-West Pomerania: female, Müritz National Park, Neustrelitz, soil 0–5 cm, alder swamp woods not on acid peat, 16.X.2013, leg. U. Burkhardt, 264-F865; 4 females, 2 males, Serrahn, Hauptmannsberg near Feldberg, sandy-gravelly moraine, largely unforested since the Middle Ages, 1973, leg. Hiebsch/ILN Greifswald, 11915; female, Serrahn, Klockenbruch, active, relatively undamaged raised bogs, moss/*Sphagnum*, 16.X.2013, leg. R. Lehmitz and U. Burkhardt, 261-01; male, Serrahn, Klockenbruch, active, relatively undamaged raised bogs, moss/*Sphagnum*, 5.XI.2014, leg. R. Lehmitz and U. Burkhardt, 401-12; female, Serrahn, “Kesselmoor” nature reserve, active, relatively undamaged raised bogs, moss/*Sphagnum*, 16.X.2013, leg. R. Lehmitz, 49077-08; male, Serrahn, soil 0–5 cm, Medio-European collinear woodrush beech forest, 16.X.2013, leg. U. Burkhardt, 263-03. Saxony: female and juv., Erzgebirge, Kleiner Kranichsee, *Sphagnum*, 22.VII. 1971, leg. W. Dunger, 7871. LUXEMBOURG, subadult male, Vallée d’Our: Tintesmühle, near the river, 21.VII.1991, leg. M. Ursone, L-91-101 (ISEZ). NORWAY (AF, leg. A. Fjellberg): Akershus: 4 females, “Östmarka” nature reserve, Tappenbergvann, old spruce cones, 18.V.1995, 95.163; female, Barum, Dalivannet, 16.XI.1997. Vestfold: male, 32/93; 2 females, Larvik, N. Holtesetra, Hvarnes, lush *Alnus* and *Fraxinus* forest, 24.XI.2007, 7.290; female and male, Larvik, Granasnekollen, Hvarnes, litter, oak/beech, 25.IX.2004, 04.086; 3 females, Brunlanes, Hummerbakken, Telemark Camp., plant debris, beach, 14.XI.1993, 93.077; female, Tjøme, Sandø, N-stranda, spongy *Pinus* litter behind beach, 22.IV.2009, 9.086. POLAND (Carpathians, DIBEC): female, 3 males, 2 juv., Beskid Sądecki Mts: “Las



Figures 3, 4. *Ceratophysella stachi* sp. nov. **3** chaetotaxy of thoracic tergum II **4** chaetotaxy of abdominal terga III–VI.

Lipowy Obrozyska” nature reserve near Muszyna, 600 m a.s.l., mosses on rocks and trees, 1.V.2004, 25.VI.2005, leg. A. Smolis, D. Skarżyński; female, Roztoka Ryterska, 600 m a.s.l., litter and mosses near stream, 3.V.2004, leg. A. Smolis, D. Skarżyński; 5 females, “Uhryń” nature reserve, 850 m a.s.l., litter of fir-beech forest, 3.V.2000, leg. A. Smolis; female, 3 males, 2 juv., “Barnowiec” nature reserve, 850 m a.s.l., mosses on rocks in an old beech forest, 10.V.2003, leg. A. Smolis, D. Skarżyński; 4 females, 2 males, SE slopes of Jaworzyna Krynicka, litter in a beech forest, ca 800 m a.s.l., 2.V.2004, leg. A. Smolis, D. Skarżyński. Bieszczady Mts: 2 females, N slopes of Krzemieniec, 1000 m a.s.l., litter in a stream valley, 19.V.2000, leg. A. Smolis. UKRAINE: male, Ivano-Frankove village, Lviv District, beech and elm forest, leaf litter and soil, leg. S. Bakaeva, 2.2.4.8 (SMNHL).

Etymology. Dedicated to Jan Stach, the excellent specialist in Collembola.

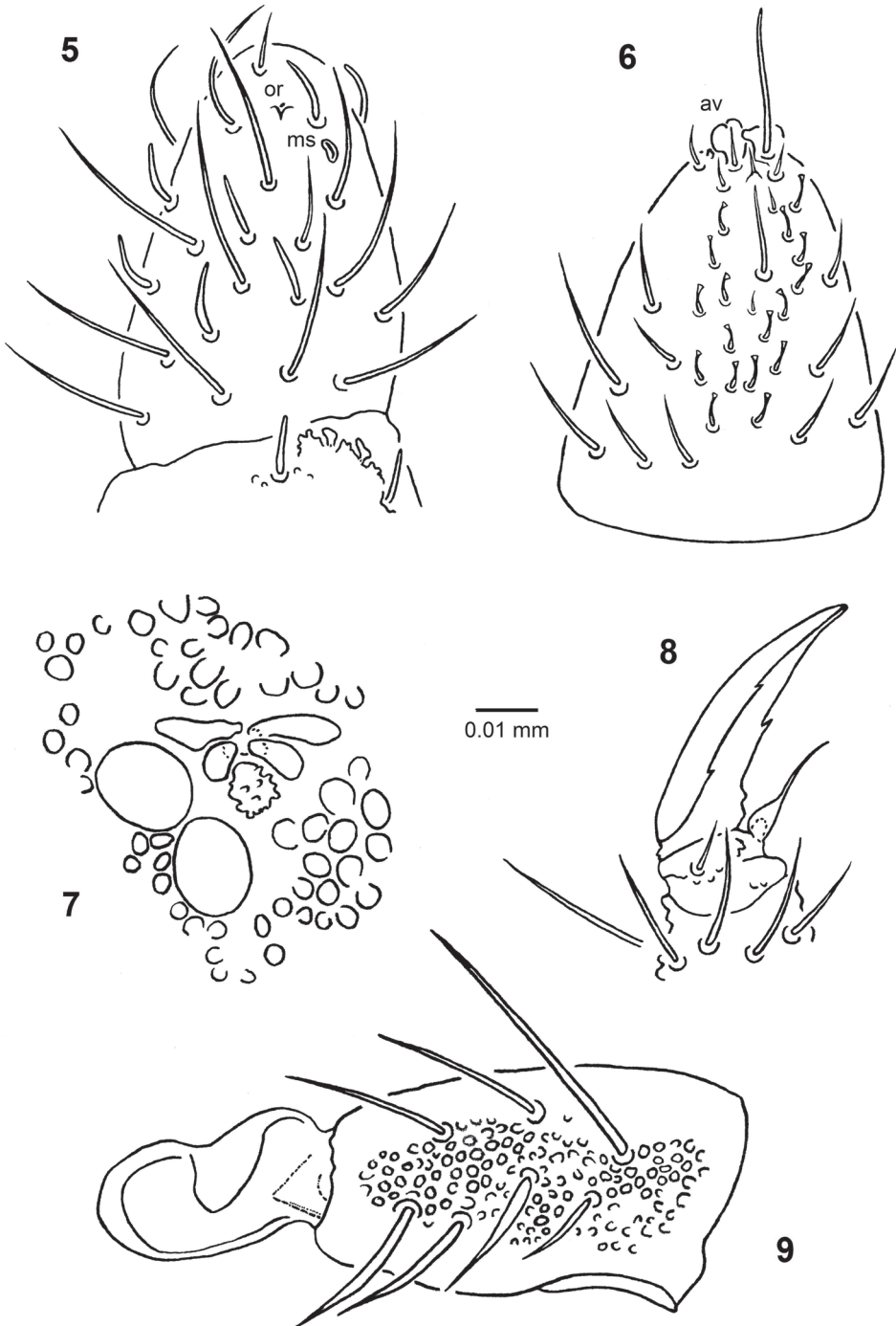
Description. Body length 1–2 mm. Colour (in alcohol) bluish-gray to bluish-black. Tegumental granulation strong, with fields of especially coarse granules on head (large uniform field covering whole dorsal side except antennal bases), thoracic terga II–III (two large subaxial fields and two lateral ones of medium size, Fig. 3), abdominal terga I–III (variable distribution: from four – Fig. 4 to seven fields of medium size as in *C. granulata*; see Skarżyński 2004a: fig. 8), abdominal tergum IV (medium axial field and two lateral large ones, Fig. 4) and abdominal terga V–VI (large uniform fields covering almost whole dorsal side, Fig. 4). 6–9 granules between macrosetae p_1 on abdominal tergum V.

Arrangement of setae on head typical for the genus, spine-like setae absent. Dorsal chaetotaxy of type B (Figs 3, 4). Thoracic terga II–III with setae m_6 present and one additional seta outside lateral sensillum m_7 present or absent. Setae p_1 on abdominal tergum IV developed as macrosetae, p_2 as microsetae, setae p_3 present. Differentiation of dorsal setae into micro- and macrosetae distinct. Setae long (ratio p_1 microsetae and p_2 macrosetae on thoracic tergum II/inner edge of claws III = 1–1.3 and 1.8–2.8, respectively), thick, curved, pointed at tips and only slightly serrate. Body sensilla (s) short (ratio sensillum p_4 and m_7 on thoracic tergum II/inner edge of claws III = 0.6–1 and 0.4–0.6, respectively), thin and smooth. Microsensilla (ms) on thoracic tergum II present (Fig. 3). Subcoxae I, II, III with 1, 2, 3 setae, respectively.

Antennal segment IV with simple or lobed apical vesicle, subapical organite (or), microsensillum (ms), 7 (2 lateral, 5 dorsal) cylindrical, subequal sensilla and 15–25 slightly curved blunt-tipped sensilla in ventral field (Figs 5, 6). Antennal segment III organ with two long (lateral) and two short (internal), curved sensilla (Fig. 5). Microsensillum on antennal segment III present. Eversible sac between antennal segments III and IV present. Antennal segment I with 7 setae.

Ocelli: 8 + 8. Postantennal organ 1.8–2.3 times as large as single ocellus; the former with four lobes, its anterior pair larger than posterior pair. Accessory boss large (equal to or only slightly smaller than posterior lobes of postantennal organ), often granulated (Fig. 7).

Labrum with 5, 5, 4 setae; 4 prelabrals present. Maxillary head of *C. armata* type (Fjellberg 1984: fig. 18). Labial palp as shown in Fjellberg (1999: Fig. 4), but with 6 proximal setae. Outer maxillary lobe with one sublobal hair.



Figures 5–9. *Ceratophysella stachi* sp. nov. **5** chaetotaxy of dorsal side of antennal segments III–IV **6** chaetotaxy of ventral side of antennal segment IV **7** postantennal organ and neighbor ocelli **8** claw I **9** dens and mucro.

Tibiotarsi I, II, III with 19, 19, 18 setae, respectively, clavate setae absent. Claws with inner tooth and a pair of lateral teeth. Empodial appendage with broad lamelliform base and filiform apex reaching inner tooth or slightly beyond, ratio empodial appendage/ inner edge of claws = 0.4–0.7 (Fig. 8).

Ventral tube with 4 + 4 setae. Furca well developed. Ratio dens + mucro/inner edge of claw III = 1.8–2.2, ratio dens/mucro = 1.7–2.2. Dens with uniform fine granules and 7 dorsal setae (2–4 inner setae modified) (Fig. 9). Mucro wide at tip (ratio width of apical part/length of mucro = 0.4–0.6, usually 0.5), boat-like, with large outer lamella, (Fig. 9). Retinaculum with 4 + 4 teeth.

Anal spines yellowish, slightly curved, situated on high basal papillae, 1.1–1.7 times as long as inner edge of claws III (Fig. 4).

Distribution and ecology. The range of distribution of *C. stachi* sp. nov. appears to be relatively wide. It is known from Denmark (Jutland, Funen), Germany (Brandenburg, Hesse, Mecklenburg-West Pomerania, Saxony), Luxembourg, southern Norway (Akershus, Vestfold), Poland (Carpathians: Beskid Niski, Beskid Sądecki, Bieszczady mountains) and Ukraine (Lviv District) (Fig. 1). Probably this species is distributed much more widely in Europe, but additional research is needed to prove this thesis. *Ceratophysella stachi* sp. nov. lives in lowlands and in the mountains (up to ca. 1000 m a.s.l.) where it inhabits litter and mosses in different types of forests, and also heathlands and bogs.

Remarks. *Ceratophysella stachi* sp. nov. belongs to a small European branch of species of the *C. armata*-group, which have strong tegumentary granulation, with distinct fields of coarse granules: *C. granulata*, *C. lawrencei* (Gisin, 1963), *C. neomeridionalis* (Nosek & Červek, 1970), *C. scotica* (Carpenter & Evans, 1899), and *C. silvatica*. It differs from all of them in the chaetotaxy of the lateral parts of the thoracic terga II–III (setae m_6 present and one additional seta outside lateral sensillum m_7 present or absent vs setae m_6 and additional setae absent) which is exceptional within the whole *C. armata*-group (both characters are found in the genus, but in other groups of species: formerly classified as *Mitchellania* Wray, 1953 and *C. denticulata*). The remaining differences between *C. stachi* sp. nov. and related species mentioned above are summarized in Table 4.

Ceratophysella granulata Stach, 1949

Ceratophysella granulata Stach 1949: 133

Material. POLAND (Carpathians): ISEZ: 2 syntypes on slide (formerly in alcohol), Tatra Mts, Dziura cave, 15.VII.1909, leg. J. Stach; 29 spp. on slides, Tatra Mts, leg. J. Stach; Beskid Mały Mts, male, juv., Zagórze near Skawce, Grota Piaskowa cave, 350 m.a.s.l., XI.1951, leg. Szymczakowski; DIBEC: Tatra Mts (leg. D. Skarżyński): 74 females, 17 males, litter of dwarf mountain pine shrubs on the slopes of the Gładkie Uplaziańskie, at an altitude of 1500–1600 m a.s.l., 13.VII.2001, 14.IX.2002,

Table 4. Characteristics of *Ceratophysella stachi* sp. nov., *C. granulata* and related species. Based on Carpenter and Evans (1899), Gisin (1963), Rusek (1964), Nosek and Červek (1967, 1970), Christian (1987), Babenko et al. (1994), Fjellberg (1998), Skarżyński (2004a, 2006), Thibaud et al. (2004), Kaprus' et al. (2006), Danyi and Traser (2008), Kováč et al. (2016), and our own data. Abbreviations: d_2 - spine-like setae d_2 on head, oc_2 - spine-like setae oc_2 on head, m_6 - setae m_6 on thoracic terga II–III, p_3 - setae p_3 on abdominal tergum IV, e/cl - ratio empodium/claw.

Species	d_2	oc_2	m_6	p_3	e/cl	Distribution	Habitat preferences
<i>C. granulata</i> ¹	-	-	-	+	0.5–0.7	Polish and Slovak Carpathians (Fig. 1)	Cold and humid places in the mountains: mosses in alpine zone, litter and mosses in dwarf mountain pine zone and deep gorges and caves in montane forests zone
<i>C. lawrencei</i>	+	+	-	+	0.5–1	Austrian, Italian and Swiss Alps, Apennines, Polish Tatra Mts.	Litter, mosses on rocks in upper montane zone and above, caves
<i>C. neomeridionalis</i>	+	+	-	-	0.2–0.3	Slovenian Dinaric Mts, Polish and Ukrainian Carpathians	Litter, mosses on rocks in montane zone
<i>C. scotic</i> ²	-	-	-	-	0.7–1.1	Belarus, Denmark, Finland, Germany, Great Britain, Ireland, Norway, Poland, Russia, Sweden, Ukraine	Hygrophilous and tyrophilous species living in lowlands and mountains
<i>C. silvatica</i>	+	-	-	-	0.3–0.4	Hungary, Italy, Poland, Romania, Slovakia, Ukraine	Litter, mosses on rocks in upland and mountain forests
<i>C. stachi</i> sp. nov. ³	-	-	+	+	0.4–0.7	Denmark, Germany, Luxembourg, Norway, Poland, Ukraine (Fig. 1)	Litter and mosses in different types of forests in lowlands and mountains, also heathlands and bogs

¹ Accessory boss near post-antennal organ small (about half the size of posterior lobes of post-antennal organ), mucro narrow at tip (ratio width of apical part/length of mucro = 0.22–0.52 (mean 39)).

² Fields of especially coarse granules only on abdominal terga IV–VI.

³ Thoracic terga II–III with one additional seta outside lateral sensillum m , present or absent.

18.IX.2004, 14. VIII. 2009; 4 females, 2 males, 2 juv., Chuda Turnia, moss on rocks, 1800 m a.s.l., 19.VIII.2004; 11 females, 5 males, 2 juv., Kraków Gorge, spruce forest litter and mosses on rocks, 1050–1150 m a.s.l., 19.VIII.2004; 4 males, Mylna cave, mosses in the entrance, 1090 m a.s.l., 19.VIII.2004; female, Raptawicka cave, mosses in the entrance, 1150 m a.s.l., 19.VIII.2004; female, juv., Dziura cave, litter in the entrance, 1000 m a.s.l., 24.VIII.1991; 20 females, 15 males, litter of dwarf mountain pine shrubs on the slopes of Sucha Czuba, 1600–1700 m a.s.l., 17.IX.2004; Beskid Żywiecki Mts: 3 females, 5 males, 6 juv., Babia Góra, litter of spruce forest and dwarf mountain pine shrubs, 1300–1500 m a.s.l., 4.VI.1999, leg. A. Smolis; 4 females, 3 males, 5 juv., Piłsko, litter of spruce forest and dwarf mountain pine shrubs, 1300–1500 m a.s.l., 21.IX.2004, leg. D. Skarżyński; Pieniny Mts, 4 females, male, 2 juv., Ociemny valley, 500–600 m a.s.l., mosses on rocks, 26.V.1994, leg. R.J. Pomorski; Beskid Wyspowy Mts, 10 females, male, Zbójecka cave near Limanowa, 900 m a.s.l., bat guano, 12.VII.2007, leg. K. Piksa. SLOVAKIA (Western Carpathians): ISEZ: female, male, Pieniny Mts, Aksamitka cave, VII.1931, leg. Grochmalicki. PJSU: 4 females, 2 males, Veľká Fatra Mts, Horná Tůfna cave near Horný Harmanec village, 975 m a.s.l., entrance hall, cave sediment, 26–31.VIII.1999, leg. Ľ. Kováč, 301-99, 302-99; female, Západné Tatry Mts, Brestovská cave near Zuberec village, entrance hall, cave sediment, 22.V.-13.IX.2006, leg. A. Mock, 671-06; 2 males, 3 juv., Belianske Tatry

Mts, Kamzíčia jaskyňa cave near Ždiar village, 2002 m a.s.l., 15 m from entrance, cave sediment, 13.IX.1991, leg. Ľ. Kováč; Low Tatras Mts: Demänovská jaskyňa slobody cave near Demänová village, 812 m a.s.l.: female, male, rotten wood, 11.V.2000, leg. P. Luptáčik, 84-00; 2 females, male, Mramorové riečisko, bait, 11.V.–27.IX.2000, leg. Ľ. Kováč, 131-00, 133-00; Demänovská ľadová jaskyňa cave, 740 m a.s.l.: 2 females, entrance, talus deposit, 12.V.–28.IX.2000, Ľ. Kováč, 168-00; female, cave entrance, wood, 28.IX.2000, leg. P. Luptáčik, 170-00; female, Pustá jaskyňa cave, Hlinená chodba, surface of water puddle, 24.VI.2015, leg. Ľ. Kováč, 82-15; Pieniny Mts, Aksamitka cave near Haligovce village, 756 m a.s.l., leg. Ľ. Kováč: 6 females, 4 males, Blatistý dóm, rotten wood, cave sediment, 12.III.–26.V.1998, 45-98, 197-98, 198-98, 199-98, 200-98; 2 females, Dóm priekopníkov, bat guano, 26.V.1998, 201-98; 2 females, 1 juv., Dóm priekopníkov, cave sediment, 23.VIII.–7.X.1999, 363-98, 364-98, 366-98; male, soil of herbal cushion in front of cave, 26.V.1998, 202-98; Levočské vrchy Mts, Jaskyňa pod Jankovcom 2 cave near Ľubica village: 3 females, male, Hall A, bat guano, Hall II rotten wood, 5.XI.2010, leg. P. Luptáčik, 747-10, 758-10; male, passage B, surface of water puddle, 5.XI.2010, leg. Z. Višňovská, 755-10; Slovak Paradise: Dobšinská ľadová jaskyňa cave near Stratená village, 969 m a.s.l.: female, male, moss on rocks in front of cave, 23.VII.1997, leg. Ľ. Kováč, 126-130-97, 2 females, humus and soil in front of cave, 7.X.2004, leg. V. Šustr, 4 females, male, Psie Diery cave, cave sediment, 6.II.1997, leg. V. Košel, female, Vojenská cave, 20 m from entrance, bait, 6.XII.1998, leg. V. Košel, 22-99, 3 females, cave sediment, 28.I.–6.II.1997, leg. V. Košel, 3 females, Kláštorňá cave, cave sediment, 27.I.–4.II.1997, leg. V. Košel, female, 2 males, Duča cave, Dóm, bait, 4.XII.1998, leg. V. Košel, 25-99, male, Stratenská cave, 200 m from entrance, rotten wood, 9.X.1997, leg. Ľ. Kováč, 184-97; male, Muránska planina Plateau, Bobačka cave near Muránska Huta village, 30 m from entrance, cave sediment, 5.X.–9.XI.2000, Ľ. Kováč, 219-00; Čierna hora Mts: 2 females, Veľká ružínska jaskyňa cave near Malá Lodina village, 614 m a.s.l., 100 m from entrance, cave sediment, 10.VIII.–14.X.1996, leg. Ľ. Kováč, 1327-96, male, juv., Malý Ružinok Valley, *Tilio-Acerion*, humus and soil, rotten wood, 19.IX.2009, 23.IV.2010, leg. Ľ. Kováč, 610-09, 139-10; male, Slovak Karst, Šingliarova priepať cave near Honce village, 680 m a.s.l., 1st Hall, rotten wood, 4.V.2008, leg. P. Luptáčik, 215-08.

Remarks. Specification of *C. granulata* morphology is provided by Skarżyński (2004a). COI sequences of this species were examined and deposited on BOLD and GenBank by Porco et al. (2012). *Ceratophysella granulata*, with strong tegumentary granulation and distinct fields of coarse granules, resembles *C. stachi* sp. nov. and four other European species of the *C. armata*-group: *C. lawrencei*, *C. neomeridionalis*, *C. scotica*, and *C. silvatica*. Differences between these species are presented in Table 4. The presence of true *C. granulata* is so far confirmed only for the Polish Carpathians (Tatra Mts, Pieniny Mts, Beskid Żywiecki Mts, Beskid Wyspowy Mts, Beskid Mały Mts) and Slovak (Veľká Fatra Mts, Západné Tatry Mts, Belianske Tatry Mts, Low Tatras Mts, Pieniny Mts, Levočské vrchy Mts, Slovak Paradise, Muránska planina Plateau, Čierna hora Mts, Slovak Karst) (Fig. 1), where it inhabits cold and humid places: mosses in the alpine zone, litter and mosses in the dwarf mountain pine zone, deep

gorges (litter and mosses), and caves (mosses, litter, and rotten wood at cave the entrance, and bat guano and cave sediments even 100 m from the entrance) in mountain forests zone. At the end of the Pleistocene, this psychro- and hygrophilous species was probably more common in the periglacial region, and due to the warming Holocene climate, its range became limited to scattered, high-mountain refuges and cold caves and other subterranean habitats at lower elevations. Based on the current distribution data, it is concluded that *C. granulata* is endemic to the Western Carpathians. However, to verify this thesis, additional research should be undertaken covering the rest of the Carpathians, the Alps, and other mountainous areas of central Europe.

Discussion

Traditionally, the most commonly used method in the taxonomy of the genus *Ceratophysella*, as in other Collembola, is the analysis of morphological features (Gisin 1949; Stach 1949; Cassagnau 1959; Yosii 1960; Bourgeois and Cassagnau 1972; Babenko et al. 1994; Jordana et al. 1997; Christiansen and Bellinger 1998; Fjellberg 1998; Thibaud et al. 2004). Recently, hybridization in laboratory conditions and DNA barcoding have also been used, although on a small scale (Skarżyński 2004a, b, c, 2005; Porco et al. 2012; Nakamori 2013). Research on the *Xenylla maritima* complex (Skarżyński et al. 2018) and *Ceratophysella comosa* Nakamori, 2013 showed that combined use of the morphological and genetic criteria may bring good results in establishing species status and support in the family Hypogastruridae. The use of integrative taxonomy methods in this study allowed for the revision of “*C. granulata*” status and the description of a species new to science. Considering its effectiveness and its relative low cost, this method has the potential to bring a significant contribution in the field of taxonomic revision.

Acknowledgements

We wish to thank Birgit Balkenhol (Senckenberg Museum of Natural History, Görlitz, Germany), László Dányi (Hungarian Natural History Museum, Budapest, Hungary), Arne Fjellberg (Norway), Igor Kaprus’ (State Museum of Natural History, Ukrainian National Academy of Sciences, Lviv, Ukraine), Peter Schwendinger (Muséum d’histoire naturelle, Geneva, Switzerland), and Wanda M. Weiner (Institute of Systematics and Evolution of Animals, Polish Academy of Sciences, Cracow, Poland), for the loan of the material. We also thank Harald Bruckner for searching for *C. granulata* in the collection of Natural History Museum in Vienna, Austria. We are grateful to Michał Furgol (Poland) for collecting *C. stachi* sp. nov. for DNA barcoding. We also express our sincere thanks to Arne Fjellberg for inspiration to undertake the research. Anatoly Babenko (The Severtsov Institute of Ecology & Evolution, Russian Academy of Sciences, Moscow, Russia) and Arne Fjellberg kindly reviewed the manuscript.

References

- Babenko AB, Chernova NM, Potapov MB, Stebaeva SK (1994) Collembola of Russia and Adjacent Countries: Family Hypogastruridae. Nauka, Moscow, 336 pp.
- Bagnall RS (1941) Notes on British Collembola. VIII. The Entomologist's Monthly Magazine 77: 217–226.
- Bellinger P, Christiansen KA, Janssens F (1996–2021) Checklist of the Collembola of the World. <http://www.collembola.org> [Accessed on: 14.I.2021]
- Bogojevič J (1968) Collembola. Catalogus Faunae Jugoslaviae. III./6, Ljubljana, 33 pp.
- Börner C (1932) Apterygota. In: Brohmer P (Ed.) Fauna von Deutschland, Auflage 4. Quelle & Meyer, Leipzig, 136–143.
- Bourgeois A, Cassagnau P (1972) La différenciation du type Ceratophysellien chez les collemboles Hypogastruridae. Nouvelle Revue d'Entomologie 2: 271–291.
- Carpenter GH, Evans W (1899) The Collembola and Thysanura of the Edinburgh district. Proceedings of the Royal Society of Edinburgh 14: 221–266.
- Cassagnau P (1959) Faune française des Collembolés (IX). Les *Hypogastrura* s.l. du massif du Néouvielle (Hautes-Pyrénées). Remarques sur la chétotaxie des espèces. Vie et Milieu 9: 476–503.
- Christian E (1987) Catalogus Faunae Austriae. XIIa, U. Kl.: Collembola (Springschwänze). Verlag der Österreichischen Akademie der Wissenschaften, Wien, 80 pp.
- Christiansen K, Bellinger P (1998) The Collembola of North America North of the Rio Grande. A Taxonomic Analysis. Grinnell College, Grinnell, 1520 pp.
- Danyi L, Traser G (2008) An annotated checklist of the springtail fauna of Hungary (Hexapoda: Collembola). Opuscula Zoologica 38: 3–82.
- Danyi L, Traser G, Fiera C, Radwański M (2006) Preliminary data on the Collembola fauna of Maramureş County. Studia Universitatis Vasile Goldiș, Seria Științele Vieții 17: 47–51.
- Eckert R, Palissa A (1999) Beiträge zur Collembolenfauna von Höhlen der deutschen Mittelgebirge (Harz, Kyffhäuser, Thüringer Wald, Zittauer Gebirge) (Insecta, Collembola). Beiträge zur Entomologie 49: 211–255. <https://doi.org/10.21248/contrib.entomol.49.1.211-255>
- Fjellberg A (1984) Maxillary structures in Hypogastruridae (Collembola). Annales de la Société Royale Zoologique de Belgique 114: 89–99.
- Fjellberg A (1998) The Collembola of Fennoscandia and Denmark. Part 1 Poduromorpha. Fauna Entomologica Scandinavica. Brill, Leiden–Boston–Köln, 184 pp.
- Fjellberg A (1999) The labial palp in Collembola. Zoologischer Anzeiger 237: 309–330.
- Folmer O, Black M, Hoeh W, Lutz R, Vrijenhoek R (1994) DNA primers for amplification of mitochondrial cytochrome c oxidase subunit i from diverse metazoan invertebrates. Molecular Marine Biology and Biotechnology 3: 294–299.
- Gisin H (1949) Notes sur les Collembolés avec description de quatorze espèces et d'un genre nouveaux. Mitteilungen der Schweizerischen Entomologischen Gesellschaft 22: 385–400.
- Gisin H (1963) Collembolés d'Europe V. Revue suisse de Zoologie 70: 77–101.
- Goto HE (1955a) Collembola from Shillay, Outer Hebrides, including new British and local records. The Scottish Naturalist 67: 29–33.
- Goto HE (1955b) Some new British and local records of Collembola. The Entomologist's Monthly Magazine 91: 267–268.

- Grinbergs A (1960) On the fauna of springtails (Collembola) of the Soviet Union. Part I. Catalogue of Collembola of the USSR. *Latvijas Entomologs Riga* 2: 21–68.
- Hajibabaei M, DeWaard JR, Ivanova NV, Ratnasingham S, Dooh RT, Kirk SL, Mackie PM, Hebert PDN (2005) Critical factors for assembling a high volume of DNA barcodes. *Philosophical Transactions of the Royal Society B-Biological Sciences* 360: 1959–1967. <https://doi.org/10.1098/rstb.2005.1727>
- Hall TA (1999) Bioedit: A user-friendly biological sequence alignment editor and analysis program for windows 95/98/nt. *Nucleic Acids Symposium Series* 41: 95–98.
- Hopkin SP (2007) A Key to the Springtails (Collembola) of Britain and Ireland. Field Studies Council (AIDGAP Project), Shropshire, 245 pp.
- Ivanova NV, Dewaard JR, Hebert PDN (2006) An inexpensive, automation-friendly protocol for recovering high-quality DNA. *Molecular Ecology Notes* 6: 998–1002. <https://doi.org/10.1111/j.1471-8286.2006.01428.x>
- Jordana R, Arbea JI, Simón C, Lucíañez MJ (1997) Collembola, Poduromorpha. In: Ramos MA, et al. (Eds) *Fauna Ibérica* (Vol. 8). Museo Nacional de Ciencias Naturales, CSIC, Madrid, 807 pp.
- Kaprus' IJ, Shrubovych JJ, Taraschuk MV (2006) Catalogue of the Collembola and Protura of Ukraine. SNHMU, NASU, Lviv, 164 pp.
- Kimura M (1980) A simple method for estimating evolutionary rates of base substitutions through comparative studies of nucleotide-sequences. *Journal of Molecular Evolution* 16: 111–120.
- Kováč L, Parimuchová A, Miklisová D (2016) Distributional patterns of cave Collembola (Hexapoda) in association with habitat conditions, geography and subterranean refugia in the Western Carpathians. *Biological Journal of the Linnean Society* 119: 571–592. <https://doi.org/10.1111/bij.12555>
- Nakamori T (2013) A new species of *Ceratophysella* (Collembola: Hypogastruridae) from Japan, with notes on its DNA barcode and a key to Japanese species in the genus. *Zootaxa* 3641(4): 371–378. <https://doi.org/10.11646/zootaxa.3641.4.3>
- Nei M, Kumar S (2000) *Molecular Evolution and Phylogenetics*. Oxford University Press, Oxford, 333 pp.
- Nilsai A, Jantarit S, Satasook C, Zhang F (2017) Three new species of *Coecobrya* (Collembola: Entomobryidae) from caves in the Thai Peninsula. *Zootaxa* 4286(2): 187–202. <https://doi.org/10.11646/zootaxa.4286.2.3>
- Nosek J (1958) Príspevek k faune Apterygot lesnich pud. *Časopis Česke Společnosti Entomologické* 55 (4): 357–360.
- Nosek J (1969) The investigation on the Apterygotan fauna of the Low Tatras. *Acta Universitatis Carolinae Biologica, Praha* 5/6(1967): 349–528.
- Nosek J, Červek S (1967) A new species of springtail from the mediterranean region *Hypogastrura* (*Ceratophysella*) *meridionalis* sp. n. (Collembola: Hypogastruridae). *Acta Societatis Zoologicae Bohemoslovenicae* 31: 245–249.
- Nosek J, Červek S (1970) Beseitigung eines Homonyms in der Gattung *Hypogastrura* (Insecta: Collembola). *Revue suisse de Zoologie* 77: 207. <https://www.biodiversitylibrary.org/page/40807834>

- Popa I (2012) Two new records of springtails (Hexapoda: Collembola) for the Romanian fauna – Maramureş County. *Travaux de l'Institut de Spéologie "Émile Racovitza"*, Bucarest 51: 73–79.
- Porco D, Rougerie R, Deharveng L, Hebert P (2010) Coupling non-destructive DNA extraction and voucher retrieval for small soft-bodied arthropods in a high-throughput context: the example of Collembola. *Molecular Ecology Resources* 10: 942–945. <https://doi.org/10.1111/j.1755-0998.2010.2839.x>
- Porco D, Bedos A, Greenslade P, Janion C, Skarżyński D, Stevens MI, Jansen van Vuuren B, Deharveng L (2012) Challenging species delimitation in Collembola: cryptic diversity among common springtails unveiled by DNA barcoding. *Invertebrate Systematics* 26: 470–477. <https://doi.org/10.1071/IS12026>
- Porco D, Skarżyński D, Decaens T, Hebert PDN, Deharveng L (2014) Barcoding the Collembola of Churchill: a molecular taxonomic reassessment of species diversity in a sub-arctic area. *Molecular Ecology Resources* 14: 249–261. <https://doi.org/10.1111/1755-0998.12172>
- Ratnasingham S, Hebert PDN (2007) BOLD: The Barcode of Life Data System (www.barcodinglife.org). *Molecular Ecology Notes* 7: 355–364. <https://doi.org/10.1111/j.1471-8286.2007.01678.x>
- Rusek J (1964) Zwei neue Collembolenarten aus der Mittel-Slowakei (ČSSR). *Zoologischer Anzeiger* 173: 432–440.
- Saitou N, Nei M (1987) The neighbor-joining method – a new method for reconstructing phylogenetic trees. *Molecular Biology and Evolution* 4: 406–425.
- Skarżyński D (2004a) Taxonomic position of *Ceratophysella granulata* STACH, 1949 and *Ceratophysella silvatica* (RUSEK, 1964) in the light of morphological and laboratory hybridization studies. *Acta Zoologica Cracoviensia* 47(3–4): 147–153. <https://doi.org/10.3409/173491504783995825>
- Skarżyński D (2004b) Generic status of *Bonetogastrura cavicola* (Börner, 1901) (Collembola: Hypogastruridae) in the light of laboratory hybridization studies. *Annales Zoologici* 54(2): 461–466.
- Skarżyński D (2004c) Taxonomic status of *Ceratophysella denticulata* (Bagnall, 1941), *C. engadinensis* (Gisin, 1949) and *C. stercoraria* Stach, 1963 (Collembola: Hypogastruridae) in the light of laboratory hybridisation studies. *Insect Systematics and Evolution* 35(3): 277–284. <https://doi.org/10.1163/187631204788920176>
- Skarżyński D (2005) Taxonomy of the ceratophysellan lineage (Collembola: Hypogastruridae) in the light of laboratory hybridization studies. *Zootaxa* 1043: 47–59. <https://doi.org/10.11646/zootaxa.1043.1.4>
- Skarżyński D (2006) Redescription of *Ceratophysella lawrencei* (Gisin, 1963) (Collembola: Hypogastruridae). *Revue suisse de Zoologie* 113(2): 291–296. <https://doi.org/10.5962/bhl.part.80352>
- Skarżyński D, Piwnik A, Porco D (2018) Integrating morphology and DNA barcodes for species delimitation within the species complex *Xenylla maritima* (Collembola: Hypogastruridae). *Arthropod Systematics & Phylogeny* 76(1): 31–43.

- Smolis A, Skarżyński D (2003) Springtails (Collembola) of the “Przełom Jasiołki” reserve in the Beskid Niski Mountains (Polish Carpathians). *Fragmenta Faunistica* 46: 121–129. <https://doi.org/10.3161/00159301FF2003.46.2.121>
- Smolis A, Skarżyński D (2006) Springtails (Collembola) of the “Barnowiec” Reserve in the Beskid Sądecki Mountains (Polish Carpathians). *Naukovi Zapysky Derzhavnoho Prirodnavczoho Muzeiu, Lviv* 22: 69–77.
- Stach J (1949) The apterygotan fauna of Poland in relation to the world fauna of this group of insects. Families Neogastruridae and Brachystomellidae. *Acta Monographica Musei Historiae Naturalis, Polish Academy of Sciences and Letters, Kraków*, 341 pp.
- Stach J (1964) Owady bezskrzydłe (Apterygota). In: Mroczkowski M (Ed.) *Katalog Fauny Polski* (Vol. 15). PWN, Warszawa, 103 pp.
- Sterzyńska M, Kaprus’ I (2000) Owady bezskrzydłe (Apterygota). Skoczogonki (Collembola) Bieszczadzkiego Parku Narodowego i otuliny. *Monografie Bieszczadzkie* 7: 131–141.
- Tamura K, Dudley J, Nei M, Kumar S (2007) MEGA4: molecular evolutionary genetics analysis (MEGA) software version 4.0. *Molecular Biology and Evolution* 24: 1596–1599. <https://doi.org/10.1093/molbev/msm092>
- Thibaud J-M, Schulz H-J, Gama Assalino MM da (2004) Hypogastruridae. In: Dunger W (Ed.) *Synopses on Palaearctic Collembola* (Vol. 4). *Abhandlungen und Berichte des Naturkundemuseums Görlitz* 75: 1–287.
- Weiner WM (1981) Collembola of the Pieniny National Park in Poland. *Acta Zoologica Cracoviensia* 25(18): 417–500.
- Wray D (1953) Some new species of springtail insects (Collembola). *Nature Notes* 1: 1–7.
- Yosii R (1960) Studies on the Collembolan genus *Hypogastrura*. *American Midland Naturalist* 64: 257–281. <https://doi.org/10.2307/2422661>

A new species of the genus *Euxaldar* Fennah, 1978 (Hemiptera, Fulgoromorpha, Issidae) from China and revision on the molecular phylogeny of the family

Liang-Jing Yang^{1,2,4}, Zhi-Min Chang^{1,2,3}, Lin Yang^{1,2}, Xiang-Sheng Chen^{1,2}

1 Institute of Entomology, Guizhou University, Guiyang, Guizhou, 550025, China **2** The Provincial Special Key Laboratory for Development and Utilization of Insect Resources, Guizhou University, Guiyang, Guizhou, 550025, China **3** College of Animal Science, Guizhou University, Guiyang, Guizhou, 550025, China **4** Office of Academic Affairs, Liupanshui Normal College, Liupanshui, Guizhou, 55300, China

Corresponding author: Xiang-Sheng Chen (chenxs3218@163.com)

Academic editor: Mike Wilson | Received 17 April 2019 | Accepted 4 January 2021 | Published 1 March 2021

<http://zoobank.org/DE22C878-1AE5-4798-84B5-8FCB4A37A73B>

Citation: Yang L-J, Chang Z-M, Yang L, Chen X-S (2021) A new species of the genus *Euxaldar* Fennah, 1978 (Hemiptera, Fulgoromorpha, Issidae) from China and revision on the molecular phylogeny of the family. ZooKeys 1021: 19–35. <https://doi.org/10.3897/zookeys.1021.35510>

Abstract

A new species *Euxaldar daweshanensis* Yang, Chang & Chen, **sp. nov.** is described and illustrated from southwestern China. The female genitalia of the genus *Euxaldar* is described and presented for the first time. A checklist and key to the known species of the genus are provided. A revised molecular phylogenetic analysis of the family Issidae based on combined partial sequences of *18S*, *28S*, *COI*, and *Cytb* is provided using both Maximum likelihood and Bayesian inference analyses.

Keywords

Checklist, DNA sequence, Hemisphaeriini, identification key, morphology, planthopper, taxonomy

Introduction

The planthopper genus *Euxaldar* Fennah, 1978 is a small group in the Issidae tribe Hemisphaeriini Melichar, 1906, established for a single species *E. jehucal* Fennah, 1978, recorded from Ninh Binh, Ha Noi, Vinh Phuc, Hoa Binh, and Haiphong Province in northern Vietnam (Fennah 1978; Gnezdilov and Constant 2012). Recently

Gnezdilov et al. (2017a) reviewed the genus and described *E. lenis* Gnezdilov, Bourgoïn & Wang, 2017 from Lam Dong Province (Da Lat) of southern Vietnam. Later, Zhang et al. (2018) recorded the genus for the first time from southeastern China and described *E. guangxiensis* Zhang, Chang & Chen, 2018 from Guangxi Province. Previously, Gnezdilov placed *Euxaldar* into the tribe Issini Spinola, 1839 (Gnezdilov 2013). However, Wang et al. (2016) moved it to Hemisphaeriini Mongolianina. Recently, this genus was placed in subgroups of Mongolianina: *Mongoliana* + (*Euxaldar* + *Macrodaruma*) by Zhao et al. (2019), but as shown in this study it is better placed in the subgroup (*Retaldar* + (*Clypeosmilus* + *Eusudasina*)) because all genera in this subgroup have the same characteristic protruded clypeus.

Below, we describe and illustrate a new species of *Euxaldar* from Yunnan Province in China, provide a checklist and key to *Euxaldar* species, and describe and photograph the female genitalia of the new species. The partial DNA sequences (*16S*, *28S* (d6-d7), *COI*, *Cytb*) of the new species are briefly analyzed. A revised molecular phylogeny is analyzed by Bayesian and Maximum likelihood based on seven sequences of four genes (*18S*, *28S*, *COI* and *Cytb*), providing molecular evidence of phylogenetic relationships within the Issidae and enabling a reevaluation of the current classification of the family Issidae by Wang et al. (2016), Zhao et al. (2019) and Gnezdilov et al. (2020).

Materials and methods

The morphological terminology used for body appearance follows Chan and Yang (1994) and Anufriev and Emeljanov (1988). Forewing venation pattern follows Bourgoïn et al. (2015). The terminologies of male and female genitalia follow Bourgoïn (1987, 1993) and Chang et al. (2015). Body length (included forewings) is given in millimeters (mm).

The genital segments of the specimens were macerated in a boiling solution of 10% NaOH for about 5 minutes, washed in distilled water, then immersed in glycerine for observation, dissection, drawing, and photography. They were stored in a micro vial in glycerol for further examination. A Leica MZ 12.5 stereomicroscope was used for illustrations. A KEYENCE VHX-1000C was used to acquire photographs. All specimens studied are deposited in the Institute of Entomology, Guizhou University, Guiyang, China (GUGC).

The molecular phylogenetic study included 71 species belonging to 48 genera as ingroups from Issidae (Wang et al. 2016; Zhao et al. 2019; Gnezdilov et al. 2020) and five species as outgroups from the families Cixidae, Caliscelidae, Delphacidae, Dictyopharidae, Tropiduchidae. Data for the 71 included species were downloaded from NCBI. Five ingroup species including the new species were newly sequenced, for which total DNA was extracted using the Animal Tissue Genomic DNA Kit (Tiangen Biotech Company, Beijing, China). Primers and PCR procedures are listed in Tables 1, 2 and carried out in 30 µl volume reaction. Accession numbers for species used in the phylogenetic analysis are shown in Table 4.

Table 1. Primers used for amplification and sequencing.

Gene	Primer	Sequence (5'–3')
<i>COI</i>	COI (LCO18)-PF	GGTCAACAAATCATAAAGATATTG
	COI (HCO29)-PR	TAAACTTCAGGGTGACCAAAAAAT
<i>16S</i> (Clary and Wolstenholme 1985)	16S-PF	GCCTGTTTATCAAAAACAT
	16S-PR	CCGGTCTGAACTCAGATCA
<i>Cytb</i> (Bourgoin et al. 1997)	Cytb-PF	TATGTACTACCATGAGGACAAATATC
	Cytb-PR	ATCTTAATGCAATAACTCCTCC
28S d6–d7 (Cryan et al. 2000)	28S EE	CCGCTAAGGAGTGTGTAA
	28S MM	GAAGTTAGGGATCTARTTTG
28S d3–d5 (Belshaw and Quicke 2002)	28S Ai	GACCCGTCTTGAAACACG
	28S D4D5r	GTTACACACTCCTTAGCGGA

Table 2. PCR procedures.

Gene	<i>COI</i>	<i>16S</i>	<i>Cytb</i>	28S d3–d5	28S d6–d7
Initial denaturation	94 °C 5 min	95 °C 7 min	94 °C 5 min	94 °C 3 min	94 °C 3 min
95 °C 7 min	94 °C 30 sec	95 °C 50 sec	94 °C 1 min	94 °C 1 min	94 °C 1 min
Annealing	55 °C 1 min	50 °C 1 min	47 °C 1 min	54 °C 1 min	55 °C 1 min
Extension	72 °C 1 min				
Cycles	35 Cycles	35 Cycles	35 Cycles	35 Cycles	40 Cycles
Annealing	72 °C 10 min				

Table 3. Nucleotide gene composition of *Euxaldar daweshanensis* Yang, Chang & Chen, sp. nov.

Gene	A%	T%	G%	C%	A+T%
<i>COI</i>	33.2	36.3	17.8	12.7	69.5
<i>16S</i>	27.4	48.6	14.9	9.1	76.0
<i>Cytb</i>	35.3	34.5	11.6	18.6	69.8
28S d6–d7	20.4	18.9	33.7	27.0	39.2

The DNA sequencing was performed at Sangon Company (Shanghai, China). Sequence chromatograms were checked and assembled by Seqman from the package DNASTAR v5.01 (www.dnastar.com), calculated by MEGA 6.06 and Notepad 7.6.2. The Maximum likelihood (ML) phylogenetic analysis was performed by IQtree v1.6.7 and visualized by Figtree v1.1.2. A Bayesian estimation search (BI) was performed using MrBayes (Ronquist et al. 2011) on the CIPRES Science Gateway V3.1 Portal (<https://www.phylo.org/portal2/home.action>). Best partitions and models were chosen by PartitionFinder 2 (Lanfear et al. 2017), running conditions as described in Appendix 1.

Taxonomy

Genus *Euxaldar* Fennah, 1978

Euxaldar Fennah, 1978: 267.

Type species. *Euxaldar jehucal* Fennah, 1978, by monotypy.

Diagnosis. Coryphe transverse, 2–3 times as wide as long. Metope flat and elongate, disc smooth or densely covered by pustules. Anteclypeus with distinct median

Table 4. Species used in the phylogeny analysis with accession number. “*” denotes new added sequences in this study.

Species	COI	Cytb	Gene 18S (A2–9R)	Gene 28S (D3–D5)	Gene 28S (D6–D7)	Collection
<i>Agalmatium flavescens</i> (Olivier, 1791)	MN194180	MN191521	MN165781	MN266987	MN266956	Russia
<i>Anatolodus musivus</i> Dlabola, 1982	MN194181	–	MN165782	MN266988	MN266957	Turkey
<i>Balduza una</i> (Ball, 1910)	–	MN191522	MN165783	MN266989	MN266958	Mexico
<i>Bootheca taurus</i> (Oshanin, 1870)	MN194182	MN191523	MN165784	MN266990	MN266959	Bulgaria
<i>Bubastia josifovi</i> Dlabola, 1980	–	MN191524	MN165785	MN266991	MN266960	Bulgaria
<i>Bubastia</i> sp.	–	MN191525	MN165786	MN266992	MN266961	Greece
<i>Caloscelis wallengreni</i> Stål, 1863	KX702956	KX702901	KX702855	KX761436	KX702877	China
<i>Celyphoma quadrupla</i> Meng & Wang, 2012	KX702919	KX702906	KX761576	KX761444	KX702806	China
<i>Ceratogerrithus pseudotesellatus</i> (Che, Zhang & Wang, 2007)	KX761502	KX761513	KX761491	KX761532	KX761521	China
<i>Ceratogerrithus spinosus</i> (Che, Zhang & Wang, 2007)	KX761502	KX761513	KX761491	KX761532	KX761521	China
<i>Chontagus longicephalus</i> Zhang, Wang & Che, 2006	KX761460	–	KX650620	KX761450	KX702810	China
<i>Cixius</i> sp.	KR343731	KX702891	JQ982514	KX761413	–	France
<i>Clypeosmilus centrodasus</i> Gnezdilov & Soulier-Perkins, 2017	KX761470	KX761474	KX761575	–	–	Vietnam
<i>Conosimus coelatus</i> Mulsant & Rey, 1855	MN194183	MN191526	MN165787	MN266993	MN266962	France
<i>Dicranotropis hamata</i> (Boheman, 1847)	KX76146	–	KX702837	KX761409	–	Austria
<i>Dictyophana europaea</i> (Linnaeus, 1767)	KJ911190	KX702896	KX702851	KX761427	–	Russia
<i>Euroxenus vayssièresi</i> (Bonfils, Artie & Reynaud, 2001)	–	–	MN165789	MN266995	MN266964	China, Reunion
<i>Eusulasina nantouensis</i> Yang, 1994	HM052838	HM452266	–	–	–	China
<i>Euxalder daweihsanensis</i> sp. nov.*	MK441660	MK441661	–	–	MK441662	China
<i>Euxalder lenis</i> Gnezdilov, Bourgoïn & Wang, 2017	–	–	KX761565	KX761412	–	Vietnam
<i>Falcidius limbatus</i> (A. Costa, 1864)	MN194185	–	MN165790	MN266996	MN266965	Italy
<i>Flavina hainana</i> (Wang & Wang, 1999)	–	KX702912	KX702824	KX761453	MN381846	China
<i>Fortunia</i> sp.	KX761498	KX761509	KX761487	–	KX761518	China
<i>Gerrithoides carinatifrons</i> Schumacher, 1915	KX761555	KX702905	KX761538	–	KX702805	China
<i>Gerrithoides caudospinosus</i> Chen, Zhang & Chang, 2014*	MN171521	MW233581	–	–	MW228374	China
<i>Gerrithoides rugulosus</i> (Melichar, 1906)	HM052835	HM452279	–	–	–	China
<i>Gerrithus frontilongus</i> Meng, Webb & Wang, 2017*	MN171522	MW233582	–	–	MW228375	China
<i>Gerrithus parallelus</i> Che, Zhang & Wang, 2007*	MN171523	MW233583	–	–	MW228376	China
<i>Gerrithus yunnanensis</i> Che, Zhang & Wang, 2007	KX702924	KX702915	KX702831	KX761456	MN381848	China
<i>Gnezdilovius</i> sp.*	MN171524	–	–	–	MW228377	China
<i>Hemisphaerius coccinelloides</i> (Burmeister, 1834)	KX702934	KX702884	KX702834	KX761405	KX702861	Philippines
<i>Hemisphaerius bysantia</i> Fennah, 1978	KX702933	KX702883	KX702833	KX761404	KX702860	Vietnam
<i>Hemisphaerius palaemon</i> Fennah, 1978	KX761497	KX761508	KX761486	KX761526	KX761517	China
<i>Hemisphaerius rufovarivus</i> Walker, 1858	KX702923	KX702913	KX702825	KX761454	KX702812	China
<i>Hemisphaerius</i> sp.	KX761556	KX702885	KX702835	KX761406	KX702862	Laos
<i>Hemisphaerius testaceus</i> Distant, 1906	HM052831	HM452258	–	–	–	China
<i>Hysteropterum dolichotum</i> Gnezdilov & Mazzoni, 2004	–	–	MN165791	MN266997	MN266966	France
<i>Issus coleopratus</i> (Fabricius, 1781)	KX702932	KX761550	KX761568	KX761403	KX761560	France
<i>Issus lauri</i> Ahrens, 1814	–	MN191528	MN165793	MN266999	MN266968	Italy
<i>Kervillea conspurcata</i> (Spinola, 1839)	MN194187	MN191529	MN165794	MN267000	MN266969	Slovenia
<i>Kodaiannela bicinctifrons</i> Fennah, 1956	KX761458	KX702902	KX702814	KX761441	KX702802	China
<i>Kodaiannelus intorques</i> Wang, Bourgoïn & Zhang, 2017	–	KX761472	KX761476	KX761480	KX761482	China
<i>Latematium latifrons</i> (Fieber, 1877)	MN194188	MN191530	MN165795	MN267001	MN266970	Bulgaria

Species	COI	Cytb	Gene 18S (A2–9R)	Gene 28S (D3–D5)	Gene 28S (D6–D7)	Collection
<i>Latilica antalyica</i> (Dlabola, 1986)	–	MN191531	MN165796	MN267002	MN266971	Greece
<i>Latisus dilatatus</i> (Fourcroy, 1785)	–	MN191532	MN165797	MN267003	MN266972	Greece
<i>Macrodaruma pertinax</i> Fennah, 1978	KX702931	KX702882	KX702832	KX761402	KX702859	Vietnam
<i>Macrodaruma</i> sp.	KX702927	KX702881	KX702828	KX761399	KX702857	China
<i>Maculegithus multipunctatus</i> (Che, Zhang & Wang, 2007)	KX702918	KX702904	KX702816	KX761443	KX702804	China
<i>Maculegithus nonomaculatus</i> (Meng & Wang, 2012)	KX761503	KX761514	KX761492	KX761533	KX761522	China
<i>Mongoliana serrata</i> Che, Wang & Chou, 2003	HM052830	HM452272	–	–	–	China
<i>Mongoliana sinuata</i> Che, Wang & Chou, 2003	KX761459	KX702908	KX702820	KX761448	–	China
<i>Mongoliana</i> sp. 2	–	–	KX761566	KX761534	MN381849	China
<i>Mongoliana</i> sp.1	–	MN332233	MN422135	MN381854	–	Thailand
<i>Mongoliana triangularis</i> Che, Wang & Chou, 2003	–	KX761510	KX761561	KX761528	–	China
<i>Mulsantereum maculifrons</i> (Mulsant & Rey, 1855)	KX702928	KX761551	KX761569	KX761400	MN381847	France
<i>Mycterodus drosopouloisi</i> Dlabola, 1982	MN194189	MN191533	MN165798	MN267004	MN266973	Greece
<i>Mycterodus goricus</i> (Dlabola, 1958)	MN194190	MN191534	MN165799	MN267005	MN266974	Greece
<i>Neodurium hamatum</i> Wang & Wang, 2011	KX702920	–	KX702818	KX761446	MN381844	China
<i>Neogergithoides tubercularis</i> Sun, Meng & Wang, 2012	KX761558	KX702910	KX702822	KX761451	MN381845	China
<i>Ophthalmosphaerius trilobulus</i> (Che, Zhang & Wang, 2006)	KX761462	KX702914	KX702826	KX761455	KX702813	China
<i>Palmallicus punctulatus</i> (Rambur, 1840)	KX761462	KX702914	MN165800	MN267006	MN266975	Greece
<i>Proteinissus bilimeki</i> Fowler, 1904	MN194193	MN191537	MN165803	MN267009	MN266978	Greece
<i>Retalard yanitubus</i> sp. nov.	MN381857	MN332232	MN381856	MN381853	MN381851	China
<i>Rhombissus</i> sp.	–	MN332231	MN381855	MN381852	MN381850	China
<i>Sarima bifurca</i> Meng & Wang, 2016	KX702921	KX761552	KX702819	KX761447	KX702808	China
<i>Scorlupaster heptapotamicum</i> Mirjaev, 1971	–	–	–	MN267010	MN266979	Kazakhstan
<i>Scorlupella discolor</i> (Germar, 1821)	–	–	MN165804	MN267011	MN266980	Bulgaria
<i>Tetrica</i> sp.	KX702922	KX702909	KX702821	KX761449	KX702809	China
<i>Thalassana ephialtes</i> (Linnavuori, 1971)	MN194194	MN191538	MN165805	MN267012	MN266981	Turkey
<i>Tingissus guadarramense</i> (Melichar, 1906)	KX702935	KX702886	MN165806	MN267013	MN266982	Portugal
<i>Traxus fulvus</i> Metcalf, 1923	MN194195	MN191539	MN165807	MN267014	MN266983	Mexico
<i>Trypetimorpha occidentalis</i> Huang & Bourgoin, 1993	KX702957	–	KX761546	KX761437	–	Kazakhstan
<i>Tshurshurnella bicolorata</i> Gnezdilov & Oezgen, 2018	MN194196	MN191540	MN165808	MN267015	MN266984	Turkey
<i>Tshurshurnella zelleri</i> (Kirschbaum, 1868)	–	MN191541	MN165809	MN267016	MN266985	Italy
<i>Zopherisca penelopae</i> (Dlabola, 1974)	–	–	MN165810	MN267017	MN266986	Greece

carinae. Forewings with costal margin basally angled and convex below eyes, claval suture developed, venation hazily reticulate, CuP distinct. Hind tibia with 2 lateral spines. Spinal formula of hind leg (7–9)–(6–8)–2. Pygofer with posterior margin distinctly convex. Male anal tube apically enlarged or elongated in dorsal view. Perianthrium asymmetrical.

Distribution. China, Vietnam.

Checklist of *Euxaldar* species

E. dawuishanensis sp. nov. (Southwestern China: Yunnan Province)

- E. guangxiensis* Zhang, Chang & Chen, 2018 (Southeastern China: Guangxi Province)
E. jehucal Fennah, 1978 (Northern Vietnam: Ninh Binh, Ha Noi, Vinh Phuc, Hoa Binh, and Haiphong Provinces)
E. lenis Gnezdilov, Bourgoïn & Wang, 2017 (Southern Vietnam: Lam Dong Province)

Key to male species of *Euxaldar*

Modified from Gnezdilov et al. (2017a) and Zhang et al. (2018).

- 1 Metope smooth. Forewings without coloured bands or spots (Gnezdilov et al. 2017a: fig. 23) ***E. lenis***
 – Metope with a row of distinct pustules along lateral margins. Forewings with coloured bands or spots (Figs 9, 11; Zhang et al. 2018: fig. 5; Gnezdilov et al. 2017a: figs 20, 33) **2**
 2 Metope without median carinae. Metopoclypeal suture incomplete medially. Hind wings rudimentary, shorter than half length of forewings (Zhang et al. 2018: fig. 5) ***E. guangxiensis***
 – Metope with weak median carinae running from upper margin to middle. Metopoclypeal suture complete, straightly, or weakly concave. Hind wings developed, longer than half length of forewings (Gnezdilov et al. 2017a: figs 20, 33) **3**
 3 Coryphe about 3 times as wide as long in the middle. Male anal tube enlarging from base to apical margin and deeply concave at posteromedial part in dorsal view (Gnezdilov et al. 2017a: fig. 6) ***E. jehucal***
 – Coryphe about 4 times as wide as long in middle. Male anal tube elongated in dorsal view, enlarging from base to apical fourth and narrowing at apical part, lateral margins with a triangular process in the upper half on each side (Figs 8, 13) ***E. daweishanensis* sp. nov.**

***Euxaldar daweishanensis* sp. nov.**

<http://zoobank.org/663A901A-6FF8-4BC9-A6B9-C9D1244AAB5B>

Figs 1–26

Type material. *Holotype*: ♂, **China**: Yunnan Province, Pingbian County, Mt: Daweishan National Nature Reserve (23°07'N, 103°20'E), 8 August, 2017, Qiang Luo, Nian Gong, Y.-J Sui, Yan Zhi. *Paratypes*: 7♂♂ 36♀♀, same data as holotype.

Measurements. Total length (from apex of coryphe to tip of forewing): male 4.1–4.3 mm ($N = 6$), female 4.6–4.9 mm ($N = 10$); forewing length: male 3.8–4.0 mm ($N = 7$), female 4.2–4.4 mm ($N = 10$).

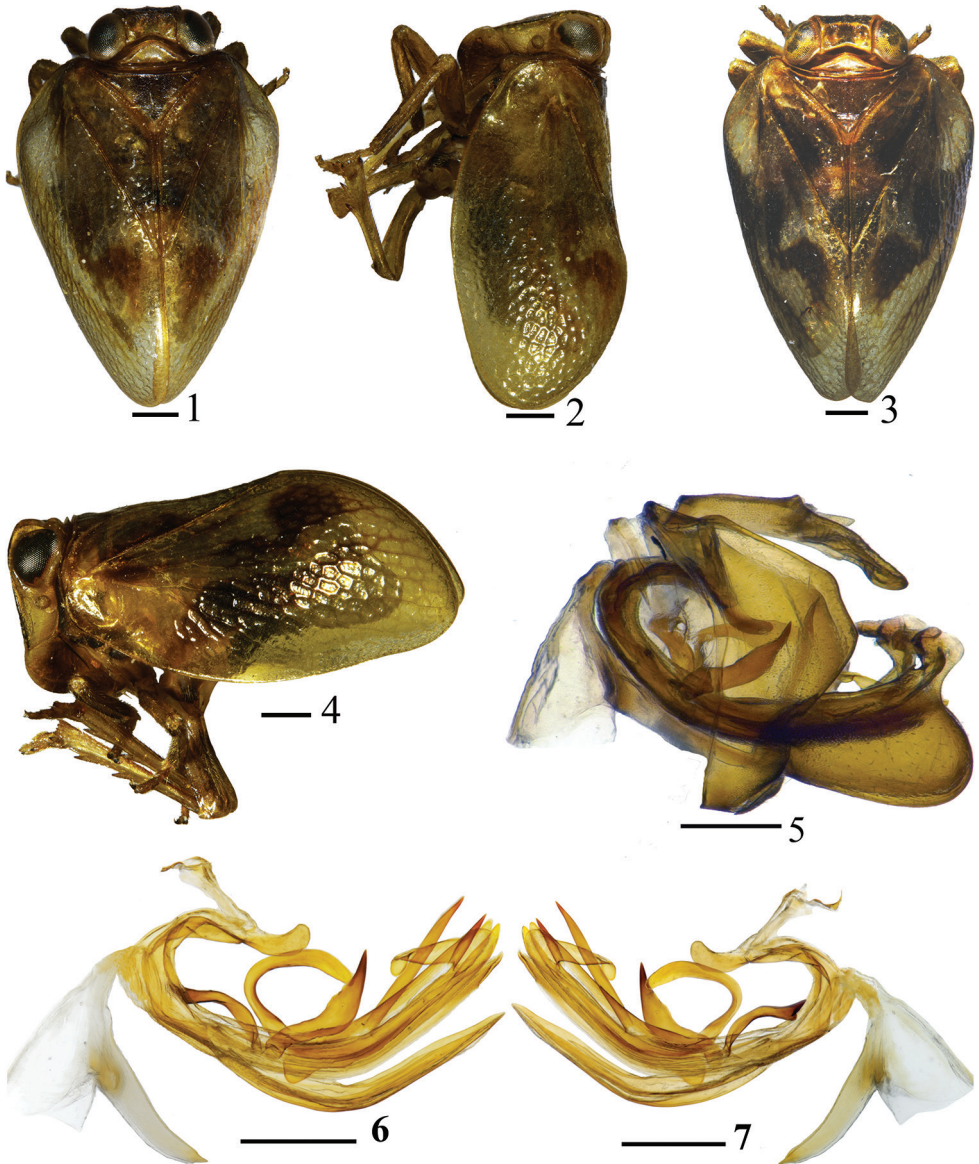
Diagnosis. This species differs from other *Euxaldar* species by the following characters: (1) coryphe about 2.3 times wider than long (less, or more than 2.3 times as wide as long in other species of *Euxaldar*); (2) first metatibiotarsal of hind leg with 8 intermediate spines (other species of *Euxaldar* with first metatarsomere of hind leg

with 6 or 7 intermediate spines); (2) penis with 3 different ribbon-shaped processes at middle (Figs 16, 17, pp, paed), dorsal lobe of periandrium with 2 asymmetrical sword-shaped subapical processes in apical half (Figs 16, 17, sap) (other species without sword-shaped subapical processes in apical half of dorsal lobe of periandrium).

Coloration. Male body brown yellowish, with irregular dark brown bands on forewings. Coryphe brown (Fig. 8). Metope with all margins, pustules, and median carinae pale yellow, disc dark brown (Fig. 9). Metopoclypeal suture light yellow. Anteclypeus straw yellow. Postclypeus pale yellow (Figs 9, 10). Rostrum and antenna straw yellow (Fig. 10). Eyes dark brown (Figs 8–10). Pronotum straw yellow. Mesonotum dark brown (Fig. 8). Forewings slightly hyaline, with 2 irregular brown bands (Figs 1, 2, 11): a large one derived from costal margin to almost C2 of radial cell, small one derived from apical half of median cell, extended to areola postica (anterior cubital area). Legs (Figs 2, 4) light brown. Abdomen brown, male genital segment light straw yellow. Females generally darker than males (Figs 3, 4).

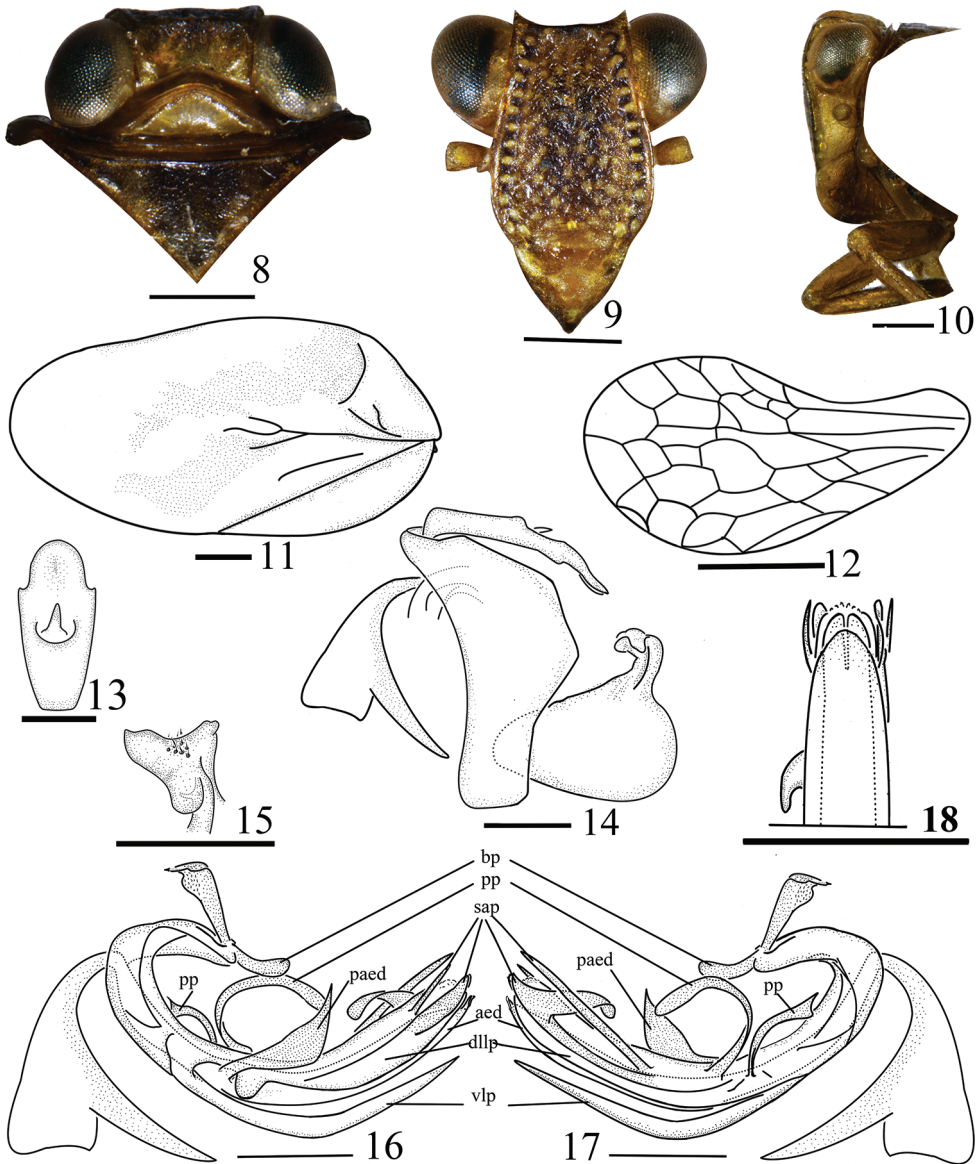
Head and thorax. Coryphe transverse, about 2.3 times wider than long, anterior margin weakly prominent in the middle, posterior margin angularly concave (Fig. 8). Metope flat, median carinae weak, running from upper margin and reaching middle, with a row of distinct pustules along lateral margins, disc with weak pustules (Fig. 9). Metopoclypeal suture complete (Fig. 9). Anteclypeus with distinct median carinae (Figs 9, 10). Pronotum with disc depressed (Fig. 8). Mesonotum about 2.1 times longer than pronotum. Forewings (Figs 1–4, 11) with distinct claval suture and CuP venation, the other venation reticulate, poorly recognizable. Hind wings about 0.7 times as long as forewings, venation reticulate (Fig. 12). Hind tibiae with 2 lateral teeth. Metatibiotarsal formula (9–8)–8–2.

Male genitalia. Anal tube (Fig. 13) enlarging from base to apical fourth in dorsal view, narrowing to apex, apical margin convex in the middle, laterally with 2 small triangular processes in apical fourth. Pygofer with hind margin distinctly convex (Figs 5, 14). Gonostyli triangular, hind margin convex, caudo-dorsal angle rounded (Fig. 14). Capitulum of gonostyli style with wide and short neck, with a wide lateral tooth and 2 apical teeth (Figs 14, 15). Corpus of connective rod-like (Figs 5–7, 16, 17), curved, cuticularized, reaching middle of periandrium; tectiductus of connective cup-shaped, third ventral part separated from corpus (Fig. 14). Periandrium asymmetrical (Figs 6, 7, 16, 17), suspensorium V-shaped in dorsal view, membranaceous in the middle; base with process claval (Figs 16, 17, bp), dorsal periandrium lobe with 2 ribbon-like processes in center near right edge (Figs 16, 17, pp), directed dorsad, respectively curved caudad and cephalad; dorsal lobe in left lateral view with 2 subapical processes near apex (Fig. 16, sap): one crescent-shaped, above base with another process shortly sword-shaped, directed caudad; in right lateral view (Fig. 17, sap) with two subapical processes derived from apical third, directed apically, one process base movable, sword-shaped, below base another process crutch-like and sclerotized. Ventral periandrium lobe (Fig. 18, vlp) with apical margin convex, shorter than dorso-lateral lobe of periandrium (Figs 16, 17, dllp, 18) in ventral view. Aedeagus (Figs 16, 17, aed) with dagger-shaped process, base slightly movable, directed dorsad, slightly inclined caudad (Figs 16, 17, paed).



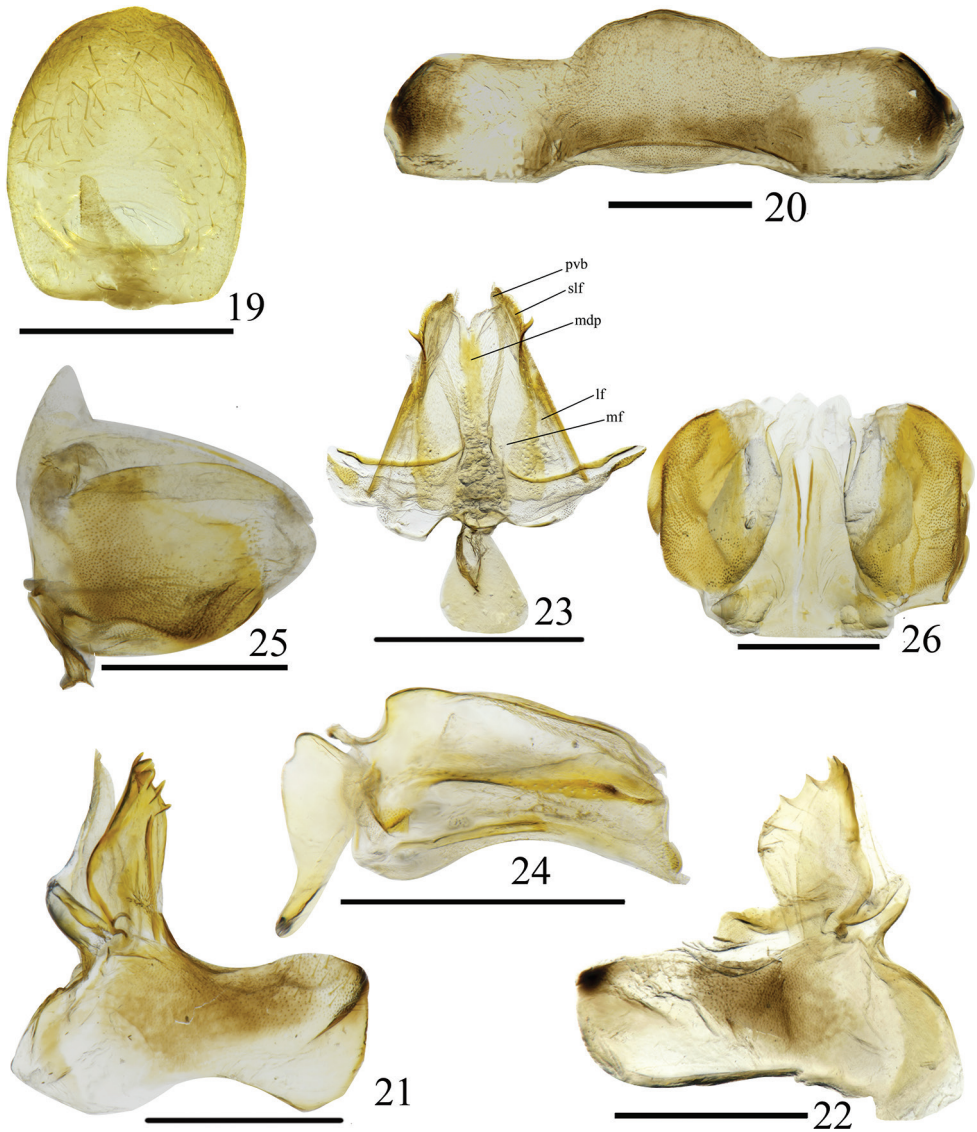
Figures 1–7. *Euxaldar daweshanensis* sp. nov. (adult) **1** male dorsal view **2** male lateral view **3** female dorsal view **4** female lateral view **5** male genitalia, lateral view **6** penis, left lateral view **7** penis, right lateral view. Scale bars: 0.5 mm.

Female genitalia. Anal tube ovate in dorsal view, about 1.3 times longer than maximal width at second part (Fig. 19). Anal style long, located at basal fifth of anal tube. In ventral view, Sternite VII with hind margin convex medially, without any process in ventral view, disc arched ventrad (Fig. 20). Anterior connective lamina of gonapophysis VIII nearly rectangular, with 3 or 4 apical teeth on inner lateral margin and 3 lateral teeth bearing 3 keels on outer lateral margin (Figs 21, 22); endogonocoxal



Figures 8–18. *Euxaldar daweishanensis* sp. nov. (male adult) **8** head and thorax, dorsal view **9** face, front view **10** head and thorax, lateral view **11** forewings **12** hind wing **13** anal tube, dorsal view **14** pygofer, anal tube and genital style, lateral view **15** capitulum of gonostyli, dorsal view **16** penis, lateral view (left) **17** penis, lateral view (right) **18** penis, ventro-apical view. Abbreviations: **aed**—aedeagus; **bp**—basal process of the periandrium; **dllp**—dorso-lateral lobe of periandrium; **paed**—process of aedeagus; **pp**—process of periandrium; **sap**—subapical processes of periandrium; **vlp**—ventral lobe of periandrium. Scale bars: 0.5 mm

lobe developed, membranous in distal part (Figs 21, 22). Posterior connective lamina of gonapophyses IX triangular in dorsal view (Fig. 23), narrowing; median field with leaf-like process bearing apical margin, deeply incised in the middle (Fig. 23, mdp);



Figures 19–26. *Euxaldar dawweishanensis* sp. nov. (female adult) **19** female anal tube, dorsal view **20** sternite VII, ventral view **21, 22** gonocoxa VIII and gonapophysis VIII, ventral view **23** gonapophysis IX and gonaspiculum bridge, dorsal view **24** gonapophysis IX and gonaspiculum bridge, lateral view **25** gonoplacs, lateral view **26** gonoplacs, dorsal view Abbreviations: **lf**–lateral field of posterior connective lamina of gonapophyses IX; **mdp**–medial dorsal process; **mf**–medial field of posterior connective lamina of gonapophyses IX; **pvd**–posterior ventral lobes; **slf**–sublateral field of posterior connective lamina of gonapophyses IX. Scale bars: 0.5 mm.

lateral field (Fig. 23, lf) without obvious process; distal parts of laminae (Fig. 23, slf) with tooth-like process on each lateral margin; posterior ventral lobes bent at slender angle (Figs 23, pvb, 24). Gonoplacs in lateral view irregularly elliptical (Fig. 25), without carinae, with apical half fused, apical margin membranous (Fig. 26).

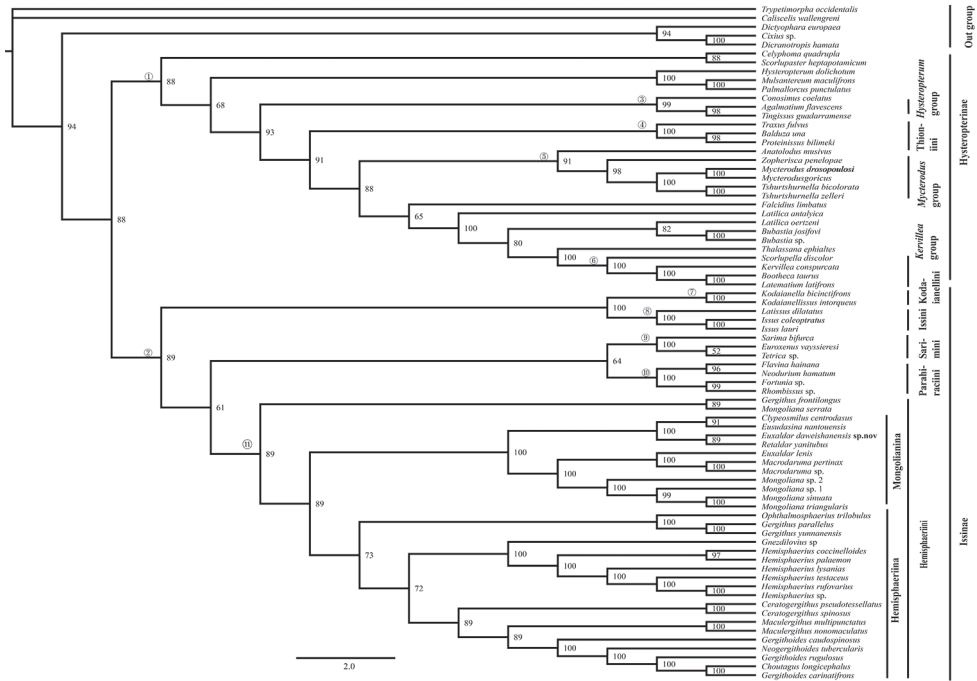


Figure 28. Bayesian 50% consensus tree based on combined dataset. Nodes of the major clades are numbered and refer to text. Each node is documented with its posterior probability (PP) value.

1906 sensu (Gnezdilov et al. 2020) and Issinae Spinola, 1839 sensu (Gnezdilov et al. 2020) are both recovered (nodes 1 and 2: ML: 47, 67; BI: 88, 89, respectively).

Node 1 includes almost all tribal level genera group of the subfamily Hysteropterinae sensu Gnezdilov (2016a, b, 2020) and the tribe Thioniini Melichar, 1906 sensu (Gnezdilov 2018): 1) Node 4 (ML: 75, BI: 100) corresponds to the subtribe Thioniina sensu Gnezdilov (2018) with the inclusion of American taxa, characterized by hind wings reduced or rudimentary, A2 vein branched; 2) Nodes 5 and 6 corresponds to the monophyletic *Kervillea*, and *Mycterodus* genera group sensu Gnezdilov (2016 a, b); monophyly of the *Hysteropterum* genera group was not supported by this analysis (node 3).

Node 2 (ML: 67, BI: 89) includes five monophyletic tribes (nodes 7–11): Issinae, Kodaianellini and Hemisphaeriini sensu (Gnezdilov 2020), Parahiraciini, and Sarimini sensu (Wang et al. 2016), while the monophyly of Sarimini and Parahiraciini was not supported by Gnezdilov (2020).

Discussion

According to our analysis, the tribe Thioniini was recovered as monophyletic, split from the subfamily Issinae sensu Gnezdilov et al. (2020), and placed in the subfamily

Hysteropterinae sensu Gnezdilov et al. (2020). Herein, we suggest that the subtribe Thioniina sensu Gnezdilov et al. (2020) should be a tribe of Hysteropterinae (Thioniini + tribal level groups of genera (Gnezdilov 2016a, b)), sharing the common characteristic of this subfamily: hind wings reduced or rudimentary. Conversely, most taxa of the subfamily Issinae Spinola, 1839 sensu Gnezdilov et al. (2020) have developed hind wings. The Issinae, including five tribes distributed in the Oriental Region, is recovered and well supported in the following topology (node 2): [(Kodaianellini, Issini) + (Sarimini, Parahiraciini) + Hemisphaeriini].

The monophyletic tribe Hemisphaeriini Melichar, 1906 is confirmed by our data, characterized by hemispherical forewings and single-lobed or rudimentary hind wings (Gnezdilov et al. 2020). The monophyly of the subtribes Hemisphaeriina and Mongolianina Wang et al. (2016) is not supported: the genus *Gergithus* shows a sister relationship with (Hemisphaeriina + Mongolianina) in this analysis (ML: 97, BI: 89).

Mongoliana serrata Che, Wang & Chou, 2003 is isolated from *Mongoliana* Distant, 1909 (ML:58, BI:89), confirming the hypothesis of Meng et al. (2017) that the genus *Mongoliana* could be divided into two species groups. It probably contains two different genera: one of them *M. serrata* is a new genus with the smooth frons, pale brown tegmina having dark fasciae and spots and the ventral hooks of the aedeagus variable in shape and usually unparallel. *Gergithus yunnanensis* and *G. parallelus* show a sister relationship with *Ophthalmosphaerius* Gnezdilov, 2017, probably belonging to a new genus with *Ophthalmosphaerius*; this finding agrees with Gnezdilov (2017c) and Zhao et al. (2019), but we still consider it incertae sedis until more evidence is presented.

The third lineage of Mongolianina (Zhao et al. 2019) is recovered only in our ML analysis. *Euxaldar daweshanensis* sp. nov. and *E. lenis* are grouped into a different cluster in our research: the genera of the cluster ((*E. daweshanensis* sp. nov. + *Retaldar*) + (*Clypeosmilus* + *Eusudasina*)) share a protruded clypeus, and forewings CuP clear; another cluster (*E. lenis* + *Macrodaruma*) recovered by Zhao et al. (2019) share a smooth metope without pustules, and sexual dimorphism. *Euxaldar lenis* probably belongs to a new genus.

Euxaldar is similar to the genus *Paramongoliana* Chen, Zhang & Chang, 2014 which is here formally placed in the subtribe Mongolianina according to Wang et al. (2016), but differs by the following characters: metope smooth or with pustules (metope roughly corrugated, without pustules in *Paramongoliana*, see Chen et al. 2014: figs 2–33E); forewings with CuP distinct (forewings with CuP poorly recognizable in *Paramongoliana*, see Chen et al. 2014: figs 2–33A, B, F); anal tube with apical margin not straight (anal tube nearly quadrilateral, apical margin straight in *Paramongoliana*, see Chen et al. 2014: figs 2–33H).

The genus *Euxaldar* is also similar to the genus *Clypeosmilus* (Gnezdilov et al. 2017b) in having forewings with reticulate venation and a distinct claval suture, but can differ from the latter in the following characters: postclypeus with complete median carina and anteclypeus with distinct median carina (*Clypeosmilus* with postclypeus large, flattened laterally, bearing a thick chisel-like median carina); perianthrium asymmetrical (perianthrium symmetrical, with pair of long and narrow subapical processes directed apically).

Euxaldar dawuishanensis sp. nov., *E. jehucal*, and *E. guangxiensis* share several compelling characters: 1) *E. dawuishanensis* sp. nov., *E. jehucal*, and *E. guangxiensis* share a metope disc with relatively weak pustules distributed in a row along the lateral margins; and 2) *E. dawuishanensis* sp. nov. and *E. guangxiensis* have an anal tube with a triangular process on each lateral margin (Fig. 13; Zhang et al. 2018: figs 12, 13). Other noteworthy characters: 1) *E. guangxiensis* exhibits a vestigial hind wing; 2) *E. lenis* has a smooth metope without pustules, and sexual dimorphism. All species of this genus probably belong to different species groups or even different genera. More molecular data and other convincing morphological evidence are expected in the future, enabling further discussion of the taxonomic status of *Euxaldar*.

Acknowledgements

We thank Dr V. M Gnezdilov for proofreading the manuscript. This work was supported by the National Natural Science Foundation of China (No. 31601886), the Program of Science and Technology Innovation Talents Team, Guizhou Province (No. 20144001), the Program of Excellent Innovation Talents, Guizhou Province (No. 20154021), the Science and Technology Project of Guiyang (No. 2017525), the Program of Science and Technology Program in Guizhou Province (No. 20177267) and the New Academic Seedlings Cultivation and Innovation Exploration Special Project of Guizhou University (No. 20175788).

References

- Anufriev GA, Emeljanov AF (1988) Cicadinea (Auchenor rhyncha). In: Lehr PA (Ed.) Key to the insects of the Far East of the USSR, 2. Leningrad, Nauka, 12–495.
- Belshaw R, Quicke DLJ (2002) Robustness of ancestral state estimates: evolution of life history strategy in ichneumonoid parasitoids. *Systematic Biology* 51: 450–477. <https://doi.org/10.1080/10635150290069896>
- Bourgoin T (1987) A new interpretation of the homologies of the Hemiptera male genitalia, illustrated by the Tettigometridae (Hemiptera, Fulgoromorpha). Proceedings of the 6th Auchenorrhyncha Meeting, Turin (Italy), September 1987, 113–120.
- Bourgoin T (1993) Female genitalia in Hemiptera Fulgoromorpha, morphological and phylogenetic data. *Annales de la Société Entomologique de France* 29(3): 225–244.
- Bourgoin T, Steffen-Campbell JD, Campbell BC (1997) Molecular phylogeny of Fulgoromorpha (Insecta, Hemiptera, Archaeorrhyncha) the enigmatic tettigometridae: evolutionary affiliations and historical biogeography. *Cladistics-the International Journal of the Willi Hennig Society* 13(3): 207–224. <https://doi.org/10.1111/j.1096-0031.1997.tb00316.x>
- Bourgoin T, Wang RR, Asche M, Hoch H, Soulier-Perkins A, Stroiński A, Yap S, Szvedo J (2015) From micropterism to hyperpterism: recognition strategy and standardized homol-

- ogy driven terminology of the forewing veins patterns in planthoppers (Hemiptera: Fulgoromorpha). *Zoomorphology* 134(1): 63–77. <https://doi.org/10.1007/s00435-014-0243-6>
- Chan ML, Yang CT (1994) Issidae of Taiwan (Homoptera: Fulgoroidea). Chen Chung Book, Taichung, 188 pp.
- Chang ZM, Yang L, Zhang ZG, Chen XS (2015) Review of the genus *Neotetricodes* Zhang et Vhen (Hemiptera: Fulgoromorpha: Issidae) with description of two new species. <https://doi.org/10.11646/zootaxa.4057.3.2>
- Clary DO, Wolstenholme DR (1985) The mitochondrial DNA molecule of *Drosophila yakuba*: nucleotide sequence, gene organization, and genetic code. *Journal of Molecular Evolution* 22(3): 252–271. <https://doi.org/10.1007/BF02099755>
- Chen XS, Zhang ZG, Chang ZM (2014) Issidae and Caliscelidae (Hemiptera: Fulgoroidea) from China. Guizhou Science and Technology Publishing House, Guiyang, 242 pp.
- Cryan JR, Wiegmann BM, Deitz LL, Dietrich CH (2000) Phylogeny of the treehoppers (Insecta: Hemiptera: Membracidae): evidence from two nuclear genes. *Molecular Phylogenetics & Evolution* 17(2):317–334. <https://doi.org/10.1006/mpev.2000.0832>
- Fennah RG (1978) Fulgoroidea (Homoptera) from Vietnam. *Annales Zoologici* 34(9): 207–279.
- Gnezdilov VM (2003) Review of the family Issidae (Homoptera, Cicadina) of the European fauna, with notes on the structure of ovipositor in planthoppers. *Chteniya pamyati NA Kholodkovskogo [Meetings in memory of NA Cholodkovsky]*, St. Petersburg 56(1): 1–145. [In Russian with English summary]
- Gnezdilov VM, Constant J (2012) Review of the family Issidae (Hemiptera: Fulgoromorpha) in Vietnam with description of a new species. *Annales Zoologici* 62(4): 571–576. <https://doi.org/10.3161/000345412X659632>
- Gnezdilov VM (2013) Modern classification and the distribution of the family Issidae Spinola (Homoptera, Auchenorrhyncha, Fulgoroidea). *Entomologicheskoe obozrenie* 92(4): 724–738. [English translation published in *Entomological Review* 94(5): 687–697.] <https://doi.org/10.1134/S0013873814050054>
- Gnezdilov VM (2016a) Planthoppers of the family Issidae (Hemiptera, Fulgoroidea) of Western Palaearctic. Thesis of Doctoral Dissertation (Dr. Sci. habilitation), St.-Petersburg, 44 pp. [In Russian]
- Gnezdilov VM (2016b) Notes on phylogenetic relationships of planthoppers of the family Issidae (Hemiptera, Fulgoroidea) of the Western Palaearctic fauna, with description of two new genera. *Entomologicheskoe Obozrenie* 95(2): 362–382. [In Russian] [English translation published in *Entomological Review* (2016) 96(3): 332–347] <https://doi.org/10.1134/S0013873816030106>
- Gnezdilov VM, Bourgoin T, Wang ML (2017a) Revision of the Genus *Euxaldar* Fennah, 1978 (Hemiptera: Fulgoroidea: Issidae). *Annales Zoologici* 67(1): 13–20. <https://doi.org/10.3161/00034541ANZ2017.67.1.002>
- Gnezdilov VM, Soulier-Perkins A (2017b) *Clypeosmilus centrodasus* gen. et sp. nov., a new genus and species of family Issidae (Hemiptera: Fulgoroidea) from Northern Vietnam. *Proceedings of the Zoological Institute RAS* 321(1): 25–31.

- Gnezdilov VM (2017c) Addenda to the revisions of the genera *Gergithus* Stål and *Hemisphaerius* Schaum (Hemiptera, Auchenorrhyncha, Fulgoroidea, Issidae). *Entomological Review* 97(9): 1338–1352. <https://doi.org/10.1134/S0013873817090123>
- Gnezdilov VM (2018) To the revision of the genus *Thionia* Stål (Hemiptera, Fulgoroidea, Issidae), with description of new genera and new subtribe. *Zootaxa* 4434(1): 158–170. <https://doi.org/10.11646/zootaxa.4434.1.10>
- Gnezdilov VM, Konstantinov FV, Bodrov SY (2020) New insights into the molecular phylogeny and taxonomy of the family Issidae (Hemiptera: Auchenorrhyncha: Fulgoroidea). *Proceedings of the Zoological Institute RAS* 324(1): 146–161. <https://doi.org/10.31610/trudyzin/2020.324.1.146>
- Lanfear R, Frandsen PB, Wright AM, Senfeld T, Calcott B (2017) PartitionFinder 2: New Methods for Selecting Partitioned Models of Evolution for Molecular and Morphological Phylogenetic Analyses. *Molecular Biology Evolutionary* 34(3): 772–773. <https://doi.org/10.1093/molbev/msw260>
- Ronquist F, Huelsenbeck J, Teslenko M (2011) MrBayes version 3.2 Manual: Tutorials and Model Summaries. http://mrbayes.sourceforge.net/mb3.2_manual.pdf
- Wang ML, Zhang Y, Bourgoin T (2016) Planthopper family Issidae (Insecta: Hemiptera: Fulgoromorpha): linking molecular phylogeny with classification. *Molecular Phylogenetics and Evolution* 105: 224–234. <https://doi.org/10.1016/j.ympev.2016.08.012>
- Meng R, Webb MD, Wang YL (2017) Nomenclatural changes in the planthopper tribe Hemisphaeriini (Hemiptera: Fulgoromorpha: Issidae), with the description of a new genus and a new species. *European Journal of Taxonomy* 298: 1–25. <https://doi.org/10.5852/ejt.2017.298>
- Zhang ZG, Chang ZM, Chen XS (2018) A new species of the genus *Euxaldar* Fennah, 1978 from China (Hemiptera, Fulgoroidea, Issidae). *ZooKeys* 781: 51–58. <https://doi.org/10.3897/zookeys.781.27059>
- Zhao S, Bourgoin T, Wang M (2019) The impact of a new genus on the molecular phylogeny of Hemisphaeriini (Hemiptera, Fulgoromorpha, Issidae). *ZooKeys* 880: 61–74. <https://doi.org/10.3897/zookeys.880.36828>

Appendix I

Partitions and models used for the Maximum likelihood tree in IQtree and Bayesian 50% consensus tree.

```
#nexus
```

```
begin sets;
```

```
  charset Subset1 = 1–1899;
```

```
  charset Subset2 = 1900–2617;
```

```
  charset Subset3 = 2618–3473;
```

```
  charset Subset4 = 3474–4194;
```

```
  charset Subset5 = 4195–4861;
```

```
charpartition PartitionFinder = GTR+I+G: Subset1, GTR+I+G: Subset2,  
GTR+I+G: Subset3, GTR+G: Subset4, GTR+I+G: Subset5;  
end;  
  
begin mrbayes;  
log start filename = log.txt;  
outgroup Caliscelis wallengreni;  
outgroup Cixius sp;  
outgroup Dicranotropis hamata;  
outgroup Dictyophara europaea;  
outgroup Trypetimorpha occidentalis;  
charset Subset1 = 1–1941;  
  charset Subset2 = 1942–2732;  
  charset Subset3 = 2733–3576;  
  charset Subset4 = 3577–4302;  
  charset Subset5 = 4303–4929;  
  
partition PartitionFinder = 5: Subset1, Subset2, Subset3, Subset4, Subset5;  
set partition = PartitionFinder;  
  
lset applyto = (1) nst = 6 rates = invgamma;  
lset applyto = (2) nst = 6 rates = invgamma;  
lset applyto = (3) nst = 6 rates = invgamma;  
lset applyto = (4) nst = 6 rates = invgamma;  
lset applyto = (5) nst = 6 rates = invgamma;  
  
prset applyto = (all) ratepr = variable revmatpr = dirichlet (1, 1, 1, 1, 1, 1) statefreqpr  
  = dirichlet (1, 1, 1, 1);  
unlink statefreq = (all) revmat = (all) shape = (all);  
  mcmcp ngen = 30000000 nruns = 2 relburnin = yes burninfrac = 0.25 printfreq =  
  1000 samplefreq = 1000 nchains = 4 savebrlens = yes;  
  mcmc;  
  sumt;;  
end;
```


Description of a new species of the genus *Ameletus* Eaton, 1885 (Ephemeroptera, Ameletidae) from Yunnan, China

Xianfu Li^{1,2,3}, Yanping Luo⁴, Jian Jiang⁴, Lili Wang⁴, Xiaoli Tong^{2,4}

1 Institute of Eastern-Himalaya Biodiversity Research, Dali University, Dali 671000, Yunnan, China **2** Collaborative Innovation Center for Biodiversity and Conservation in the Three Parallel Rivers Region of China, Dali University, Dali, Yunnan, China **3** The Provincial Innovation Team of Biodiversity Conservation and Utility of the Three Parallel Rivers Region from Dali University, Dali, Yunnan, China **4** Department of Entomology, College of Plant Protection, South China Agricultural University, Guangzhou 510642, Guangdong, China

Corresponding author: Xiaoli Tong (xtong@scau.edu.cn)

Academic editor: Ben Price | Received 22 October 2020 | Accepted 22 January 2021 | Published 1 March 2021

<http://zoobank.org/1A3C9B28-F0EA-4CAA-BE25-83CE7A6C763A>

Citation: Li X, Luo Y, Jiang J, Wang L, Tong X (2021) Description of a new species of the genus *Ameletus* Eaton, 1885 (Ephemeroptera, Ameletidae) from Yunnan, China. ZooKeys 1021: 37–51. <https://doi.org/10.3897/zookeys.1021.59927>

Abstract

A new species with primitive characteristics, *Ameletus daliensis* Tong, **sp. nov.**, is described, based on the morphology of imago, larva and egg with molecular data of the mitochondrial COI from Mount Cangshan, Dali, China. The new species is closely related to one of the most primitive mayflies, *Ameletus primitivus* Traver, 1939, by sharing persistent mouthparts in the alate stage, but it can be distinguished from the latter by the morphological differences of the mouthpart remains, wings and genitals in the imaginal stage. Both morphological and molecular evidence support that *A. daliensis* Tong, **sp. nov.** is a new member of the genus *Ameletus*. The discovery of the new species could help understand the origin and evolution of the genus *Ameletus*.

Keywords

COI, integrative taxonomy, Kimura 2-parameter, Mayfly, southwest China

Introduction

Ameletus Eaton, the largest genus of the family Ameletidae, is distributed in the Nearctic, Palearctic and Oriental Regions. The vast majority of the species of the genus are typical cold-water species and usually inhabit cold streams at mid-high latitude areas. Currently, *Ameletus* species are most diverse in the Nearctic Region with thirty-five species (Zloty 1996; Zloty and Pritchard 1997; Zloty and Harper 1999; Kondratieff and Meyer 2010). In the Palearctic Region, most species are distributed intensively in the East Palearctic areas, for example, about 12 species are known from the Russian Far East (Kluge 2007; Tiunova 2013; Tiunova et al. 2017), six species from Japan (Ishiwata 2001) and two species are reported from Korea (Bae and Yoon 1997). However, only four species are recorded from the Oriental Region (Traver 1939; Kang and Yang 2014). In China, *Ameletus* species have been paid little attention, with, so far, only five species being recorded: *A. costalis* (Matsumura) and *A. montanus* Imanishi are reported from north-eastern China (Quan et al. 2002); *A. atratus* Kang & Yang, *A. formosus* Kang & Yang and *A. montivagus* Kang & Yang are described from Taiwan, based on the larval stage (Kang and Yang 1994). During our recent survey on mayfly fauna of southwest China, many unknown species of *Ameletus* in the larval stage have been found, which suggests that the species diversity of *Ameletus* in the country is likely highly underestimated. Amongst them, an undescribed species was determined, based on larval and imaginal stages associated with laboratory rearing. Here, we describe this new *Ameletus* species by integrated approaches, including descriptions of imago, larva and egg and DNA sequence analysis (COI, Kimura 2-parameter).

Materials and methods

The specimens in this study were collected from Mount Cangshan, Dali City, Yunnan Province, China (Fig. 1). Mt. Cangshan, with 18 nearly parallel mountainous streams, is located at the southern end of the lofty Qinghai-Tibet Plateau and the southernmost mountain in Asia reached by the latest glaciation period. The summit of Mt. Cangshan reaches 4122 m a.s.l., the elevation of our collecting sites being between 2000 and 2250 m. The regional climate is influenced by plateau monsoons, being characterised by wet (May to October) and dry (November to April) seasons. The mean annual precipitation is 1683 mm, which is the major source of stream flow, while snow melt in the dry season is the minor source (Chiu et al. 2020).

The larvae were collected with a D-frame net from two small streams (Heilong and Mocan) in Mt. Cangshan, some of the larvae were then directly placed into vials containing 90% ethanol in the field, the mature larvae with black wing pads were selected for transportation to artificial rearing cages in situ (Figs 40, 41) and some larvae were taken back to the laboratory for rearing individually. Photographs were taken using a Canon EOS 5D Mark IV camera with MP-E 65 mm macro lens and a digital microscope (Keyence VHX-5000). Slide-mounted specimens were examined and photographed under the microscope with a digital camera attached. Some specimens

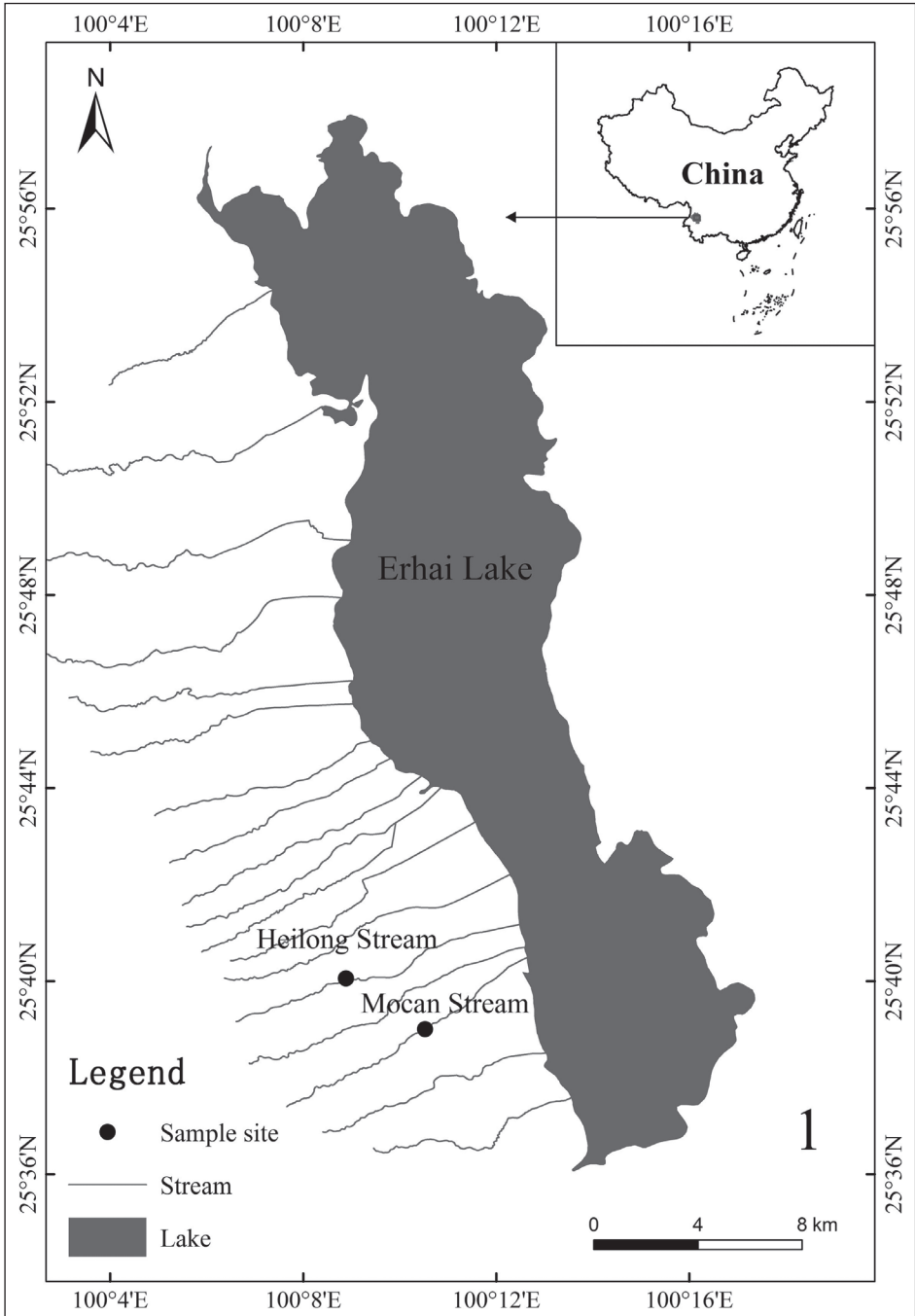


Figure 1. Map of collecting sites.

were dissected under the stereomicroscope and were mounted on slides with Hoyer's Solution for examination under the microscope. The map of the sampling sites (Fig. 1) is made in QGIS Standalone Installer Version 3.10 and the DEM data pixel is 30 m

provided by Geospatial Data Cloud site, Computer Network Information Center, Chinese Academy of Sciences (<http://www.gscloud.cn>). The holotype (mature male larva) and two paratypes (male imago and female larva) are deposited in the Museum of Biology, Institute of Eastern-Himalaya Biodiversity Research, Dali University (MBDU); the remaining paratypes are deposited in the Insect Collection, South China Agricultural University (SCAU), Guangzhou, China.

Total genomic DNA was extracted from the legs of larva using the TIANamp Genomic DNA Kit (TIANGEN, Beijing, China) according to the manufacturer's protocol. The cytochrome c oxidase subunit I (COI) gene was amplified by the universal primers LCO1490-JJ/HCO2198-JJ to obtain a 658 bp fragment corresponding to the DNA barcoding region (Astrin and Stüeben 2008). Polymerase chain reaction (PCR) conditions were referred to Wesener (2015). The COI sequence was assembled by SeqMan (DNASTAR, Inc). Sequence alignments were performed by the Mafft (codon) algorithm, then optimised with MACSE (Katoh and Standley 2013; Ranwez et al. 2018; Zhang et al. 2020). The Kimura 2-Parameter distances between sequenced species were calculated by MEGA 7.0 with default setting (Kumar et al. 2016).

Results

Morphological taxonomy

Ameletus daliensis Tong, sp. nov.

<http://zoobank.org/C2F34991-74B7-4842-8557-F97F6FEE5578>

Figs 2–39

Material examined. *Holotype*: male mature larva (in ethanol, deposited in BMDU), CHINA, Yunnan Province, Dali City, Mt. Cangshan, Mocan Stream (2020 m a.s.l.), 15.v.2020, coll. Xianfu Li. *Paratypes* (in ethanol, one male imago reared from larva and one larva are deposited in BMDU, the remaining in SCAU): 14 larvae and two imagos reared from larvae with same data as holotype; 20 larvae, one female sub-imago and one male imago reared from larvae, Yunnan, Dali City, Mt. Cangshan, Heilong Stream (2220 m a.s.l.), 1.v.2018, coll. Xianfu Li; one male sub-imago, Dali City, Mt. Cangshan, Heilong Stream, 28.v.2019, coll. Xianfu Li.

Diagnosis. *Larva* has the following combination of characters: 1) body with contrasting colour pattern; 2) labrum ventrally bordered with row of dense feathered setae (rare bi-forked setae) along anterior margin; 3) inner margin of trochanter in hind leg bearing row of brush-like fine and dense setae; 4) abdominal tergites I–X each with pointed spines on posterior margin; sternites without any spines on posterior margin, except V–VIII with tiny spines laterally; sternite IX with deep V-shaped cleft in both sexes. *Sub-imago*. 1) labial and maxillary palpi present and clearly visible; 2) wings semi-transparent, all cross-veins bordered around by dark brown. *Imago*. 1) labial and maxillary palpi present, but vestigial; 2) forewing transparent, MP2 turns downwards



Figures 2, 3. Larval habitus of *Ameletus daliensis* Tong, sp. nov. **2** dorsal view (upper: female; lower: male) **3** ventral view (upper: female; lower: male).

to meet CuA, stigmatic area suffused with milky and divided by a longitudinal vein; hind wings hyaline with short costal projection near the base; 3) genital forceps dark brown, apices of lobes round and slightly bent inwardly, ventral plates absent.

Description. Mature larva (in ethanol) (Figs 2, 3). Body length 14 (12.5–15.0) mm; cerci 7 (6.0–7.5) mm. Head brown, except ocelli pale. Eyes blackish-grey. Antenna brown dorsally at base, flagellum light brown. Clypeus brown; labrum mainly brown with two longitudinal dark brown stripes submedially. Pronotum dark brown with light brown irregular markings and one pale mesal line, meso- and metanotum brown with some irregular dark brown streaks and markings. Legs largely brown, except femora with pale patches on sub-basal and sub-distal areas, tarsi dark brown near apex. Abdominal tergites with contrasting colour pattern, tergite I white with diffuse light brown in a form of triangle medially, tergites II–III and VI–VII white, each with pair of diffuse light brown longitudinal bends sub-medially, tergites IV–V and VIII–IX mainly brown, each with longitudinal pale stripe medially, tergite X white with brown along posterior margin and pair of longitudinal light brown streaks; tergites II–IX each

with pair of dark brown oblique stripes sub-medially and pair of dark brown stripes on sides; abdominal sternites brown, except sternites I, VI, VII and IX paler; sternites II–VIII each with ganglionic marking medially (Fig. 3), II–IX each with pair of small pale spots on anterolateral corners. Generally, the above colour pattern can change slightly in intensity, depending on the life stage.

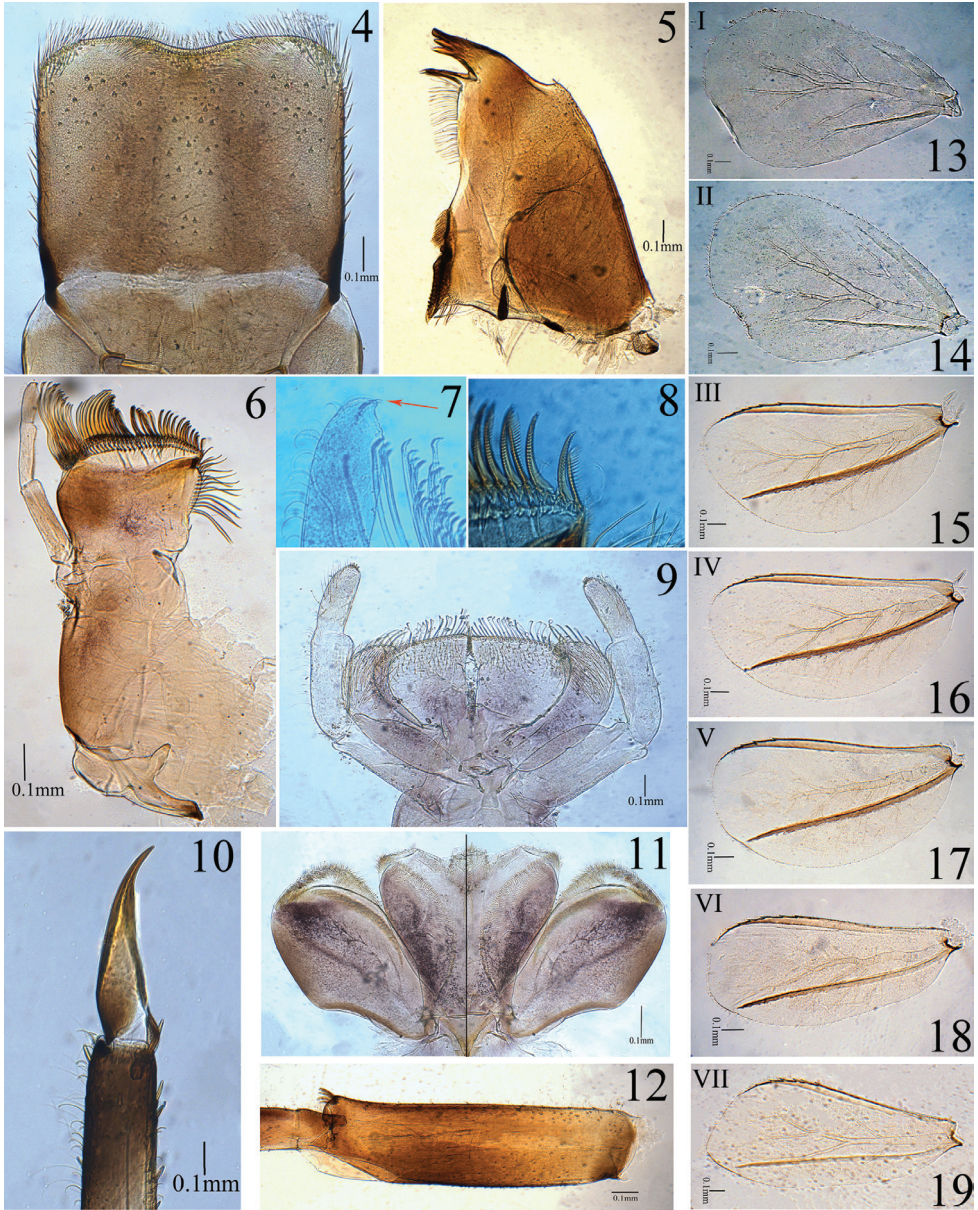
Head. Flagellum of antenna with approximately 15–17 segments. Labrum (Fig. 4) rectangle (length to width ratio approximately 0.7:1) with shallow indentation on anterior margin, ventrally bordered with row of dense feathered setae (rarely bi-forked setae) along anterior margin. Outer incisor of left mandible with 4 denticles, first denticle longest, rest gradually getting shorter; outer incisor of right mandible with 3 denticles (Fig. 5), first denticle longest, second denticle slightly shorter or subequal to third. Hypopharynx as in Fig. 11, lingua with one median projection covered with hair-like fine setae. Right and left maxillae similar in structure (Fig. 6), crown of each maxilla with 27–31 comb-shaped setae and first seta with approximately 20 pointed denticles (Fig. 8), lateral galealacinia with row of approximately 14 long, feathered setae; maxillary palp 3-segmented, length ratio from basal to apical segments = 2.3:1.4:1, apex of terminal segment with one small hook (Fig. 7). Apical margin of glossae truncate and straight with row of long, spatulate flat setae widened towards apex (Fig. 9).

Thorax. Dorsal surface of legs covered with many minute spine-like setae; apices of femora with crosswise row of distinct stout spine-like setae (Fig. 12): fore, middle and hind femora with 7–8, 4–5 and 3 stout setae at apices, respectively. Claws slightly curved and without denticles (Fig. 10). Inner margin of trochanter in hind leg bearing row of brush-like fine and dense setae (Fig. 23), fore and middle trochanters without such setae.

Abdomen. Tergites I–X each with pointed spines on posterior margin (Figs 20, 22); sternites I–IV without any spines on posterior margin, V–VIII with tiny spines (Fig. 21) on posterior margin laterally (visible only under high magnification); surfaces of tergites and sternites I–IV without spine-like setae, but V–IX covered with tiny spine-like setae (Fig. 20), sternite IX with deep V-shaped cleft in both sexes, female with acute dentate emargination medially (Fig. 24), male without any denticles, penis buds without spine-like setae (Fig. 25); posterolateral spines on abdominal segments VIII–IX relatively short. Gills on abdominal segments I–VII (Figs 13–19); gills I–II white and oval, widest at apical half, each with short costal and anal ribs (Figs 13, 14); gills III–VII white with brown ribs and black tracheae, each with one strong costal rib and distinct serrations on costal margin and with one strong anal rib far from anal margin (Figs 15–19). Ratios of maximum width to length: gill I = 0.71, gill II = 0.66, gills III–IV = 0.48, gill V–VI = 0.50 and VII = 0.45. Cerci dark brown and median caudal filament paler (Figs 2, 3).

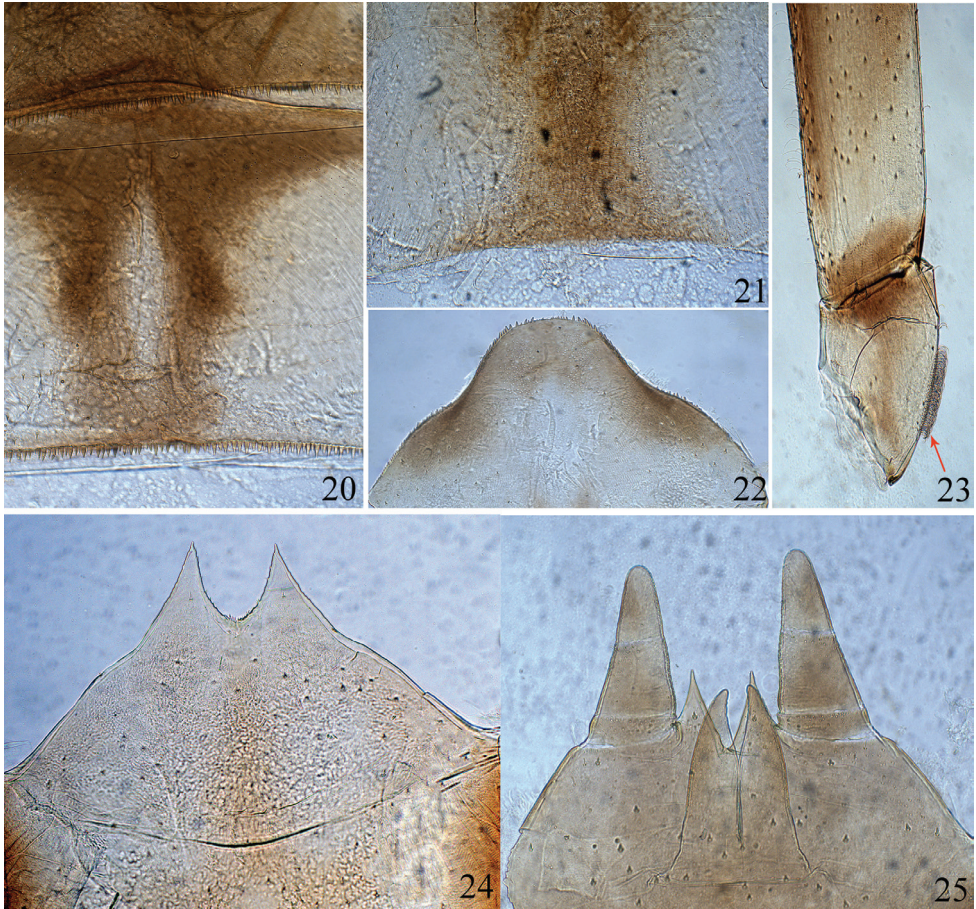
Male imago (in alcohol). Length (mm): Body 13 (12.5–14.0); forewings 12 (11.5–12.5); cerci 19 (16.0–22.0).

Head. Upper portion of compound eyes grey, lower portion dark grey (Figs 26, 27). Antennae light brown. Ocelli whitish. Labial and maxillary palpi present, but vestigial.



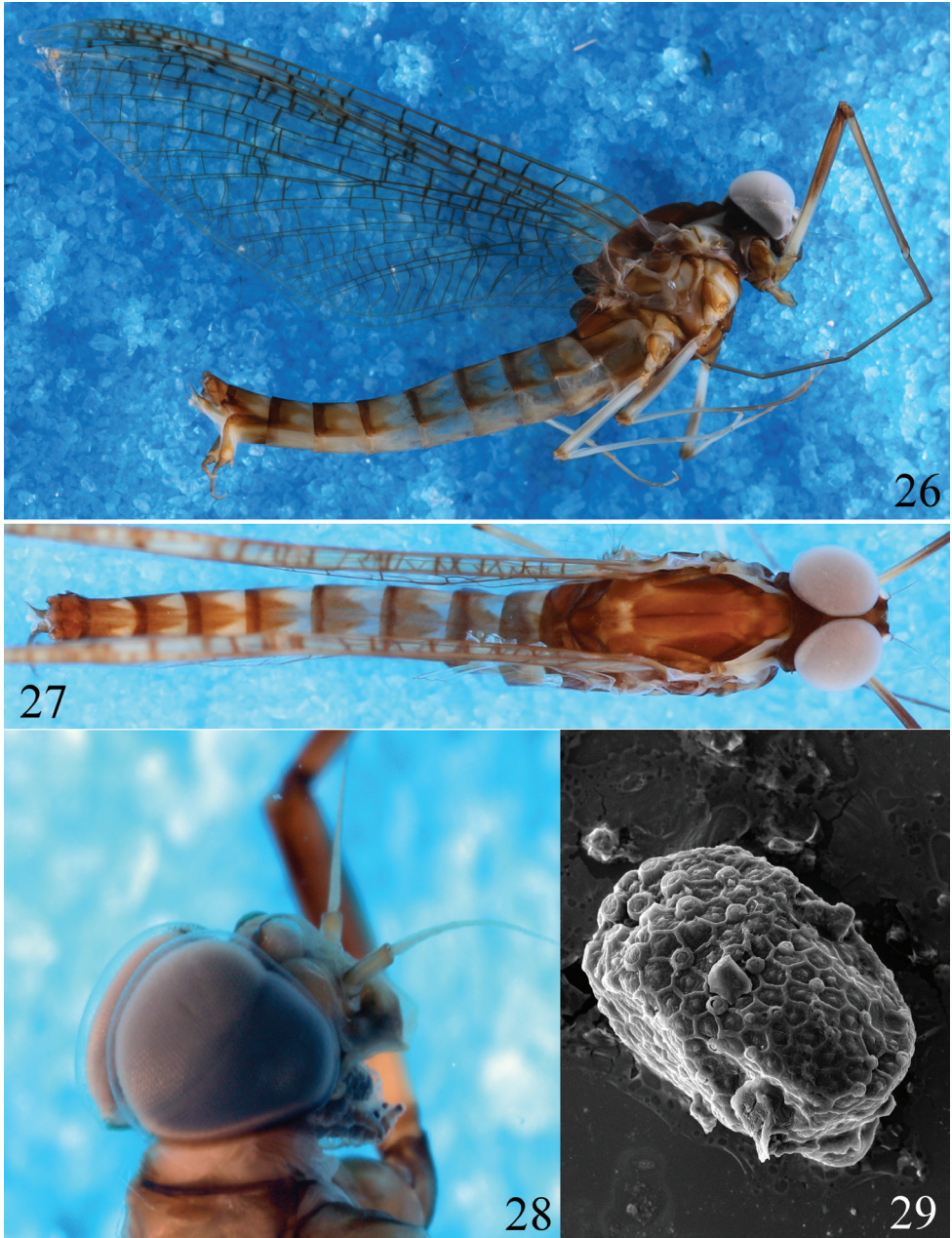
Figures 4–19. Larva of *Ameletus daliensis* Tong, sp. nov. **4** labrum (dorsal view) **5** right mandible **6** right maxillae **7** apex of terminal segment of maxillary palp (showing hook) **8** comb-shaped setae of maxilla (showing first seta) **9** labium **10** claw **11** hypopharynx (left: ventral view; right: dorsal view) **12** femur of foreleg **13–19** gills I–VII.

Thorax: Pronotum dark brown. Anteronotal protuberance brown, posterolateral sides dark brown; medioscutum brown, submedioscutum dark brown, median longitudinal suture dark brown (Fig. 27); sublateroscutum brown to dark brown; posterior scutle



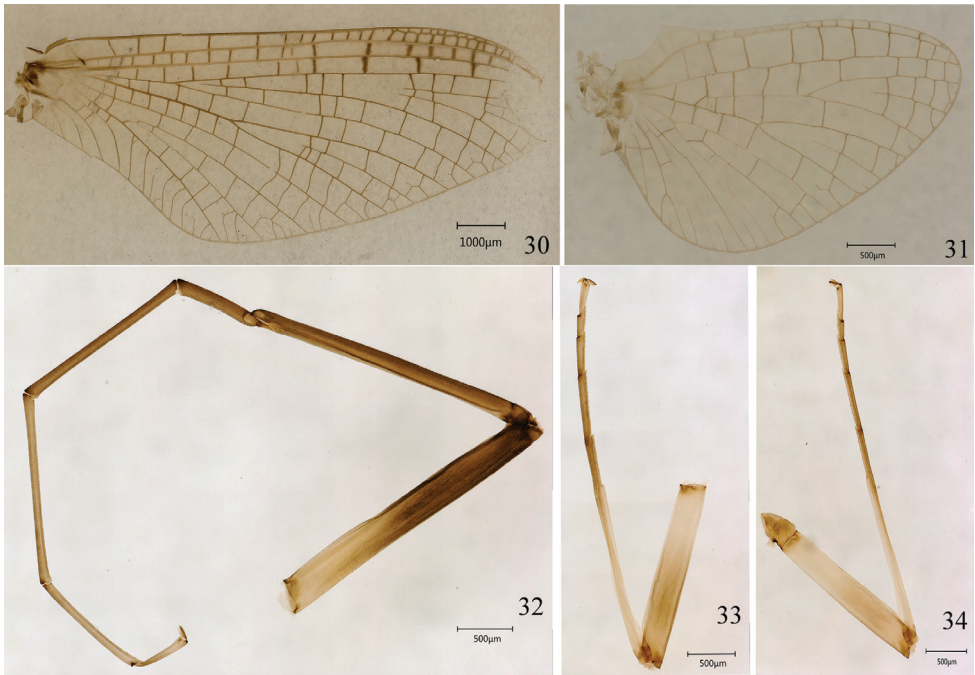
Figures 20–25. Larva of *Ameletus daliensis* Tong, sp. nov. **20** abdominal tergites VII–VIII **21** sternite VIII **22** abdominal tergite X (male) **23** trochanter of hind leg **24** female sternite IX **25** male sternite IX (showing penis buds, ventral view).

protuberance brown with narrow white patch posterolaterally; scutellum brown, infrascutellum dark brown, scuto-scutellar impression light brown with pale lateral margins. Foreleg dark brown, except light yellowish-brown at basal 1/3 of femur (Fig. 32); middle and hind legs similar in colour and lighter than forelegs (Figs 33, 34); tibia pale and tarsus light brown, dorsal surface without spinules. Length of foreleg segments (mm): femur 2.7; tibia 2.7; tarsal segments 0.8, 1.7, 1.6, 1.1 and 0.5. Fore wings membrane transparent (Fig. 30), all veins dark brown with cross-veins lighter. Vein RS forked at about 1/4 of distance from base to margin; MA forked at middle of wing; MP_2 turns downwards to meet CuA; stigmatic area suffused with milky and divided by longitudinal vein; cross-veins between C and R veins bordering around by dark brown. Hind wings hyaline with short costal projection near the base; vein MA forked at middle with one intercalary vein between MA_1 and MA_2 ; MP forked about one-third of distance from base to margin (Fig. 31).



Figures 26–29. *Ameletus daliensis* Tong, sp. nov. **26** male imago **27** male imago (dorsal view) **28** head of male sub-imago **29** egg (SEM).

Abdomen: Tergites I and X brown, tergites II–IX brown with two triangle-like white markings on anterior half (Fig. 27). Sternites II–VIII pale, each with ganglionic marking medially. Cerci dark brown.



Figures 30–34. Imago of *Ameletus daliensis* Tong, sp. nov. **30** forewing **31** hind wing **32** fore leg **33** middle leg **34** hind leg.

Genitals: Styliger white with brown markings laterally (Fig. 35); forceps dark brown, terminal segment paler (Fig. 35); penis lateral lobes with spinules, apices of lobes round and slightly bent inwardly; ventral plates absent (Figs 36–39).

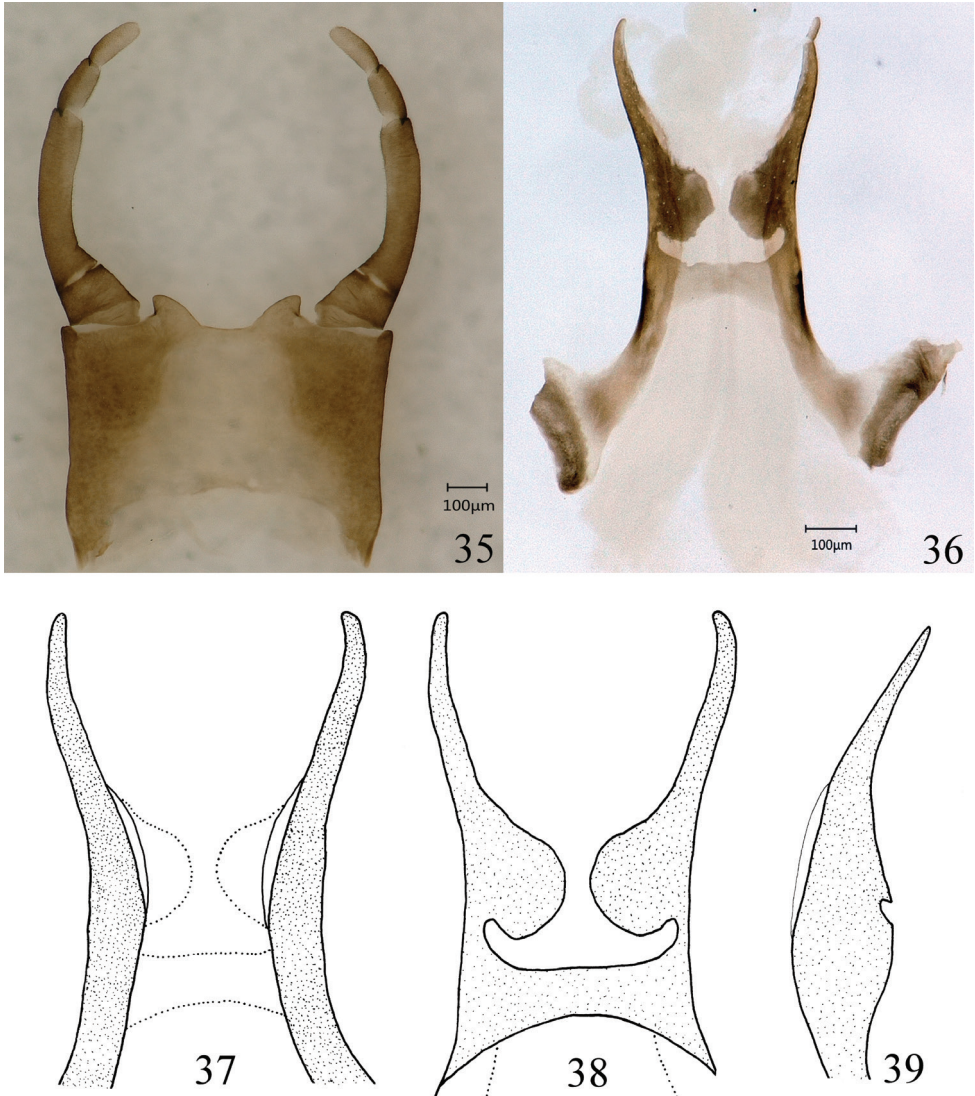
Female subimago (in alcohol). Length (mm): Body 13.5; forewings 13.5; cerci 11. Compound eyes dark grey. Lateral view of head, the labial and maxillary palpi present and clearly visible (Fig. 28). Pronotum pale. Medioscutum and median longitudinal suture pale to light brown; submedioscutum and sublateroscutum brown. Wings semi-transparent, all cross-veins bordered around by dark brown. Abdominal tergite I pale with brown markings laterally and medially, colour pattern of other tergites similar to those of male; sternites II–VIII pale, each with blackish ganglionic marking medially, subgenital plate brown with deep V-shaped cleft.

Eggs. Generally long ellipsoid shape with length 180–205 µm and width 100–115 µm (Fig. 29). The chorionic surface is covered by large-mesh polygonal cells, each cell with a small protuberance in the middle; large prominent round knobs exist on one pole only.

Etymology. The specific epithet is named after the type locality, Dali City, Yunnan Province, China.

Distribution. China (Yunnan).

Biology. Larvae of this new species prefer to live in pools or slow currents with boulder and cobble substrate in very clear small streams. At one representative location



Figures 35–39. Male genitalia of *Ameletus daliensis* Tong, sp. nov. **35** terminal abdominal sternites **36** penis lobes **37** penis lobes (ventral view) **38** penis lobes (dorsal view) **39** penis lobes (lateral view).

(Heilong Stream, Mt. Cangshan) in May, the average water temperature was 14.6 °C, pH was 6.9 and DO (mg/l) was 7.6. Mature larvae with black wing-pads could be collected from early May through to mid-July, which suggests that the emergence period of the alate stage occurs from early May to late July, from which we infer that *A. daliensis* Tong, sp. nov. is a univoltine species in Dali, Yunnan. Before emergence, the mature larvae crawled to stones protruding from the water, half submerged and moulted to sub-imago (Fig. 42). The sub-imagos usually emerged on a warm sunny daytime and were rarely collected by light-trap in the evening.



Figures 40–42. 40 rearing cage in the field 41 rearing cage 42 habitat of *Ameletus daliensis* Tong, sp. nov.

Molecular analyses

A total of 71 COI sequences of *Ameletus*, which represent all sequenced species of the genus, including 24 unidentified species and 33 valid species, with four sequences from *Ametropus neavei*, *Baetisca lacustris*, *Metreletus balcanicus* and *Siphonurus quebcensis* used as outgroups, were obtained from GenBank and BOLD for calculating genetic distances by K2P. The results showed that the interspecific genetic distances between *A. daliensis* sp. nov. and other sequenced *Ameletus* species are ranging from 5.5%–26.3%, of which the lowest K2P distance of 5.5% (Tables 1, 2) was found between the

Table 1. Collection information of the sequenced specimens from China.

Species	Collection locality	Collection date	GenBank Accession	Sources
<i>Ameletus daliensis</i> sp. nov.	Yunnan	15 May 2020	MW147549	This study
<i>Ameletus</i> sp.1 MT-2014	Sichuan	28 May 2012	KM207086.1	Tang et al. (2014)
<i>Ameletus</i> sp.1 MT-2014	Sichuan	28 May 2012	KM244682.1	Tang et al. (2014)

Table 2. Pairwise genetic distances (COI) between *Ameletus daliensis* Tong, sp. nov. and *Ameletus* sp.1 MT-2014 using the Kimura 2-parameter.

Taxa	K2P genetic distances	
	1	2
1 <i>Ameletus daliensis</i> sp. nov.		
2 KM207086 <i>Ameletus</i> sp.1 MT-2014	0.055	
3 KM244682 <i>Ameletus</i> sp.1 MT-2014	0.055	0.00

new species and *Ameletus* sp.1 MT-2014 (GenBank # KM207086 and KM244682, see Tang et al. 2014) from Sichuan, China. In general, 3.5% sequence divergence ($K2P = 0.035$) is considered as a likely maximal value for intraspecific divergence (Hebert et al. 2003; Ball et al. 2005; Zhou et al. 2010), although there is an exceptional case with 6% intraspecific distance in a mayfly in North America (Ball et al. 2005). The evidence of morphological differences in their larval stage and the genetic distance higher than 3.5% support the erection of the new species *A. daliensis* sp. nov.

Discussion

The larvae of the new species are similar to *Ameletus formosus* Kang & Yang from Taiwan with a V-shaped cleft on the posterior margin of abdominal sternite IX, but it differs from the latter by: (1) anterior margin of labrum having a row of dense feathered setae (rarely bi-forked setae); (2) gills I–II much wider (width/length ratio is 0.66–0.71) than those of *A. formosus* and each gill bearing a short costal rib and (3) V-shaped cleft on sternite IX is much deeper and more acute than that of *A. formosus*. In addition, the trochanter of the hind leg of the new species in larvae bears a row of brush-like fine and dense setae (Fig. 23). We are not sure whether this feature is unique for new species or shared by all *Ameletus* species, as it has never been mentioned in literature. The imaginal genital of the new species is characterised by being devoid of ventral plates. Interestingly, this character is also shared with *A. inopinatus* Eaton from Palearctic, *A. primitivus* Traver from Oriental and *A. velox* Dodds from Nearctic Regions. However, the lateral lobes of the penis are bent into an S-shape in *A. inopinatus* and are curved mesally in *A. velox* (Zloty 1996; Kluge 2007), in contrast to *A. primitivus*, the lateral lobes of the new species being relatively shorter and wider. Compared to the imago and larva of other *Ameletus* species, *Ameletus daliensis* Tong, sp. nov. is most closely related to *A. primitivus* Traver by its sharing retaining maxillary and labial palpi in the alate stage, in particular, these palpi (even the segmentation) were clearly visible in the sub-imago (Fig. 28). *A. primitivus* was firstly described by Traver (1939), based on the female imago, female sub-imago and the larvae from northern India. Zloty (2001) re-described the male imago of *A. primitivus* Traver and discussed its relationship with other *Ameletus* species. As the persistent mouthparts are a unique character in the winged stage of Ephemeroptera, *A. primitivus* Traver was considered as one of the most primitive in all mayflies (Traver 1939; Zloty 2001). However, the imago of the new species can be readily distinguished from that of *A. primitivus* Traver by the following combination of characteristics: (1) although maxillary and labial palpi are externally visible, they are reduced in size and atrophied and lacking in chitinisation (unlike *A. primitivus*, which are elongated and easily visible in the imago, cf. Zloty 2001: fig. 1F); (2) all wings are transparent (in contrast to both wings stained with dark brown at the basal half in *A. primitivus*) and (3) lateral lobes of penis relatively shorter (length ratio of lateral lobes to the width of penis is about 1:1, while the ratio is about 2:1 in *A. primitivus*). The larvae of the new species could be separated those of *A. primitivus* by (1) costal rib of gills III–VII with serrations and lacking spine-like

setae; (2) abdominal sternites lacking spines on posterior margin, except V–VIII with tiny spines laterally and (3) surfaces of abdominal segments I–IV lacking spine-like setae on surfaces. Obviously, the new species has the characteristics that fall somewhere between Oriental and Holarctic species. The discovery of this new species bridges the gap between *A. primitivus* Traver and other Holarctic *Ameletus* species and could help reveal the origin and evolution of the genus *Ameletus*.

Acknowledgements

This work was supported by the National Natural Science Foundation of China (U1602262, 31872265). Special thanks to Dr. Tiunova for providing helpful identification suggestions and literature and thanks are also due to Ronglong Yang and Zhen Tian (Dali University) for help with fieldwork and the referees for their advice and constructive comments.

References

- Astrin JJ, Stüben PE (2008) Phylogeny in cryptic weevils: molecules, morphology and new genera of western Palaearctic Cryptorhynchinae (Coleoptera: Curculionidae). *Invertebrate Systematics* 22(5): 503–522. <https://doi.org/10.1071/IS07057>
- Bae YJ, Yoon IB (1997) A revised catalogue of the Ephemeroptera of Korea. *Entomological Research Bulletin* 23: 43–53.
- Ball SL, Hebert PDN, Burian SK, Webb JM (2005) Biological identifications of mayflies (Ephemeroptera) using DNA barcodes. *Journal of the North American Benthological Society* 24: 508–524. <https://doi.org/10.1899/04-142.1>
- Chiu MC, Ao SC, He FZ, Resh VH, Cai QH (2020) Elevation shapes biodiversity patterns through metacommunity-structuring processes. *Science of the Total Environment* 743: e140548. <https://doi.org/10.1016/j.scitotenv.2020.140548>
- Hebert PDN, Cywinska A, Ball SL, DeWaard JR (2003) Biological identifications through DNA barcodes. *Proceedings of the Royal Society B-Biological Sciences* 270: 313–321. <https://doi.org/10.1098/rspb.2002.2218>
- Ishiwata S (2001) A checklist of Japanese Ephemeroptera. In: Bae YJ (Ed.) *The 21st Century and Aquatic Entomology in East Asia*, Proceedings of the 1st Symposium of Aquatic Entomologists in East Asia. The Korean Society of Aquatic Entomology, Korea, 55–84.
- Kang SC, Yang CT (1994) Three new species of the genus *Ameletus* from Taiwan (Ephemeroptera: Siphonuridae). *Chinese Journal of Entomology* 14: 261–269. <https://doi.org/10.1007/BF00160820>
- Kluge NJ (2004) *The phylogenetic system of Ephemeroptera*. Kluwer Academic Publishers, 442 pp. <https://doi.org/10.1007/978-94-007-0872-3>
- Kluge NJ (2007) Review of Ameletidae (Ephemeroptera) of Russia and adjacent lands. *Russian Entomological Journal* 16(3): 245–258.

- Katoh K, Standley DM (2013) MAFFT multiple sequence alignment software version 7: improvements in performance and usability. *Molecular Biology and Evolution* 30(4): 772–780. <https://doi.org/10.1093/molbev/mst010>
- Kondratieff BC, Meyer MD (2010) *Ameletus janetae*, a new species of mayfly (Ephemeroptera: Ameletidae) from West Virginia. *Proceedings of the Entomological Society of Washington* 112(4): 526–529. <https://doi.org/10.4289/0013-8797.112.4.526>
- Kumar S, Stecher G, Tamura K (2016) MEGA7: Molecular evolutionary genetics analysis version 7.0 for bigger datasets. *Molecular Biology and Evolution* 33(7): 1870–1874. <https://doi.org/10.1093/molbev/msw054>
- Quan YT, Bae YJ, Jung JC, Lee JW (2002) Ephemeroptera (Insecta) fauna of Northeast China. *Insecta Koreana* 19(3–4): 241–269.
- Ranwez V, Douzery EJP, Cambon C, Chantret N, Delsuc F (2018) MACSE v2: Toolkit for the alignment of coding sequences accounting for frameshifts and stop codons. *Molecular Biology and Evolution* 35(10): 2582–2584. <https://doi.org/10.1093/molbev/msy159>
- Tang M, Tan MH, Meng GL, Yang SZ, Su X, Liu SL, Song WH, Li YY, Wu Q, Zhang AB, Zhou X (2014) Multiplex sequencing of pooled mitochondrial genomes—a crucial step toward biodiversity analysis using mito-metagenomics. *Nucleic Acids Research* 42(22): e166. <https://doi.org/10.1093/nar/gku917>
- Tiunova TM (2013) New species of *Ameletus* Eaton, 1885 and redescription of *Ameletus longulus* Sinichenkova, 1981 from the Russian Far East (Ephemeroptera: Ameletidae). *Zootaxa* 3630(3): 519–533. <https://doi.org/10.11646/zootaxa.3630.3.7>
- Tiunova TM, Semenchenko AA, Velyaev OA (2017) New species of *Ameletus* Eaton, 1885 from the Russian Far East with notes on *Ameletus camtschaticus* Ulmer 1927 (Ephemeroptera: Ameletidae). *Zootaxa* 4276(2): 151–176. <https://doi.org/10.11646/zootaxa.4276.2.1>
- Wesener T (2015) No millipede endemics north of the Alps? DNA-Barcoding reveals *Glomeris malmivaga* Verhoeff, 1921 as a synonym of *G. ornate* Koch, 1847 (Diplopoda, Glomerida, Glomeridae). *Zootaxa* 3999(4): 571–580. <https://doi.org/10.11646/zootaxa.3999.4.7>
- Zhang D, Gao F, Jakovlic I, Zou H, Zhang J, Li WX, Wang GT (2020) PhyloSuite: An integrated and scalable desktop platform for streamlined molecular sequence data management and evolutionary phylogenetics studies. *Molecular Ecology Resources* 20(1): 348–355. <https://doi.org/10.1111/1755-0998.13096>
- Zhou X, Jacobus LM, DeWalt RE, Adamowicz SJ, Hebert PDN (2010) Ephemeroptera, Plecoptera, and Trichoptera fauna of Churchill (Manitoba, Canada): insights into biodiversity patterns from DNA barcoding. *Journal of the North American Benthological Society* 29: 814–837. <https://doi.org/10.1899/09-121.1>
- Zloty J (1996) A revision of the Nearctic *Ameletus* mayflies based on adult males, with description of seven new species (Ephemeroptera: Ameletidae). *Canadian Entomologist* 128: 293–346. <https://doi.org/10.4039/Ent128293-2>
- Zloty J, Harper F (1999) Two new *Ameletus* mayflies (Ephemeroptera: Ameletidae) from western North America. *Canadian Entomologist* 131: 1–9. <https://doi.org/10.4039/Ent1311-1>
- Zloty J, Pritchard G (1997) Larvae and adults of *Ameletus* mayflies (Ephemeroptera, Ameletidae) from Alberta. *Canadian Entomologist* 129: 251–289. <https://doi.org/10.4039/Ent129251-2>

Two new species of *Paraphytis* (Hymenoptera, Aphelinidae) from Southwest China

Ye Chen¹, Hai-feng Chen¹, Cheng-de Li²

1 Hebei Key Laboratory of Animal Diversity, College of Life Science, Langfang Normal University, Langfang, 065000, China **2** School of Forestry, Northeast Forestry University, Harbin, 150040, China

Corresponding author: Hai-feng Chen (chenhaifeng@lfnu.edu.cn); Cheng-de Li (lichengde0608@sina.com)

Academic editor: A. Köhler | Received 25 September 2020 | Accepted 25 January 2021 | Published 1 March 2021

<http://zoobank.org/CFB9ECD6-F7CD-49FA-B7AC-8FB3714A72B0>

Citation: Chen Y, Chen H-f, Li C-d (2021) Two new species of *Paraphytis* (Hymenoptera, Aphelinidae) from Southwest China. ZooKeys 1021: 53–63. <https://doi.org/10.3897/zookeys.1021.58962>

Abstract

Two new species of *Paraphytis* Compere, *P. bannaensis* **sp. nov.** and *P. pseudovittatus* **sp. nov.**, are described from the Xishuangbanna Rainforest (Southwest China). A key to species from China based on females is provided.

Keywords

Aphelininae, Aphytini, Chalcidoidea, parasitic wasp, rainforest, taxonomy

Introduction

The genus *Paraphytis* was established by Compere (1925), with *Paraphytis vittatus* as the type species. Afterwards, it was treated as a synonym under *Marietta* (Compere 1936), and later as a synonym under *Aphytis* (DeBach & Rosen, 1976). It was resurrected by Kim and Heraty (2012). Currently, *Paraphytis* comprises 26 valid species (Kim and Heraty 2012; Noyes 2019). Species are distributed in the Australian, Oriental and Neotropical regions, with 11, 8 and 7 species respectively.

All species of this genus with known biology are primary endoparasitoids of Diapriidae (Rosen and DeBach 1979; Kim and Heraty 2012; Noyes 2019). Rosen and DeBach (1979) provided a detailed taxonomic treatment for the species which were then placed in the *Aphytis vittatus*-group, including a key to species, descriptions or redescriptions, and photos. Kim and Heraty (2012) resurrected *Paraphytis*, and provided diagnoses to distinguish this and similar genera, including *Aphytis* and *Marietta*.

The Chinese fauna of *Paraphytis* includes five species: *P. vittatus* described by Compere (1925) from Fujian Province; *P. angustus* by Compere (1955) from Taiwan; *P. breviclavatus*, *P. densiciliatus* and *P. transversus* by Huang (1994) from Fujian Province. Herein we describe two new species and provide an identification key to Chinese species of *Paraphytis*.

Materials and methods

In May 2019, arthropods were sampled in the rainforest canopy at the Xishuangbanna Tropical Botanical Garden in Menglun Town, Yunnan Province. Samples were obtained using a pyrethroid fog generated from a thermal fogger (Swingfog SN50, Germany, Model 2610E, Series 3). All individuals in the present study were collected from these samples.

Specimens were dissected and mounted in Canada Balsam on slides following the method described by Noyes (1982). Prior to slide mounting, specimens in ethanol were photographed with an Olympus C7070 digital camera attached to an Olympus BX51 compound microscope. Slide-mounted specimens were photographed with a digital CCD camera attached to an Olympus BX53 compound microscope. Final modifications to the images were made using Helicon Focus 6 and Adobe Photoshop CS5. Measurements were made from the slide-mounted specimens using a reticle micrometer, except for the total body length (excluding the ovipositor), which was measured from ethanol-preserved specimens before dissection. All measurements are given in micrometers (μm) except body length, which is measured in millimetres (mm). The measurements of length and width of body parts generally follows Hayat (1998), except pedicel and flagellomeres which are measured as shown in Fig. 3. Scale bars are 100 μm except where otherwise indicated. All specimens listed below are deposited in Langfang Normal University (LFNU), Langfang, China.

Terminology follows the Hymenoptera Anatomy Consortium (2020) for most body parts, Rosen and DeBach (1979) for bullae, and Hayat (1998) for basal cell and lineae calva.

The following abbreviations are used in the text:

- F1–3** funicle segments 1–3;
Gt₁, Gt₂ etc. tergites 1, 2, etc. of gaster.

Taxonomy

Genus *Paraphytis* Compere, 1925

Paraphytis Compere, 1925: 129. Type species: *Paraphytis vittata*, by monotypy. Synonymy under *Marietta* by Compere 1936: 311; synonymy under *Aphytis* by DeBach and Rosen 1976: 541; revived by Kim and Heraty 2012: 544.

Syediella Shafee, 1970: 144. Type species: *Syediella maculata*, by original designation. Synonymy under *Aphytis* by Hayat 1982: 169 and under *Paraphytis* by Kim and Heraty 2012: 544.

Diagnosis. Species of *Paraphytis* can be recognized by the following combination of characters: antenna (Figs 3, 15) with 6 or rarely 5 antennomeres; distinctly mottled forewings (Figs 6, 18) and heavily pigmented body (Figs 1, 11); mesopleuron convex, large and undivided; axilla with one seta (Figs 4, 16); propodeum more than 2× as long as metanotum and with crenulae on posterior margin (Figs 5, 10, 17, 22); seta anterior to propodeal spiracle thin and not flattened as in *Aphytis* (Figs 4, 16; cf. fig. 243 in Kim and Heraty 2012).

Key to Chinese species (female) of *Paraphytis* Compere

- 1 Antenna with 5 antennomeres **2**
- Antenna with 6 antennomeres **3**
- 2 Clava with an incomplete transverse suture (cf. fig. 9B in Huang 1994) at about basal one third; dorsum of mesoscutum and mesoscutellum without dark longitudinal stripes; forewing mostly infusate, with a hyaline crossband near apex (cf. fig. 9C in Huang 1994)..... ***P. densiciliatus* (Huang)**
- Clava without any sutures, dorsum of mesoscutum and mesoscutellum with 2 and 4 dark longitudinal stripes respectively (Figs 1, 4); forewing with a brown band below apex of submarginal vein, and with a broad infuscated patch below stigmal vein, otherwise uniformly hyaline (Fig. 6)..... ***P. bannaensis* sp. nov.**
- 3 Body extensively pale yellow, with 4 dark longitudinal stripes (Figs 11, 16) on dorsum of mesoscutum and mesoscutellum **4**
- Body extensively yellow or dark; if yellow, then without any dark longitudinal stripes, at most with some dark patches (cf. fig. 11E in Huang 1994) **5**
- 4 Mesoscutellum with submedian dark longitudinal stripes that do not merge with lateral stripes at posterior margin (Figs 11, 16); forewing with delta area having “F” shaped pattern formed by dark and hyaline setae and dark membrane; forewing disc with pattern posterior to linea calva formed by a transparent round patch and other irregular transparent and dark patches (Fig. 18); clava relatively slender, 3.0–3.6× as long as wide ***P. pseudovittatus* sp. nov.**
- Mesoscutellum with submedian dark longitudinal stripes merging with lateral stripes at posterior margin (cf. fig. 265 in Rosen and DeBach 1979); forewing

- with delta area having an infuscated ring formed by dark and hyaline setae, without dark membrane; forewing disc with different pattern posterior to linea calva formed mainly by several subelliptical transparent patches against a dark background (cf. fig. 268 in Rosen and DeBach 1979); clava about 2.5× as long as wide *P. vittatus* **Compere**
- 5 Scape pale; forewing at most faintly infuscated; midlobe of mesoscutum about 1.6× as wide as long (cf. Fig. 10E in Huang 1994) **6**
- Scape with a dark brown oblique band apically; forewing with an “M” shaped transparent patch (cf. fig. 11C in Huang 1994); midlobe of mesoscutum 1.9× as wide as long (cf. fig. 11E in Huang 1994)..... *P. transversus* **(Huang)**
- 6 Mesofemur with a dark patch medially on outer surface; clava more than 2× as long as wide *P. angustus* **(Compere)**
- Mesofemur pale; clava 1.8× as long as wide.....*P. breviclavatus* **(Huang)**

***Paraphytis bannaensis* Chen & Li, sp. nov.**

<http://zoobank.org/21D4E45E-F23E-4A0B-9824-1AF5C3B34EF8>

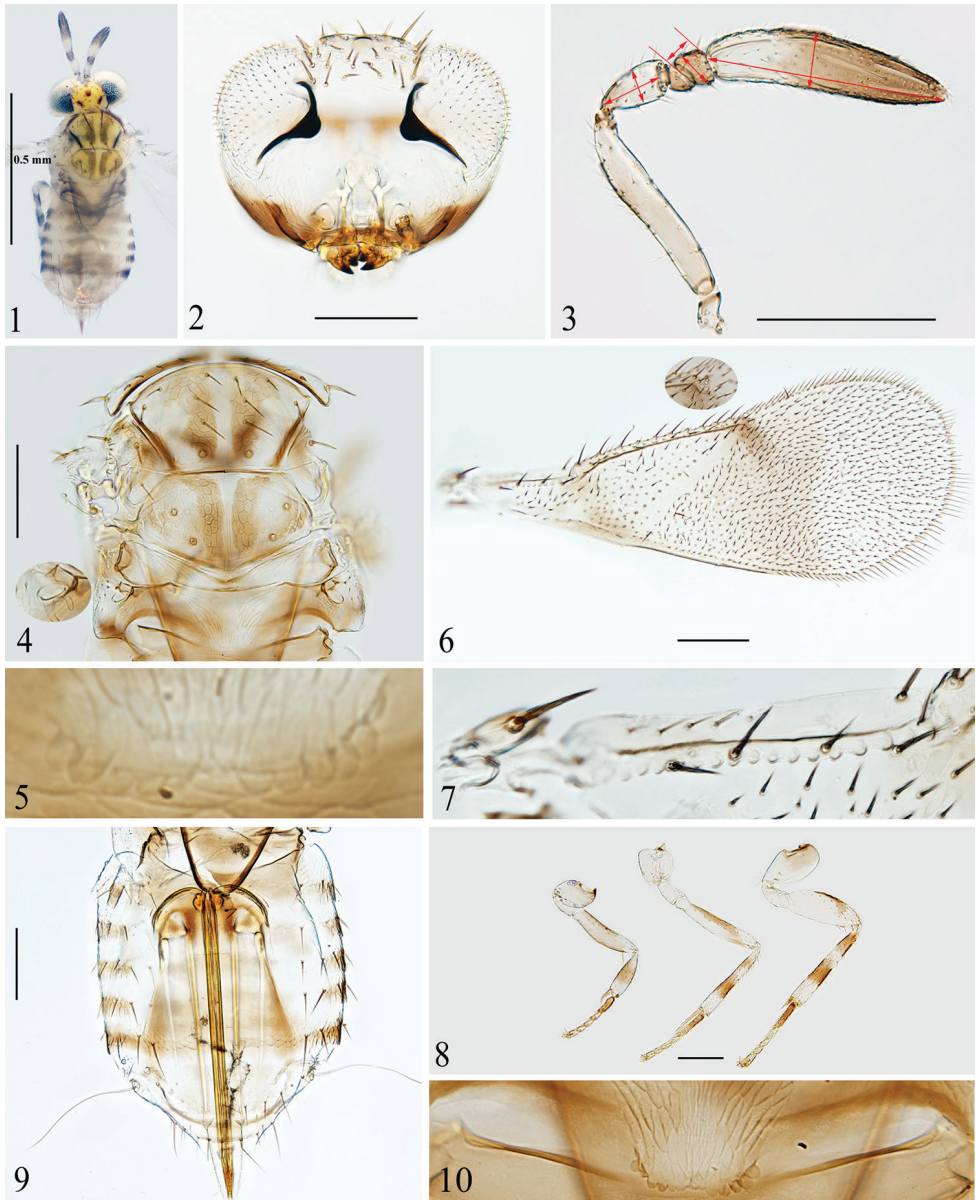
Figs 1–10

Type material. Holotype: ♀ [on slide, A-Pa2020011], CHINA, Yunnan Province, Xishuangbanna, Mengla County, Menglun Town (21°54.24'N, 101°15.98'E, elevation ca 541 m), 13.v.2019, Zi-long Bai, Zhi-gang Chen, Cheng Wang, Hao Yu leg; deposited in LFNU. **Paratypes:** 17♀♀ [10♀♀ on slides, A-Pa202001– A-Pa2020010; 7♀♀ in alcohol, LFNU], same data as holotype. 1♀ [on slide, A-Pa2020012, LFNU], CHINA, Yunnan Province, Xishuangbanna, Mengla County, Menglun Town (21°54.34'N, 101°16.79'E, elevation ca 618 m), 2.v.2019, Zi-long Bai, Zhi-gang Chen, Cheng Wang, Yan-feng Tong, Hao Yu leg.

Diagnosis. *Paraphytis bannaensis* sp. nov. can be distinguished from other species in this genus by the following combination of characters: 5 antennomeres, midlobe of mesoscutum with two dark stripes, mostly dark brown profemur, dark tarsomeres, forewing with a brown band below apex of submarginal vein, with a broad infuscated patch below stigmal vein, and relatively long ovipositor which at least 2.0× as long as mesotibia.

Description. Female. Holotype. Length 0.8 mm.

Coloration (Fig. 1). Head mostly pale yellow, with vertex orange yellow, lower half of malar space and mouth margin dark. Occipital foramen with a dark brown transverse line on upper margin, and with lateral margins dark brown. Ocelli orange red. Setae on head dark. Antenna with funicle segments and distal half of clava dark brown, remainder yellow somewhat suffused with brown. Mandible brown with apex darker. Pronotum yellow but with central region and posterior margin dark. General coloration of mesosoma (Fig. 1) yellow, but with dark markings as followings: anterior margin of midlobe of mesoscutum and notauli; midlobe with a pair of submedian longitudinal stripes, which curve out at anterior ends; mesoscutellum with similar submedian longitudinal stripes as on midlobe, and additionally with two oblique stripes



Figures 1–10. *Paraphytis bannaensis* sp. nov., holotype female (except Fig. 10) **1** body, dorsal view **2** head, frontal view **3** antenna, red arrows indicate measurements of length and width **4** mesosoma and propodeal seta **5** crenulae **6** forewing **7** submarginal vein **8** legs **9** metasoma **10** crenulae, paratype.

along lateral margins (not clearly visible in Fig. 1, but in the fresh specimen the lateral oblique stripes obviously merge with the submedian stripes at each posterior margin). Mesopleuron with posterior half dark brown; propodeum with lateral sides brown, and with a dark “V” shaped streak along posterior margin. Forewing (Fig. 6) with veins and

posterior margin brown; disc with an oblique brown band below apex of submarginal vein, and with broad infuscated patch below stigmal vein and area around stigmal vein darker. Legs (Fig. 8) pale yellow with brown parts as followings: extreme base of procoxae; profemur dorsally except apical one third; protibiae with a broad ring basally; mesofemur with dorsal surface and distal one third; mesotibia with two rings, one near base, the other on medial area; base of metacoxae, metafemur with a curved band on dorsal surface distally, metatibia pigmented as mesotibia; all tarsomeres brown, with basitarsi darker. Metasoma (Figs 1, 9) with petiole dark, Gt_{1-5} each with pale brown to brown bands on dorsal surface medially and dark bands on lateral sides, the median bands connecting the lateral bands on Gt_1 and Gt_5 ; Gt_6 brown, the following two tergites pale yellow. Ovipositor brown.

Head (Fig. 2), in frontal view, $0.8\times$ as high as wide; weakly reticulated. Frontover-
tex $0.4\times$ head width, with two pairs of long setae, one on vertex and another along occipital margin, and with about 20 short brown setae. Ocellar triangle (Fig. 1) with apical angle 94° . Mandible bidentate. Antenna (Fig. 3) with 5 antennomeres, scape $5.0\times$ as long as wide, slightly shorter than clava; pedicel $2.0\times$ as long as wide, $1.2\times$ as long as F1 and F2 combined; F1 triangular, ventral margin longer than dorsal margin, a little longer than wide; F2 trapezoidal, dorsal margin $1.6\times$ longer than ventral margin, $0.8\times$ as long as wide, subequal to F1 in length, $1.7\times$ width of F1; clava slightly curved medially, $4.1\times$ as long as wide with 7 longitudinal sensilla. Measurements, length (width): scape 112.5 (22.5); pedicel 45 (22.5); F1 17.5 (15); F2 20 (25); clava 145 (35).

Mesosoma (Figs 4, 5). Dorsum of mesosoma reticulate, with sculpture on dark areas more evident. Mesoscutum with midlobe $0.6\times$ as long as wide, about as long as mesoscutellum, and with 12 setae; lateral lobe of mesoscutum with 4 setae; axilla with 1 seta; mesoscutellum pentagonal, $0.6\times$ as long as wide with 2 pairs of setae. Distance between anterior pair of scutellar setae $1.4\times$ that between posterior pair. Placoid sensilla just mesad of anterior scutellar setae, and distance between sensilla about equal to distance between the posterior scutellar setae. Metanotum narrow. Propodeum with a thin seta (Fig. 4, inset) anterior to propodeal spiracle, $4.7\times$ length of metanotum, and posterior margin with 5 (left side) + 6 (right side) crenulae (Fig. 5).

Wings. Forewing (Figs 6, 7) $2.6\times$ as long as wide, marginal setae $0.1\times$ wing width. Costal cell $0.7\times$ length of marginal vein, with 4 fine setae medially and 2 coarse setae apically; submarginal vein (Fig. 7) with 5 setae and 18 bullae; marginal vein with 9 setae along anterior margin; basal cell with about 17 setae in nearly 4 transverse lines. Hind wing hyaline, $5.0\times$ as long as wide, with marginal setae $0.5\times$ wing width. Measurements, length (width): forewing 760 (290); costal cell 150; submarginal vein 130; marginal vein 230; stigma vein 15; hind win, 600 (120); marginal setae of hind wing 60.

Legs (Fig. 8). Mesotibial spur as long as corresponding basitarsus. Length measurements: mesotibia 190; mesotibial spur 75; mesobasitarsus 75.

Metasoma (Fig. 9). Petiole strongly reticulated on central area just below crenulae. Gt_{1-5} with elongate reticulations on lateral sides, Gt_5 with imbricate sculpture on dorsal surface. Setation of tergites on dorsal surface as follows: Gt_1 with 3 setae on each side, Gt_2 with 4 setae on left side and 3 setae on right side (4+3), Gt_3 5+4, Gt_4 4+4, Gt_5 4+4,

Gt₆ and Gt₇ each with 10 setae, Gt₈ with 4 setae. Ovipositor originating from apex of Gt₁, 2.4× as long as mesotibia, and slightly exerted. Second valvifer 3.1× as long as third valvula; third valvula with several pale setae apically, and 1.5× as long as mesobasitarsus. Length measurements: ovipositor 450; second valvifer 340; third valvula 110.

Male. Unknown.

Variation. Scape 5.0–6.4× as long as wide, clava 3.6–4.8× as long as wide. Forewing 2.6–2.9× as long as wide, hind wing 5.0–5.7× as long as wide. Basal cell with 15–22 setae. Posterior margin of propodeum with 5+6 to 6+7 crenulae (Figs 5, 10). Gt_{2–5} each with 7–10 setae. Ovipositor originating from apex of Gt₁ to apex of Gt₂, and 2.1–2.4× as long as mesotibia.

Remarks. This species resembles *P. maculatus* (Shafee), with both having 5 antennomeres and similar coloration. They can be distinguished from each other by the following: midlobe of mesoscutum with only a pair of submedian longitudinal dark brown stripes, which are obviously curving out at anterior ends (vs with four longitudinal brown stripes, and with the pair of submedian stripes not curving out at anterior ends in *P. maculatus*, cf. fig. 467 in Rosen and DeBach 1979; fig. 151 in Hayat 1998; fig. 39 in Kim and Heraty 2012); legs with profemur extensively brown and all tarsomeres brown to dark brown (vs profemur pale yellow somewhat faintly suffused with dusky distally, tarsomeres mostly pale except all basitarsi and the second tarsomere of fore leg dark brown); forewing with a brown band and broad infuscated patch, without a patch of thick, darker setae in middle of proximal margin of linea calva (vs with only an oval infuscated patch below stigmal vein and with a patch of thick, darker setae in middle of proximal margin of the linea calva cf. fig. 152 in Hayat 1998); Ovipositor at least 2.0× as long as mesotibia (vs less than 2.0×).

Host. Unknown.

Etymology. Named after the locality of type specimen.

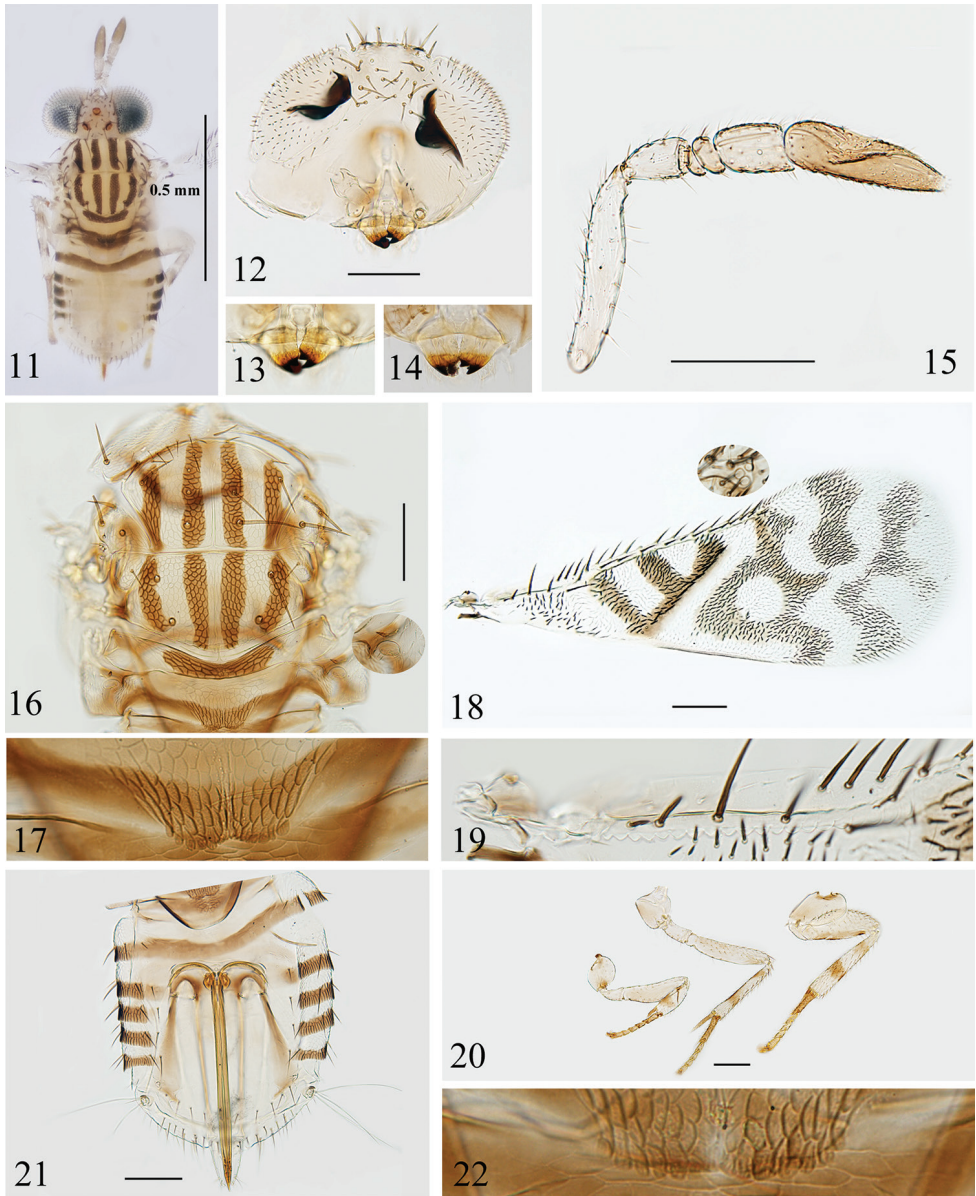
Distribution. China (Xishuangbanna of Yunnan Province).

***Paraphytis pseudovittatus* Chen & Li, sp. nov.**

<http://zoobank.org/FE45DA92-F1FE-4D56-B577-3D5248ED8148>

Figs 11–22

Type material. *Holotype*: ♀ [on slide, A-Pa2020020], CHINA, Yunnan Province, Xishuangbanna, Mengla County, Menglun Town (21°54.55'N, 101°16.31'E, elevation ca 570 m), 14.v.2019, Zi-long Bai, Zhi-gang Chen, Cheng Wang, Hao Yu leg; deposited in LFNU. *Paratypes*: 1♀ [on slide, A-Pa2020021, LFNU], CHINA, Yunnan Province, Xishuangbanna, Mengla County, Menglun Town (21°53.68'N, 101°17.41'E, elevation ca 539 m), 8.v.2019, Zi-long Bai, Ye-jie Lin, Cheng Wang, Yan-feng Tong, Hao Yu leg. 1♀ [on slide, A-Pa2020022, LFNU], CHINA, Yunnan Province, Xishuangbanna, Mengla County, Menglun Town (21°54.34'N, 101°16.79'E, elevation ca 618 m), 2.v.2019, Zi-long Bai, Zhi-gang Chen, Cheng Wang, Yan-feng Tong leg. 2♀ [on slides, A-Pa2020023, A-Pa2020024, LFNU], CHINA, Yunnan Province,



Figures 11–22. *Paraphytis pseudovittatus* sp. nov., holotype female (except Figs 14, 22) **11** body, dorsal view **12** head, frontal view **13** mandible **14** mandible, paratype **15** antenna **16** mesosoma and propodeal seta **17** crenulae **18** forewing **19** submarginal vein **20** legs **21** gaster **22** crenulae, paratype.

Xishuangbanna, Mengla County, Menglun Town (21°54.37'N, 101°16.71'E, elevation ca 623 m), 6.v.2019, Zi-long Bai, Ye-jie Lin, Cheng Wang, Yan-feng Tong, Hao Yu leg. 1♀ [in alcohol, LFNU], CHINA, Yunnan Province, Xishuangbanna, Mengla County, Menglun Town (21°53.59'N, 101°17.29'E, elevation ca 546 m), 4.v.2019,

Zi-long Bai, Zhi-gang Chen, Cheng Wang, Yan-feng Tong, Hao Yu leg. 1 ♀ [on slide, A-Pa2020025, LFNU], same data as holotype.

Diagnosis. *Paraphytis pseudovittatus* can be distinguished from other species in this genus by the following combination of characters: antenna with 6 antennomeres; mesoscutum and mesoscutellum each with four dark stripes; forewing with “F” shaped pattern in delta area and intricate mottled pattern posterior to linea calva (Fig. 18); F3 obviously longer than wide, clava more than 3.0× as long as wide; and posterior margin of propodeum with 6+5 to 6+6 crenulae.

Description. Female. Holotype. Length 0.8 mm.

Coloration (Fig. 11). Head mostly pale yellow, with upper margin and lateral margins of occipital foramen brown. Ocelli orange red. Setae on head dark. Antenna generally yellow, funicle segments with brownish suffusion, clava brown. Mandible (Fig. 13) with distal proximal brown to dark brown. Pronotum yellow except posterior margin dark. General coloration of mesosoma pale yellow, but with a distinctive pattern of dark markings as followings: midlobe of mesoscutum and mesoscutellum each with a pair of submedian longitudinal stripes and two stripes on lateral sides (Figs 11, 16); central region of metanotum with a transverse band; propodeum with a broad “V” shaped band along posterior margin. Forewing (Fig. 18) with delta area having “F” shaped pattern formed by dark and hyaline setae and dark membrane; disc with intricate pattern posterior to linea calva formed by a transparent round patch and other irregular transparent and dark patches (Fig. 18). Legs (Fig. 20) mostly pale yellow; coxae and femur more pale brown; tibiae with two brown rings, with basal rings at protibiae opened on dorsal surface; tarsomeres yellowish brown and with basitarsi darker. Metasoma mostly pale yellow, except the following: petiole dark except sides, with a dark band along posterior margin of Gt₁, Gt₂₋₅ with a dark patch on each side; Gt₂ with two brownish blotches on sides interior to the dark patches; cercal plates brown; ovipositor brown.

Head (Fig. 12), in frontal view 0.7× as high as wide; weakly reticulated. Frontover-
tex 0.3× head width, with about 30 coarse and brown setae. Ocellar triangle with apical
angle 76°. Mandible bidentate (Fig. 13). Antenna (Fig. 15) with 6 antennomeres, scape
5.5× as long as wide, slightly longer than clava; pedicel 1.6× as long as wide, about as
long as F3; F1 triangular, ventral margin longer than dorsal margin, about as long as
wide; F2 with dorsal margin a little longer than ventral margin, 0.5× as long as wide,
as long as F1; F3 cylindrical, 1.3× as long as wide, 3.4× as long as and 1.2× as wide as
F2; clava 3.2× as long as wide, 2.8× the length of F3. F3 and clava each with 2 and 6
longitudinal sensilla. Measurements, length (width): scape 137.5 (25); pedicel 40 (25);
F1 12.5 (15); F2 12.5 (27.5); F3 42.5 (32.5); clava 120 (37.5).

Mesosoma (Figs 16, 17). Dorsum of mesosoma faintly reticulate, with sculpture
on dark areas more evident. Mesoscutum with midlobe 0.6× as long as wide, about as
long as mesoscutellum, and with 14 setae in 4 lines; lateral lobe of mesoscutum with
4 setae; axilla with 1 seta; mesoscutellum 0.5× as long as wide, with 2 pairs of setae.
Distance between anterior pair of scutellar setae 1.3× that between posterior pair. Pla-
coid sensilla just mesad of and slightly posterior to anterior scutellar setae, and distance
between sensilla equal to distance between posterior scutellar setae. Propodeum with a

thin seta (Fig. 16, inset) anterior to propodeal spiracle, 2.6× length of metanotum, and bearing 6+5 crenulae (Fig. 17) on posterior margin.

Wings. Forewing (Fig. 18) 2.6× as long as wide; marginal setae 0.1× wing width. Costal cell 0.6× the length of marginal vein, with a row of fine setae and 4 coarse setae near apex; submarginal vein (Fig. 19) with 5 setae and 17 bullae; marginal vein with 10 setae along anterior margin; basal cell with about 40 dark setae. Hind wing hyaline, 4.7× as long as wide, with marginal setae 0.4× wing width. Measurements, length (width): forewing 870 (340); costal cell 170; submarginal vein 150; marginal vein 280; stigma vein 17.5; hind wing 660 (140); marginal setae of hind wing 50.

Legs (Fig. 20). Mesotibial spur slightly shorter than corresponding basitarsus. Length measurements: mesotibia 210; mesotibial spur 80; mesobasitarsus 85.

Metasoma (Fig. 21). Petiole strongly reticulated on central pigmented area just below the crenulae. Gt_{1–5} with reticulations on lateral sides, and bearing some setae on each reticulated area, setation as followings: Gt₁ with 3 setae on each side, Gt_{2–5} with 4 setae on each side respectively, Gt₆ with 10 setae between spiracles, Gt₇ with 17 setae, Gt₈ with 14 setae. Ovipositor originating from Gt₂, 1.9× as long as mesotibia, and slightly exerted. Second valvifer 3.9× as long as third valvula; the latter with some hyaline setae apically, and slightly shorter than mesobasitarsus. Length measurements: ovipositor 390; second valvifer 310; third valvula 80.

Male. Unknown.

Variation. Mandible bidentate, but a paratype specimen with mandible having a small denticulation attached to ventral tooth (Fig. 14). Scape 5.0–5.7× as long as wide, clava 3.0–3.6× as long as wide. Midlobe of mesoscutum bearing 12–15 setae. Forewing 2.4–2.7× as long as wide, hind wing 4.5–4.9× as long as wide. Posterior margin of propodeum with 6+5 to 6+6 crenulae (Figs 17, 22). Gt₈ bearing 10–14 setae. Ovipositor 1.6–2.1× as long as mesotibia.

Remarks. This species is similar to *Paraphytis vittatus* Compere in having a similar body colour. It can be separated from the latter by differences listed in the key. Apart from these differences, the new species has F3 obviously longer than wide (vs as long as or slightly wider than long), clava relatively slender, more than 3.0× (3.0–3.6×) as long as wide (vs about 2.5× as long as wide), propodeum bearing 6+5 to 6+6 crenulae on the posterior margin (vs only 4+4 to 4+5 crenulae).

Host. Unknown.

Etymology. From the Latin prefix *pseudo-*, and *vittatus* reference to the fact that this species is easily confused with *P. vittatus*.

Distribution. China (Xishuangbanna of Yunnan Province).

Acknowledgements

We would like to thank John Heraty and Jason Mottern for providing valuable comments on earlier drafts of this manuscript. This study was supported by the National Natural Science Foundation of China (Grant No. 31970396) to Hai-feng Chen, the

Doctoral Scientific Research Foundation of Langfang Normal University (Grant No. XBQ202034) and the project of Langfang Science and Technology Bureau (Grant No. 2020013024) to Ye Chen. We are grateful to Professor Shu-qiang Li (Chinese Academy of Sciences, Beijing) for providing the materials. Special thanks to Professor Mohammad Hayat (Aligarh Muslim University, Aligarh) for his kindly help of sending some papers by E-mail. We thank all specimen collectors.

References

- Compere H (1925) A new genus and species of Aphelinidae (Hymenoptera) from China. *Transactions of the American Entomological Society* 51(2): 129–133.
- Compere H (1936) Notes on the classification of the Aphelinidae with descriptions of new species. *University of California Publications in Entomology* 6(12): 277–322.
- Compere H (1955) A systematic study of the genus *Aphytis* Howard (Hymenoptera, Aphelinidae) with description of new species. *University of California Publications in Entomology* 10(4): 271–319.
- DeBach P, Rosen D (1976) Twenty new species of *Aphytis* (Hymenoptera: Aphelinidae) with notes and new combinations. *Annals of the Entomological Society of America* 69: 541–545. <https://doi.org/10.1093/aesa/69.3.541>
- Hayat M (1982) On the taxonomic status of *Syediella* (Hymenoptera: Aphelinidae). *Colemania* 1(3): 169–170.
- Hayat M (1998) Aphelinidae of India (Hymenoptera: Chalcidoidea): A taxonomic revision. *Memoirs on Entomology, International* 13: 1–416.
- Huang J (1994) *Systematic Studies on Aphelinidae of China* (Hymenoptera: Chalcidoidea). Chongqing Publishing House, Chongqing, 348 pp.
- Hymenoptera Anatomy Consortium (2020) Hymenoptera Anatomy Ontology Portal. <http://glossary.hymao.org> [accessed 8 July 2020]
- Kim JW, Heraty J (2012) A phylogenetic analysis of the genera of Aphelininae (Hymenoptera: Aphelinidae), with a generic key and descriptions of new taxa. *Systematic Entomology* 37: 479–549. <https://doi.org/10.1111/j.1365-3113.2012.00625.x>
- Noyes JS (1982) Collecting and preserving chalcid wasps (Hymenoptera: Chalcidoidea). *Journal of Natural History* 16: 315–334. <https://doi.org/10.1080/00222938200770261>
- Noyes JS (2019) Universal Chalcidoidea Database. <http://www.nhm.ac.uk/chalcidoids> [accessed September 2020]
- Rosen D, DeBach P (1979) *Species of Aphytis of the World*. Dr. W. Junk BV, Publishers, The Hague, 765 pp. <https://doi.org/10.1007/978-94-009-9603-8>
- Shafee SA (1970) A new genus of Aphelinidae recorded from Ootacumund (India) (Hym.). *Mushi* 43: 143–147.

A multilocus assessment reveals two new synonymies for East Asian *Cyclommatus* stag beetles (Coleoptera, Lucanidae)

Jiao Jiao Yuan^{1,2}, Dan Chen^{1,2}, Xia Wan^{1,2}

1 Department of Ecology, School of Resources and Engineering, Anhui University, 111 Jiulong Rd., Hefei 230601, China **2** Anhui Province Key Laboratory of Wetland Ecosystem Protection and Restoration, Hefei 230601, China

Corresponding author: Xia Wan (wanzia@ahu.edu.cn)

Academic editor: A. Frolov | Received 26 September 2020 | Accepted 31 January 2021 | Published 2 March 2021

<http://zoobank.org/23EF341F-3DAF-4D3C-8292-4AE87334E1B9>

Citation: Yuan JJ, Chen D, Wan X (2021) A multilocus assessment reveals two new synonymies for East Asian *Cyclommatus* stag beetles (Coleoptera, Lucanidae). ZooKeys 1021: 65–79. <https://doi.org/10.3897/zookeys.1021.58832>

Abstract

Cyclommatus scutellaris Möllenkamp, 1912, *Cyclommatus elsae* Kriesche, 1921 and *Cyclommatus tamdaoensis* Fujita, 2010 are East Asian stag beetle species with long-debated taxonomic relationships due to high intraspecific morphological variability. In this study, we applied multilocus phylogenetic analyses to reassess their relationships. Two mitochondrial genes (16S rDNA, COI) and two nuclear genes (28S rDNA, Wingless) were used to reconstruct the phylogeny through the Bayesian inference (BI) and Maximum Likelihood (ML) methods. Both topologies supported two clades: the clade *C. scutellaris* was sister to the clade (*C. elsae* + *C. tamdaoensis*) with the subclade *C. tamdaoensis* embedded in the subclade *C. elsae*. The Kimura 2-parameter (K2P) genetic distance analysis yielded a low mean value (≤ 0.035) among the three taxa, which was well below the minimum mean value between other *Cyclommatus* species (≥ 0.122). We also compared the accuracy and efficiency of two approaches, GMYC and ABGD, in delimitating the three lineages. The result shows that ABGD is a better approach than GMYC. Our molecular data recognizes the three species as different populations of a single species, ranging from Taiwan Island to the continent. Therefore, we propose two new junior synonymy for *C. scutellaris*: *C. tamdaoensis*, **syn. nov.** and *C. elsae* **syn. nov.**

Keywords

East Asia, Lucanidae, molecular phylogeny, morphology, new synonym, species delimitation

Introduction

The genus *Cyclommatus* Parry, 1863 (Lucanidae), includes some of the most striking stag beetles with enormous male mandibles and metallic body colorations. Many species display strong sexual dimorphism and male polymorphism, causing substantial confusion in morphological-based species delimitation. Phylogenetic analysis using molecular markers such as mitochondrial and nuclear genes can clarify many morphology-based species/subspecies' taxonomic positions. Yet, in *Cyclommatus*, only a few such studies have been performed for a limited number of species (Kim and Farrell 2015; Tsai and Yeh 2016) and only mitogenomic data of *Cyclommatus vitalisi* Pouillaude, 1913 from southwestern China have been reported (Liu et al. 2017). To our knowledge, no multilocus phylogenetic analysis has been applied to resolve taxonomic debates in this genus to date.

This study aims to resolve the long-debated taxonomic relationships among three *Cyclommatus* species, namely *C. scutellaris* Möllenkamp, 1912; *C. elsae* Kriesche, 1921 and *C. tamdaoensis* Fujita, 2010. *C. scutellaris* was first described by Möllenkamp (1912) and believed to be endemic to Taiwan Island. *Cyclommatus elsae* and *C. tamdaoensis* are distributed in southeastern China and the China-Vietnam border, respectively (Fig. 1). The three lineages' taxonomic relationships were frequently revised by different studies, resulting in inconsistent conclusions (Möllenkamp 1912; Kurosawa 1974; Bomans 1979; Lacroix 1988; Maes 1992; Fujita 2010; Schenk and Nguyen 2015). Most of these revisions, however, lack sufficient data support. For instance, Fujita (2010) treated *C. scutellaris* and *C. elsae* as valid species and described the new taxon *C. tamdaoensis* from northern Vietnam. More recently, Huang and Chen (2017) considered them three subspecies based on morphological characters and considered *C. princeps* Schenk & Nguyen, 2015 from northern Vietnam as a junior synonym of *C. tamdaoensis*. Both studies used some key morphological diagnostic traits showing a considerable degree of intraspecific variabilities, such as the stripes on the pronotum and the male genitalia. The black lateral stripes in male individuals of *C. elsae* display two forms: the complete-form extending to the anterior angle of the pronotum and the partly patched form along the margins [see pl. 194, figs 8–2–2, 8–2–4 in Huang and Chen (2017)]. The black median stripe shows three forms: ranging from the broadly diamond shape to the reduced midline, then disappearing completely [see pl. 194, figs 8–2–2, 8–2–4 in Huang and Chen (2017)]. The lateral stripes of male *C. scutellaris* are patched and the middle one is absent, while those of *C. tamdaoensis* are the complete-form and diamond-shaped, respectively [see pl. 194, figs 8–1, 8–3 in Huang and Chen (2017)]. Moreover, characters of male genitalia, including the median lobes and the basal piece, which are very important in lucanid taxonomy (Holloway 2007), show variability within the samples of *C. elsae*, *C. scutellaris* and *C. tamdaoensis* [see pl. 196 in Huang and Chen (2017)]. The protibiae of males of all three taxa consistently show yellow setae along 3/5 of their inner margin [see pl. 194, figs 8–1–1, 8–2–1, 8–3–1 in Huang and Chen (2017)]. Finally, the females of all three taxa look uniform with broad lateral stripes and a

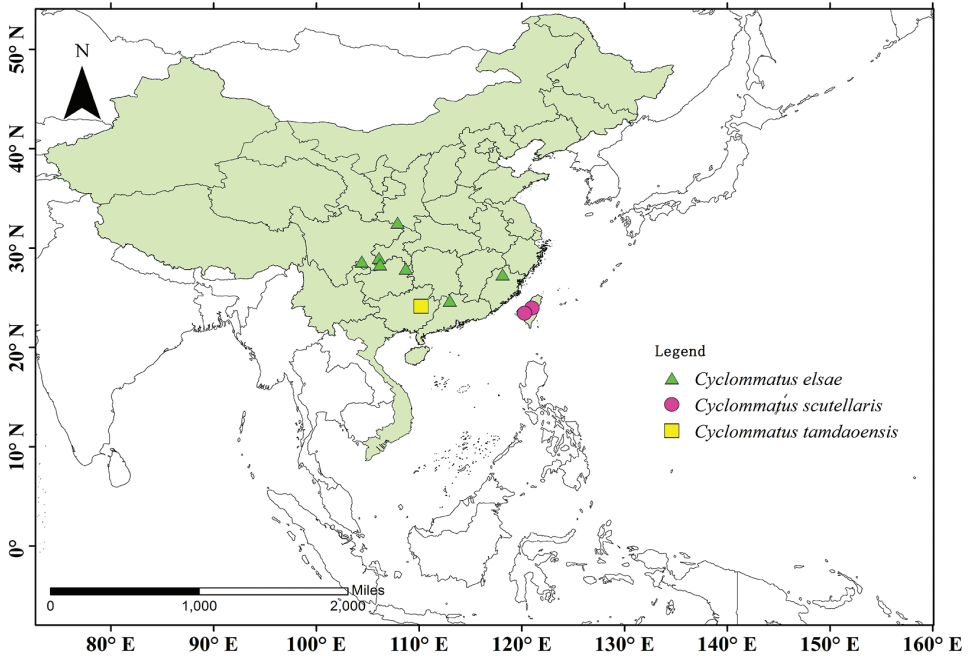


Figure 1. Collection localities of *C. scutellaris*, *C. elsaе* and *C. tamdaoensis*. The map is generated using ARCGIS 10.2 software based on the geospatial data from the National Geomatics Center of China.

diamond-shaped median stripe [see pl. 195 figs 8–1–4, 8–2–19, 8–3–4 in Huang and Chen (2017)].

The broadly distributed *C. elsaе* displays substantial morphological variability within its range. Populations from Mt. Nanling in Guangdong are morphologically almost identical to *C. scutellaris*, whereas the Mt. Simianhshan (Chongqing) population are nearly indistinguishable from *C. tamdaoensis*. The three groups' intraspecific variations and interlineage morphological convergence suggest that they are likely different populations of the same species. Yet, the lack of molecular data makes it difficult to clarify their conspecific status. In the current study, we applied the multilocus approach to recognize the three species' relationship. Our goal is to resolve this long-debated issue in *Cyclommatus* species phylogeny while testing the multilocus molecular approach's power and efficiency in resolving species delimitation problems for lucanid beetles.

Materials and methods

Taxon sampling

Thirty-three stag beetle specimens were examined, including 29 samples of *Cyclommatus* (15 *C. elsaе*; 9 *C. scutellaris*; 5 *C. tamdaoensis*) as in groups, and 4 samples as outgroups

(*C. albersi* Kraatz, 1894, *C. mniszzechi* (Thomson, 1856); *C. nagaii* Fujita, 2010; *C. vitalisi*). Voucher specimens and their extracted genomic DNA are deposited in the research collection at the Museum of Anhui University, China (Suppl. material 1: Table S1).

Laboratory protocols

The specimens were stored in 100% ethanol at -20 °C for molecular analysis. A small muscle was extracted from the sample using the Blood and Tissue Kit for total DNA extraction (Qiagen, Germany). Extracted DNA was stored at -20 °C until needed for the polymerase chain reaction (PCR). Four gene regions were targeted using the PCR. These regions included mitochondrial genes (16S rDNA, COI) and two nuclear genes (28S rDNA, Wingless). COI is often used in DNA barcoding because of its strong species identification ability (Han et al. 2016; Thormann et al. 2016). 16S rDNA is a conserved gene in animal mitochondria, which has a slow evolution rate. This gene is suitable for the study of distant taxa (Simon et al. 1994). COI and 16SrDNA are the most commonly used mitochondrial genes in the Lucanidae phylogeny (Tsai and Yeh 2016). 28S rDNA is relatively conservative in the evolutionary process and contains a highly variable region in the conserved sequence. It is also an excellent molecular marker to solve the phylogenetic relationship from species to families. Because wing pattern is a vital criterion for insect identification, Wingless is a necessary candidate gene for studying insect phylogeny. Still, the gene is only used in Lepidoptera and Coleoptera systematics (Liu and Jiang 2005). So, all specimens were sequenced for 16S rDNA, COI, 28S rDNA, and Wingless.

The primer sets used to amplify 16S rDNA, COI, 28S rDNA, and Wingless are shown in Table 1. PCR amplification reaction was carried out in a volume of 25 µL, in which 10 µM of each primer (forward and reverse) 1 µL, 2 µL template DNA, 12.5 µL 2×EasyTaq SuperMix (dye) and 8.5 µL sterile double distilled water (ddH₂O) constituted a final volume of 25µL. PCR conditions were as followed: initial denaturation at 94 °C for 2 minutes, followed by 35–37 cycles of denaturation at 94 °C for the 40 s and annealing at 52–58 °C for 50s, and elongation at 70 °C for 50s, and then a final extension step at 72 °C for 7 min. The length of the fragments determined the annealing temperature. For sequencing, we used the ABI PRISM BigDye terminator version 3.1

Table 1. List of the primer pairs and their respective reference used during the present study.

Gene	Primer name	Sequence (5'–3')	Reference
COI	COI-F1	CAACATTTATTTTGATTTTTTGG	Simon et al. (1994)
	COI-R1	TCCAATGCACTAATCTGCCATATTA	Simon et al. (1994)
16S rDNA	16S-F1	CCGGTTTGAACCTCAGATCATG	Hosoya et al. (2001)
	16S-R1	TAATTTATTGTACCTTGTGTATCAG	Hosoya et al. (2001)
28S rDNA	28SDD	GGGACCCGTCCTTGAAACAC	Monaghan et al. (2007)
	28SFF	TTACACACTCCTTAGCGGAT	Monaghan et al. (2007)
Wingless	Wg550F	ATGCGTCAGGARTGYAARTGYCAYGGYATGTC	Wild and Maddison (2008)
	WgAbRZ	CACTTNACYTCRCARCACCARTG	Wild and Maddison (2008)
	Wg578F	TGCACNGTGAARACYTGCTGGATG	Ward and Downie (2005)
	WgAbR	ACYTCGCAGCACCARTGGAA	Abouheif and Wray (2002)

sequencing kit (Life Technologies, USA) and cycle sequencing reactions were performed on ABI PRISM 3730xl automated sequencers (Life Technologies, USA) at Sangon Biotech Company, China. The sequences were submitted to GenBank with the accession number (Suppl. material 1: Table S1).

Phylogenetic analyses

Sequences were assembled in GENEIOUS PRIME 2019.1.1. All sequences were aligned in MEGA 7 (Kumar et al. 2016). Divergences among taxa were analyzed using MEGA 7.0 based on the Kimura 2-parameter model. DNA COI sequences of *Cyclommatus* were assembled for genetic distance analyses. Bayesian inference (BI) and Maximum Likelihood (ML) analyses were conducted using MRBAYES 3.2.7a and IQ-TREE web server, respectively. The BI and ML analysis was conducted on the CIPRES Science Gateway (Miller et al. 2011). Two independent chains starting from a random tree were run for 20,000 generations, sampling the tree every 10 generations. The initial 25% trees of each Markov Chain Monte Carlo (MCMC) chain were discarded as burn-in. A consensus tree was computed from the remaining 1500 trees combined from two runs, and the two runs converged at a maxdiff of less than 0.1. For ML analyses, the “automatic” option was set under the optimal evolution model, and the phylogenetic trees were constructed using an ultrafast bootstrap approximation approach with 10,000 replicates. Phylogenetic trees were viewed and edited in FIGTREE 1.4.4.

Divergence time analysis

Divergence time was estimated with a relaxed clock Exponential model (Drummond and Rambaut 2007) in BEAST 2.6.0 (Bouckaert et al. 2014). The MCMC chain was run for 8.5×10^8 generations, with four independent runs. Substitution rates of 1.77% per lineage in a million years (Myr) for COI combining with 0.54%/lineage/Myr for 16S rDNA have been suggested optimally for beetles (Papadopoulou et al. 2010). The resultant BEAST log files were viewed using TRACER 1.7 (Rambaut et al. 2018) to analyze the output results of the Effective Sample Size (ESS) for the posterior distribution of estimated parameter values. With a 25% burn-in threshold, all post-burn-in trees from the four independent runs were combined using the software LOG COMBINER 2.6.0 (Bouckaert et al. 2014). TREE ANNOTATOR 2.5.1 (Bouckaert et al. 2014) was used to summarize information (i.e., Nodal posterior probabilities, posterior estimates and highest posterior density limits) from the individual post-burn-in trees onto a single maximum clade credibility (MCC) tree. The summarized information was visualized on the MCC tree using FIGTREE 1.4.4.

Species delimitation

We performed species delimitation using Automatic Barcode Gap Discovery (ABGD) and Generalized Mixed Yule Coalescent (GMYC) methods. The ABGD detects a gap

in divergence distribution, which corresponds to differences between intraspecific and interspecific distances. When a gap exists, the process works well for species delimitation (Puillandre et al. 2012a). The ABGD analyses were performed at the webserver (<https://bioinfo.mnhn.fr/abi/public/abgd/abgdweb.html>). The following setting was used: steps (20), distance Kimura (K80) TS/TV (2.0), other parameter values employed defaults. GMYC delimits distinct genetic clusters by optimizing the set of nodes defining the transitions between inter- and intraspecific processes (Pons et al. 2006). The analysis was conducted using BEAST 2.6.0 under a relaxed clock Exponential model. ESS values assessed convergence. A burn-in with 25% was set to obtain an optimal consensus tree. The resulting tree was then used to analyze the data under the GMYC species delimitation approach in the software R with the package ‘splits’ using the single-threshold method (Ezard et al. 2015).

Results

Phylogenetic relationships

The BI and ML analysis showed consistent topology with a highly supported backbone (Fig. 2; Suppl. material 2: Fig. S1). The clade *C. scutellaris* was sister to *C. elsae* + *C. tamdaoensis* (Bayesian posterior probability, BPP = 1, Maximum Likelihood Bootstrap, MLB = 100). And the subclade *C. tamdaoensis* embedded in *C. elsae* (BPP = 0.7, MLB = 76). *Cyclommatus scutellaris* was an early branch in the three taxa and the species was monophyletic.

Genetic distances

The genetic distances using the COI gene were calculated among the three taxa. The mean genetic distances between the *C. scutellaris*, *C. elsae* and *C. tamdaoensis* were no more than 0.035 (Table 2). The numbers were well below the minimum mean genetic distances of 0.122 among interspecific taxa of *Cyclommatus*.

Divergence time analysis

Based on the COI gene and 16S rDNA gene, calibration time was analyzed to describe these taxonomically controversial species’ possible differentiation history. The analysis under BI converged well as all parameters had ESS values above 200. The mean divergence age estimates and 95% High Posterior Density (HPD) for nodes of interest based on the BEAST analysis are presented in Fig. 3, and Suppl. material 3: Fig. S2. Among the three taxa, *C. scutellaris* diverged during the Middle Pleistocene circa 1.23 million years ago (Mya) (95% HPD: 0.58–2.28 Mya). Within the clade *C. elsae* + *C. tamdaoensis*, the crown node’s age estimate was dated to be 0.62 Mya (95% HPD: 0.32–1.06 Mya) in the Late Pleistocene. The age of *C. tamdaoensis* was estimated to be 0.49 Mya (95% HPD: 0.27–0.82 Mya) in the Late Pleistocene.

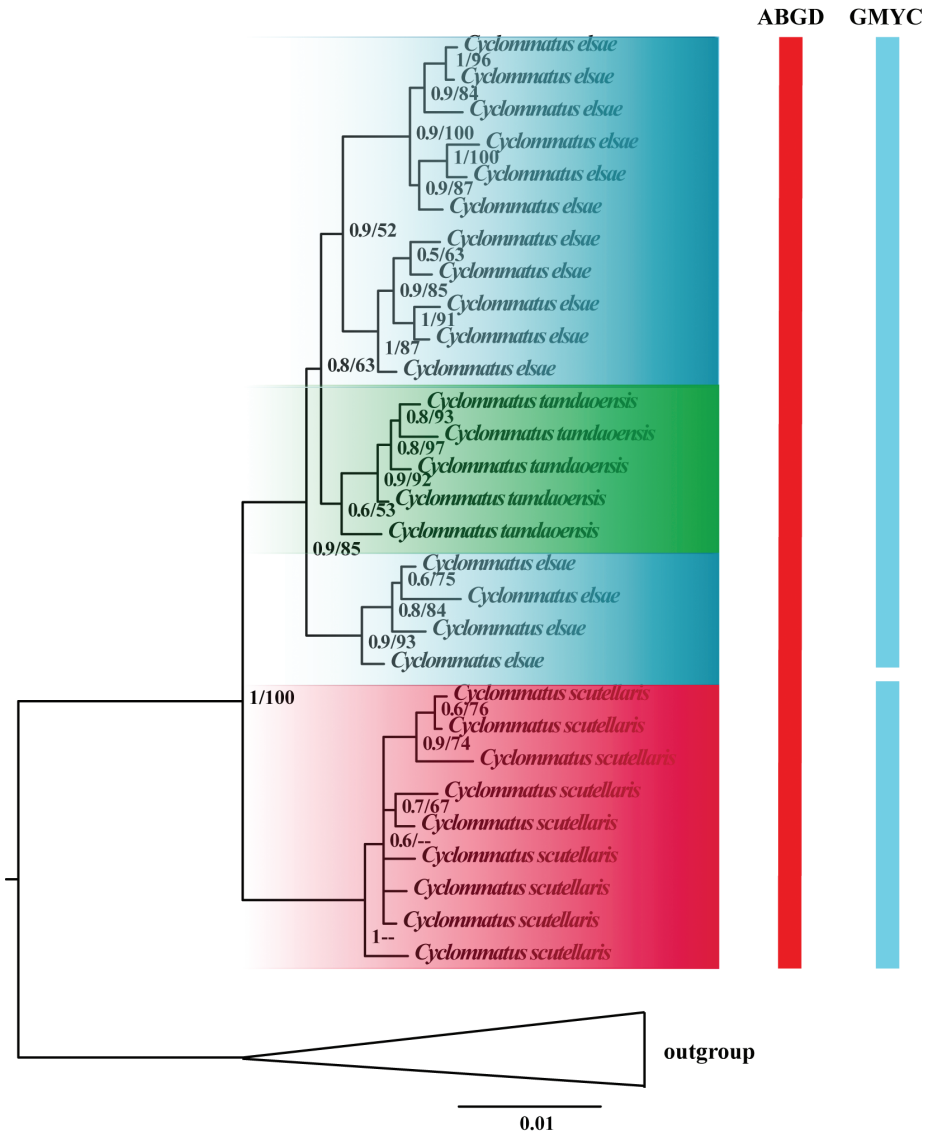


Figure 2. Bayesian topology showing the relationships within *C. scutellaris*, *C. elsae*, *C. tamdaoensis* and outgroups. Values next to each node represent Bayesian posterior probabilities (first number) and maximum likelihood bootstrap support (second number). The phylogenetic tree is based on Bayesian inference analysis of concatenated DNA sequence data from 16S rDNA, 28S rDNA, COI and Wingless. The columns on the right show numbers of entities identified by the ABGD, GMYC.

Species delimitation

Two species delimitation methods were employed to evaluate which one was most suitable for multilocus phylogenetic analyses. ABGD analyses suggested the three taxa were one molecular operational taxonomic unit (MOTU), whereas GMYC divided *C. scutellaris*, *C. elsae* and *C. tamdaoensis* into two MOTUs (Fig. 2).

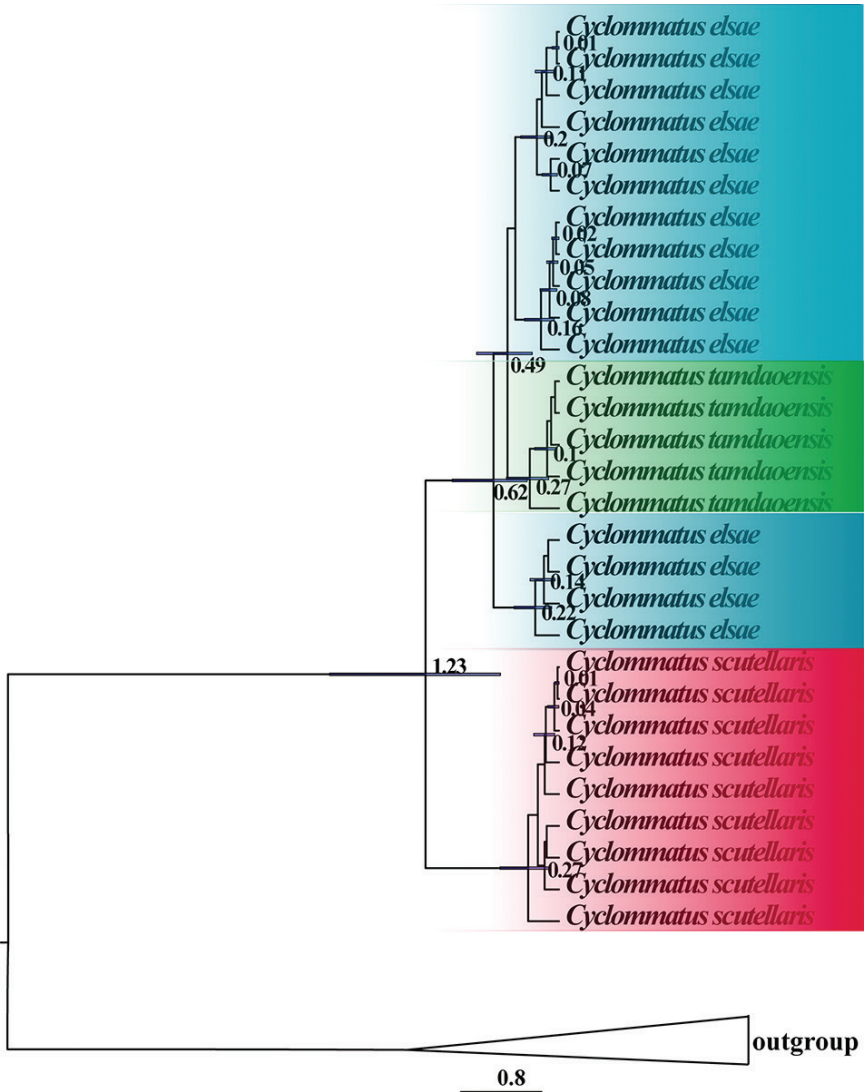


Figure 3. Maximum clade credibility time-tree obtained from BEAST based on COI and 16S rDNA. Divergence time estimates are represented next to the nodes (in millions of years) with horizontal bars indicating 95% highest posterior density intervals.

Table 2. The mean genetic distances among all the taxa (Kimura 2-parameter)

	1	2	3	4	5	6
<i>C. albersi</i>						
<i>C. elsae</i>	0.159					
<i>C. mniszecchi</i>	0.166	0.164				
<i>C. nagaii</i>	0.142	0.124	0.175			
<i>C. scutellaris</i>	0.166	0.035	0.169	0.129		
<i>C. tamdaoensis</i>	0.155	0.016	0.158	0.122	0.031	
<i>C. vitalisi</i>	0.152	0.150	0.145	0.146	0.159	0.146

Taxonomic account

Cyclommatus scutellaris Möllenkamp, 1912

Cyclommatus scutellaris Möllenkamp, 1912: 7.

Cyclommatus elsae Kriesche, 1921: 95. syn. nov.

Cyclommatus tamdaoensis Fujita, 2010:14. syn. nov.

Cyclommatus princeps Schenk & Nguyen, 2015: 7. (Synonymized as a junior synonym of *Cyclommatus tamdaoensis* by Huang and Chen 2017: 193)

Material examined. CHINA • 1 male; Yunnan Province, Shuifu County; 27 Jul. 2010; JS Xu and LX Chang leg. • 1 male; Shaanxi Province, Zhenba County; 10 Jul. 1996. • 3 males; Chongqing Province, Mt. Simianshan; 29 Aug. 2014. • 3 males; Guizhou Province, Mt. Fanjingshan; 29 Jul. 2014; YF Wu. • 1 male; Guizhou Province, Xishui County, 18 Jul. 2015, LX Zhu. • 1 male; Fujian Province, Mt. Wuyishan; 18 Jul. 2011; Q Zhang and YY Cao. • 1 male; same locality as for preceding; 18 Aug. 2010; F Zhong and XY Hu. • 3 males; Taiwan Island; 29 Aug. 1995. • 1 male; same locality as for preceding; 17 May 2008. • 1 male; same locality as for preceding; 5 Oct. 2008. • 2 males; same locality as for preceding; 20 Jul. 2010; • 2 males; same locality as for preceding; 21 Jul. 2011. • 3 males; Guangdong Province, Mt. Nanling; 18 Aug. 2010; HY Liu. • 1 male; same locality as for preceding; 9 Aug. 2011, F Zhong; • 4 males; Guangxi Autonomous Region, Jinxiu County; 18 Jul. 2012. • 1 male; same locality as for preceding; 28 Jun. 2013.

Diagnosis. The species is characterized in the male by the matt dorsal surface of the entire body and the long seta-range on the inner margin of the protibial, and in the female by the elytra usually without black stripes. The female can be distinguished from other members of *Cyclommatus* by the following combination of characters: 1) ground color of the dorsal surface of the body redder; 2) canthus often short, with lateral end blunt, and usually with a convex or straight outer margin; 3) central black band on the pronotum clearly defined and often narrower than the lateral orange band (Huang and Chen 2017).

Distribution. China (Yunnan, Shaanxi, Chongqing, Guizhou, Fujian, Taiwan Island, Guangdong, Guangxi).

Discussion

This study presents consistent phylogenetic relationships inferred by the BI and ML methods. The trees' identical topology strongly supports that *C. scutellaris* is sister to the clade *C. elsae* + *C. tamdaoensis*. The nested structure of *C. elsae* and *C. tamdaoensis* suggests that the two nominal taxa should be treated as one species. The genetic distance also indicates that *C. elsae* and *C. tamdaoensis* are most likely two continental populations of the Taiwanese species *C. scutellaris*.

The divergence time estimation shows that *C. scutellaris* began to diverge from the Middle Pleistocene with subsequent deep genetic isolation during the Late Pleistocene. During the glacial maxima, a land bridge facilitated the contraction of the geographical ranges of some species southwards into Taiwan (Kawamura et al. 2016). Once the glaciations ended, the rising sea levels resulted in vicariant isolation. The relict populations might have retreated to the montane habitat of Taiwan Island, causing the present disjunct distributions (Päckert et al. 2011; Wang et al. 2013). Many studies interpreted the global cooling and aridification, the Qinghai–Tibet Plateau uplift and the abrupt climate change in East Asia during the Neogene and Quaternary as responsible for the speciation, intraspecific divergence, genetic diversification, and significant phylogeographic break between the western and eastern clade in Chinese fauna (Meng et al. 2015; Qiu et al. 2017; Ye et al. 2017; Zhou et al. 2017).

Accurate species delimitations are critical in many biology areas, such as conservation biology (designating endangered species) and evolutionary biology (describing diversification patterns). Traditionally, species are identified and described by morphological characters. However, using morphological data alone may underestimate the number of species (Yang and Rannala 2010). Therefore, molecular data are used to delimitate species in the present study. However, GMYC and ABGD methods obtained different results. GMYC has been developed to delimit species according to single-locus data, which has a strong theoretical basis. Although the method is based on a reliable phylogenetic framework, it largely depends on the ultrametric gene tree's correctness. Errors in the framework underpinning the analysis may affect the final results (Kekkonen and Hebert 2014). Also, GMYC usually over-splits species, mainly due to low genetic divergence between lineages and overlap of interspecific and intraspecific divergences, or due to lack of reciprocal monophyly between sister clades (Talavera et al. 2013; Pentinsaari et al. 2016; Stokkan et al. 2018). Evaluations of the accuracy and efficiency of ABGD conducted by different researchers reached a consensus that ABGD is more conservative and faster than other methods (Puillandre et al. 2012a; Puillandre et al. 2012b; Kekkonen and Hebert 2014; Guillemin et al. 2016). Our results also produced a consistent conclusion. ABGD produced one MOTU, which agrees with the number of species defined based on multilocus phylogenetic analyses.

In summary, our study resolved a long-standing debate on species recognition in the genus *Cyclommatus* while illustrating the necessity of employing multiple data types, both morphological and molecular, for efficient and accurate species delimitation in taxa with a high degree of phenotypic convergence and variations.

Acknowledgements

We want to express our gratitude to Dr Jian-Yue Qiu, Dr Hao Xu, Dr Yun-Fei Wu, Prof. Ai-Min Shi and Mr Chang-Chin Chen for their kind donation of specimens. This work was supported by research grants from the National Natural Science Foundation of China (No. 31872276; 31572311).

References

- Abouheif E, Wray GA (2002) Evolution of the gene network underlying wing polyphenism in ants. *Science* 297: 249–252. <https://doi.org/10.1126/science.1071468>
- Bomans HE (1979) Contribution à l'étude des Coléoptères Lucanides. Description de l'allo-type de *Cyclommatus elsa* Kriesche. *Bulletin et Annales de la Société Royale d'Entomologie de Belgique* 115: 194–196.
- Bouckaert R, Heled J, Kuhnert D, Vaughan T, Wu CH, Xie D, Suchard MA, Rambaut A, Drummond AJ (2014) BEAST 2: A software platform for Bayesian evolutionary analysis. *PLoS Computational Biology* 10: e1003537. <https://doi.org/10.1371/journal.pcbi.1003537>
- Drummond AJ, Rambaut A (2007) BEAST: Bayesian evolutionary analysis by sampling trees. *BMC Evolutionary Biology* 7: e214. <https://doi.org/10.1186/1471-2148-7-214>
- Ezard T, Fujisawa T, Barraclough T (2015) R package splits: Species' limits by threshold statistics, version 1.0–18/r45. <http://R-Forge.R-project.org/projects/splits/>
- Fujita H (2010) *The Lucanid Beetles of the World*. Mushi-sha, Tokyo, 472 pp.
- Guillemin ML, Contreras-Porcía L, Ramírez ME, Macaya EC, Contador CB, Woods H, Wyatt C, Brodie J (2016) The bladed Bangiales (Rhodophyta) of the South Eastern Pacific: Molecular species delimitation reveals extensive diversity. *Molecular Phylogenetics and Evolution* 94: 814–826. <https://doi.org/10.1016/j.ympev.2015.09.027>
- Han T, Lee W, Lee S, Park IG, Park H (2016) Reassessment of Species Diversity of the Subfamily Denticollinae (Coleoptera: Elateridae) through DNA Barcoding. *PLoS ONE* 11: e0148602. <https://doi.org/10.1371/journal.pone.0148602>
- Holloway BA (2007) Lucanidae (Insecta: Coleoptera). *Fauna of New Zealand* 61: 1–254.
- Hosoya T, Honda M, Araya K (2001) Genetic variations of 16S rRNA gene observed in *Ceruchus lignarius* and *Dorcus rectus rectus* (Coleoptera: Lucanidae). *Entomological Science* 4: 335–344.
- Huang H, Chen CC (2017) *Stag Beetles of China III*. Formosa Ecological Company, Taiwan, 540 pp.
- Kawamura A, Chang CH, Kawamura Y (2016) Middle Pleistocene to Holocene mammal faunas of the Ryukyu Islands and Taiwan: An updated review incorporating results of recent research. *Quaternary International* 397: 117–135. <https://doi.org/10.1016/j.quaint.2015.06.044>
- Kekkonen M, Hebert PDN (2014) DNA barcode-based delineation of putative species: Efficient start for taxonomic workflows. *Molecular Ecology Resources* 14: 706–715. <https://doi.org/10.1111/1755-0998.12233>
- Kim SI, Farrell BD (2015) Phylogeny of world stag beetles (Coleoptera: Lucanidae) reveals a Gondwanan origin of Darwin's stag beetle. *Molecular Phylogenetics and Evolution* 86: 35–48. <https://doi.org/10.1016/j.ympev.2015.02.015>
- Kraatz G (1894) *Cyclommatus albersi* nov. sp., Hirschkäfer von Birma. *Deutsche Entomologische Zeitschrift* 1894: 268–269. <https://doi.org/10.1002/mmnd.48018940522>
- Kriesche R (1921) Zur Kenntnis der Lucaniden. *Archiv für Naturgeschichte* 86: 92–107.
- Kumar S, Stecher G, Tamura K (2016) MEGA7: Molecular evolutionary genetics analysis version 7.0 for bigger datasets. *Molecular Biology and Evolution* 33: 1870–1874. <https://doi.org/10.1093/molbev/msw054>

- Kurosawa Y (1974) A stag-beetle new to the Formosan fauna (Coleoptera: Lucanidae). Bulletin of the National Science Museum. Series A: Zoology 17: 103–104.
- Lacroix JP (1988) Descriptions de Coleoptera Lucanidae nouveaux ou peu connus (6eme note). Bulletin de la Société Sciences Nat 1988: 5–7.
- Liu DF, Jiang GF (2005) The application of nuclear genes sequences in insect molecular systematics. Zoological Systematics 30: 484–492. <https://doi.org/10.3969/j.issn.1000-0739.2005.03.007>
- Liu J, Li C, You S, Wan X (2017) The first complete mitogenome of *Cyclommatus* stag beetles (Coleoptera: Lucanidae) with the phylogenetic implications. Entomotaxonomia 39: 294–299.
- Maes JM (1992) Lista de los Lucanidae (Coleoptera) del Mundo. Revista Nicaraguense de Entomologia 22: 1–121.
- Meng HH, Gao XY, Huang JF, Zhang ML (2015) Plant phylogeography in arid Northwest China: Retrospectives and perspectives. Journal of Systematics and Evolution 53: 33–46. <https://doi.org/10.1111/jse.12088>
- Miller MA, Pfeiffer W, Schwartz T (2011) The CIPRES Science Gateway: A community resource for phylogenetic analyses. In: Cordero Rivera A (Ed.) Proceedings of the 2011 Tera-Grid Conference: Extreme Digital Discovery. Association for Computing Machinery, New York, NY, United States, Article 41: 1–8. <https://doi.org/10.1145/2016741.2016785>
- Möllenkamp W (1912) H. Sauter's Formosa Ausbeute. Lucanidae. (Coleoptera). Entomologische Mitteilungen 1: 6–8. <https://doi.org/10.5962/bhl.part.25903>
- Monaghan MT, Inward DJG, Hunt T, Vogler AP (2007) A molecular phylogenetic analysis of the Scarabaeinae (dung beetles). Molecular Phylogenetics and Evolution 45: 674–692. <https://doi.org/10.1016/j.ympev.2007.06.009>
- Päckert M, Martens J, Sun YH, Severinghaus LL, Nazarenko AA, Ting J, Töpfer T, Tietze DT (2011) Horizontal and elevational phylogeographic patterns of Himalayan and Southeast Asian forest passerines (Aves: Passeriformes). Journal of Biogeography 39: 556–573. <https://doi.org/10.1111/j.1365-2699.2011.02606.x>
- Papadopoulou A, Anastasiou I, Vogler AP (2010) Revisiting the insect mitochondrial molecular clock: The Mid-Aegean trench calibration. Molecular Biology and Evolution 27: 1659–1672. <https://doi.org/10.1093/molbev/msq051>
- Parry FJS (1863) A few remarks upon Mr. James Thomson's catalogue of Lucanidae, published in the 'Annales de la Société Entomologique de France, 1862.' Transactions of the Royal Entomological Society of London 1: 442–452. <https://doi.org/10.1111/j.1365-2311.1863.tb01291.x>
- Pentinsaari M, Vos R, Mutanen M (2016) Algorithmic single-locus species delimitation: Effects of sampling effort, variation and nonmonophyly in four methods and 1870 species of beetles. Molecular Ecology Resources 17: 393–404. <https://doi.org/10.1111/1755-0998.12557>
- Pons J, Barraclough TG, Gomez-Zurita J, Cardoso A, Duran DP, Hazell S, Kamoun S, Sumlin WD, Vogler AP (2006) Sequence-Based Species Delimitation for the DNA Taxonomy of Undescribed Insects. Systematic Biology 55: 595–609. <https://doi.org/10.1080/10635150600852011>
- Pouillaude I (1913) Note sur quelques Lucanidae d'Indo-Chine. Insecta, revue illustree d'Entomologie 3: 332–337.

- Puillandre N, Lambert A, Brouillet S, Achaz G (2012a) ABGD, automatic barcode gap discovery for primary species delimitation. *Molecular Ecology* 21: 1864–1877. <https://doi.org/10.1111/j.1365-294X.2011.05239.x>
- Puillandre N, Modica MV, Zhang Y, Sirovich L, Boisselier MC, Cruaud C, Holford M, Samadi S (2012b) Large-scale species delimitation method for hyperdiverse groups. *Molecular Ecology* 21: 2671–2691. <https://doi.org/10.1111/j.1365-294X.2012.05559.x>
- Qiu YX, Lu QX, Zhang YH, Cao YN (2017) Phylogeography of East Asia's Tertiary relict plants: Current progress and future prospects. *Biodiversity Science* 25: 136–146. <https://doi.org/10.17520/biods.2016292>
- Rambaut A, Drummond AJ, Xie D, Baele G, Suchard MA (2018) Posterior summarization in bayesian phylogenetics using Tracer 1.7. *Systematic Biology* 67: 901–904. <https://doi.org/10.1093/sysbio/syy032>
- Schenk KD, Nguyen TQ (2015) Description of two new taxa of the genus *Cyclommatus* Parry, 1863 from Central Vietnam (Coleoptera: Lucanidae). *Beetles World* 11: 7–11.
- Simon C, Frati F, Beckenbach A, Crespi B, Liu H, Flook P (1994) Evolution, weighting, and phylogenetic utility of mitochondrial gene sequences and a compilation of conserved polymerase chain reaction primers. *Annals of the Entomological Society of America* 87: 651–701. <https://doi.org/10.1093/aesa/87.6.651>
- Stokkan M, Jurado-Rivera JA, Oromí P, Juan C, Jaume D, Pons J (2018) Species delimitation and mitogenome phylogenetics in the subterranean genus *Pseudoniphargus* (Crustacea: Amphipoda). *Molecular Phylogenetics and Evolution* 127: 988–999. <https://doi.org/10.1016/j.ympev.2018.07.002>
- Talavera G, Dincă V, Vila R (2013) Factors affecting species delimitations with the GMYC model: Insights from a butterfly survey. *Methods in Ecology and Evolution* 4: 1101–1110. <https://doi.org/10.1111/2041-210X.12107>
- Thomson J (1856) Description de quatre Lucanides nouveaux de ma collection, précédée du catalogue des Coléoptères lucanoïdes de Hope (1845), et de l'arrangement méthodique adopté par Lacordaire pour sa famille des Pectinicornes. *Revue et magasin de zoologie pure et appliquée* 8: 516–528.
- Thormann B, Ahrens D, Marín Armijos D, Peters MK, Wagner T, Wägele JW (2016) Exploring the Leaf Beetle Fauna (Coleoptera: Chrysomelidae) of an Ecuadorian Mountain Forest Using DNA Barcoding. *PLoS ONE* 11: e0148268. <https://doi.org/10.1371/journal.pone.0148268>
- Tsai CL, Yeh WB (2016) Subspecific differentiation events of montane stag beetles (Coleoptera: Lucanidae) endemic to Formosa island. *PLoS ONE* 11: e0156600. <https://doi.org/10.1371/journal.pone.0156600>
- Wang W, McKay BD, Dai C, Zhao N, Zhang R, Qu Y, Song G, Li SH, Liang W, Yang X, Pasquet E, Lei F (2013) Glacial expansion and diversification of an East Asian montane bird, the green-backed tit (*Parus monticolus*). *Journal of Biogeography* 40: 1156–1169. <https://doi.org/10.1111/jbi.12055>
- Ward PS, Downie DA (2005) The ant subfamily Pseudomyrmecinae (Hymenoptera: Formicidae): Phylogeny and evolution of big-eyed arboreal ants. *Systematic Entomology* 30: 310–335. <https://doi.org/10.1111/j.1365-3113.2004.00281.x>

- Wild AL, Maddison DR (2008) Evaluating nuclear protein-coding genes for phylogenetic utility in beetles. *Molecular Phylogenetics and Evolution* 48: 877–891. <https://doi.org/10.1016/j.ympev.2008.05.023>
- Yang Z, Rannala B (2010) Bayesian species delimitation using multilocus sequence data. *Proceedings of the National Academy of Sciences of the United States of America* 107: 9264–9269. <https://doi.org/10.1073/pnas.0913022107>
- Ye JW, Zhang Y, Wang XJ (2017) Phylogeographic breaks and the mechanisms of their formation in the Sino-Japanese floristic region. *Chinese Journal of Plant Ecology* 41: 1003–1019. <https://doi.org/10.17521/cjpe.2016.0388>
- Zhou Z, Huang J, Ding W (2017) The impact of major geological events on Chinese flora. *Biodiversity Science* 25: 123–135. <https://doi.org/10.17520/biods.2016120>

Supplementary material 1

Table S1. A list of specimens' voucher information and GenBank accession numbers used in this study

Authors: Jiao Jiao Yuan

Data type: phylogenetic

Copyright notice: This dataset is made available under the Open Database License (<http://opendatacommons.org/licenses/odbl/1.0/>). The Open Database License (ODbL) is a license agreement intended to allow users to freely share, modify, and use this Dataset while maintaining this same freedom for others, provided that the original source and author(s) are credited.

Link: <https://doi.org/10.3897/zookeys.1021.58832.suppl1>

Supplementary material 2

Figure S1. Bayesian topology showing the relationships within *C. scutellaris*, *C. elsae*, *C. tamdaoensis* and outgroups

Authors: Jiao Jiao Yuan

Data type: phylogenetic

Explanation note: The figure also indicates outgroups and accession numbers. The columns on the right show numbers of entities identified by the ABGD, GMYC.

Copyright notice: This dataset is made available under the Open Database License (<http://opendatacommons.org/licenses/odbl/1.0/>). The Open Database License (ODbL) is a license agreement intended to allow users to freely share, modify, and use this Dataset while maintaining this same freedom for others, provided that the original source and author(s) are credited.

Link: <https://doi.org/10.3897/zookeys.1021.58832.suppl2>

Supplementary material 3

Figure S2. Maximum clade credibility time-tree based on COI and 16S rDNA

Authors: Jiao Jiao Yuan

Data type: phylogenetic

Explanation note: Age estimates are indicated at the nodes (Mya). The outgroups are shown in the figure.

Copyright notice: This dataset is made available under the Open Database License (<http://opendatacommons.org/licenses/odbl/1.0/>). The Open Database License (ODbL) is a license agreement intended to allow users to freely share, modify, and use this Dataset while maintaining this same freedom for others, provided that the original source and author(s) are credited.

Link: <https://doi.org/10.3897/zookeys.1021.58832.suppl3>

A new species of the Asian leaf litter toad genus *Leptobrachella* Smith, 1925 (Anura, Megophryidae) from northwest Guizhou Province, China

Yan-Lin Cheng^{1*}, Sheng-Chao Shi^{2*}, Jiaqi Li³, Jing Liu¹, Shi-Ze Li^{1,2}, Bin Wang^{1,2}

1 Department of Resources and Environment, Moutai Institute, Renhuai 564500, China **2** Chengdu Institute of Biology, Chinese Academy of Sciences, Chengdu 610041, China **3** Nanjing Institute of Environmental Sciences, Ministry of Ecology and Environment of China, Nanjing 210042, China

Corresponding author: Shi-Ze Li (976722439@qq.com); Bin Wang (wangbin@cib.ac.cn)

Academic editor: A. Ohler | Received 13 November 2020 | Accepted 4 February 2021 | Published 2 March 2021

<http://zoobank.org/0C8921F1-7D8B-417C-B10F-55787C19E501>

Citation: Cheng Y-L, Shi S-C, Li J, Liu J, Li S-Z, Wang B (2021) A new species of the Asian leaf litter toad genus *Leptobrachella* Smith, 1925 (Anura, Megophryidae) from northwest Guizhou Province, China. ZooKeys 1021: 81–107. <https://doi.org/10.3897/zookeys.1021.60729>

Abstract

A new species of the Asian leaf litter toad genus *Leptobrachella* is described from Guizhou Province, China. Molecular phylogenetic analyses support the new species as an independent lineage deeply nested in the *Leptobrachella* clade. The new species is distinguished from its congeners by a combination of the following morphological characters: body size medium (SVL 29.7–31.2 mm in five adult males); dorsal skin shagreened, some of the granules forming longitudinal short skin ridges; tympanum distinctly discernible, slightly concave; supra-axillary, femoral, pectoral and ventrolateral glands distinctly visible; absence of webbing and lateral fringes on fingers; toes with narrow lateral fringes but without webbing; heels overlapping when thighs are positioned at right angles to the body; tibia-tarsal articulation reaching the middle of eye when leg stretched forward. The discovery highlighted the underestimated species diversity in the *Leptobrachella* toads in southwestern China.

Keywords

Leptobrachella jinshaensis sp. nov., molecular phylogenetic analyses, morphology, Taxonomy

* These authors have contributed equally to this work.

Introduction

The Asian leaf litter toads of the genus *Leptobrachella* Smith, 1925 (Anura, Megophryidae) are widely distributed from southern China west to northeastern India and Myanmar, through mainland Indochina to peninsular Malaysia and the island of Borneo (Frost 2020). Many species in this genus have been classified into *Leptolalax* Dubois, 1983 (e.g., Fei et al. 2009, 2012), but Chen et al. (2018) placed *Leptolalax* as a junior synonym of *Leptobrachella* based on large-scale molecular analyses. Currently, the genus *Leptobrachella* contains 82 species (Frost 2020) but a series of cryptic species is still suggested by molecular phylogenetic analyses (Chen et al. 2018). To date, 25 species of this genus have been recorded in China, i.e., *L. alpina* (Fei, Ye & Li, 1990) and *L. bourreti* (Dubois, 1983) from Yunnan and Guangxi; *L. eos* (Ohler, Wollenberg, Grosjean, Hendrix, Vences, Ziegler & Dubois, 2011), *L. nyx* (Ohler, Wollenberg, Grosjean, Hendrix, Vences, Ziegler & Dubois, 2011), *L. pelodytoides* (Boulenger, 1893), *L. tengchongensis* (Yang, Wang, Chen & Rao, 2016), *L. yingjiangensis* (Yang, Zeng & Wang, 2018), *L. feii* (Chen, Yuan & Che, 2020), *L. flaviglandulosa* (Chen, Wang & Che, 2020), and *L. niveimontis* (Chen, Poyarkov, Yuan & Che, 2020) from Yunnan; *L. laui* (Sung, Yang & Wang, 2014) and *L. yunkaiensis* Wang, Li, Lyu & Wang, 2018 from Guangdong and Hong Kong; *L. liui* (Fei & Ye, 1990) from Fujian, Jiangxi, Guangdong, Guangxi, Hunan, and Guizhou; *L. oshanensis* (Liu, 1950) from Gansu, Sichuan, Chongqing, Guizhou, and Hubei; *L. purpuraventra* (Wang, Li, Li, Chen & Wang, 2019), *L. bijie* (Wang, Li, Li, Chen & Wang, 2019), *L. chishuiensis* (Li, Liu, Wei & Wang, 2020), and *L. suiyangensis* (Luo, Xiao, Gao & Zhou, 2020) from Guizhou; *L. purpurus* (Yang, Zeng & Wang, 2018), *L. ventripunctata* (Fei, Ye & Li, 1990) from Guizhou and Yunnan; *L. mangshanensis* (Hou, Zhang, Hu, Li, Shi, Chen, Mo & Wang, 2018) from Hunan; and *L. sungi* (Lathrop, Murphy, Orlov & Ho, 1998), *L. maoershanensis* (Yuan, Sun, Chen, Rowley & Che, 2017), *L. shangsiensis* (Chen, Liao, Zhou & Mo, 2019), and *L. wubuangmontis* (Wang, Yang & Wang, 2018) from Guangxi. Among them, ten *Leptobrachella* species occur in Guizhou Province, China, highlighting the high species diversity of the genus in this region.

In recent years, we collected some specimens of *Leptobrachella* from northwest Guizhou Province, China. Molecular phylogenetic analyses, morphological comparisons, and bioacoustics data consistently indicated these specimens as an undescribed species of *Leptobrachella*. We describe it herein as a new species.

Materials and methods

Specimens

Five adult males of the new species were collected on 16 May 2020 from Lengshuihe Nature Reserve, Jinsha County, Guizhou Province, China (Fig. 1; Table 1). After taking photographs, toads were euthanised using isoflurane, and then the specimens were fixed in 10% buffered formalin. Tissue samples were taken and preserved separately

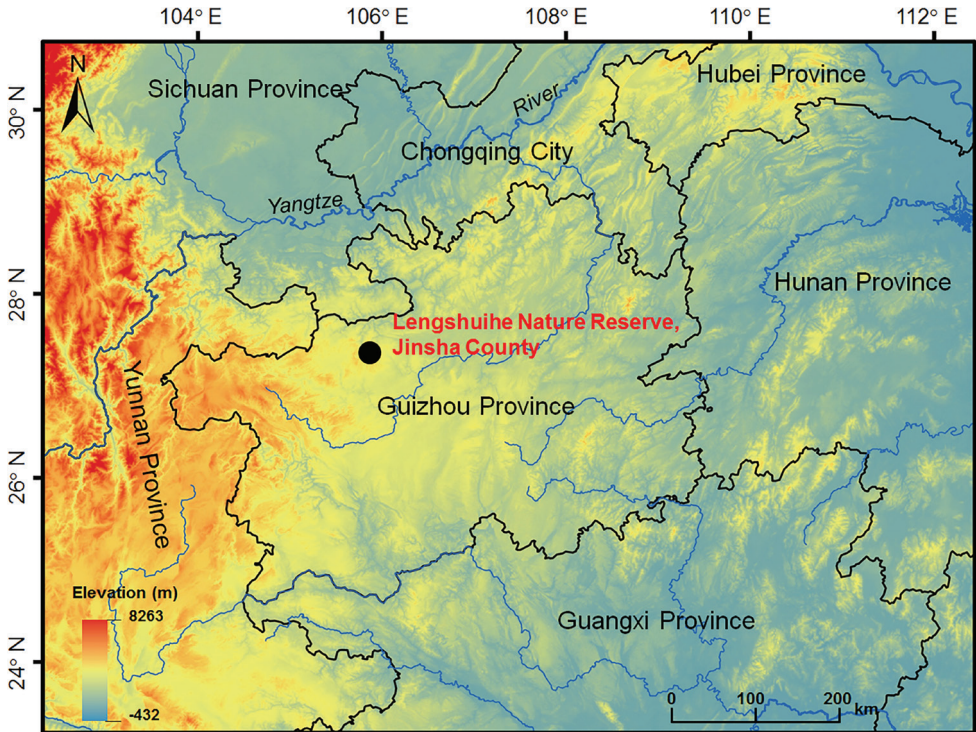


Figure 1. Location of the type locality of *Leptobrachella jinshaensis* sp. nov., Lengshuihe Nature Reserve, Jinsha County, Guizhou Province, China.

in 95% ethanol prior to fixation. Specimens were deposited in Chengdu Institute of Biology, Chinese Academy of Sciences (**CIB, CAS**).

Molecular phylogenetic analyses

All five adult male specimens of the new species collected in this work were included in the molecular phylogenetic analyses (Table 1). For phylogenetic analyses, the corresponding gene sequences for all those related species for which comparable sequences were available were also downloaded from GenBank (Table 1). Corresponding sequences of one *Leptobrachium tengchongensis*, one *Leptobrachium huashen*, and one *Megophrys major* were downloaded (Table 1) and used as outgroups based on previous studies (Chen et al. 2018; Li et al. 2020a).

Total DNA was extracted using a standard phenol-chloroform extraction protocol (Sambrook et al. 1989). The mitochondrial 16S rRNA genes were amplified, and the primers P7 (5'-CGCCTGTTTACCAAAAACAT-3') and P8 (5'-CCGGTCT-GAACTCAGATCACGT-3') were used following Simon et al. (1994). Gene fragments were amplified under the following conditions: an initial denaturing step at 95 °C for 4 min; 36 cycles of denaturing at 95 °C for 30 sec, annealing at 51 °C for 30 sec and extending at 72 °C for 70 sec. Sequencing was conducted using an ABI3730 automated

Table 1. Information for samples used in molecular phylogenetic analyses in this study.

ID	Species	Voucher	Locality	GenBank accession number
1	<i>Leptobranchella jinshaensis</i> sp. nov.	CIBJS20200516001	Lengshuihe Nature Reserve, Jinsha County, Guizhou Province, China	MT814014
2	<i>Leptobranchella jinshaensis</i> sp. nov.	CIBJS20200516002	Lengshuihe Nature Reserve, Jinsha County, Guizhou Province, China	MT814015
3	<i>Leptobranchella jinshaensis</i> sp. nov.	CIBJS20200516003	Lengshuihe Nature Reserve, Jinsha County, Guizhou Province, China	MT814016
4	<i>Leptobranchella jinshaensis</i> sp. nov.	CIBJS20200516004	Lengshuihe Nature Reserve, Jinsha County, Guizhou Province, China	MT814017
5	<i>Leptobranchella jinshaensis</i> sp. nov.	CIBJS20200516005	Lengshuihe Nature Reserve, Jinsha County, Guizhou Province, China	MT814018
6	<i>Leptobranchella chishuiensis</i>	CIBCS20190518047	Alsophila National Nature Reserve, Chishui City, Guizhou Province, China	MT117053
7	<i>Leptobranchella chishuiensis</i>	CIBCS20190518042	Alsophila National Nature Reserve, Chishui City, Guizhou Province, China	MT117054
8	<i>Leptobranchella chishuiensis</i>	CIBCS20190518043	Alsophila National Nature Reserve, Chishui City, Guizhou Province, China	MT117055
9	<i>Leptobranchella bijie</i>	SYS a007313/ CIB110002	Mt. Zhaozi Nature Reserve, Bijie City, Guizhou Province, China	MK414532
10	<i>Leptobranchella bijie</i>	SYS a007314	Mt. Zhaozi Nature Reserve, Bijie City, Guizhou Province, China	MK414533
11	<i>Leptobranchella bijie</i>	SYS a007315	Mt. Zhaozi Nature Reserve, Bijie City, Guizhou Province, China	MK414534
12	<i>Leptobranchella suiyangensis</i>	GZNU20180606002	Huoqiuba Nature Reserve, Suiyang County, Guizhou, China	MK829648
13	<i>Leptobranchella suiyangensis</i>	GZNU20180606006	Huoqiuba Nature Reserve, Suiyang County, Guizhou, China	MK829649
14	<i>Leptobranchella suiyangensis</i>	GZNU20180606005	Huoqiuba Nature Reserve, Suiyang County, Guizhou, China	MK829650
15	<i>Leptobranchella niveimontis</i>	KIZ015744	Daxueshan Nature Reserve, Yunnan, China	MH055878
16	<i>Leptobranchella purpuraventra</i>	SYS a007081	Wujing Nature Reserve, Bijie City, Guizhou Province, China	MK414517
17	<i>Leptobranchella purpuraventra</i>	SYS a007277/ CIB110003	Wujing Nature Reserve, Bijie City, Guizhou Province, China	MK414518
18	<i>Leptobranchella purpuraventra</i>	SYS a007278	Wujing Nature Reserve, Bijie City, Guizhou Province, China	MK414519
19	<i>Leptobranchella bouwreti</i>	AMS R 177673	Lao Cai Province, Vietnam	KR018124
20	<i>Leptobranchella purpurus</i>	SYS a006530	Yingjiang County, Yunnan Province, China	MG520354
21	<i>Leptobranchella alpina</i>	KIZ046816	Huangcaoling, Yunnan Province, China	MH055866
22	<i>Leptobranchella oshanensis</i>	KIZ025776	Emei Shan, Emei Shan City, Sichuan Province, China	MH055895
23	<i>Leptobranchella eos</i>	MNHN:2004.0278	Phongsaly Province, Laos	JN848450
24	<i>Leptobranchella tengchongensis</i>	SYS a004598	Tengchong County, Yunnan Province, China	KU589209
25	<i>Leptobranchella puboatensis</i>	AMS:R184852	Pu Hoat Nature Reserve, Nghe An Province, Vietnam	KY849588
26	<i>Leptobranchella namdongensis</i>	VNUF A.2017.37	Thanh Hoa Provincen, Vietnam	MK965389
27	<i>Leptobranchella petrops</i>	AMS:R184826	Vietnam	KY459997
28	<i>Leptobranchella khasiorum</i>	SDBDU 2009.329	East Khasi Hills, Meghalaya, India	KY022303
29	<i>Leptobranchella yingjiangensis</i>	SYS a006532	Yingjiang County, Yunnan Province, China	MG520351
30	<i>Leptobranchella mangshanensis</i>	MSZTC201701	Mt. Mang, Yizhang County, Hunan Province, China	MG132196
31	<i>Leptobranchella liui</i>	SYS a001597	Mt. Wuyi, Wuyishan City, Fujian Province, China	KM014547
32	<i>Leptobranchella laui</i>	SYS a001507	Mt. Wutong, Shenzhen City, Guangdong Province, China	KM014544
33	<i>Leptobranchella yunkaiensis</i>	SYS a004664 / CIB107272	Dawuling Forest Station, Maoming City, Guangdong Province, China	MH605585
34	<i>Leptobranchella maershanensis</i>	KIZ019385	Mt. Maer Nature Reserve, Ziyuan County, Guangxi Province, China	KY986930
35	<i>Leptobranchella flaviglandulosa</i>	KIZ016072	Xiaoqiaogou Nature Reserve, Yunnan, China	MH055934
36	<i>Leptobranchella zhangyapingi</i>	KIZ07258	Pang Num Poo, Chiang Mai Province, Thailand	MH055864
37	<i>Leptobranchella sungi</i>	ROM 20236	Tam Dao, Vinh Phuc, Vietnam	MH055858
38	<i>Leptobranchella isos</i>	VNMN A 2015.4/ AMS R 176480	Gia Lai Province, Vietnam	KT824769
39	<i>Leptobranchella firthi</i>	AMS R 176524	Kon Tum Province, Vietnam	JQ739206
40	<i>Leptobranchella minimus</i>	KUHE:19201	Thailand	LC201981
41	<i>Leptobranchella ventripunctata</i>	SYS a004536	Zhushihe, Yunnan Province, China	MH055831
42	<i>Leptobranchella feii</i>	KIZ048893	Xiaoqiaogou Nature Reserve, Yunnan, China (E)	MH055841
43	<i>Leptobranchella aerea</i>	ZFMK 86362	Quang Binh Province, Vietnam	JN848409
44	<i>Leptobranchella pluvialis</i>	MNHN:1999.5675	Mt. Fan Si Pan, Lao Cai Province, Vietnam	JN848391
45	<i>Leptobranchella shangsiensis</i>	NHMG1704003	Shangsi County, Guangxi Zhuang minority Autonomous Region, China	MK095463
46	<i>Leptobranchella wuhuangmontis</i>	SYS a003500 / CIB107274	Mt. Wuhuang, Pubei County, Guangxi Zhuang minority Autonomous Region, China	MH605581

ID	Species	Voucher	Locality	GenBank accession number
47	<i>Leptobranchella nahangensis</i>	ROM 7035	Na Hang Nature Reserve, Tuyen Quang, Vietnam	MH055853
48	<i>Leptobranchella nyx</i>	AMNH A163810	Ha Giang Province, Vietnam	DQ283381
49	<i>Leptobranchella tuberosa</i>	ZMMU-NAP-02275	Kon Ka Kinh National Park, Gia Lai, Vietnam	MH055959
50	<i>Leptobranchella botsfordi</i>	VNMN 03682	Fansipan, Lao Cai, Vietnam	MH055953
51	<i>Leptobranchella pallida</i>	UNS00510	Lam Dong Province, Vietnam	KR018112
52	<i>Leptobranchella kalonensis</i>	IEBR A.2015.15	Binh Thuan Province, Vietnam	KR018114
53	<i>Leptobranchella bidoupensis</i>	NAP-01453	Lam Dong Province, Vietnam	KP017573
54	<i>Leptobranchella tadungensis</i>	UNS00515	Dak Nong Province, Vietnam	KR018121
55	<i>Leptobranchella maculosa</i>	AMS R 177660	Ninh Thuan Province, Vietnam	KR018119
56	<i>Leptobranchella pyrrhops</i>	ZMMU ABV-00148	Loc Bao, Lam Dong Province, Vietnam	KP017575
57	<i>Leptobranchella macrops</i>	IEBR A.2017.9	Hon Den Mt., Phu Yen Province, Vietnam	MG787990
58	<i>Leptobranchella melica</i>	MVZ 258197	Virachey National Park, Ratanakiri Province, Cambodia	HM133599
59	<i>Leptobranchella applebyi</i>	AMS R171704	Song Thanh, Quang Nam, Vietnam	HM133598
60	<i>Leptobranchella rowleyae</i>	ITBCZ 2783	Son Tra, Da Nang City, Vietnam	MG682552
61	<i>Leptobranchella ardens</i>	AMS R 176463	Gia Lai Province, Vietnam	KR018110
62	<i>Leptobranchella crocea</i>	AMS R 173740	Kon Tum, Vietnam	MH055954
63	<i>Leptobranchella melanoleuca</i>	KUHE 23840	Thailand	LC201997
64	<i>Leptobranchella fuliginosa</i>	KUHE:20172	Thailand	LC201985
65	<i>Leptobranchella itiokai</i>	KUHE:55897	Mulu NP, Sarawak, Borneo, Malaysia	LC137805
66	<i>Leptobranchella brevicrus</i>	ZMH A09365	Sarawak: Gunung Mulu National Park: Small stream of the Sungei Tapin, Malaysia	KJ831302
67	<i>Leptobranchella parva</i>	KUHE 55308	Mulu NP, Sarawak, Borneo, Malaysia	LC056791
68	<i>Leptobranchella baluensis</i>	SP 21604	Tambunan, Sabah, Borneo, Malaysia	LC056792
69	<i>Leptobranchella mjobergi</i>	KUHE 17064	Gading NP, Sarawak, Borneo, Malaysia	LC056785
70	<i>Leptobranchella juliandringi</i>	SRC 00230/KUHE 49815	Mulu NP, Sarawak, Borneo, Malaysia	LC056779
71	<i>Leptobranchella arayai</i>	BORNEEISIS 22931	Liwagu, Kinabalu, Borneo, Malaysia	AB847558
72	<i>Leptobranchella bamidi</i>	KUHE 17545	Borneo, Malaysia	AB969286
73	<i>Leptobranchella marmorata</i>	KUHE 53227	Annah Rais, Padawan, Kuching Division, Sarawak, Malaysia	AB969289
74	<i>Leptobranchella maura</i>	SP 21450	Kinabalu, Sabah, Malaysia	AB847559
75	<i>Leptobranchella gracilis</i>	KUHE 55624	Camp 1, Gunung Mulu, Borneo, Malaysia	AB847560
76	<i>Leptobranchella sabahmontana</i>	BORNEENSIS 12632	Borneo, Malaysia	AB847551
77	<i>Leptobranchella dringi</i>	KUHE 55610	Camp 4 of Gunung Mulu, Malaysia	AB847553
78	<i>Leptobranchella picta</i>	UNIMAS 8705	Borneo, Malaysia	KJ831295
79	<i>Leptobranchella fritiniensis</i>	KUHE 55371	Headquarters, Gunung Mulu, Malaysia	AB847557
80	<i>Leptobranchella sola</i>	KUHE 23261	Hala Bala, Thailand	LC202007
81	<i>Leptobranchella heteropus</i>	KUHE 15487	Larut, Peninsular, Malaysia	AB530453
82	<i>Leptobranchella kecil</i>	KUHE 52440	Malaysia	LC202004
83	<i>Leptobranchella kajangensis</i>	LSUHC 4439	Tioman, Malaysia	LC202002
84	<i>Leptobranchium tengchongense</i>	SYSa004604d	Yunnan Province, China	KX066880
85	<i>Leptobranchium huashen</i>	KIZ049025	Yunnan Province, China	KX811931
86	<i>Megophrys major</i>	AMS R 173870	Kon Tum, Vietnam	KY476333

Table 2. Measurements of adult males of *Leptobranchella jinshaensis* sp. nov. Units given in mm. See abbreviations for morphometric characters in Materials and methods section.

Voucher number	Sex	SVL	HDL	HDW	SL	IND	IOD	UEW	ED	TYD	LAL	LW	ML	THL	TW	TL	TFL	FL
CIBCS20200516001	male	31.1	11.4	10.1	4.9	3.4	3.1	2.8	3.9	2.5	15.4	2.6	8.4	15.0	4.9	15.3	21.4	14.4
CIBCS20200516002	male	31.2	10.8	10.4	4.6	3.2	3.2	2.7	3.9	2.8	13.7	2.1	7.7	15.2	3.2	15.6	19.3	13.0
CIBCS20200516003	male	29.7	10.0	10.1	4.6	3.2	3.4	3.0	4.2	2.5	14.4	2.2	7.2	14.0	3.6	15.1	19.5	13.0
CIBCS20200516004	male	31.1	10.3	10.0	4.5	2.8	3.7	2.9	4.3	2.6	15.2	2.4	8.2	14.6	3.5	15.1	21.4	14.2
CIBCS20200516005	male	30.9	11.3	10.4	4.6	3.5	4.0	3.2	3.7	3.2	14.1	2.2	8.2	14.1	3.6	14.5	21.2	14.2

DNA sequencer in Shanghai DNA BioTechnologies Co., Ltd. (Shanghai, China). New sequences were deposited in GenBank (for GenBank accession numbers see Table 1).

Sequences were assembled and aligned using the Clustalw module in BioEdit v. 7.0.9.0 (Hall 1999) with default settings. Alignments were checked by eye and revised

manually if necessary. Phylogenetic analyses were conducted using maximum likelihood (ML) and Bayesian Inference (BI) methods, implemented in PhyML v. 3.0 (Guindon et al. 2010) and MrBayes v. 3.12 (Ronquist and Huelsenbeck 2003), respectively. We ran Jmodeltest v. 2.1.2 (Darriba et al. 2012) with Akaike and Bayesian information criteria on the alignment, resulting in the best-fitting nucleotide substitution models of GTR + I + G for the data. For the ML tree, branch supports were drawn from 10,000 nonparametric bootstrap replicates. In BI analyses, the parameters for each partition were unlinked, and branch lengths were allowed to vary proportionately across partitions. Two runs each with four Markov chains were simultaneously run for 50 million generations with sampling every 1,000 generations. The first 25% trees were removed as the “burn-in” stage followed by calculations of Bayesian posterior probabilities and the 50% majority-rule consensus of the post burn-in trees sampled at stationarity. Finally, genetic distance between *Leptobranchella* species based on uncorrected *p*-distance model was estimated on 16S gene using MEGA v. 6.06 (Tamura et al. 2013).

Morphological comparisons

All five adult male specimens of the new species were measured (Table 2). The terminology and methods followed Fei et al. (2005), Mahony et al. (2011), and Wang et al. (2019). Measurements were made with a dial caliper to the nearest 0.1 mm (Watters et al. 2016) with digital calipers. Corresponding measurements of *L. bijie* and *L. chishuiensis* were retrieved from Wang et al. (2019) and Li et al. (2020a). Nineteen morphometric characters of adult specimens were measured:

- ED** eye diameter (distance from the anterior corner to the posterior corner of the eye);
- FL** foot length (distance from tarsus to the tip of the fourth toe);
- HDL** head length (distance from the tip of the snout to the articulation of jaw);
- HDW** head width (greatest width between the left and right articulations of jaw);
- HLL** hindlimb length (distance from tip of fourth toe to vent);
- IND** internasal distance (minimum distance between the inner margins of the external nares);
- IOD** interorbital distance (minimum distance between the inner edges of the upper eyelids);
- LAL** length of lower arm and hand (distance from the elbow to the distal end of the Finger IV);
- LW** lower arm width (maximum width of the lower arm);
- ML** manus length (distance from tip of third digit to proximal edge of inner palmar tubercle);
- SL** snout length (distance from the tip of the snout to the anterior corner of the eye);
- SVL** snout-vent length (distance from the tip of the snout to the posterior edge of the vent);

- TEY** tympanum-eye distance (distance from anterior edge of tympanum to posterior corner of eye);
- TFL** length of foot and tarsus (distance from the tibiotarsal articulation to the distal end of the toe IV);
- THL** thigh length (distance from vent to knee);
- TL** tibia length (distance from knee to tarsus);
- TW** maximal tibia width;
- TYD** maximal tympanum diameter;
- UEW** upper eyelid width (greatest width of the upper eyelid margins measured perpendicular to the anterior-posterior axis).

In order to reduce the impact of allometry, the correct value from the ratio of each character to SVL was calculated and then all of the data were log-transformed for the following morphometric analyses. Mann-Whitney *U* tests were conducted to test the significance of differences on morphometric characters between *Leptobrachella jinshaensis* sp. nov., *L. bijie* and *L. chishuiensis*. The significance level was set at 0.05. Furthermore, principal component analyses (PCA) were conducted to highlight whether the different species were separated in morphometric space. Due to only the measurements SVL, HDL, HDW, SL, IND, IOD, ED, TYD, TEY, LAL, ML, TL, HLL, and FL of male *L. bijie* being available from Wang et al. (2019), the morphometric analyses were conducted only based on these 14 morphometric characters for male group.

Leptobrachella jinshaensis sp. nov. was also compared with all other congeners of *Leptobrachella* based on morphological characters. Comparative morphological data were obtained from literatures (Table 3).

Bioacoustics data

The advertisement calls of *L. jinshaensis* sp. nov. were recorded from the holotype specimen CIBJS20200516004 in the field on 16 May 2020 in Lengshuihe Nature Reserve, Jinsha County, Guizhou Province, China. The advertisement call of *L. jinshaensis* sp. nov. was recorded in the stream at ambient air temperature of 20 °C and air humidity of 87%. A SONY PCM-D50 digital sound recorder was used to record within 20 cm of the calling individual. The sound files in wave format were resampled at 48 kHz with sampling depth 24 bits. Calls were recorded and examined as described by Wijayathilaka and Meegaskumbura (2016). Call recordings were visualised and edited with SoundRuler 0.9.6.0 (Gridi-Papp 2003–2007) and Raven Pro 1.5 software (Cornell Laboratory of Ornithology, Ithaca, NY, USA). Ambient temperature of the type locality was taken by a digital hygrothermograph. For comparison, bioacoustics data for the related species *L. bijie* and *L. chishuiensis* were obtained from Li et al. (2020a).

Table 3. References for morphological characters for congeners of the genus *Leptobranchella*.

No.	<i>Leptobranchella</i> species	References
1	<i>L. aerea</i> (Rowley, Stuart, Richards, Phimmachak & Sivongxay, 2010)	Rowley et al. 2010a
2	<i>L. alpina</i> (Fei, Ye & Li, 1990)	Fei et al. 1990
3	<i>L. applebyi</i> (Rowley & Cao, 2009)	Rowley and Cao 2009
4	<i>L. arayai</i> (Matsui, 1997)	Matsui 1997
5	<i>L. ardens</i> (Rowley, Tran, Le, Dau, Peloso, Nguyen, Hoang, Nguyen & Ziegler, 2016)	Rowley et al. 2016
6	<i>L. baluensis</i> (Smith, 1931)	Dring 1983; Eto et al. 2016, 2018
7	<i>L. bidoupensis</i> (Rowley, Le, Tran & Hoang, 2011)	Rowley et al. 2011
8	<i>L. bijie</i> (Wang, Li, Li, Chen & Wang, 2019)	Wang et al. 2019
9	<i>L. bondangensis</i> (Eto, Matsui, Hamidy, Munir & Iskandar, 2018)	Eto et al. 2018
10	<i>L. botsfordi</i> (Rowley, Dau & Nguyen, 2013)	Rowley et al. 2013
11	<i>L. bourreti</i> (Dubois, 1983)	Ohler et al. 2011
12	<i>L. brevicrus</i> (Dring, 1983)	Dring 1983; Eto et al. 2015
13	<i>L. chishuiensis</i> Li, Liu, Wei & Wang, 2020	Li et al. 2020a
14	<i>L. crocea</i> (Rowley, Hoang, Le, Dau & Cao, 2010)	Rowley et al. 2010b
15	<i>L. dringi</i> (Dubois, 1987)	Inger et al. 1995; Matsui and Dehling 2013
16	<i>L. eos</i> (Ohler, Wollenberg, Grosjean, Hendrix, Vences, Ziegler & Dubois, 2011)	Ohler et al. 2011
17	<i>L. feii</i> (Chen, Yuan & Che, 2020)	Chen et al. 2020
18	<i>L. firthi</i> (Rowley, Hoang, Dau, Le & Cao, 2012)	Rowley et al. 2012
19	<i>L. flaviglandulosa</i> (Chen, Yuan & Che, 2020)	Chen et al. 2020
20	<i>L. fritinniens</i> (Dehling & Matsui, 2013)	Dehling and Matsui 2013
21	<i>L. fuliginosa</i> (Matsui, 2006)	Matsui 2006
22	<i>L. fusca</i> (Eto, Matsui, Hamidy, Munir & Iskandar, 2018)	Eto et al. 2018
23	<i>L. gracilis</i> (Günther, 1872)	Günther 1872; Dehling 2012a
24	<i>L. hamidi</i> (Matsui, 1997)	Matsui 1997
25	<i>L. heteropus</i> (Boulenger, 1900)	Boulenger 1900
26	<i>L. isos</i> (Rowley, Stuart, Neang, Hoang, Dau, Nguyen & Emmett, 2015)	Rowley et al. 2015
27	<i>L. itiokai</i> Eto, Matsui & Nishikawa, 2016	Eto et al. 2016
28	<i>L. juliandrangi</i> Eto, Matsui & Nishikawa, 2015	Eto et al. 2015
29	<i>L. kajangensis</i> (Grismer, Grismer & Youmans, 2004)	Grismer et al. 2004
30	<i>L. kalonensis</i> (Rowley, Tran, Le, Dau, Peloso, Nguyen, Hoang, Nguyen & Ziegler, 2016)	Rowley et al. 2016
31	<i>L. kecil</i> (Matsui, Belabut, Ahmad & Yong, 2009)	Matsui et al. 2009
32	<i>L. khasiorum</i> (Das, Tron, Rangad & Hooroo, 2010)	Das et al. 2010
33	<i>L. lateralis</i> (Anderson, 1871)	Anderson 1871; Humtsoe et al. 2008
34	<i>L. laui</i> (Sung, Yang & Wang, 2014)	Sung et al. 2014
35	<i>L. liui</i> (Fei & Ye, 1990)	Fei et al. 2009; Sung et al. 2014
36	<i>L. macrops</i> (Duong, Do, Ngo, Nguyen & Poyarkov, 2018)	Duong et al. 2018
37	<i>L. maculosa</i> (Rowley, Tran, Le, Dau, Peloso, Nguyen, Hoang, Nguyen & Ziegler, 2016)	Rowley et al. 2016
38	<i>L. mangshanensis</i> (Hou, Zhang, Hu, Li, Shi, Chen, Mo & Wang, 2018)	Hou et al. 2018
39	<i>L. maoershanensis</i> (Yuan, Sun, Chen, Rowley & Che, 2017)	Yuan et al. 2017
40	<i>L. marmorata</i> (Matsui, Zainudin & Nishikawa, 2014)	Matsui et al. 2014a
41	<i>L. maura</i> (Inger, Lakim, Biun & Yambun, 1997)	Inger et al. 1997
42	<i>L. melanoleuca</i> (Matsui, 2006)	Matsui 2006
43	<i>L. melica</i> (Rowley, Stuart, Neang & Emmett, 2010)	Rowley et al. 2010c
44	<i>L. minima</i> (Taylor, 1962)	Taylor 1962; Ohler et al. 2011
45	<i>L. mjobergi</i> (Smith, 1925)	Eto et al. 2015, 2018
46	<i>L. nabangensis</i> (Lathrop, Murphy, Orlov & Ho, 1998)	Lathrop et al. 1998
47	<i>L. namdongensis</i> (Hoang, Nguyen, Luu, Nguyen & Jiang, 2019)	Hoang et al. 2019
48	<i>L. natunae</i> (Günther, 1895)	Günther 1895
49	<i>L. neangi</i> (Stuart & Rowley, 2020)	Stuart and Rowley 2020
50	<i>L. niveimontis</i> (Chen, Yuan & Che, 2020)	Chen et al. 2020
51	<i>L. nokrekensis</i> (Mathew & Sen, 2010)	Mathew and Sen 2010
52	<i>L. nyx</i> (Ohler, Wollenberg, Grosjean, Hendrix, Vences, Ziegler & Dubois, 2011)	Ohler et al. 2011
53	<i>L. oshanensis</i> (Liu, 1950)	Liu 1950, 1961; This paper
54	<i>L. pallida</i> (Rowley, Tran, Le, Dau, Peloso, Nguyen, Hoang, Nguyen & Ziegler, 2016)	Rowley et al. 2016
55	<i>L. palmata</i> Inger & Stuebing, 1992	Inger and Stuebing 1992
56	<i>L. parva</i> Dring, 1983	Dring 1983
57	<i>L. pelodytoides</i> (Boulenger, 1893)	Boulenger 1893; Ohler et al. 2011
58	<i>L. petrops</i> (Rowley, Dau, Hoang, Le, Cutajar & Nguyen, 2017)	Rowley et al. 2017a
59	<i>L. picta</i> (Malkmus, 1992)	Malkmus 1992
60	<i>L. platycephala</i> (Dehling, 2012)	Dehling 2012b

No.	<i>Leptobrachella</i> species	References
61	<i>L. pluvialis</i> (Ohler, Marquis, Swan & Grosjean, 2000)	Ohler et al. 2000, 2011
62	<i>L. puhoatensis</i> (Rowley, Dau & Cao, 2017)	Rowley et al. 2017b
63	<i>L. purpuraventra</i> Wang, Li, Li, Chen & Wang, 2019	Wang et al. 2019
64	<i>L. purpurus</i> (Yang, Zeng & Wang, 2018)	Yang et al. 2018
65	<i>L. pyrhaps</i> (Poyarkov, Rowley, Gogoleva, Vassilieva, Galoyan & Orlov, 2015)	Poyarkov et al. 2015
66	<i>L. rowleyae</i> (Nguyen, Poyarkov, Le, Vo, Ninh, Duong, Murphy & Sang, 2018)	Nguyen et al. 2018
67	<i>L. sabahmontana</i> (Matsui, Nishikawa & Yambun, 2014)	Matsui et al. 2014b
68	<i>L. serasanae</i> Dring, 1983	Dring 1983
69	<i>L. shangsiensis</i> Chen, Liao, Zhou & Mo, 2019	Chen et al. 2019
70	<i>L. sola</i> (Matsui, 2006)	Matsui 2006
71	<i>L. suiyangensis</i> (Luo, Xiao, Gao & Zhou, 2020)	Luo et al. 2020
72	<i>L. sungi</i> (Lathrop, Murphy, Orlov & Ho, 1998)	Lathrop et al. 1998
73	<i>L. tadungensis</i> (Rowley, Tran, Le, Dau, Peloso, Nguyen, Hoang, Nguyen & Ziegler, 2016)	Rowley et al. 2016
74	<i>L. tamdil</i> (Sengupta, Sailo, Lalremanga, Das & Das, 2010)	Sengupta et al. 2010
75	<i>L. tengchongensis</i> (Yang, Wang, Chen & Rao, 2016)	Yang et al. 2016
76	<i>L. tuberosa</i> (Inger, Orlov & Darevsky, 1999)	Inger et al. 1999
77	<i>L. ventripunctata</i> (Fei, Ye & Li, 1990)	Fei et al. 2009
78	<i>L. wubuangmontis</i> Wang, Yang & Wang, 2018	Wang et al. 2018
79	<i>L. wulingensis</i> Qian, Xiao, Cao, Xiao & Yang, 2020	Qian et al. 2020
80	<i>L. yingjiangensis</i> (Yang, Zeng & Wang, 2018)	Yang et al. 2018
81	<i>L. yunkaiensis</i> Wang, Li, Lyu & Wang, 2018	Wang et al. 2018
82	<i>L. zhangyapingi</i> (Jiang, Yan, Suwannapoom, Chomdej & Che, 2013)	Jiang et al. 2013

Results

Aligned sequence matrix of 16S rRNA gene contained 537 bps. ML and BI analyses resulted in essentially identical topologies (Fig. 2). All samples of *L. jinshaensis* sp. nov. were clustered into one independent clade nested into the *Leptobrachella* clade. The relationships between *L. jinshaensis* sp. nov. and its congeners are not resolved though it is likely sister to a clade in comprising of *L. bijie* and *L. chishuiensis* (Fig. 2). The smallest pairwise genetic divergence between *L. jinshaensis* sp. nov. and all other species of the genus *Leptobrachella* is 2.6% (vs. *L. niveimontis* or vs. *L. purpurus*), being at the same level with or higher than that between some pairs of substantial species, such as *L. bijie* vs. *L. chishuiensis* (2.1%), and *L. chishuiensis* vs. *L. alpina* (2.6%; Suppl. material 1: Table S1).

For the male group, PCA extracted five principal component axes with eigenvalues greater than one, and the percentage of variance of the first five principal components are 37.7%, 15.7%, 13.0%, 9.0% and 8.1%, with percentage of cumulative is 83.5% (Suppl. material 2: Table S2). There were 14 morphological features with major contributions in the first five principal components, and these morphological features were distributed in the anterior, middle, and posterior parts of the body (Suppl. material 2: Table S2). The total variation of the first two principal components was 53.4% (Suppl. material 2: Table S2). On the PCA plot (PC1 vs. PC2), the first principal component axis could separate *L. jinshaensis* sp. nov. from *L. bijie* and *L. chishuiensis* (Fig. 3) mainly based on SVL, HDL, HDW, SL, ED, IND, TEY, and FL, and the second component axis mainly based on ML, FL, and LAL. Mann-Whitney *U* tests indicated that *L. jinshaensis* sp. nov. was significantly different from *L. bijie* on HDW, SL, IOD, TYD, TEY, LW, and FL, and from *L. chishuiensis* on SVL, TYD, and TL (*p*-values < 0.05; Table 4).

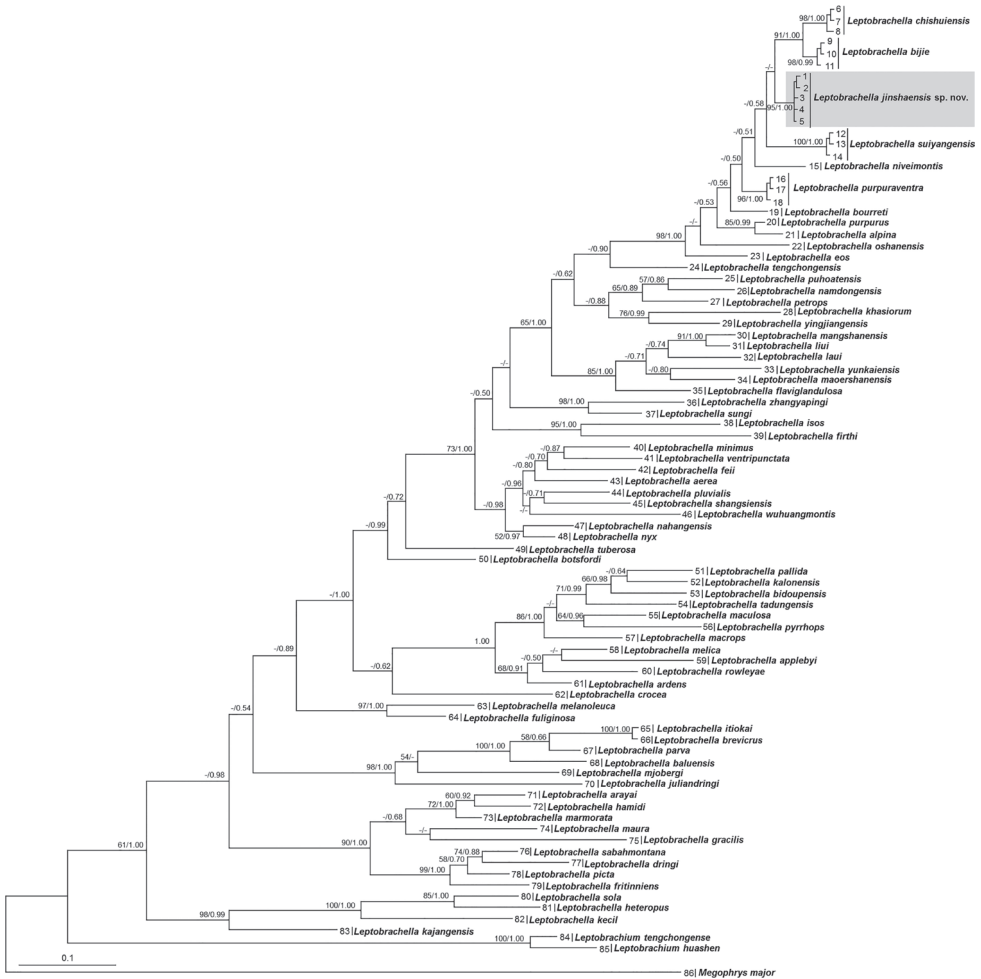


Figure 2. Bayesian Inference (BI) tree based on the mitochondrial 16S rRNA sequences. Bootstrap supports from Maximum Likelihood analyses/Bayesian posterior probabilities from BI analyses are labelled beside nodes. Information of samples 1–86 refer to Table 1.

In total, 109 advertisement calls of *Leptobranchella jinshaensis* sp. nov. were recorded in Lengshuihe Nature Reserve, Jinsa County, Guizhou Province, China on 16 May 2020 between 21:00–22:00. The call description is based on recordings of the holotype CIB-JS20200516004 under a stone nearby a stream, and the ambient air temperature was 20 °C. The call characters of *L. jinshaensis* sp. nov. were demonstrated in the following section for describing it. There were some differences in sonograms and waveforms of calls between *L. jinshaensis* sp. nov., *L. bijie*, and *L. chishuiensis* (Suppl. material 3: Table S3). *Leptobranchella jinshaensis* sp. nov. has longer call interval (132.7 ± 8.6 , $N = 109$) than *L. bijie* (101.9 ± 6.4 , $N = 33$), and has lower dominant frequency (4525 ± 0.065 Hz) than *L. bijie* (4780.4 ± 76.5 Hz) and *L. chishuiensis* (6064–6284 H). Each call of *L. jinshaensis* sp. nov. has two kinds of notes, while each call of *L. chishuiensis* only has one kind of note.

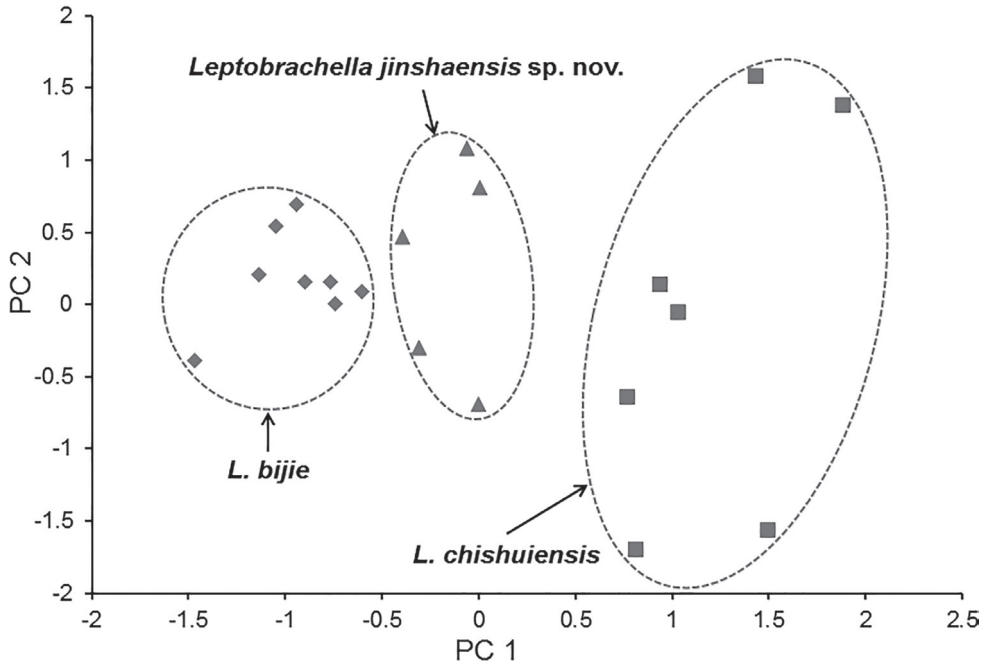


Figure 3. Plots of the first principal component (PC1) versus the second (PC2) for *Leptobrachella jinshaensis* sp. nov., *L. bijie*, and *L. chishuiensis* in males from a principal component analysis based on morphometric data.

***Leptobrachella jinshaensis* sp. nov.**

<http://zoobank.org/C2982600-D9EF-46C1-A539-CC1151444B18>

Figs 3–6; Tables 1, 2, 4, Suppl. material 1: Table S1, Suppl. material 2: Table S2

Holotype. CIBJS20200516004, adult male (Figs 4, 5), collected from Lengshuihe Nature Reserve, Jinsha County (27.536944°N, 105.999166°E, ca. 770 m a. s. l.), Guizhou Province, China by Shi-Ze Li on 16 May 2020.

Paratypes. Four adult males from the same place as holotype. Two adult males CIBJS20200516001 and CIBJS20200516002 collected by Shi-Ze LI, and two adult males CIBJS20200516003 and CIBJS20200516005 collected by Jing LIU, all of them were collected on 16 May 2020.

Diagnosis. *Leptobrachella jinshaensis* sp. nov. is assigned to the genus *Leptobrachella* based on molecular phylogenetic analyses and the following morphological characters: medium size, rounded finger tips, the presence of an elevated inner palmar tubercle not continuous to the thumb, the presence of macroglands on body (including supra-axillary, pectoral, and femoral glands), vomerine teeth absent, tubercles on eyelids, and the anterior tip of snout with a vertical white bar.

Leptobrachella jinshaensis sp. nov. can be distinguished from its congeners by a combination of the following characters: body of medium size (SVL 29.7–31.2 mm in five adult males); dorsal skin shagreened, some of the granules forming longitudi-

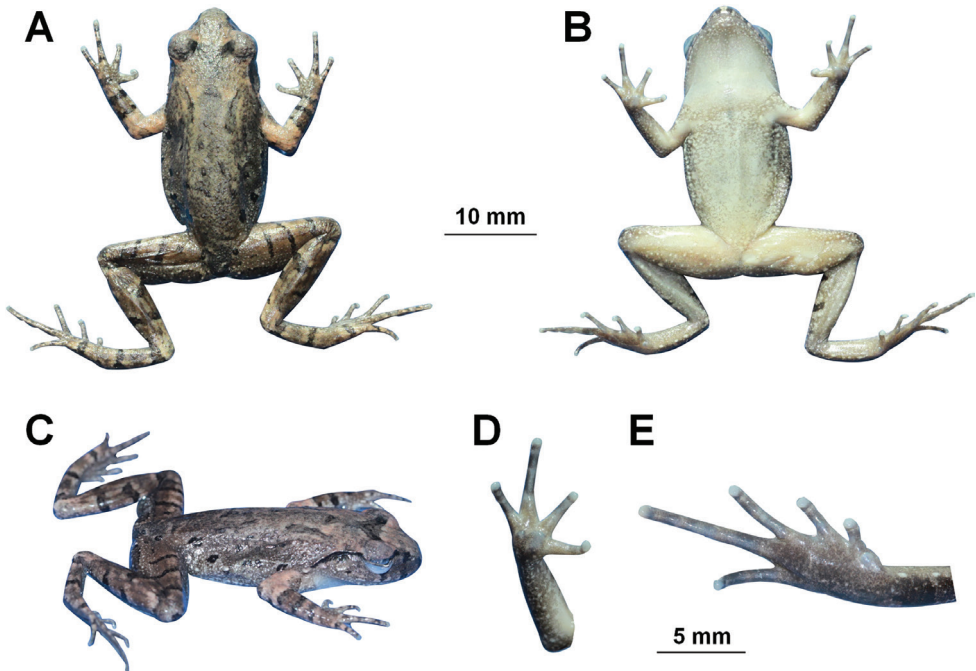


Figure 4. Photos of the holotype specimen CIBCS20200516004 of *Leptobrachella jinshaensis* sp. nov. **A** dorsal view **B** ventral view **C** lateral view **D** ventral view of hand **E** ventral view of foot.

nal short skin ridges; tympanum distinctly discernible, slightly concave; supra-axillary, femoral, pectoral, and ventrolateral glands distinctly visible; absence of webbing and lateral fringes on fingers; toes with narrow lateral fringes and without webbing; heels overlapping when thighs positioned at right angles to the body; tibia-tarsal articulation reaching the middle eye when leg stretched forward.

Description of holotype (Figs 4, 5). Adult male. SVL in 31.1 mm. **Head** length slightly longer than head width (HDL/HDW 1.02); snout slightly protruding, projecting slightly beyond margin of the lower jaw; nostril closer to snout than eye; canthus rostralis gently rounded; loreal region slightly concave; interorbital space flat, interorbital distance slightly longer than internarial distance; pineal ocellus absent; vertical pupil; eye diameter slightly shorter than snout length; tympanum distinct, rounded, and slightly concave, diameter smaller than that of the eye (TMP/ED 0.61); upper margin of tympanum in contact with supratympanic ridge; vomerine teeth absent; tongue notched behind; supratympanic ridge distinct, extending from posterior corner of eye to supra-axillary gland.

Forelimbs slender, 48.9% of snout-vent length; tips of fingers rounded, slightly swollen; relative finger lengths I < II <= IV < III; absence of webbing; nuptial pad and subarticular tubercles absent; inner palmar tubercle large, rounded separated from the smaller, round outer palmar tubercle.

Hindlimbs slender, tibia slightly longer than thigh length and 48.4% of snout-vent length; heels overlapping when thighs are positioned at right angles to the body,

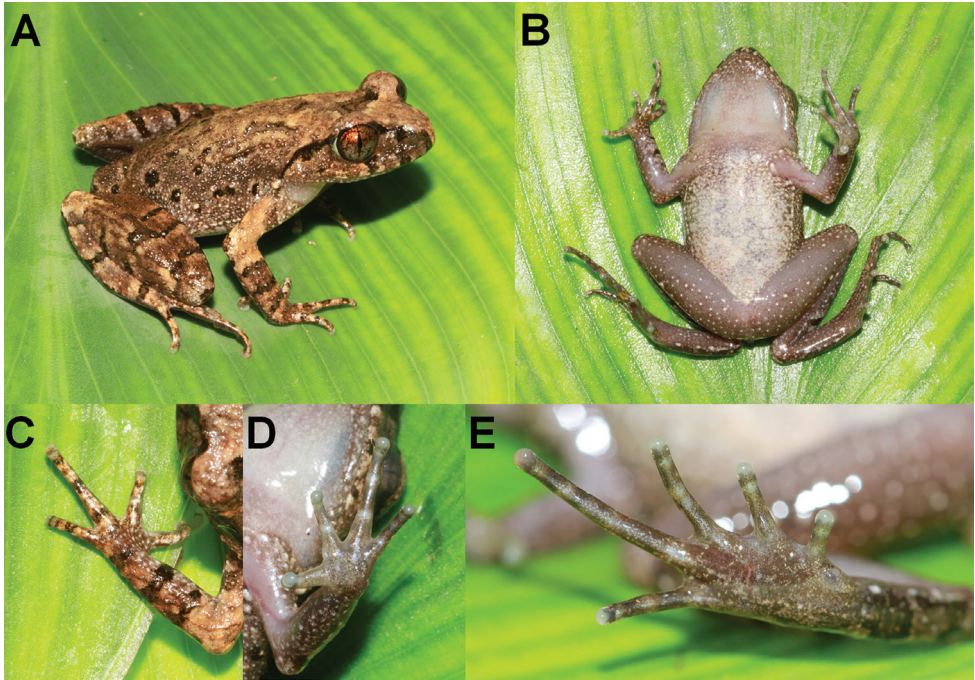


Figure 5. Photos of the holotype CIBCS20200516004 of *Leptobranchella jinshaensis* sp. nov. in life **A** dorsal view **B** ventral view **C** dorsal view of hand **D** ventral view of hand **E** ventral view of foot.

tibiotarsal articulation reaching middle eye when leg stretched forward; relative toe lengths $I < II < V < III < IV$; tips of toes round, slightly dilated; subarticular tubercle at the articulations of the toes absent; toes without webbing; lateral fringes narrow on all toes; inner metatarsal tubercle present, large, oval, outer metatarsal tubercle absent.

Dorsal surface shagreened and granular, some of the granules forming short longitudinal folds dorsally on the flank; ventral skin smooth; dense tiny granules present on ventral surface of thigh and tibia; pectoral gland and femoral gland white, oval, distinctly visible. Ventrolateral gland distinctly visible and forming an incomplete line.

Colouration of holotype in life. Dorsum brown, with small, distinct darker brown markings and spots, and irregularly dispersed light orange speckles. A dark brown inverted triangular pattern between anterior corners of eyes. Tympanum brown, a dark brown bar above tympanum, and a dark brown bar under the eye, distinct black supratympanic line present; transverse dark brown bars on dorsal surface of limbs; distinct dark brown blotches on flanks from groin to axilla, longitudinally in two rows; elbow and upper arms with dark bars and distinct coppery orange colouration; fingers and toes with distinct dark bars. Ventral surface of throat cream white, chest, and belly cream yellow with purple speckling, and on flanks presence of distinct nebulous greyish speckling; ventral surface of limbs grey purple. Supra-axillary gland, femoral, pectoral, and ventrolateral glands white (Fig. 5).

Colouration of holotype in preservation. Dorsum of body and limbs fade to brown copper; transverse bars on limbs become more distinct. Ventral surface of body

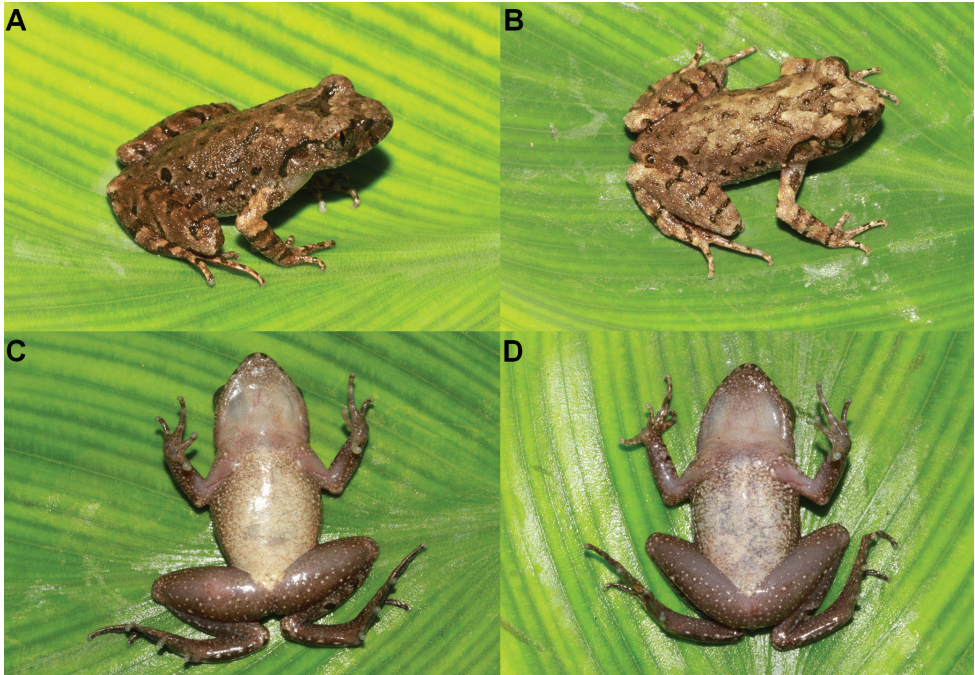


Figure 6. Colour variation in *Leptobrachella jinshaensis* sp. nov. **A** dorsal view of the male specimen CIBJS20200516002 **B** dorsal view of the male specimen CIBJS20200516005 **C** ventral view of the male specimen CIBJS20200516005 **D** ventral view of the male specimen CIBJS20200516003.

and limbs fade to cream white. Supra-axillary, femoral, and pectoral glands fade to creamy yellow (Fig. 4).

Variation. Measurements of adult specimens were presented in Tables 2 and 4. All specimens were similar but some individuals different from the holotype in colour pattern. In CIBJS20200516002, the tympana are dark brown (Fig. 6A); in CIBJS20200516005, the dorsum is olive grey (Fig. 6B) and the pectoral glands on the left side not obviously (Fig. 6D); in CIBJS20200516003 ventrolateral glands scattered and unlined (Fig. 6C).

Advertisement call. In total, 109 advertisement calls of *Leptobrachella jinshaensis* sp. nov. were recorded in Lengshuihe Nature Reserve, Jinsa County, Guizhou Province, China on 16 May 2020 between 21:00–22:00. The call description is based on recordings of the holotype CIBJS20200516004 under a stone nearby a stream, and the ambient air temperature was 20 °C. The sonograms and waveforms of the new species are shown in Fig. 7 and Suppl. material 2: Table S2. The call has two kinds of notes, and each call contains two or three notes (mean 2.12 ± 0.33 , $n = 109$). Call duration was 117–156 ms (mean 132.7 ± 8.6 , $n = 109$). Call interval was 62–106 ms (mean 84.3 ± 10.4 , $n = 108$), and each consists of two types of note. The first type of note is the start note in each call and beginning with lowest energy pulses, then increasing to the peak; in the second type, the amplitude begins with highest pulses and then decreasing

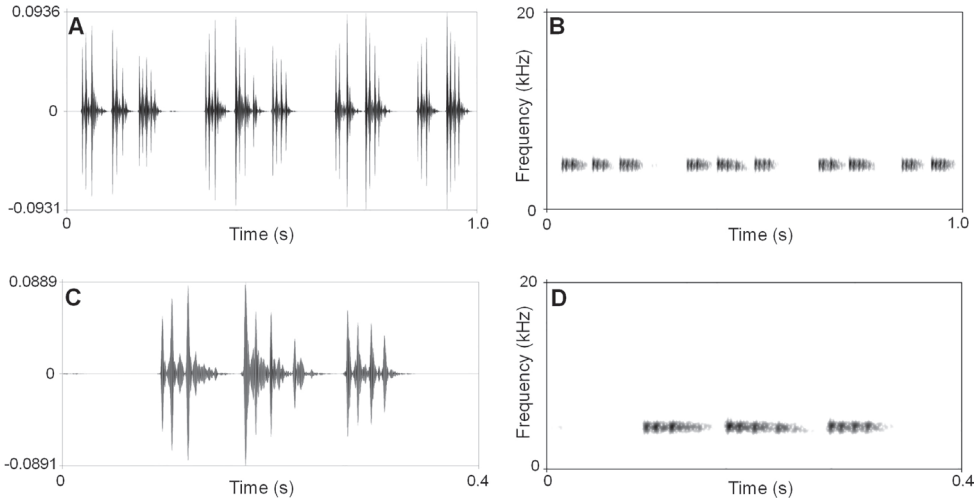


Figure 7. Advertisement calls of the holotype CIBCS20200516004 of *Leptobrachella jinshaensis* sp. nov. **A** waveform showing one second contains 4 calls **B** sonogram showing one second contains 4 calls **C** waveform showing 0.4 second contains a call **D** sonogram showing 0.4 second contains a call.

towards the end of each note. The duration of first type of note with 35–71 ms (mean 48.77 ± 7.90 , $n = 109$), the duration of the second type of note with 39–78 ms (mean 52.93 ± 8.85 , $n = 122$), the duration between notes 18–40 ms (mean 23 ± 5.68 , $n = 122$). The dominant frequency of calls is 4500–4688 Hz (mean 4525 ± 0.065 Hz).

Secondary sexual characteristics. Adult males with a comparatively large single subgular vocal sac and nuptial pads and spines absent.

Comparisons. Measurements were given in mm. In male, by body size moderate in male (SVL 29.7–31.2, $n = 5$), *Leptobrachella jinshaensis* sp. nov. is larger than *L. aerea* (25.1–28.9), *L. alpina* (24.0–26.4), *L. applebyi* (19.6–22.3), *L. ardens* (21.3–24.7), *L. baluensis* (14.9–15.9), *L. bidoupensis* (18.5–25.4), *L. bondangensis* (17.8), *L. brevicrus* (17.1–17.8), *L. crocea* (22.2–27.3), *L. feii* (21.5–22.8), *L. flaviglandulosa* (23.0–27.0), *L. fusca* (16.3), *L. isos* (23.7–27.9), *L. itiokai* (15.2–16.7), *L. juliandringi* (17.0–17.2), *L. khasiorum* (24.5–27.3), *L. laui* (24.8–26.7), *L. maculosa* (24.2–26.6), *L. mangshanensis* (22.22–27.76), *L. maura* (26.1), *L. melica* (19.5–22.8), *L. mjobergi* (15.7–19.0), *L. natunae* (17.6), *L. niveimontis* (22.5–23.6), *L. parva* (15.0–16.9), *L. palmata* (14.4–16.8), *L. pallida* (24.5–27.7), *L. petrops* (23.6–27.6), *L. pluvialis* (21.3–22.3), *L. purpurus* (25.0–27.5), *L. rowleyae* (23.4–25.4), *L. serasanae* (16.9), *L. tengchongensis* (23.9–26.0), *L. ventripunctata* (25.5–28.0), and *L. yingjiangensis* (25.7–27.6); and smaller than *L. eos* (33.1–34.7), *L. gracilis* (34.3–39.0), *L. marmorata* (32.3–38.0), *L. nahangensis* (40.8), *L. platycephala* (35.1), *L. sungi* (48.3–52.7), *L. tamdil* (32.0), and *L. zhangyapingi* (45.8–52.5).

By the presence of supra-axillary and ventrolateral glands, *Leptobrachella jinshaensis* sp. nov. can be easily distinguished from *L. arayai*, *L. dringi*, *L. fritinniensis*, *L. gracilis*, *L. hamidi*, *L. heteropus*, *L. kajangensis*, *L. kecil*, *L. marmorata*, *L. melanoleuca*, *L. maura*,

L. picta, *L. platycephala*, *L. sabahmontana*, and *L. sola* (vs. lacking supra-axillary and ventrolateral glands in the latter).

By tympanum distinctly visible, *Leptobrachella jinshaensis* sp. nov. differs from *L. crocea* and *L. tuberosa* (vs. invisible in the latter).

By having black spots on flanks, *Leptobrachella jinshaensis* sp. nov. differs from *L. aerea*, *L. botsfordi*, *L. firthi*, *L. crocea*, *L. isos*, *L. pallida*, *L. petrops*, and *L. tuberosa* (vs. lacking in the latter).

By toes without webbing, *Leptobrachella jinshaensis* sp. nov. differs from *L. aerea*, *L. alpina*, *L. applebyi*, *L. bidoupensis*, *L. bijie*, *L. botsfordi*, *L. bourreti*, *L. chishuiensis*, *L. crocea*, *L. eos*, *L. feii*, *L. firthi*, *L. fuliginosa*, *L. isos*, *L. khasiorum*, *L. lateralis*, *L. laui*, *L. liui*, *L. macrops*, *L. mangshanensis*, *L. maershanensis*, *L. marmorata*, *L. melica*, *L. minima*, *L. nahangensis*, *L. namdongensis*, *L. niveimontis*, *L. nokrekensis*, *L. nyx*, *L. pluviialis*, *L. pluviialis*, *L. puhoatensis*, *L. purpureus*, *L. purpuraventra*, *L. pyrrhops*, *L. sabahmontana*, *L. shangsiensis*, *L. suiyangensis*, *L. tengchongensis*, *L. tuberosa*, *L. ventripunctata*, *L. wuhuangmontis*, *L. yingjiangensis*, *L. yunkaiensis*, and *L. zhangyapingi* (vs. webbing rudimentary in the latter); and differs from *L. flaviglandulosa* and *L. pelodytoides* (vs. webbing present in the latter).

By toes with narrow lateral fringes, *Leptobrachella jinshaensis* sp. nov. differs from *L. aerea*, *L. alpina*, *L. firthi*, *L. laui*, *L. liui*, *L. khasiorum*, and *L. yunkaiensis* (vs. wide in the latter); and differs from *L. kalonensis*, *L. macrops*, *L. minima*, *L. marmorata*, *L. namdongensis*, *L. nyx*, *L. oshanensis*, *L. pyrrhops*, *L. rowleyae*, and *L. tuberosa* (vs. lacking in the latter).

By dorsal surface shagreened and granular, lacking enlarge tubercles or warts, *Leptobrachella jinshaensis* sp. nov. differs from *L. applebyi*, *L. bidoupensis*, *L. kalonensis*, *L. melica*, *L. minima*, *L. nahangensis*, *L. shangsiensis*, and *L. tadungensis* (all of which have the dorsum smooth), and *L. bourreti* (dorsum smooth with small warts), *L. fuliginosa* (dorsum smooth with fine tubercles), *L. liui* (dorsum with round tubercles), *L. macrops* (dorsum roughly granular with large tubercles), *L. maershanensis* (dorsum shagreened with tubercles), *L. minima* (dorsum smooth), *L. nyx* (dorsum with round tubercles), *L. nokrekensis* (dorsum tubercles and longitudinal folds), *L. pelodytoides* (dorsum with small, smooth warts), *L. tamdil* (dorsum weakly tuberculate, with low, oval tubercles), *L. tuberosa* (dorsum very tuberculate), *L. yunkaiensis* (dorsum with raised warts), and *L. wuhuangmontis* (dorsum rough with conical tubercles).

By having higher dominant frequency (4.5–4.7 kHz, 20 °C), *Leptobrachella jinshaensis* sp. nov. differs from *L. applebyi* (3.9–4.3 kHz, 21.5 °C), *L. ardens* (3.1–3.4 kHz, 23.6 °C), *L. bidoupensis* (1.9–2.3 kHz, 19.9 °C), *L. botsfordi* (2.6–3.2 kHz, 14 °C), *L. crocea* (2.6–3.0 kHz, 21.6–25.1 °C), *L. fuliginosa* (2.3–2.4 kHz, 19.3–19.6 °C), *L. heteropus* (2.8 kHz, 21 °C), *L. maculosa* (2.7 kHz, 23.3–24.1 °C), *L. melanoleuca* (3.1–3.3 kHz, 23.9 °C), *L. melica* (2.9–3.8 kHz, 26.1 °C), *L. pallida* (2.4–2.7 kHz, 18.9 °C), *L. pyrrhops* (1.9–2.2 kHz, 25 °C), *L. rowleyae* (2.6–3.0 kHz, 21.6–25.1 °C), *L. sola* (3.1–3.2 kHz, 24.2–24.3 °C), *L. tadungensis* (2.6–3.1 kHz, 12.9–22.3 °C) and *L. tuberosa* (2.6–2.8 kHz, 22.5–24.5 °C). The call of the new species appears to have lower frequency compared to the calls attributed to *L. aerea* (6.2–6.4 kHz, 22.4 °C), *L. isos* (7.83–8.55 kHz, 26.4 °C), *L. marmorata* (6.0–6.2 kHz, 22.8 °C), *L. pelodytoides* (6.4–6.6 kHz, 22.7 °C), *L. ventripunctata* (6.1–6.4 kHz, 15 °C) and *L. yingjiangensis* (5.7–5.9 kHz, 19 °C).

By call duration 117–156 ms, *Leptobrachella jinshaensis* sp. nov. differs from *L. aerea* (16–28 ms), *L. bidoupensis* (308–400), *L. botsfordi* (239–303 ms), *L. firthi* (18–24 ms), *L. fuliginosa* (51–80 ms), *L. isos* (31–38 ms), *L. maculosa* (889–907 ms), *L. marmorata* (1900–6700 ms), *L. melanoleuca* (40–63 ms), *L. pallida* (627–729 ms), *L. petrops* (44–57 ms), *L. puhoatensis* 6–14 ms, *L. shangsiensis* (64–69 ms), *L. tadungensis* (248–353 ms) and *L. yingjiangensis* (28–42 ms).

Seven species (*L. liui*, *L. oshanensis*, *L. purpuraventra*, *L. bijie*, *L. suiyangensis*, *L. chishuiensis*, and *L. ventripunctata*) of the genus occur in Guizhou Province, China (Fei et al. 2012; Wang et al. 2019; Luo et al. 2020; Li et al. 2020a). The new species differs from *L. liui* by having narrow lateral fringes on toes (vs. wide in the latter), dorsal surface shagreened with small granules, and lacking enlarge tubercles or warts (vs. dorsum with round tubercles in the latter); differs from *L. oshanensis* by having narrow lateral fringes on toes (vs. lacking in the latter); differs from *L. purpuraventra* and *L. suiyangensis* by heels overlapping when thighs are positioned at right angles to the body (vs. just meeting in the latter); differs from *L. purpuraventra* by tibia-tarsal articulation reaches the middle eye when leg stretched forward (vs. only reaches the level between tympanum to eye in the latter).

In mitochondrial DNA trees, *Leptobrachella jinshaensis* sp. nov. clustered as an independent clade and appears to be sister to a clade in comprising of *L. bijie* and *L. chishuiensis*. The latter two species also occur near the type locality of the new species. The new species differs from *L. bijie* by the following characters: webbing on toes absent (vs. webbing rudimentary in the latter), heels overlapping when thighs are positioned at right angles to the body (vs. just meeting in the latter), having longer call interval (132.7 ± 8.6 , $N = 109$ in the new species vs. 101.9 ± 6.4 , $N = 33$ in the latter),

Table 4. Morphometric comparisons between *Leptobrachella jinshaensis* sp. nov. and its relatives. Units given in mm. See abbreviations for morphometric characters in Materials and methods section. *P*-value was resulted from Mann-Whitney *U* test. Significant level at 0.05. Abbreviations for species name: *LJ*, *Leptobrachella jinshaensis* sp. nov.; *LC*, *L. chishuiensis*; *LB*, *L. bijie*.

Character	<i>Leptobrachella jinshaensis</i> sp. nov.		<i>L. chishuiensis</i>		<i>L. bijie</i>		<i>P</i> -value	
	Male (n = 5)		Male (n = 7)		Male (n = 8)		<i>LJ</i> vs. <i>LC</i>	<i>LJ</i> vs. <i>LB</i>
	Ranging	Mean \pm SD	Ranging	Mean \pm SD	Ranging	Mean \pm SD		
SVL	29.7–31.2	30.8 \pm 0.6	30.8–33.4	32.1 \pm 1.0	29.0–30.4	29.7 \pm 0.6	0.088	0.019
HDL	10.0–11.4	10.7 \pm 0.6	11.1–12.3	11.8 \pm 0.4	10.0–10.6	10.2 \pm 0.2	0.123	0.661
HDW	10.0–10.4	10.2 \pm 0.2	10.6–11.9	11.4 \pm 0.5	9.5–10.2	9.8 \pm 0.3	0.012	0.463
SL	4.5–4.9	4.6 \pm 0.1	4.8–5.8	5.2 \pm 0.3	4.0–4.7	4.2 \pm 0.2	0.019	0.057
IND	2.8–3.5	3.2 \pm 0.3	3.5–3.8	3.7 \pm 0.1	2.8–3.4	3.1 \pm 0.2	0.062	0.464
IOD	3.1–4.0	3.5 \pm 0.4	2.7–3.1	3.0 \pm 0.2	2.8–3.4	3.1 \pm 0.2	0.004	0.242
UEW	2.7–3.2	2.9 \pm 0.2	3.0–3.3	3.2 \pm 0.1	/	/	0.223	/
ED	3.7–4.3	4.0 \pm 0.2	4.0–5.0	4.4 \pm 0.4	3.6–4.1	3.8 \pm 0.2	0.064	0.558
TYD	2.5–3.2	2.7 \pm 0.3	2.0–2.6	2.3 \pm 0.2	1.9–2.2	2.0 \pm 0.1	0.019	0.003
TEY	0.9–1.4	1.0 \pm 0.2	1.2–1.6	1.4 \pm 0.2	0.9–1.1	1.0 \pm 0.1	0.042	0.464
LAL	13.7–15.4	14.6 \pm 0.7	14.7–17.0	15.6 \pm 0.8	14.0–14.8	14.3 \pm 0.3	0.570	0.661
LW	2.1–2.6	2.3 \pm 0.2	2.6–3.2	3.0 \pm 0.2	/	/	0.004	/
ML	7.2–8.4	7.9 \pm 0.5	7.9–8.8	8.2 \pm 0.39	7.4–8.3	7.8 \pm 0.3	0.935	0.770
HLL	41.3–46.4	44.4 \pm 2.0	43.3–49.7	49.7 \pm 2.7	43.0–45.5	43.7 \pm 0.8	0.291	0.464
THL	14.0–15.2	14.6 \pm 0.5	13.7–17.1	15.1 \pm 1.2	/	/	0.465	/
TW	3.2–4.9	3.8 \pm 0.7	3.3–4.3	3.8 \pm 0.4	/	/	0.935	/
TL	14.5–15.6	15.1 \pm 0.4	14.9–16.8	15.6 \pm 0.6	13.5–14.4	13. \pm 0.3	0.685	0.008
TFL	19.3–21.4	20.6 \pm 1.0	20.9–22.3	21.7 \pm 0.6	/	/	0.962	/
FL	13.0–14.4	13.7 \pm 0.7	14.4–15.9	15.1 \pm 0.5	13.0–13.8	13.3 \pm 0.2	0.019	0.558



Figure 8. Habitats of *Leptobrachella jinshaensis* sp. nov. in the type locality Lengshuihe Nature Reserve, Jinsha County, Guizhou Province, China. Forest and a mountain stream in the type locality (insert holo-type CIBCS20200516004 in life in the field).

having lower dominant frequency of 4525 ± 0.065 Hz vs. 4780.4 ± 76.5 Hz in the latter, having significantly higher value of SVL in males, and having significantly higher value of TYD and TL to SVL in males. *Leptobrachella jinshaensis* sp. nov. differs from *L. chishuiensis* by webbing on toes absent (vs. webbing rudimentary in the latter), tibiotarsal articulation reaches the middle of eye when leg stretched forward (vs. reaches the tympanum or the level between tympanum to eye in the latter), the lower dominant frequency of calls 4500–4688 Hz (mean 4525 ± 0.065 , 20 °C) vs. 6064–6284 Hz (6140.15 ± 69.35 , 20 °C) in the latter, each call with two kinds of notes vs. only one kind of note in the latter, and having significantly higher value of HDW, SL, IOD, TYD, TEY and FL to SVL in males (all p -values < 0.05; Table 4).

Ecology. *Leptobrachella jinshaensis* sp. nov. is known from the type locality, Lengshuihe Nature Reserve, Jinsha County, Guizhou Province, China. Specimens of the new species are frequently found from stream covered with reeds, and under the rocks (Fig. 8).

Etymology. The specific name *jinshaensis* refers to the distribution of this species, Jinsha County, Guizhou Province, China. We suggest its English common name “Jinsha leaf litter toads” and Chinese name “Jin Sha Zhang Tu Chan (金沙掌突蟾)”.

Discussion

Molecular phylogenetic analyses, detailed morphological comparisons, and advertisement call data all supported the new species distinctly separated from its congeners especially the superficially-morphological-similar species, *L. bijie* and *L. chishuiensis*. Although the relationships between the new species and other closely related species were not resolved, the new species appears to be phylogenetically closer to *L. bijie* and *L. chishuiensis*, corresponding to their high similarity on morphology. However, the new species appears to have lower dominant frequency on calling than the two closely related species. Moreover, they could be separated by morphometric analyses on contributions of some characters, for example, on PC1 of PCA, several characters of head, SVL and FL, which might be associated the calling behaviours, breeding behaviours, and jumping behaviours. We need future work to detect the function of the characters of these species to explore the ecological differences between them.

The large-scale molecular phylogenetic analyses in Chen et al. (2018) revealed many cryptic species in the genus *Leptobrachella* but did not included samples of *Leptobrachella jinshaensis* sp. nov. Similarly, this large phylogenetic framework likely included a few population samples in Guizhou Province, China. However, the phylogenetic framework indicated that Guizhou Province might be the biogeographical zone of transition for western-to-eastern or southwestern-to-northeastern clades (Chen et al. 2018). The findings of series of new species (*Leptobrachella jinshaensis* sp. nov., *L. chishuiensis*, *L. suiyangensis*, *L. bijie*, and *L. purpuraventra*) obviously supply important supplemental materials for detecting detailed evolutionary and biogeographical models of the genus. Moreover, the findings of the new species also indicated a high degree of localised diversification and micro-endemism for the species in the genus *Leptobrachella* because in Guizhou Province, China, the five recent-described *Leptobrachella* species are just known only from their type localities or nearby areas. In addition, in recent years, large number of discoveries have been made from Guizhou, dramatically raising the number of frog species known from the region (Zhang et al. 2017; Li et al. 2018a, b, 2019a, b, 2020a, b, c; Lyu et al. 2019; Wang et al. 2019; Luo et al. 2020; Su et al. 2020; Xu et al. 2020; Wei et al. 2020). This further indicated that more investigations should be conducted in Guizhou Province to define more precisely distribution area of the new species and detect more cryptic species especially in the poorly-investigated areas.

Acknowledgements

This work was supported by Project supported by the National Natural Science Foundation of China (Nos. 32070426 and 31960099), Biodiversity Conservation Key Laboratory of Guizhou Province Education Department, Guiyang College, Basic research project of science and technology department of Guizhou Province (Nos. [2020]1Y083), Guizhou Provincial Science and Technology Project (No. [2020]4Y029), Guizhou

Provincial Department of Education Youth Science and Technology Talents Growth Project (Nos. KY[2018]455 and KY[2018]468), and China Biodiversity Observation Networks (Sino BON–Amphibian & Reptile).

References

- Anderson J (1871) A list of the reptilian accession to the Indian Museum, Calcutta from 1865 to 1870, with a description of some new species. *Journal of the Asiatic Society of Bengal* 40: 12–39.
- Boulenger GA (1893) Concluding report on the reptiles and batrachians obtained in Burma by Signor L. Fea dealing with the collection made in Pegu and the Karin Hills in 1887–88. *Annali del Museo Civico di Storia Naturale di Genova* 13: 304–347.
- Boulenger GA (1900) Descriptions of new batrachians and reptiles from the Larut Hills, Perak. *Annals and Magazine of Natural History* 6: 186–194. <https://doi.org/10.1080/00222930008678356>
- Chen JM, Poyarkov NJ, Suwannapoom C, Lathrop A, Wu YH, Zhou WW, Yuan ZY, Jin JQ, Chen HM, Liu HQ, Nguyen TQ, Nguyen SN, Duong TV, Eto K, Nishikawa K, Matsui M, Orlov NL, Stuart BL, Brown RM, Rowley J, Murphy RW, Wang YY, Che J (2018) Large-scale phylogenetic analyses provide insights into unrecognized diversity and historical biogeography of Asian leaf-litter frogs, genus *Leptolalax* (Anura: Megophryidae). *Molecular Phylogenetics and Evolution* 124: 162–171. <https://doi.org/10.1016/j.ympev.2018.02.020>
- Chen WC, Liao X, Zhou SC, Mo YM (2019) A new species of *Leptobranchella* (Anura: Megophryidae) from southern Guangxi, China. *Zootaxa* 4563: 67–82. <https://doi.org/10.11646/zootaxa.4563.1.3>
- Chen JM, Xu K, Poyarkov NA, Wang K, Yuan ZY, Hou M, Suwannapoom C, Wang J, Che J (2020) How little is known about “the little brown frogs”: description of three new species of the genus *Leptobranchella* (Anura: Megophryidae) from Yunnan Zoological Research 41(3): 292–313. <https://doi.org/10.24272/j.issn.2095-8137.2020.036>
- Darriba D, Taboada GL, Doallo R, Posada D (2012) jModelTest 2: more models, new heuristics and parallel computing. *Nature Methods* 9(8): 772–772. <https://doi.org/10.1038/nmeth.2109>
- Das I, Tron RKL, Rangad D, Hooroo RN (2010) A new species of *Leptolalax* (Anura: Megophryidae) from the sacred groves of Mawphlang, Meghalaya, north-eastern India. *Zootaxa* 2339: 44–56. <https://doi.org/10.11646/zootaxa.2339.1.2>
- Dehling JM (2012a) Eine neue Art der Gattung *Leptolalax* (Anura: Megophryidae) vom Gunung Benom, Westmalaysia/A new species of the genus *Leptolalax* (Anura: Megophryidae) from Gunung Benom, Peninsular Malaysia. *Sauria* 34: 9–21.
- Dehling JM (2012b) Redescription of *Leptolalax gracilis* (Günther, 1872) from Borneo and taxonomic status of two populations of *Leptolalax* (Anura: Megophryidae) from Peninsular Malaysia. *Zootaxa* 3328: 20–34. <https://doi.org/10.11646/zootaxa.3328.1.2>
- Dehling JM, Matsui M (2013) A new species of *Leptolalax* (Anura: Megophryidae) from Gunung Mulu National Park, Sarawak, East Malaysia (Borneo). *Zootaxa* 3670: 33–44.

- Dring J (1983) Frogs of the genus *Leptobrachella* (Pelobatidae). *Amphibia-Reptilia* 4: 89–102. <https://doi.org/10.1163/156853883X00012>
- Dubois A (1983) Note preliminaire sur le genre *Leptolalax* Dubois, 1980 (Amphibiens, Anoures), avec diagnose d'une espece nouvelle du Vietnam. *Alytes* 2: 147–153.
- Duong TV, Do DT, Ngo CD, Nguyen TQ, Poyarkov Jr NA (2018) A new species of the genus *Leptolalax* (Anura: Megophryidae) from southern Vietnam. *Zoological Research* 39: 181–196. <https://doi.org/10.24272/j.issn.2095-8137.2018.009>
- Eto K, Matsui M, Nishikawa K (2015) Description of a new species of the genus *Leptobrachella* (Amphibia, Anura, Megophryidae) from Borneo. *Current Herpetology* 34(2): 128–139. <https://doi.org/10.5358/hsj.34.128>
- Eto K, Matsui M, Nishikawa K (2016) A new highland species of dwarf litter frog genus *Leptobrachella* (Amphibia, Anura, Megophryidae) from Sarawak. *Raffles Bulletin of Zoology*. Singapore 64: 194–203.
- Eto K, Matsui M, Hamidy A, Munir M, Iskandar DT (2018) Two new species of the genus *Leptobrachella* (Amphibia: Anura: Megophryidae) from Kalimantan, Indonesia. *Current Herpetology* 37(2): 95–105. <https://doi.org/10.5358/hsj.37.95>
- Fei L, Ye CY, Huang YZ (1990) Key to Chinese Amphibians. Publishing House for Scientific and Technological Literature, Chongqing, 364 pp.
- Fei L, Ye CY (2005) The key and illustration of Chinese. Sichuan Publishing House of Science and Technology, Chongqing, 253–255.
- Fei L, Hu SQ, Ye CY, Huang YZ (2009) Fauna Sinica. Amphibia Vol. 2 Anura. Science Press, Beijing, 957 pp.
- Fei L, Ye CY, Jiang JP (2012) Colored atlas of Chinese amphibians and their distributions. Sichuan Publishing House of Science and Technology, Chengdu, 619 pp.
- Fouquet A, Gilles A, Vences M, Marty C, Blanc M, Gemmell NJ (2007) Underestimation of species richness in Neotropical frogs revealed by mtDNA analyses. *PLoS ONE* 2(10): e1109. <https://doi.org/10.1371/journal.pone.0001109>
- Frost DR (2020) Amphibian species of the world. Version 6.0. New York: American Museum of Natural History. <http://research.amnh.org/vz/herpetology/amphibia/index.html> [accessed 22 Sep 2020]
- Gosner KL (1960) A simplified table for staging anuran embryos and larvae with notes on identification. *Herpetologica* 16(3): 183–190.
- Grismer LL, Grismer JL, Youmans TM (2004) A new species of *Leptolalax* (Anura: Megophryidae) from Pulau Tioman, West Malaysia. *Asiatic Herpetological Research* 10: 8–11.
- Guindon S, Dufayard JF, Lefort V, Anisimova M, Hordijk W, Gascuel O (2010) New algorithms and methods to estimate maximum-likelihood phylogenies: assessing the performance of PhyML 3.0. *Systematic Biology* 59(3): 307–321. <https://doi.org/10.1093/sysbio/syq010>
- Günther A (1872) On the reptiles and amphibians of Borneo. *Proceedings of the Scientific Meetings of the Zoological Society of London* 1872: 586–600.
- Günther A (1895) The reptiles and batrachians of the Natuna Islands. *Novitates Zoologicae* 2: 499–502.
- Hall TA (1999) BIOEDIT: a user-friendly biological sequence alignment editor and analysis program for Windows 95/98/NT. *Nucleic Acids Symposium Series* 41(41): 95–98. <https://doi.org/10.1021/bk-1999-0734.ch008>

- Hoang CV, Nguyen TT, Luu VQ, Nguyen TQ, Jiang JP (2019) A new species of *Leptobranchella* Smith 1925 (Anura: Megophryidae) from Thanh Hoa Province, Vietnam. *Raffles Bulletin of Zoology*. Singapore 67: 536–556. <https://doi.org/10.26107/RBZ-2019-0042>
- Hou YM, Zhang MF, Hu F, Li SY, Shi SC, Chen J, Mo XY, Wang B (2018) A new species of the genus *Leptolalax* (Anura, Megophryidae) from Hunan, China. *Zootaxa* 4444(3): 247–266. <https://doi.org/10.11646/zootaxa.4444.3.2>
- Humtsoe LN, Bordoloi S, Ohler A, Dubois A (2008) Rediscovery of a long known species, *Ixalus lateralis* Anderson, 1871. *Zootaxa* 1921: 24–34. <https://doi.org/10.11646/zootaxa.1921.1.2>
- Inger RE, Stuebing RB (1992 [“1991”]) A new species of frog of the genus *Leptobranchella* Smith (Anura: Pelobatidae), with a key to the species from Borneo. *Raffles Bulletin of Zoology*. Singapore 39: 99–103.
- Inger RE, Stuebing RB, Tan F (1995) New species and new records of anurans from Borneo. *Raffles Bulletin of Zoology*. Singapore 43: 115–132.
- Inger RE, Lakim M, Biun A, Yambun P (1997) A new species of *Leptolalax* (Anura: Megophryidae) from Borneo. *Asiatic Herpetological Research* 7: 48–50. <https://doi.org/10.5962/bhl.part.18855>
- Inger RE, Orlov N, Darevsky I (1999) Frogs of Vietnam: a report on new collections. *Fieldiana Zoology* 92: 1–46.
- Jiang K, Yan F, Suwannapoom C, Chomdej S, Che J (2013) A new species of the genus *Leptolalax* (Anura: Megophryidae) from northern Thailand. *Asian Herpetological Research* 4: 100–108. <https://doi.org/10.3724/SPJ.1245.2013.00100>
- Lathrop A, Murphy RW, Orlov N, Ho CT (1998) Two new species of *Leptolalax* (Anura: Megophryidae) from northern Vietnam. *Amphibia-Reptilia* 19: 253–267. <https://doi.org/10.1163/156853898X00160>
- Li SZ, Xu N, Lv JC, Jiang JP, Wei G, Wang B (2018a) A new species of the odorous frog genus *Odorrana* (Amphibia, Anura, Ranidae) from southwestern China. *PeerJ* 6(e5695): 1–28. <https://doi.org/10.7717/peerj.5695>
- Li SZ, Xu N, Liu J, Jiang JP, Wei G, Wang B (2018b) A new species of the Asian Toad genus *Megophrys sensu lato* (Amphibia: Anura: Megophryidae) from Guizhou Province, China. *Asian Herpetological Research* 9: 224–239. <https://doi.org/10.16373/j.cnki.ahr.180072>
- Li SZ, Wei G, Xu N, Cui JG, Fei L, Jiang JP, Liu J, Wang B (2019a) A new species of the Asian music frog genus *Nidirana* (Amphibia, Anura, Ranidae) from Southwestern China. *PeerJ* 7: e7157. <https://doi.org/10.7717/peerj.7157>
- Li SZ, Zhang MH, Xu N, Lv JC, Jiang JP, Liu J, Wei G, Wang B (2019b) A new species of the genus *Microhyla* (Amphibia: Anura: Microhylidae) from Guizhou Province, China. *Zootaxa* 4624: 551–575. <https://doi.org/10.11646/zootaxa.4624.4.7>
- Li SZ, Liu J, Wei G, Wang B (2020a) A new species of the Asian leaf litter toad genus *Leptobranchella* (Amphibia, Anura, Megophryidae) from southwest China. *ZooKeys* 943: 91–118. <https://doi.org/10.3897/zookeys.943.51572>
- Li SZ, Lu NN, Liu J, Wang B (2020b) Description of a new *Megophrys* Kuhl & Van Hasselt, 1822 (Anura, Megophryidae) from Guizhou Province, China. *ZooKeys* 986: 101–126. <https://doi.org/10.3897/zookeys.986.57119>

- Li SZ, Wei G, Cheng YL, Zhang BW, Wang B (2020c) Description of a new species of the Asian newt genus *Tylototriton sensu lato* (Amphibia: Urodela: Salamandridae) from South-west China. *Asian Herpetological Research* 11(4): 282–296. <https://doi.org/10.16373/j.cnki.ahr.200026>
- Liu CC (1950) Amphibians of western China. *Fieldiana Zoology Memoires* 2: 1–397. [+ 10 pl.] <https://doi.org/10.5962/bhl.part.4737>
- Luo T, Xiao N, Gao K, Zhou J (2020) A new species of *Leptobrachella* (Anura, Megophryidae) from Guizhou Province, China. *ZooKeys* 923: 115–140. <https://doi.org/10.3897/zookeys.923.47172>
- Lyu ZT, Zeng ZC, Wan H, Yang JH, Li YL, Pang H, Wang YY (2019) A new species of *Amolops* (Anura: Ranidae) from China, with taxonomic comments on *A. liangshanensis* and Chinese populations of *A. marmoratus*. *Zootaxa* 4609: 247–268. <https://doi.org/10.11646/zootaxa.4609.2.3>
- Mahony S, Sengupta S, Kamei RG, Biju SD (2011) A new low altitude species of *Megophrys* Kuhl and van Hasselt (Amphibia: Megophryidae), from Assam, Northeast India. *Zootaxa* 3059: 36–46. <https://doi.org/10.11646/zootaxa.3059.1.2>
- Malkmus R (1992) *Leptolalax pictus* sp. nov. (Anura: Pelobatidae) vom Mount Kinabalu/Nord Borneo. *Sauria* 14: 3–6.
- Mathew R, Sen N (2010 [“2009”]) Description of a new species of *Leptobrachium* Tschudi, 1838 (Amphibia: Anura: Megophryidae) from Meghalaya, India. *Records of the Zoological Survey of India* 109: 91–108.
- Matsui M (1997) Call characteristics of Malaysian *Leptolalax* with a description of two new species (Anura: Pelobatidae). *Copeia* 1997: 158–165. <https://doi.org/10.2307/1447851>
- Matsui M (2006) Three new species of *Leptolalax* from Thailand (Amphibia, Anura, Megophryidae). *Zoological Science* 23 (9): 821–830. <https://doi.org/10.2108/zsj.23.821>
- Matsui M, Belabut DM, Ahmad N, Yong HS (2009) A new species of *Leptolalax* (Amphibia, Anura, Megophryidae) from Peninsular Malaysia. *Zoological Science* 26(3): 243–247. <https://doi.org/10.2108/zsj.26.243>
- Matsui M, Dehling JM (2012) Notes on an enigmatic Bornean megophryid, *Leptolalax dringi* Dubois, 1987 (Amphibia: Anura). *Zootaxa* 3317(1): 49–58. <https://doi.org/10.11646/zootaxa.3317.1.4>
- Matsui M, Zainudin R, Nishikawa K (2014a) A new species of *Leptolalax* from Sarawak, Western Borneo (Anura: Megophryidae). *Zoological Science* 31(11): 773–779. <https://doi.org/10.2108/zs140137>
- Matsui M, Nishikawa K, Yambun P (2014b) A new *Leptolalax* from the mountains of Sabah, Borneo (Amphibia, Anura, Megophryidae). *Zootaxa* 3753(3): 440–452. <https://doi.org/10.11646/zootaxa.3753.5.3>
- Nguyen LT, Poyarkov Jr NA, Le DT, Vo BD, Ninh HT, Duong TV, Murphy RW, Sang NV (2018) A new species of *Leptolalax* (Anura: Megophryidae) from Son Tra Peninsula, central Vietnam. *Zootaxa* 4388: 1–21. <https://doi.org/10.11646/zootaxa.4388.1.1>
- Ohler A, Marquis O, Swan S, Grosjean S (2000) Amphibian biodiversity of Hoang Lien Nature Reserve (Lao Cai Province, northern Vietnam) with description of two new species. *Herpetozoa* 13(1/2): 71–87.

- Ohler A, Wollenberg KC, Grosjean S, Hendrix R, Vences M, Ziegler T, Dubois A (2011) Sorting out *Lalos*: description of new species and additional taxonomic data on megophryid frogs from northern Indochina (genus *Leptolalax*, Megophryidae, Anura). *Zootaxa* 3147: 1–83. <https://doi.org/10.11646/zootaxa.3147.1.1>
- Poyarkov NJ, Rowley JJ, Gogoleva SI, Vassilieva AB, Galoyan EA, Orlov NL (2015) A new species of *Leptolalax* (Anura: Megophryidae) from the western Langbian Plateau, southern Vietnam. *Zootaxa* 3931(2): 221–252. <https://doi.org/10.11646/zootaxa.3931.2.3>
- Qian TY, Xiao X, Cao Y, Xiao NW, Yang DD (2020) A new species of *Leptobranchella* (Anura: Megophryidae) Smith, 1925 from Wuling Mountains in Hunan Province, China. *Zootaxa* 4816: 491–526. <https://doi.org/10.11646/zootaxa.4816.4.4>
- Ronquist FR, Huelsenbeck JP (2003) MrBayes3: Bayesian phylogenetic inference under mixed models. *Bioinformatics* 19(12): 1572–1574. <https://doi.org/10.1093/bioinformatics/btg180>
- Rowley JJ, Cao TT (2009) A new species of *Leptolalax* (Anura: Megophryidae) from central Vietnam. *Zootaxa* 2198: 51–60. <https://doi.org/10.11646/zootaxa.2198.1.5>
- Rowley JJ, Hoang DH, Le TTD, Dau QV, Cao TT (2010a) A new species of *Leptolalax* (Anura: Megophryidae) from Vietnam and further information on *Leptolalax tuberosus*. *Zootaxa* 2660: 33–45.
- Rowley JJ, Stuart BL, Neang T, Emmett DA (2010b) A new species of *Leptolalax* (Anura: Megophryidae) from northeastern Cambodia. *Zootaxa* 2567: 57–68. <https://doi.org/10.11646/zootaxa.2567.1.3>
- Rowley JJ, Stuart BL, Richards SJ, Phimmachak S, Sivongxay N (2010c) A new species of *Leptolalax* (Anura: Megophryidae) from Laos. *Zootaxa* 2681: 35–46. <https://doi.org/10.11646/zootaxa.2681.1.3>
- Rowley JJ, Le DTT, Tran DTA, Hoang DH (2011) A new species of *Leptobranchella* (Anura: Megophryidae) from southern Vietnam. *Zootaxa* 2796: 15–28. <https://doi.org/10.11646/zootaxa.4563.1.3>
- Rowley JJ, Hoang HD, Dau VQ, Le TTD, Cao TT (2012) A new species of *Leptolalax* (Anura: Megophryidae) from central Vietnam. *Zootaxa* 3321: 56–68. <https://doi.org/10.11646/zootaxa.3321.1.4>
- Rowley JJ, Dau VQ, Nguyen TT (2013) A new species of *Leptolalax* (Anura: Megophryidae) from the highest mountain in Indochina. *Zootaxa* 3737(4): 415–428. <https://doi.org/10.11646/zootaxa.3737.4.5>
- Rowley JJ, Stuart BL, Neang T, Hoang HD, Dau VQ, Nguyen TT, Emmett DA (2015) A new species of *Leptolalax* (Anura: Megophryidae) from Vietnam and Cambodia. *Zootaxa* 4039: 401–417. <https://doi.org/10.11646/zootaxa.4039.3.1>
- Rowley JJ, Tran DTA, Le DTT, Dau VQ, Peloso PLV, Nguyen TQ, Hoang HD, Nguyen TT, Ziegler T (2016) Five new, microendemic Asian Leaf-litter Frogs (*Leptolalax*) from the southern Annamite mountains, Vietnam. *Zootaxa* 4085: 63–102. <https://doi.org/10.11646/zootaxa.4085.1.3>
- Rowley JJ, Dau VQ, Hoang HD, Le DTT, Cutajar TP, Nguyen TT (2017a) A new species of *Leptolalax* (Anura: Megophryidae) from northern Vietnam. *Zootaxa* 4243: 544–564. <https://doi.org/10.11646/zootaxa.4243.3.7>

- Rowley JJ, Dau VQ, Cao TT (2017b) A new species of *Leptolalax* (Anura: Megophryidae) from Vietnam. *Zootaxa* 4273(1): 61–79. <https://doi.org/10.11646/zootaxa.4273.1.5>
- Sambrook J, Fritsch EF, Maniatis T (1989) Molecular cloning: a laboratory manual. Cold Spring Harbor Laboratory Press, New York.
- Sengupta S, Sailo S, Lalremsanga HT, Das A, Das I (2010) A new species of *Leptolalax* (Anura: Megophryidae) from Mizoram, north-eastern India. *Zootaxa* 2406: 56–68. <https://doi.org/10.11646/zootaxa.2406.1.3>
- Stuart BL, Rowley JJJ (2020) A new *Leptobrachella* (Anura: Megophryidae) from the Cardamom Mountains of Cambodia. *Zootaxa* 4834: 556–572. <https://doi.org/10.11646/zootaxa.4834.4.4>
- Simon C, Frati F, Beckenbach A, Crespi B, Liu H, Flook P (1994) Evolution, weighting and phylogenetic utility of mitochondrial gene sequences and a compilation of conserved polymerase chain reaction primers. *Annals of the Entomological Society of America* 87(6): 651–701. <https://doi.org/10.1093/aesa/87.6.651>
- Su H, Shi S, Wu Y, Li G, Yao X, Wang B, Li S (2020) Description of a new horned toad of *Megophrys* Kuhl & Van Hasselt, 1822 (Anura, Megophryidae) from southwest China. *ZooKeys* 974: 131–159. <https://doi.org/10.3897/zookeys.974.56070>
- Sung YH, Yang JH, Wang YY (2014) A new species of *Leptolalax* (Anura: Megophryidae) from southern China. *Asian Herpetological Research* 5(2): 80–90. <https://doi.org/10.3724/SPJ.1245.2014.00080>
- Tamura K, Stecher G, Peterson D, Fiipiski A, Kumar S (2013) MEGA6: Molecular Evolutionary Genetics Analysis Version 6.0. *Molecular Phylogenetics and Evolution* 28: 2725–2729. <https://doi.org/10.1093/molbev/mst197>
- Taylor EH (1962) The amphibian fauna of Thailand. *University of Kansas Science Bulletin* 43: 265–599. <https://doi.org/10.5962/bhl.part.13347>
- Wang J, Yang JH, Li Y, Lyu ZT, Zeng ZC, Liu ZY, Ye YH, Wang YY (2018) Morphology and molecular genetics reveal two new *Leptobrachella* species in southern China (Anura, Megophryidae). *ZooKeys* 776: 105–137. <https://doi.org/10.3897/zookeys.776.22925>
- Wang J, Li YL, Li Y, Chen HH, Zeng YJ, Shen JM, Wang YY (2019) Morphology, molecular genetics, and acoustics reveal two new species of the genus *Leptobrachella* from northwestern Guizhou Province, China (Anura, Megophryidae). *ZooKeys* 848: 119–154. <https://doi.org/10.3897/zookeys.848.29181>
- Watters JL, Cummings ST, Flanagan RL, Siler CD (2016) Review of morphometric measurements used in anuran species descriptions and recommendations for a standardized approach. *Zootaxa* 4072(4): 477–495. <https://doi.org/10.11646/zootaxa.4072.4.6>
- Wei G, Li SZ, Liu J, Cheng YL, Xu N, Wang B (2020) A new species of the Music frog *Nidirana* (Anura, Ranidae) from Guizhou Province, China. *ZooKeys* 904: 63–87. <https://doi.org/10.3897/zookeys.904.39161>
- Wijayathilaka N, Meegaskumbura M (2016) An acoustic analysis of the genus *Microhyla* (Anura: Microhylidae) of Sri Lanka. *PLoS ONE* 11: e0159003. <https://doi.org/10.1371/journal.pone.0159003>
- Xu N, Li S-Z, Liu J, Wei G, Wang B (2020) A new species of the horned toad *Megophrys* Kuhl & Van Hasselt, 1822 (Anura, Megophryidae) from southwest China. *ZooKeys* 943: 119–144. <https://doi.org/10.3897/zookeys.943.50343>

- Yang JH, Wang YY, Chen GL, Rao DQ (2016) A new species of the genus *Leptolalax* (Anura: Megophryidae) from Mt. Gaoligongshan of western Yunnan Province, China. *Zootaxa* 4088: 379–394. <https://doi.org/10.11646/zootaxa.4088.3.4>
- Yang JH, Zeng ZC, Wang YY (2018) Description of two new sympatric species of the genus *Leptolalax* (Anura: Megophryidae) from western Yunnan of China. *PeerJ* 6(e4586): 1–32. <https://doi.org/10.7717/peerj.4586>
- Yuan ZY, Sun RD, Chen JM, Rowley JJ, Wu ZJ, Hou SB, Wang SN, Che J (2017) A new species of the genus *Leptolalax* (Anura: Megophryidae) from Guangxi, China. *Zootaxa* 4300: 551–570. <https://doi.org/10.11646/zootaxa.4300.4.5>
- Zhang Y, Li G, Xiao N, Li J, Pan T, Wang H, Zhang B, Zhou J (2017) A new species of the genus *Xenophrys* (Amphibia: Anura: Megophryidae) from Libo County, Guizhou, China. *Asian Herpetological Research* 8: 75–85.

Supplementary material 1

Table S1. Uncorrected *p*-distance between *Leptobranchella* species on the 16S rRNA gene

Authors: Bin Wang

Data type: molecular data

Copyright notice: This dataset is made available under the Open Database License (<http://opendatacommons.org/licenses/odbl/1.0/>). The Open Database License (ODbL) is a license agreement intended to allow users to freely share, modify, and use this Dataset while maintaining this same freedom for others, provided that the original source and author(s) are credited.

Link: <https://doi.org/10.3897/zookeys.1021.60729.suppl1>

Supplementary material 2

Table S2. Variable loadings for principal components with Eigenvalue greater than 1, from morphometric characters corrected by SVL

Authors: Yan-Lin Cheng, Sheng-Chao Shi, Jiaqi Li, Jing Liu, Shi-Ze Li, Bin Wang

Data type: species data

Copyright notice: This dataset is made available under the Open Database License (<http://opendatacommons.org/licenses/odbl/1.0/>). The Open Database License (ODbL) is a license agreement intended to allow users to freely share, modify, and use this Dataset while maintaining this same freedom for others, provided that the original source and author(s) are credited.

Link: <https://doi.org/10.3897/zookeys.1021.60729.suppl2>

Supplementary material 3

Table S3. Advertisement call comparisons between *Leptobrachella jinshaensis* sp. nov. and its congeners

Authors: Yan-Lin Cheng, Sheng-Chao Shi, Jiaqi Li, Jing Liu, Shi-Ze Li, Bin Wang

Data type: statistical data

Copyright notice: This dataset is made available under the Open Database License (<http://opendatacommons.org/licenses/odbl/1.0/>). The Open Database License (ODbL) is a license agreement intended to allow users to freely share, modify, and use this Dataset while maintaining this same freedom for others, provided that the original source and author(s) are credited.

Link: <https://doi.org/10.3897/zookeys.1021.60729.suppl3>

A new species of *Cyrtodactylus* Gray, 1827 (Squamata, Gekkonidae) from Yunnan, China

Shuo Liu¹, Dingqi Rao²

1 Kunming Natural History Museum of Zoology, Kunming Institute of Zoology, Chinese Academy of Sciences, 32 Jiaochang Donglu, Kunming, Yunnan 650223, China **2** Kunming Institute of Zoology, Chinese Academy of Sciences, 32 Jiaochang Donglu, Kunming, Yunnan 650223, China

Corresponding authors: Dingqi Rao (raodq@mail.kiz.ac.cn); Shuo Liu (liushuo@mail.kiz.ac.cn)

Academic editor: T. Ziegler | Received 5 November 2020 | Accepted 27 January 2021 | Published 2 March 2021

<http://zoobank.org/07E7157B-C336-448B-BD4B-CE6053D919DE>

Citation: Liu S, Rao D (2021) A new species of *Cyrtodactylus* Gray, 1827 (Squamata, Gekkonidae) from Yunnan, China. ZooKeys 1021: 109–126. <https://doi.org/10.3897/zookeys.1021.60402>

Abstract

A new species of *Cyrtodactylus* is described on the basis of five specimens collected from the karst formations of Zhenkang County, Yunnan Province, China. *Cyrtodactylus zhenkangensis* **sp. nov.** is recognized by having a unique combination of morphological characters, the most diagnostic being: 12–15 enlarged femoral scales on each thigh; 2–5 femoral pores on each thigh in males, 0–3 pitted scales on each thigh in females; eight or nine preloacal pores in a continuous row or separated by one poreless scale in males, 7–9 pitted scales in females; subcaudals enlarged, arranged alternately as single and double on anterior and mostly single at middle and posterior; dorsal surface of head with obvious reticulations. Phylogenetic analyses show that the new species is a member of the *C. wayakonei* species group and a sister taxon to a clade consisting of *C. wayakonei* and *C. martini* based on Maximum Likelihood analyses and Bayesian Inference and differs from its congeners by at least 12.0% genetic divergence in a fragment of the COI gene.

Keywords

Bent-toed gecko, *Cyrtodactylus wayakonei*, karst-dwelling, taxonomy, Zhenkang

Introduction

Bent-toed geckos of the genus *Cyrtodactylus* are one of the most species-diverse genera of gekkonid lizards (Kluge 2001; Uetz 2020), and many of these species are thought to be highly localized with extremely narrow geographic ranges (Nazarov et al. 2012; Luu et al. 2016; Grismer et al. 2018, 2020; Murdoch et al. 2019). At present, the genus contains more than 300 recognized species (Uetz et al. 2020), and approximately 150 new species have been described since 2010 and most of these new discoveries were from Southeast Asia (Schneider et al. 2020).

During our recent fieldwork in Yunnan Province, China, a series of bent-toed geckos was collected from the karst formations of Zhenkang County. Morphological and molecular phylogenetic analyses revealed that the new collection belonged to an unnamed species of *Cyrtodactylus*. We describe it as a new species.

Materials and methods

Sampling

Fieldwork was conducted at night. Specimens were collected by hand. Photographs were taken to document color pattern in life prior to euthanization. Liver tissues were stored in 99% ethanol and specimens were preserved in 75% ethanol. Specimens were deposited at Kunming Natural History Museum of Zoology, Kunming Institute of Zoology, Chinese Academy of Sciences (**KIZ**).

Molecular analyses

Molecular data were generated for three specimens and analyzed with the available homologous sequences of the *Cyrtodactylus wayakonei* species group obtained from GenBank. The new sequences were deposited in GenBank under accession numbers MW593136–MW593138. Sequences of *C. cf. interdigitalis* Ulber, 1993 and *C. elok* Dring, 1979 were used as outgroups according to Nguyen et al. (2017) and Schneider et al. (2020).

We used the protocols of Le et al. (2006) for DNA extraction, amplification, and sequencing. DNA extraction used the standard three-step phenol/trichloromethane protocol (Sambrook et al. 1989). A fragment of the mitochondrial gene, cytochrome c oxidase subunit 1 (COI) was amplified in a volume consisted of 25 μ l (10 μ l of mastermix, 5 μ l of water, 2 μ l of each primer at 10 pmol/ μ l and 6 μ l of DNA) by the polymerase chain reaction (PCR; 35 cycles of 95 °C for 30 s, 53 °C for 40 s, 72 °C for 90 s) and sequenced using the primer pair VF1-d (TTCTCAACCAACCACAARGAYATYGG) and VR1-d (TAGACTTCTGGGTGGC-CRAARAAYCA) (Ivanova et al. 2006). PCR products were cleaned using ExoSAP-IT (Applied Biosystems) and sequenced in both directions by direct double strand cycle sequencing using the BigDye Terminator v. 3.1 Cycle Sequencing Kit on a

3130 DNA Analyzer (Applied Biosystems). Sequences were edited with Sequencher v. 5.4.6 (Gene Codes).

Sequences were aligned using ClustalW (Thompson et al. 1994) integrated in MEGA v. 7 (Kumar et al. 2016) with default parameters. Pairwise distances between species were calculated in MEGA v. 7 with the parameters Transitions + Transversions, Uniform rates, and Pairwise deletion (Kumar et al. 2016). The substitution model GTR+G+I was selected using the corrected Akaike Information Criterion (AICc) in MODELTEST v. 3.7 (Posada and Crandall 1998). Bayesian inference (BI) was performed in MrBayes v. 3.2.6 (Ronquist et al. 2012) based on the selected substitution model. Two runs were performed simultaneously with four Markov chains starting from random tree. The chains were run for 10,000,000 generations and sampled every 1000 generations. The first 25% of the sampled trees was discarded as burn-in after the standard deviation of split frequencies of the two runs reached a value of less than 0.01, and then the remaining trees were used to create a 50% majority-rule consensus tree and to estimate Bayesian posterior probabilities (BPP). Nodes with BPP of 95 and above were considered strongly supported (Huelsenbeck et al. 2001; Wilcox et al. 2002; Alfaro et al. 2003) and nodes with values of 90–94 as well supported (Chomdej et al. 2020). Maximum Likelihood (ML) analysis was performed in RaxmlGUI v. 1.5 (Silvestro and Michalak 2012), and nodal support was estimated by 1,000 rapid bootstrap replicates. Nodes with bootstrap values of 70 and above were considered significantly supported (Alfaro et al. 2003; Sitnikova 1996).

Morphological analyses

Measurements were taken with digital calipers to the nearest 0.1 mm. Bilateral scale counts were given as left/right. The methodology of measurements and meristic counts followed Ngo (2011) and Schneider et al. (2020):

AG	axilla to groin distance;
DTR	dorsal tubercle rows, number of dorsal, longitudinal rows of tubercles at midbody between the ventrolateral folds;
ED	ear diameter, greatest diameter of ear;
EE	eye orbit to ear distance, from posterior corner of eye orbit to anterior margin of ear opening;
EFS	enlarged femoral scales, number of enlarged femoral scale beneath each thigh;
ForeaL	forearm length, from the base of the palm to the elbow;
FP	femoral pores;
GSDT	granular scales surrounding dorsal midbody tubercles;
HH	maximum head height, from occiput to underside of jaws;
HL	head length, from tip of snout to posterior margin of ear;
HW	maximum head width;
I	postrostrals or internasals;
IFL	infralabials;
IND	internarial distance, measured between inner borders of nostrils;

IOD	interorbital distance, measured across narrowest point of frontal bone;
LD4	subdigital lamellae under the fourth finger;
LT4	subdigital lamellae under the fourth toe;
ML	mental length;
MW	mental width;
OD	greatest diameter of orbit;
PAT	postcloacal tubercles, number of tubercles on each side of postcloacal region;
PM	postmentals, i.e. scales bordering mental shield, except infralabials;
PP	precloacal pores;
PVT	paravertebral tubercles, counted in a single paravertebral row from the level of the forelimb insertions to the level of the hind limb insertion;
RH	rostral height;
RW	rostral width;
SC5SPL	scale rows between fifth supralabials;
SE	snout to eye distance, from tip of snout to anterior corner of eye orbit;
SL	shank length, from the base of heel to the knee;
SPL	supralabials;
SVL	snout-vent length, from tip of snout to anterior margin of cloaca;
TaL	tail length, from posterior margin of cloaca to tip of tail;
V	longitudinal ventral scale rows, counted across the belly between the ventro-lateral folds at midbody.

Morphological comparisons and analyses were based on specimen examination and data obtained from the literature (Hoang et al. 2007; Rösler et al. 2008; Bauer et al. 2009, 2010; Ngo and Grismer 2010; Nguyen et al. 2010, 2015, 2017; Sumontha et al. 2010; Teynie and David 2010; Luu et al. 2011, 2013, 2016; Ngo 2011; Ngo and Chan 2011; Schneider et al. 2011, 2014, 2020; Kunya et al. 2014; Nazarov et al. 2014, 2018; Nguyen et al. 2014; Le 2016; Pham et al. 2019).

Results

Molecular analyses

The obtained sequence alignment is 690 bp in length. The topologies derived from ML and BI analyses were similar and basically consistent with those of Nguyen et al. (2017), Pham et al. (2019), and Schneider et al. (2020). The sequences of three specimens collected from Zhenkang County, Yunnan, China were nested them within the *Cyrtodactylus wayakonei* group and the sister group to a clade consisting of *C. wayakonei* Nguyen, Kingsada, Rösler, Auer & Ziegler, 2010 and *C. martini* Ngo, 2011 with strong support in ML and moderate support in BI (Fig. 1). The interspecific uncorrected genetic *p*-distances between the newly collected specimens and other members of *C. wayakonei* group ranged from 12.0% to 17.8% (Table 1).

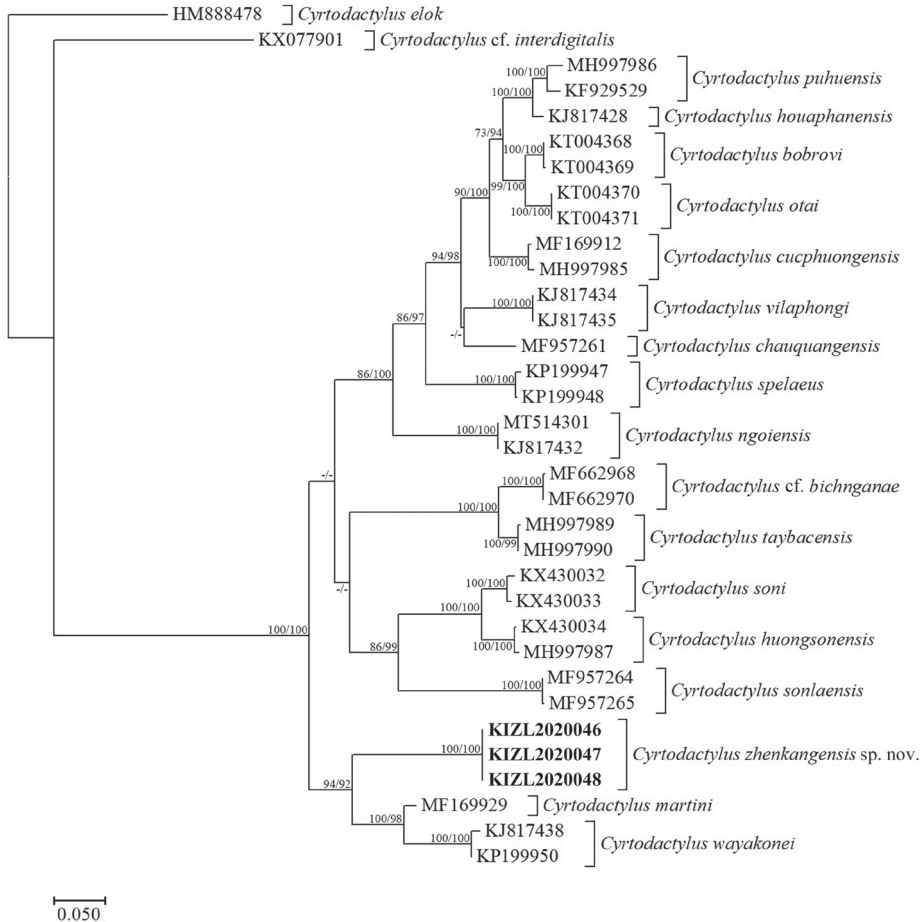


Figure 1. Bayesian Inference phylogram inferred from partial COI genes. Numbers before slashes indicate bootstrap support for Maximum Likelihood analyses and numbers after slashes indicate Bayesian posterior probabilities. The symbol “-” represents the value below 60.

Taxonomic accounts

Cyrtodactylus zhenkangensis sp. nov.

<http://zoobank.org/1CAE09BE-E522-42EF-AD5A-0E3B7A694CDB>

Figs 2–5

Holotype. KIZL2020049, adult male, China, Yunnan Province, Lincang City, Zhenkang County, Nansan town, 23°46'32"N, 98°50'28"E, 1060 m elevation, collected on 11 September 2020 by Shuo Liu.

Paratypes. KIZL2020048 and KIZL2020050, two adult females; KIZL2020046, subadult male; and KIZL2020047, subadult female; all the same collection data as the holotype.

Table 1. Mean uncorrected pairwise genetic distances (%) based on 690 base pairs of COI gene sequences.

	1	2	3	4	5	6	7	8	9	10	11	12	13	14	15	16	17	18	
1 <i>Cyrtodactylus bichnganae</i>																			
2 <i>C. bobrovi</i>	17.2																		
3 <i>C. chauquangensis</i>	15.3	9.3																	
4 <i>C. cucphuongensis</i>	16.6	6.9	8.0																
5 <i>C. houaphanensis</i>	17.3	6.2	8.8	7.2															
6 <i>C. huongsonensis</i>	14.7	15.8	14.5	14.9	16.0														
7 <i>C. martini</i>	15.6	15.1	13.7	14.1	15.6	15.0													
8 <i>C. ngoiensis</i>	15.9	12.3	11.6	13.8	13.1	14.1	14.7												
9 <i>C. otai</i>	16.7	3.8	9.3	7.2	6.2	15.4	15.9	13.1											
10 <i>C. puhensis</i>	18.8	7.2	10.3	8.2	3.4	17.7	16.1	15.0	7.3										
11 <i>C. soni</i>	13.6	16.7	14.5	15.8	16.4	5.3	15.4	15.0	16.3	18.7									
12 <i>C. sonlaensis</i>	15.4	16.3	16.8	16.7	17.7	13.4	14.6	15.4	17.3	18.8	14.0								
13 <i>C. spelaeus</i>	16.9	10.0	11.7	12.1	10.9	16.7	15.0	13.5	11.2	11.8	15.8	15.7							
14 <i>C. taybacensis</i>	5.2	16.1	14.4	15.4	16.2	15.1	14.7	15.6	16.4	17.5	14.4	16.1	15.3						
15 <i>C. vilaphongi</i>	16.4	9.3	8.2	9.5	8.2	15.3	14.7	12.9	9.4	10.1	15.9	17.1	11.8	15.9					
16 <i>C. wayakonei</i>	15.2	16.7	15.2	16.5	17.4	16.7	6.5	15.5	18.3	18.1	17.5	15.9	16.2	15.6	16.0				
17 <i>Cyrtodactylus zhenkangensis</i> sp. nov.	17.8	15.0	14.9	15.8	16.2	16.7	12.0	14.3	16.1	16.8	17.1	17.1	15.7	16.8	16.4	13.1			
18 <i>C. interdigitalis</i>	18.5	19.9	19.2	19.3	20.2	20.2	18.2	20.1	20.1	21.9	19.9	20.5	20.4	18.3	19.3	18.3	19.9		
19 <i>C. elok</i>	18.8	19.4	18.9	17.9	19.5	19.6	17.1	19.5	19.6	20.2	20.2	19.7	18.6	18.6	19.2	18.6	19.5	15.8	

Etymology. The name refers to Zhenkang County, where the new species was found.

Diagnosis. *Cyrtodactylus zhenkangensis* sp. nov. differs from all other congeners by the following combination of characters: medium size (SVL 78.1–87.4 mm); ventrolateral folds present with interspersed tubercles; 12–15 enlarged femoral scales on each thigh; 2–5 femoral pores on each thigh in males, 0–3 pitted scales on each thigh in females; eight or nine precloacal pores in a continuous row or separated by one poreless scale in males, 7–9 pitted scales in females; two or three postcloacal tubercles on each side; 18–21 lamellae under finger IV, 21–23 lamellae under toe IV; subcaudals enlarged, arranged alternately as single and double on anterior and mostly single at middle and posterior; dorsal surface of head with obvious, light-colored reticulations; eight or nine irregular transverse bands on the dorsum of body.

Description of holotype. Adult male, SVL 87.4 mm; head distinguished from neck, moderately long (HL/SVL 0.27), relatively widened (HW/HL 0.79), slightly depressed (HH/HL 0.48); two supranasals separated by one internasal; nares oval, surrounded by supranasal, rostral, first supralabial, and three or four postnasals; loreal region concave; snout long (SE/HL 0.41), round anteriorly, longer than diameter of orbit (OD/SE 0.70); snout scales small, round, granular, larger than those in frontal and parietal regions; eye large (OD/HL 0.28), pupils vertical; upper eyelid fringe with spinous scales; ear opening oval, obliquely directed, small in size (ED/HL 0.08); rostral wider than high (RH/RW 0.66), medially divided dorsally by a suture, reaching to approximately half-way down rostral, in contact with first supralabial and nostrils laterally, and supranasals and internasal dorsally; mental triangular, narrower than rostral

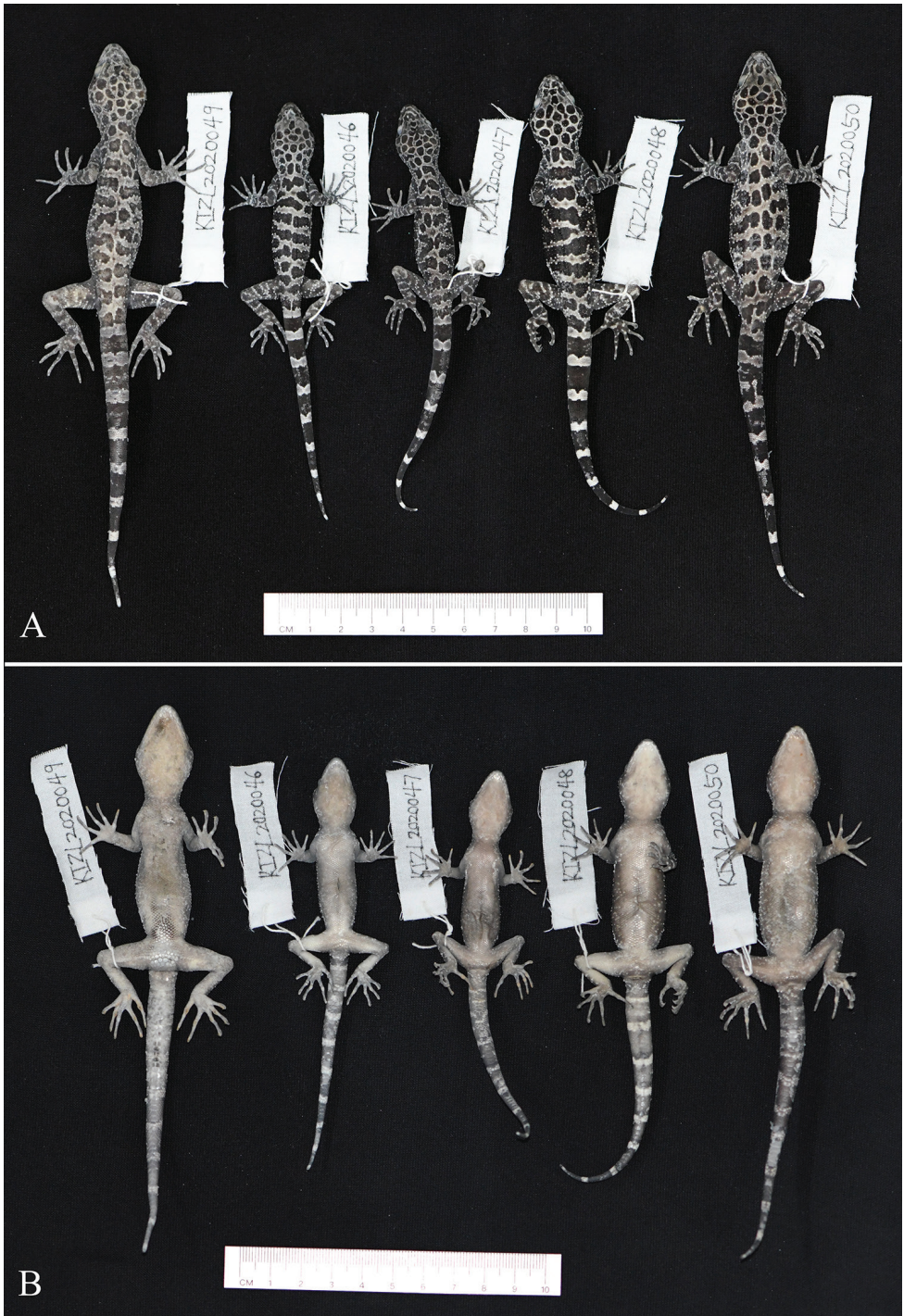


Figure 2. Type series of *Cyrtodactylus zhenkangensis* sp. nov. in preservative **A** dorsal view **B** ventral view.

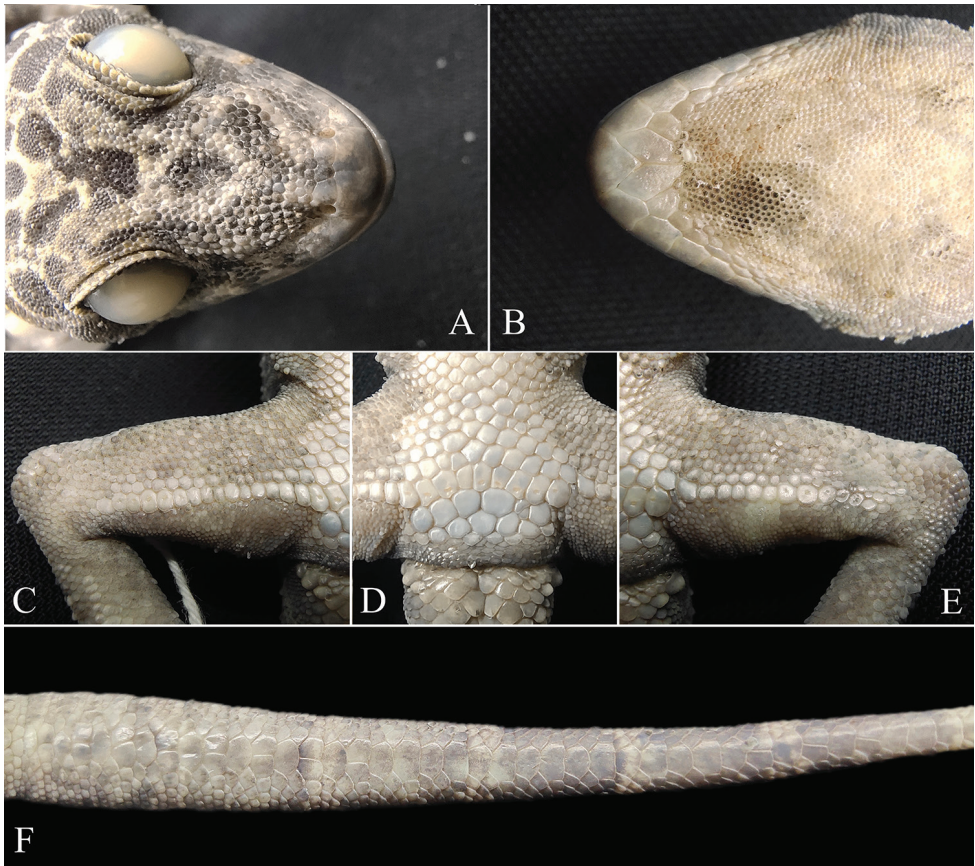


Figure 3. Close-up views of the holotype (KIZL20200049) of *Cyrtodactylus zhenkangensis* sp. nov. in preservative **A** dorsal view of head **B** ventral view of head **C** right side femoral region **D** precloacal region **E** left side femoral region **F** subcaudal scales.

(MW/RW 0.83), wider than high (ML/MW 0.82); two postmentals, enlarged, in contact posteriorly, bordered by mental anteromedially, first infralabial anterolaterally, and an enlarged chin scale posterolaterally; 10/10 supralabials; 10/10 infralabials.

Body slender (AG/SVL 0.41), ventrolateral folds slightly developed with interspersed tubercles; dorsal scales granular; dorsal tubercles round and weakly keeled, four or five times larger than the size of adjoining scales, conical, present on occiput, back and tail base, each surrounded by nine or ten granular scales, in 24 irregular longitudinal rows at the midbody, 29 paravertebral tubercles; ventral scales smooth, larger than those of dorsum, round, subimbricate, largest posteriorly, in 33 longitudinal rows at midbody; gular region with homogenous smooth scales; precloacal groove absent; three rows of enlarged scales present in posterior region of pore-bearing scales; 13/15 enlarged femoral scales beneath thighs continuous with enlarged precloacal scales; femoral pores bearing scales separated from pore-bearing precloacal scales by six poreless

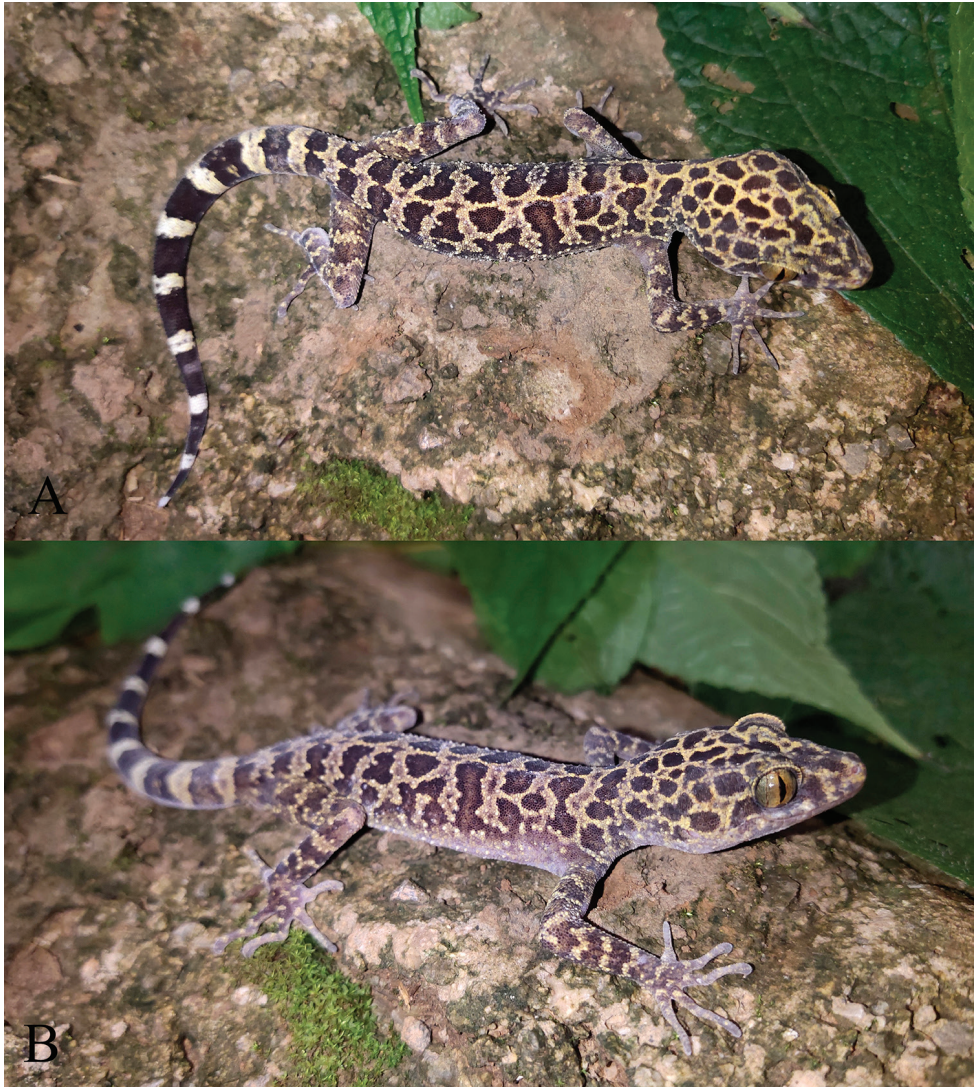


Figure 4. The holotype (KIZL20200049) of *Cyrtodactylus zhenkangensis* sp. nov. in life **A** dorsal view **B** lateral view.

or pitted femoral scales on the left side and nine poreless or pitted femoral scales on the right side; 5/5 femoral pores; 5/3 preloacal pores, separated by one poreless scale; most preloacal pores are positioned in the posterior margin of their scales and femoral pores positioned in the center of scales.

Fore and hind limbs moderately slender (ForeL/SVL 0.17, SL/SVL 0.20); dorsal surface of forelimbs covered by a few weakly developed tubercles; interdigital webbing absent; lamellae under finger IV 20/18, under toe IV 21/23; relative length of fingers $I < II < V < III < IV$, relative length of toes $I < II < III < V < IV$.

Table 2. Measurements (mm) and meristic data for the type series of *Cyrtodactylus zhenkangensis* sp. nov. Abbreviations defined in Materials and methods.

	KIZL2020049	KIZL2020046	KIZL2020047	KIZL2020048	KIZL2020050
	Holotype	Paratype	Paratype	Paratype	Paratype
Sex	Male	Subadult male	Subadult female	Female	Female
SVL	87.4	64.1	66.2	78.1	85.5
TaL	98.1	73.2	76.3	86.9	96.8
HH	11.5	9.0	8.5	10.3	10.4
HL	23.9	18.6	18.6	22.0	24.2
HW	18.8	13.9	14.2	17.1	17.8
OD	6.8	5.1	5.3	6.3	6.8
SE	9.7	7.9	8.0	9.3	9.9
EE	7.6	5.7	5.8	6.7	7.1
IND	3.1	2.5	2.6	3.0	3.2
IOD	8.3	5.8	6.1	7.2	7.7
ED	1.8	1.4	1.3	1.3	1.8
AG	35.5	25.7	25.4	33.2	36.1
ForeaL	15.2	11.5	11.6	13.1	14.5
SL	17.8	13.0	13.5	15.9	16.7
RW	4.1	3.3	3.2	3.7	4.2
RH	2.7	2.0	1.6	2.0	2.4
MW	3.4	3.1	2.7	3.2	3.8
ML	2.8	2.2	2.2	2.1	2.9
SPL	10/10	10/10	10/11	11/10	10/10
IFL	10/10	8/8	10/10	9/9	8/7
I	1	1	1	1	1
SC5SPL	37	32	34	28	33
PM	2	2	2	2	2
GSDT	9–10	9–10	8–9	8–10	8–9
DTR	24	23	21	20	22
PVT	29	27	32	33	28
V	33	32	32	34	33
EFS	13/15	14/14	14/13	13/12	14/15
PP	8	9 (pitted)	9 (pitted)	8 (pitted)	7 (pitted)
FP	5/5	2/2 (pitted)	1/0 (pitted)	3/0 (pitted)	2/2 (pitted)
PAT	2/3	2/2	2/2	3/3	2/3
LD4	20/18	19/20	19/18	21/20	21/19
LT4	21/23	23/22	22/22	22/21	22/22

Tail complete, longer than snout-vent length (TaL/SVL 1.12); 2/3 postcloacal tubercles; dorsal tail base with tubercles; subcaudals smooth, enlarged, arranged alternately in single and double series at anterior and mostly singly at middle and posterior parts.

Color of holotype in life. Head brown with pale-yellow, slightly symmetrical reticulations on either side of the midline, no dark-colored nuchal loop; dorsum of body brown with approximately nine pale-yellow, transverse, irregular bands from forelimb insertions to base of tail and one longitudinal, continuous, narrow vertebral stripe; dorsal surface of limbs brown with some light-yellow, irregularly shaped bands, some small, light-yellow spots on the dorsum of fingers and toes; ventral surface of head, body, and limbs grey with no stripes or spots; tail brownish black with ten yellowish white rings; iris copper-yellow.

Variations. Color pattern variations are shown in Figure 5, and morphometric and meristic differences are presented in Table 2. Morphologically the paratypes resemble

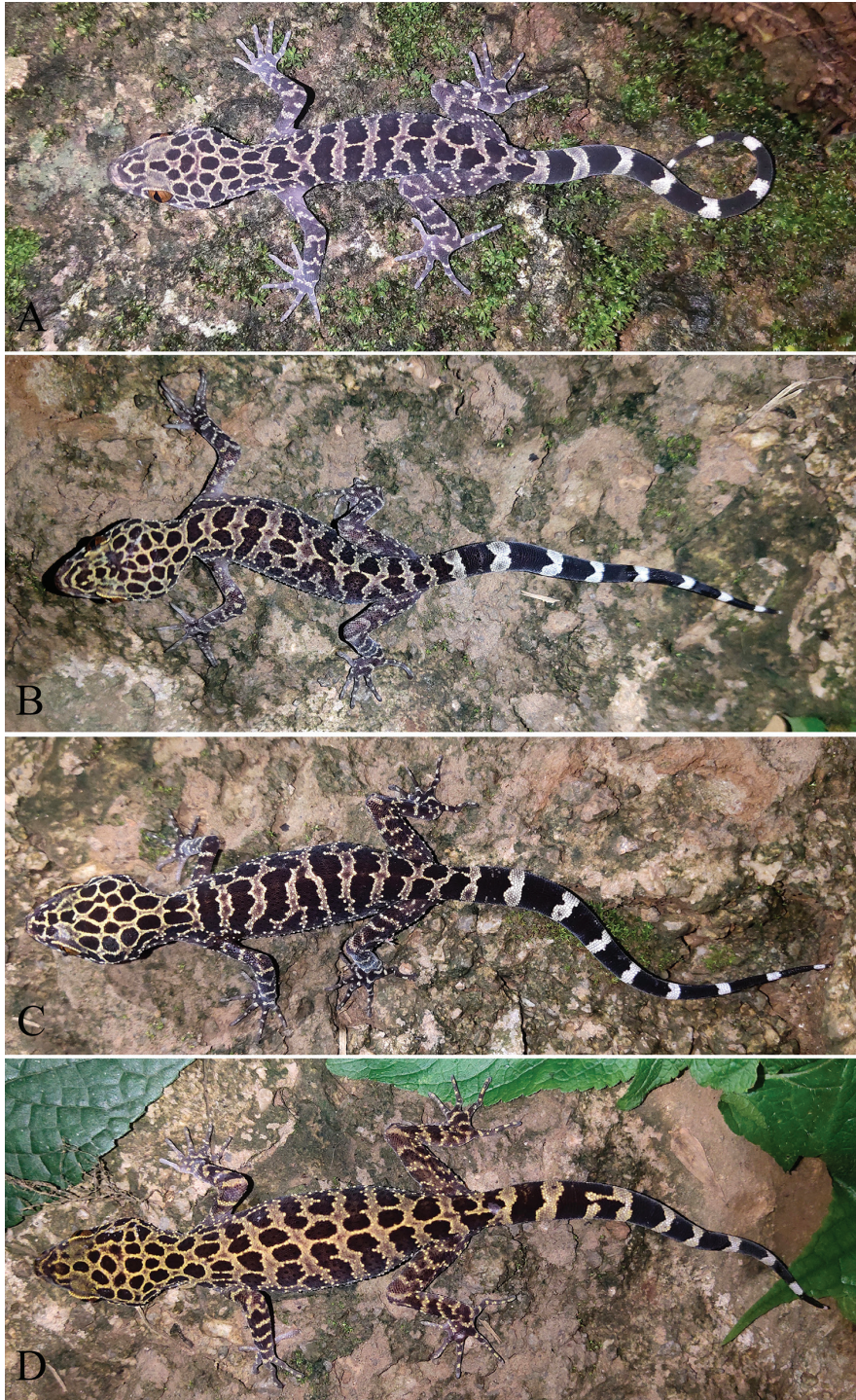


Figure 5. The paratypes of *Cyrtodactylus zhenkangensis* sp. nov. in life **A** subadult male (KIZL2020046) **B** subadult female (KIZL2020047) **C** adult female (KIZL2020048) **D** adult female (KIZL2020050).

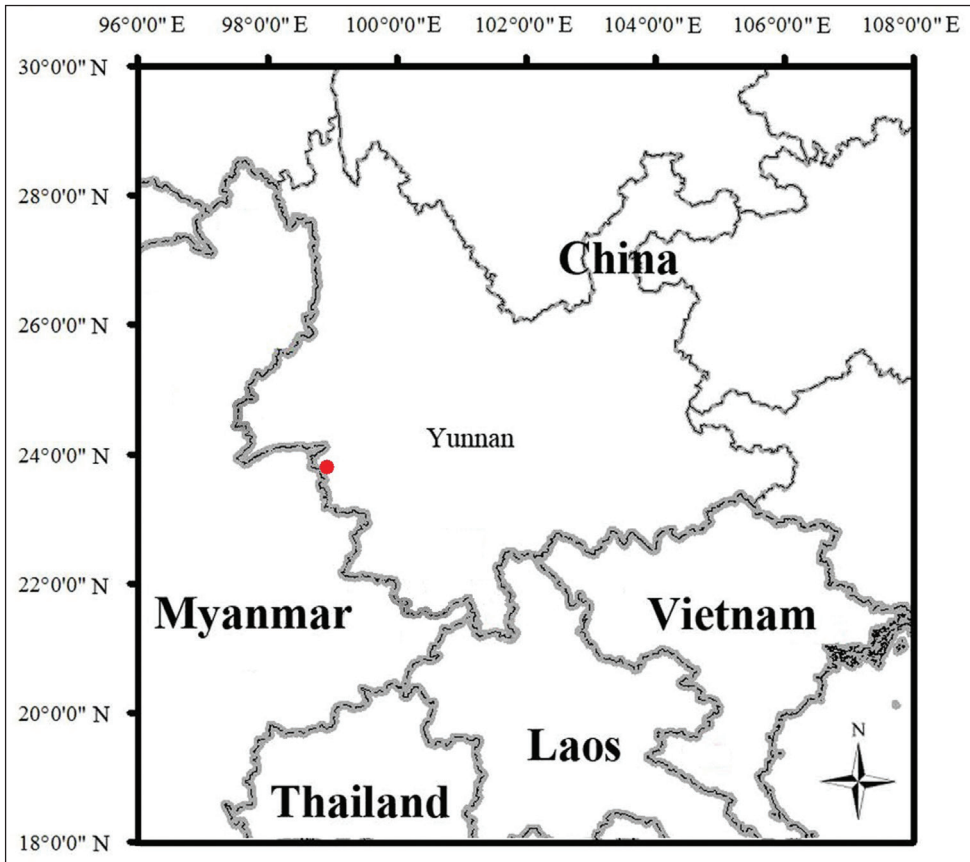


Figure 6. Map showing the type locality (red dot) of *Cyrtodactylus zhenkangensis* sp. nov. in Zhenkang County, Yunnan Province, China.

the holotype except as follows: KIZL2020046 and KIZL2020047 each has one vertebral stripe like the holotype but it is discontinuous; KIZL2020050 has one continuous vertebral strip and two discontinuous, longitudinal, narrow stripes on the sides of vertebral strip; KIZL2020048 only has transverse bands and no vertebra stripe. All paratypes have continuous preloacal pores (pitted) and fewer femoral pores (pitted).

Distribution. The new species is currently known only from the type locality in Zhenkang County, Yunnan Province, China.

Natural history. All specimens were found at night between 19:00 and 21:00 on limestone cliffs of the karst formations. The surrounding habitat was primary forest with a stream nearby. No eggs or juveniles were found.

Comparisons. *Cyrtodactylus zhenkangensis* sp. nov. is distinguishable from all other members of the *C. wayakonei* group by a unique combination of morphological characters. *Cyrtodactylus zhenkangensis* sp. nov. differs from *C. bichnganae* Ngo & Grismer, 2010;



Figure 7. Habitat of *Cyrtodactylus zhenkangensis* sp. nov. at the type locality in Zhenkang County, Yunnan Province, China.

C. huongsonensis Luu, Nguyen, Do & Ziegler, 2011; and *C. sonlaensis* Nguyen, Pham, Ziegler, Ngo & Le, 2017 in having fewer femoral pores in males (4–10 vs 15–29).

Cyrtodactylus zhenkangensis sp. nov. differs from *C. bobrovi* Nguyen, Le, Pham, Ngo, Hoang, Pham & Ziegler, 2015; *C. otai* Nguyen, Le, Pham, Ngo, Hoang, Pham & Ziegler, 2015; and *C. vilaphongi* Schneider, Nguyen, Le, Nophaseud, Bonkowski & Ziegler, 2014 in having enlarged subcaudal scales (vs lacking enlarged subcaudals).

Cyrtodactylus zhenkangensis sp. nov. differs from *C. chauquangensis* Hoang, Orlov, Ananjeva, Johns, Hoang & Dau, 2007; *C. cucphuongensis* Ngo & Chan, 2011; *C. houaphanensis* Schneider, Luu, Sitthivong, Teynié, Le, Nguyen & Ziegler, 2020; *C. pubuensis* Nguyen, Yang, Le, Nguyen, Orlov, Hoang, Nguyen, Jin, Rao, Hoang, Che, Murphy & Zhang, 2014; *C. spelaeus* Nazarov, Poyarkov, Orlov, Nguyen, Milto, Martynov, Konstantinov & Chulisov, 2014; and *C. taybacensis* Pham, Le, Ngo, Ziegler & Nguyen, 2019 in having femoral pores in males (vs lacking femoral pores in males).

Cyrtodactylus zhenkangensis sp. nov. differs from *C. martini* in having femoral pores in males (vs lacking femoral pores in males) and more irregular transverse bands on the dorsum of body (8–9 vs 5–7).

Cyrtodactylus zhenkangensis sp. nov. differs from *C. ngoiensis* Schneider, Luu, Sitthivong, Teynié, Le, Nguyen & Ziegler, 2020 and *C. soni* Le, Nguyen, Le & Ziegler, 2016 in its smaller body size (64.1–87.4 mm vs 62.9–103 mm) and having more lamellae under finger IV (18–21 vs 15–19) and toe IV (21–23 vs 18–22).

Cyrtodactylus zhenkangensis sp. nov. differs from *C. wayakonei* in having enlarged subcaudal scales (vs lacking enlarged subcaudals) and with more irregular transverse bands on the dorsum of body (8–9 vs 5–7).

For other species which were not included in the phylogenetic analyses and resemble *Cyrtodactylus zhenkangensis* sp. nov. in morphology. *Cyrtodactylus zhenkangensis* sp. nov. differs from *C. auribalteatus* Sumontha, Panitvong & Deenin, 2010 in having more transverse bands on the dorsum of body (8–9 vs 4–5), obvious reticulations on the dorsum of head (vs no obvious reticulations) and absent dark-colored nuchal loop (vs present).

Cyrtodactylus zhenkangensis sp. nov. differs from *C. doisuthep* Kunya, Panmongkol, Pauwels, Sumontha, Meewasana, Bunkhwamdi & Dangsri, 2014 in having fewer femoral pores (0–10 vs 12–14), more precloacal pores (7–9 vs 6), and absent dark-colored nuchal loop (vs present).

Cyrtodactylus zhenkangensis sp. nov. differs from *C. dumnuui* Bauer, Kunya, Sumontha, Niyomwan, Pauwels, Chanhome & Kunya, 2010 in having more lamellae under toe IV (21–23 vs 19), absent dark-colored nuchal loop (vs present), and obvious reticulations on the dorsum of head (vs not obvious or no reticulations).

Cyrtodactylus zhenkangensis sp. nov. differs from *C. erythropros* Bauer, Kunya, Sumontha, Niyomwan, Panitvong, Pauwels, Chanhome & Kunya, 2009 in having fewer femoral pores in males (4–10 vs 18–20), more lamellae under finger IV (18–21 vs 16) and toe IV (21–23 vs 20), and more transverse bands on the dorsum of body (8–9 vs 6–7).

Discussion

According to Pham et al. (2019) and Schneider et al. (2020), the *Cyrtodactylus wayakonei* species group contains 16 species, namely *C. bichnganae*, *C. bobrovi*, *C. chauquanensis*, *C. cucphuongensis*, *C. houaphanensis*, *C. huongsonensis*, *C. martini*, *C. ngoiensis*, *C. otai*, *C. pubuensis*, *C. soni*, *C. sonlaensis*, *C. spelaeus*, *C. taybacensis*, *C. vilaphongi*, and *C. wayakonei*. However, we speculate that there are still some other species (e.g., *C. auribalteatus*, *C. doisuthep*, *C. dumnuui*, and *C. erythropros*) which were not included in the phylogenetic analyses also belong to this species group based on morphology, molecular evidence is needed to clarify these problems.

Although the distribution of the new species is distant from the distributions of *C. martini* and *C. wayakonei*, the new species is most similar to the latter two in both morphology and phylogeny. The new species is not found in a protected area; the type locality is just beside the county seat, where there are human activities during the day but usually not at night. This species is nocturnal, so it may be less affected by human activities.

There are many other karst formations in Yunnan, some of which remain insufficiently surveyed. We are continuing to conduct more expeditions in these regions, and it is likely that additional new species of *Cyrtodactylus* will be found in these karst systems.

Acknowledgements

We thank Decai Ouyang for assistance in the field. We are grateful to our workmates for their help and advice. We also thank the reviewers for their valuable comments on the manuscript. This work was supported by Science-Technology Basic Condition Platform from the Ministry of Science and Technology of the People's Republic of China (grant no. 2005DKA21402) and National Natural Science Foundation Project: Investigation and Classificatory and Phylogenetic Studies on the Lizards of Gekkonidae of China (grant no. NSFC-31970404).

References

- Alfaro ME, Zoller S, Lutzoni F (2003) Bayes or bootstrap? A simulation study comparing the performance of Bayesian Markov chain Monte Carlo sampling and bootstrapping in assessing phylogenetic confidence. *Molecular Biology and Evolution* 20: 255–266. <https://doi.org/10.1093/molbev/msg028>
- Bauer AM, Kunya K, Sumontha M, Niyomwan P, Panitvong N, Pauwels OSG, Chanhom L, Kunya T (2009) *Cyrtodactylus erythrops* (Squamata: Gekkonidae), a new cave-dwelling gecko from Mae Hong Son Province, Thailand. *Zootaxa* 3811: 251–261. <https://doi.org/10.11646/zootaxa.2124.1.4>
- Bauer A, Kunya K, Sumontha M, Niyomwan P, Pauwels OSG, Chanhom L, Kunya T (2010) *Cyrtodactylus dumnuui* (Squamata: Gekkonidae), a new cave-dwelling gecko from Chiang Mai Province, Thailand. *Zootaxa* 2570: 41–50. <https://doi.org/10.11646/zootaxa.2570.1.2>
- Chomdej S, Suwannapoom C, Pawangkhanant P, Pradit W, Nazarov RA, Grismer LL, Poyarkov NA (2020) A new species *Cyrtodactylus* Gray (Squamata: Gekkonidae) from western Thailand and the phylogenetic placement of *C. inthanon* and *C. doisuthep*. *Zootaxa* 4838: 179–209. <https://doi.org/10.11646/zootaxa.4838.2.2>
- Dring JCM (1979) Amphibians and reptiles from northern Trengganu, Malaysia, with descriptions of two new geckos: *Cnemaspis* and *Cyrtodactylus*. *Bulletin of the British Museum (Natural History), Zoology* 34: 181–241.
- Grismer LL, Wood Jr PL, Thura MK, Zin T, Quah ESH, Murdoch ML, Grismer MS, Lin A, Kyaw H, Ngwe L (2018) Twelve new species of *Cyrtodactylus* Gray (Squamata: Gekkonidae) from isolated limestone habitats in east-central and southern Myanmar demonstrate high localized diversity and unprecedented microendemism. *Zoological Journal of the Linnean Society* 182: 862–959. <https://doi.org/10.1093/zoolinnean/zlx057>
- Grismer LL, Wood Jr PL, Le MD, Quah ESH, Grismer JL (2020) Evolution of habitat preference in 243 species of bent-toed geckos (genus *Cyrtodactylus* Gray, 1827) with a discussion of karst habitat conservation. *Ecology and Evolution* 10: 13717–13730. <https://doi.org/10.1002/ece3.6961>
- Hoang QX, Orlov NL, Ananjeva NB, Johns AG, Hoang TN, Dau VQ (2007) Description of a new species of the genus *Cyrtodactylus* Gray, 1827 (Squamata: Sauria: Gekkonidae) from the karst of North Central Vietnam. *Russian Journal of Herpetology* 14: 98–106.

- Ivanova NV, Dewaard JR, Hebert PDN (2006) An inexpensive, automation-friendly protocol for recovering high-quality DNA. *Molecular Ecology Notes* 6: 998–1002. <https://doi.org/10.1111/j.1471-8286.2006.01428.x>
- Kluge AG (2001) Gekkotan lizard taxonomy. *Hamadryad* 26: 1–209.
- Kumar S, Stecher G, Tamura K (2016) MEGA7: Molecular Evolutionary Genetics Analysis version 7.0 for bigger datasets. *Molecular Biology and Evolution* 33: 1870–1874. <https://doi.org/10.1093/molbev/msw054>
- Kunya K, Panmongkol A, Pauwels OGS, Sumontha M, Meewasana J, Bunkhwamdi W, Dang-sri S (2014) A new forest-dwelling Bent-toed Gecko (Squamata: Gekkonidae: *Cyrtodactylus*) from Doi Suthep, Chiang Mai Province, northern Thailand. *Zootaxa* 3811: 251–261. <https://doi.org/10.11646/zootaxa.3811.2.6>
- Huelsenbeck JP, Ronquist F, Nielsen R, Bollback JP (2001) Bayesian Inference of phylogeny and its impact on evolutionary biology. *Science* 294: 2310–2314. <https://doi.org/10.1126/science.1065889>
- Le DT, Nguyen TQ, Le MD, Ziegler T (2016) A new species of *Cyrtodactylus* (Squamata: Gekkonidae) from Ninh Binh Province, Vietnam. *Zootaxa* 4162: 268–282. <https://doi.org/10.11646/zootaxa.4162.2.4>
- Le M, Raxworthy CJ, McCord WP, Mertz L (2006) A molecular phylogeny of tortoises (Testudines: Testudinidae) based on mitochondrial and nuclear genes. *Molecular Phylogenetics and Evolution* 40: 517–531. <https://doi.org/10.1016/j.ympev.2006.03.003>
- Luu VQ, Bonkowski M, Nguyen TQ, Le MD, Schneider N, Ngo HT, Ziegler T (2016) Evolution in karst massifs: cryptic diversity among bent-toed geckos along the Truong Son Range with descriptions of three new species and one new country record from Laos. *Zootaxa* 4107: 101–140. <https://doi.org/10.11646/zootaxa.4107.2.1>
- Luu VQ, Calame T, Nguyen TQ, Soudthichak S, Bonkowski M, Ziegler T (2013) New country records of reptiles from Laos. *Biodiversity Data Journal* 1: e1015. <https://doi.org/10.3897/BDJ.1.e1015>
- Luu VQ, Nguyen TQ, Do HQ, Ziegler T (2011) A new *Cyrtodactylus* (Squamata: Gekkonidae) from Huong Son limestone forest, Hanoi, northern Vietnam. *Zootaxa* 3129: 39–50. <https://doi.org/10.11646/zootaxa.3129.1.3>
- Murdoch ML, Grismer LL, Wood Jr PL, Neang T, Poyarkov NA, Ngo TV, Nazarov RA, Aowphol A, Pauwels OSG, Nguyen HN, Grismer JL (2019) Six new species of the *Cyrtodactylus intermedius* complex (Squamata: Gekkonidae) from the Cardamom Mountains and associated highlands of Southeast Asia. *Zootaxa* 4554: 1–62. <https://doi.org/10.11646/zootaxa.4554.1.1>
- Nazarov RA, Pauwels OSG, Konstantinov EL, Chulisov AS, Orlov NL, Poyarkov NA (2018) A new karst-dwelling bent-toed gecko (Squamata: Gekkonidae: *Cyrtodactylus*) from Xiengkhoang Province, northeastern Laos. *Zoological Research* 39: 197–213.
- Nazarov RA, Poyarkov NA, Orlov NL, Nguyen SN, Milto KD, Martynov AA, Konstantinov EL, Chulisov AS (2014) A review of genus *Cyrtodactylus* (Reptilia: Sauria: Gekkonidae) in fauna of Laos with description of four new species. *Proceedings of the Zoological Institute RAS* 318: 391–423.

- Nazarov RA, Poyarkov NA, Orlov NL, Phung TM, Nguyen TT, Hoang DM, Ziegler T (2012) Two new cryptic species of the *Cyrtodactylus irregularis* complex (Squamata: Gekkonidae) from southern Vietnam. *Zootaxa* 3302: 1–24. <https://doi.org/10.11646/zootaxa.3302.1.1>
- Ngo TV (2011) *Cyrtodactylus martini*, another new karst-dwelling *Cyrtodactylus* Gray, 1827 (Squamata: Gekkonidae) from Northwestern Vietnam. *Zootaxa* 2834: 33–46. <https://doi.org/10.11646/zootaxa.2834.1.3>
- Ngo TV, Chan KO (2011) A new karstic cave-dwelling *Cyrtodactylus* Gray (Squamata: Gekkonidae) from Northern Vietnam. *Zootaxa* 3125: 51–63.
- Ngo TV, Grismer LL (2010) A new karst dwelling *Cyrtodactylus* (Squamata: Gekkonidae) from Son La Province, northwestern Vietnam. *Hamadryad* 35: 84–95. <https://doi.org/10.11646/zootaxa.2652.1.1>
- Nguyen TQ, Kingsada P, Rösler H, Auer M, Ziegler T (2010) A new species of *Cyrtodactylus* (Squamata: Gekkonidae) from northern Laos. *Zootaxa* 2652: 1–16.
- Nguyen TQ, Le MD, Pham AV, Ngo HN, Hoang CV, Pham CT, Ziegler T (2015) Two new species of *Cyrtodactylus* (Squamata: Gekkonidae) from the karst forest of Hoa Binh Province, Vietnam. *Zootaxa* 3985: 375–390. <https://doi.org/10.11646/zootaxa.3985.3.3>
- Nguyen TQ, Pham AV, Ziegler T, Ngo HT, Le MD (2017) A new species of *Cyrtodactylus* (Squamata: Gekkonidae) and the first record of *C. otai* from Son La Province, Vietnam. *Zootaxa* 4341: 25–40. <https://doi.org/10.11646/zootaxa.4341.1.2>
- Nguyen SN, Yang JX, Le NT, Nguyen LT, Orlov NL, Hoang CV, Nguyen TQ, Jin JQ, Rao DQ, Hoang TN, Che J, Murphy RW, Zhang YP (2014) DNA barcoding of Vietnamese bent-toed geckos (Squamata: Gekkonidae: *Cyrtodactylus*) and the description of a new species. *Zootaxa* 3784: 48–66. <https://doi.org/10.11646/zootaxa.3784.1.2>
- Pham AV, Le MD, Ziegler T, Nguyen TQ (2019) A new species of *Cyrtodactylus* (Squamata: Gekkonidae) from northwestern Vietnam. *Zootaxa* 4544: 360–380. <https://doi.org/10.11646/zootaxa.4544.3.3>
- Posada D, Crandall KA (1998) Modeltest: testing the model of DNA substitution. *Bioinformatics* 14: 817–818. <https://doi.org/10.1093/bioinformatics/14.9.817>
- Ronquist F, Teslenko M, van der Mark P, Ayres DL, Darling A, Höhna S, Larget B, Liu L, Suchard MA, Huelsenbeck JP (2012) MrBayes 3.2: efficient Bayesian phylogenetic inference and model choice across a large model space. *Systematic Biology* 61: 539–542. <https://doi.org/10.1093/sysbio/sys029>
- Rösler H, Vu TN, Nguyen TQ, Ngo TV, Ziegler T (2008) A new *Cyrtodactylus* (Squamata: Gekkonidae) from central Vietnam. *Hamadryad* 33: 48–63.
- Schneider N, Luu VQ, Sitthivong S, Teynié A, Le MD, Nguyen TQ, Ziegler T (2020) Two new species of *Cyrtodactylus* (Squamata: Gekkonidae) from northern Laos, including new finding and expanded diagnosis of *C. bansocensis*. *Zootaxa* 4822: 503–530. <https://doi.org/10.11646/zootaxa.4822.4.3>
- Schneider N, Nguyen TQ, Le MD, Nophaseud L, Bonkowski M, Ziegler T (2014) A new species of *Cyrtodactylus* (Squamata: Gekkonidae) from the karst forest of northern Laos. *Zootaxa* 3835: 80–96. <https://doi.org/10.11646/zootaxa.3835.1.4>

- Schneider N, Nguyen TQ, Schmitz A, Kingsada P, Auer M, Ziegler T (2011) A new species of karst dwelling *Cyrtodactylus* (Squamata: Gekkonidae) from northwestern Laos. *Zootaxa* 2930: 1–21. <https://doi.org/10.11646/zootaxa.2930.1.1>
- Silvestro D, Michalak I (2012) raxmlGUI: a graphical front-end for RAxML. *Organisms Diversity and Evolution* 12: 335–337. <https://doi.org/10.1007/s13127-011-0056-0>
- Sitnikova T (1996) Bootstrap method of interior-branch test for phylogenetic trees. *Molecular Biology and Evolution* 13: 605–611. <https://doi.org/10.1093/oxfordjournals.molbev.a025620>
- Sumontha M, Panitvong N, Deein G (2010) *Cyrtodactylus auribalteatus* (Squamata: Gekkonidae), a new cave-dwelling gecko from Phitsanulok Province, Thailand. *Zootaxa* 2370: 53–64. <https://doi.org/10.11646/zootaxa.2370.1.3>
- Teynié A, David P (2010) *Voyages naturalists au Laos. Les reptiles*. Revoir Editions, Chamalières, France, 315 pp.
- Thompson JD, Higgins DG, Gibson TJ (1994) CLUSTAL W: improving the sensitivity of progressive multiple sequence alignment through sequence weighting, position-specific gap penalties and weight matrix choice. *Nucleic Acids Research* 22: 4673–4680. <https://doi.org/10.1093/nar/22.22.4673>
- Uetz P (2020) The Reptile Database. <http://www.reptile-database.org> [Accessed on: 2020-11-5]
- Ulber T (1993) Bemerkungen über cyrtodactyline Geckos aus Thailand nebst Beschreibungen von zwei neuen Arten (Reptilia: Gekkonidae). *Mitteilungen aus dem Zoologischen Museum in Berlin* 69: 187–200. <https://doi.org/10.1002/mmnz.19930690202>
- Wilcox TP, Zwickl DJ, Heath TA, Hillis DM (2002) Phylogenetic relationships of the dwarf boas and a comparison of Bayesian and bootstrap measures of phylogenetic support. *Molecular Phylogenetics and Evolution* 25: 361–371. [https://doi.org/10.1016/S1055-7903\(02\)00244-0](https://doi.org/10.1016/S1055-7903(02)00244-0)

New record of *Cyrtonotula* Uvarov, 1939 (Blaberidae, Epilamprinae) from China, with three new species based on morphological and COI data

Yi-Shu Wang¹, Rong Chen¹, Du-Ting Jin¹, Yan-Li Che¹, Zong-Qing Wang¹

¹ College of Plant Protection, Southwest University, Beibei, Chongqing 400715, China

Corresponding author: Zong-Qing Wang (zqwang2006@126.com)

Academic editor: F. Legendre | Received 11 October 2020 | Accepted 5 February 2021 | Published 2 March 2021

<http://zoobank.org/39F17136-0F16-416F-A667-F4346CDC4F30>

Citation: Wang Y-S, Chen R, Jin D-T, Che Y-L, Wang Z-Q (2021) New record of *Cyrtonotula* Uvarov, 1939 (Blaberidae, Epilamprinae) from China, with three new species based on morphological and COI data. ZooKeys 1021: 127–143. <https://doi.org/10.3897/zookeys.1021.59526>

Abstract

The genus *Cyrtonotula* Uvarov, 1939 (Blaberidae, Epilamprinae) is recorded for the first time from Hainan Island, China. Three new species, *Cyrtonotula epunctata* Wang & Wang, **sp. nov.**, *C. maculosa* Wang & Wang, **sp. nov.**, and *C. longialata* Wang & Wang, **sp. nov.**, are described based on morphological data and a molecular analysis using Automatic Barcode Gap Discovery (ABGD). Additional barcode data of blaberid species, including these three new species, are provided to facilitate future species identification. Morphological photographs and habitat photos of these new species, as well as a key to the known species, are provided.

Keywords

ABGD, *Cyrtonota*, DNA barcodes, habitat, neighbor joining, species identification

Introduction

The Epilamprinae genus *Cyrtonota* was proposed by Hanitsch (1929), with *C. lata* as type species, on the basis of one single female specimen from Sumatra. It was characterized by its comparatively large pronotum, hind metatarsus length barely equal to the succeeding joints combined, and the reduced tergum with nearly truncate apex. Owing that the name is preoccupied by a genus of spider (Simon 1864), a replacement name, *Cyrtonotula*, was proposed by Uvarov (1939).

Since then, no more species have been reported from this genus. Roth (2003) removed it from Epilamprinae and treated it as Blaberidae *incerate sedis*. Recently, Mavropulo et al. (2015) returned it back to Epilamprinae as a result of a phylogenetic analysis based on 28S and the male genital characters; this was verified by Djernæs et al. (2020) using four mitochondrial and three nuclear genes. Mavropulo et al. (2015) described two species from Indonesia and provided a description on the male genitalia of this genus for the first time. Later, a fourth species was described from the Philippines (Lucañas 2017). To date, there are four known *Cyrtonotula* species worldwide and none from China.

Species of *Cyrtonotula* are currently identified primarily on the basis of morphological characters, mainly the shortened tegmina and wings, the shape of the pronotum, and male genitalia. DNA barcoding had not been employed to explore the diversity of *Cyrtonotula*.

DNA barcodes (the standard COI sequence) have been proven to be a useful supplementary method in identifying cockroach species and have been effective in resolving problems, such as sexual dimorphism and the identification of nymphs (Che et al. 2017; Bai et al. 2018; Wang et al. 2018). In DNA barcoding studies of cockroaches, the Automatic Barcode Gap Discovery (ABGD) method of species delineation (Puillandre et al. 2012) is widely used and has proven effective in discerning cockroach species (Bai et al. 2018; Wang et al. 2019; Li et al. 2020). Here, *Cyrtonotula* is reported from China, and three new species are described, with the aid of DNA barcoding.

Material and methods

Morphological study

Type specimens are deposited in the Institute of Entomology, College of Plant Protection, Southwest University, Chongqing, China (SWU). Male genital segments were processed with 10% NaOH for maceration of the soft tissues, observed in glycerol with a Motic K400 stereomicroscope or a Leica M205A stereomicroscope, and preserved with the remainder of the specimen in ethyl alcohol. Photographs were taken with a Leica DFC digital microscope camera attached to a Leica M205A stereomicroscope. All photos and images were processed with Adobe Photoshop CS6. Species descriptions are based on the holotype male. Measurements are given according to the whole sample studied for the description. Sclerites in male genitalia are named according to Klass (1997). The terminology of venation follows Li et al. (2018). Vein abbreviations in this article are as follows:

ScP	subcosta posterior;	M	media;
R	radius;	CuA	cubitus anterior;
RA	radius anterior;	CuP	cubitus posterior;
RP	radius posterior;	V	vannal.
Pcu	postcubitus;		

DNA extraction, amplification, and sequencing

We used standard methods to sample cytochrome c oxidase subunit I (COI) of four species (Table 1) as follows. Total DNA was extracted using Hipure Tissue DNA Mini Kit from the hind legs of alcohol-preserved specimens according to the standard DNA barcoding methods for the cockroach. The mitochondrial COI gene was amplified by PCR using primer sets of COI-F3 (5'-CAACYAATCATAAAGANATTGGAAC-3') and COI-R3 (5'-TAAACTTCTGGRTGACCAAARAATCA-3') resulting in a fragment length of 658 bp for genetic analysis after trimming the primers from the amplified product. The amplification reaction was performed in a total volume of 25 μ L, including 23 μ L T3 DNA polymerase, 1 μ L of each primer and 1 μ L DNA template. The thermal cycling conditions were as follows: initial denaturation of 2 min at 98 °C followed by 35 cycles of denaturation at 98 °C for 10 s, annealing at 53 °C for 10 s, extension at 72 °C for 10 s, and a final extension at 72 °C for 5 min; the samples were then held at 8 °C. The amplified samples were evaluated in 1% agarose gels. Sequencing in both directions was performed by BGI Technology Solutions Co. Ltd (BGI-Tech) (Beijing, China).

Sequence processing and phylogenetic analyses

A total of 11 mitochondrial COI sequences were obtained from four Epilamprinae species, plus one *Cyrtototula* sequence, another seven Epilamprinae sequences, and one sequence representing the mantis outgroup were downloaded from NCBI for phylogenetic analyses (Table 1). Sequences were aligned in online MAFFT 7 (<https://mafft.cbrc.jp/alignment/server/>) using the Q-INS-i algorithm. The alignment was then manually corrected in MEGA 7 (Kumar et al. 2007). Intraspecific and interspecific genetic distances are quantified based on the Kimura 2-parameter (K2P) distance model (Kimura 1980) in MEGA 7. The neighbor joining (NJ) tree was constructed in MEGA 7 under the Kimura 2 parameter model (K2P). Statistical support was estimated with 1000 bootstrap replicates. To determine putative species in our study, we used the species delimitation approach, Automatic Barcoding Gap Discovery (ABGD), which was performed using the online webserver (<http://wwwabi.snv.jussieu.fr/public/abgd/>). The settings were as follows: Pmin = 0.001, Pmax = 0.1, Steps = 10, X (relative gap width) = 1.0, Nb bins = 20, and using Jukes Cantor (JC69) distance.

Results

Species delimitation based on COI and morphological data

In this study, we acquired 11 COI sequences representing three *Cyrtototula* and one *Opisthoplatia* species. All new sequences were deposited in GenBank (accession numbers MW649972 to MW649982 in Table 1). An NJ analysis revealed that clades

Table 1. Samples of COI genes used in this study.

Genus	Species	Voucher number	Sequence ID	Locality (China)	Accession number
<i>Opisthoptera</i>	<i>O. orientalis</i>	C01.1M	OpisOri03	Guangzhou, Guangdong	MW649981
		C01.3M	OpisOri05	Wuzhishan, Hainan	MW649982
<i>Cyrtototula</i>	<i>C. epunctata</i> sp. nov.	M01.1M	CyrtTest01	Diaoluoshan, Hainan	MW649978
		M01.2F	CyrtTest02	Diaoluoshan, Hainan	MW649979
		M01.3F	CyrtTest03	Wuzhishan, Hainan	MW649980
	<i>C. maculosa</i> sp. nov.	K01.1M	QuadBrac01	Yinggeling, Hainan	MW649972
		K01.2M	QuadBrac02	Yinggeling, Hainan	MW649973
		K01.3F	QuadBrac03	Yinggeling, Hainan	MW649974
	<i>C. longialata</i> sp. nov.	K02.1F	QuadMacr01	Baoting, Hainan	MW649975
		K02.2M	QuadMacr02	Dalimuling, Hainan	MW649976
		K02.3M	QuadMacr03	Bawangling, Hainan	MW649977
	cf. <i>Cyrtototula</i> sp. MNHN BL13				KY497672
<i>Pseudophoraspis</i>	<i>P. kabakovi</i>				MH755938
					MH755939
<i>Rhabdoblatta</i>	<i>R. densimaculata</i>				MK547402
					MK547405
					MK547406
	<i>R. mascifera</i>				MK547407
					MK547408
Outgroup	<i>Mantis religiosa</i>				KR148854

from the same species, including male and female samples, constituted monophyletic groups with high support values (Fig. 1). We observed the lowest and highest K2P interspecies genetic distance among these species, 0.1056 for *C. maculosa* sp. nov. and *C. longialata* sp. nov., and 0.1367 for *C. epunctata* sp. nov. and *C. maculosa* sp. nov. We used the ABGD method to delimit *Cyrtototula* species. Three MOTUs were detected in the ABGD analysis, which are completely consistent with the results based on morphological characters (Fig. 1) for *C. epunctata* sp. nov., *C. maculosa* sp. nov., and *C. longialata* sp. nov.

Systematics

Cyrtototula Uvarov, 1939

Cyrtotota Hanitsch 1929: 281. Type species: *Cyrtotota lata* Hanitsch, 1929.

Cyrtototula Uvarov 1939: 459, replacement name for *Cyrtotota* Hanitsch, 1929; Princis 1967: 662; Mavropulo et al. 2015: 18; Lucañas 2017: 132. New record from China.

Diagnosis. Medium-sized cockroaches. Both sexes similar. Ocular distance slightly narrower than the distance between antennal sockets, greater than ocellar distance. Pronotum broad, anterior margin curved and posterior margin obtusely produced. Tegmina and wings usually brachypterous, not reaching the abdominal apex (except for macropterous *C. longialata* sp. nov.), their apices somewhat rounded or approximately truncated. Anteroventral margin

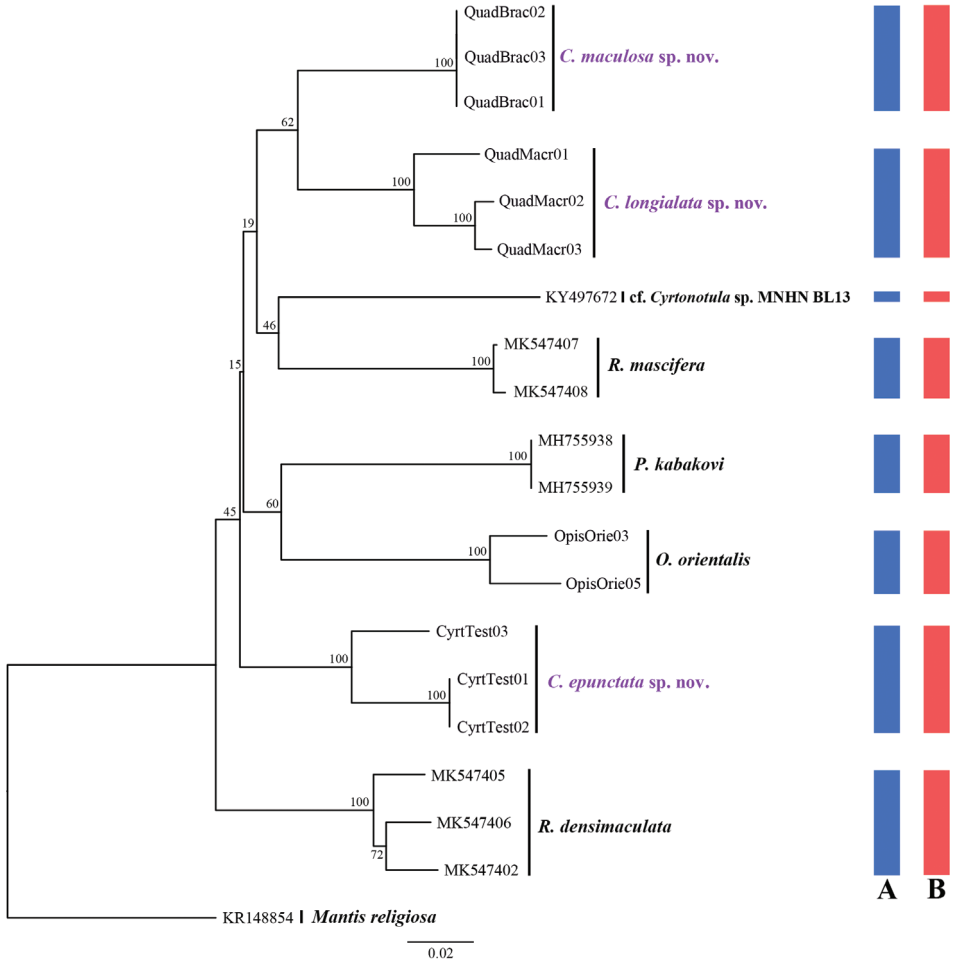


Figure 1. Neighbor joining (NJ) tree derived from COI sequences based on the K2P model. Morphospecies blue; MOTUs in ABGD red.

of front femur Type B; tarsi moderately long; hind metatarsus slender, distinctly longer or nearly equal to the remaining segments combined, armed with two or less equal rows of spines and large apical pulvilli; succeeding tarsomeres armed only with spines surrounding the large pulvilli; the pretarsus with arolium, claws symmetrical and unspecialized. Supranal plate entire, with a median incision. Cerci elongate. Subgenital plate large, nearly symmetrical or somewhat asymmetrical. Styli cylindrical.

Male genitalia. Right phallomere Morphnini-type (Anisyutkin and Yushkova 2017): consisting of sclerites R1T, R2, R3, R4, and R5; R4 irregular plate-like, separated; R3 connected to R5. The shape of apical sclerite of L2D irregular and variable. Sclerite L3 hook apically blunt; the folded structure distinct with bristles (visible at high magnification), sclerite L4U present.

Remarks. Based on the closely similar structure of right phallomere in the epilamprines, four genera have been recorded from China: *Morphna* Shelford, *Pseudophoraspis* Kirby, *Rhabdoblatta* Kirby, and *Stictolampra* Hanitsch (Beccaloni 2014; Anisyutkin and Yushkova 2017).

The genus *Cyrtonotula* differs from *Rhabdoblatta*, *Pseudophoraspis*, and *Stictolampra* principally by its reduction of the tegmina and wings. Additionally, *C. longialata* sp. nov. is morphologically somewhat similar to some *Rhabdoblatta* and *Stictolampra* species but can be distinguished by the presence of glandular specialization on the abdominal tergites, basal portion of sclerite L2D, and the non-punctate pronotum.

The genus *Cyrtonotula* can be distinguished from *Morphna* by the structure of hind tarsi: metatarsus distinctly longer or about as long as other segments combined, with relatively numerous tarsal spines (metatarsus slightly shorter or nearly equal to remaining segments combined with larger pulvilli, tarsal spines few or absent).

Key to species of *Cyrtonotula* worldwide

- 1 Tegmina and wings fully developed, both extending beyond the abdominal apex.....*C. longialata* sp. nov.
- Tegmina and wings reduced, not reaching the abdominal apex 2
- 2 Pronotum testaceous without maculae *C. epunctata* sp. nov.
- Pronotum with scattered maculae 3
- 3 Vertex with 3 longitudinal dark lines..... *C. lata* Hanitsch
- Vertex with longitudinal lines fewer than 3 4
- 4 Front femur Type B₁ *C. maquilingensis* Lucañas
- Front femur Type B₂ 5
- 5 First abdominal tergum specialized, sclerite L3 comparatively truncated at apex ...
..... *C. maculosa* sp. nov.
- Abdominal tergites unspecialized, sclerite L3 with apex rounded to truncated..... 6
- 6 Vertex with yellowish striation, tegmina and wings strongly reduced.....
C. tertia Mavropulo, Anisyutkin, Zagoskin, Zagoskina, Lukyantsev & Mukha
- Vertex speckled with black, tegmina and wings weakly reduced..... *C. secunda* Mavropulo, Anisyutkin, Zagoskin, Zagoskina, Lukyantsev & Mukha

Cyrtonotula epunctata Wang & Wang, sp. nov.

<http://zoobank.org/1B3A01E3-2D33-4263-A61F-656D79F82863>

Figs 2A–L, 5A

Type material. Holotype. CHINA • male; Hainan Prov., Lingshui County, Diaoluoshan Mountain; 916 m; 16 Apr. 2015; Lu Qiu & Qi-Kun Bai leg.; SWU-B-BB100101.

Paratypes. CHINA • 1 male & 2 females; same collection data as holotype; 18 Apr. 2015; SWU-B-BB100102 to 100104 • 1 female; Hainan Prov., Wuzhishan Nature

Reserve; 795 m; 18 May 2014; Xin-Ran Li, Shun-Hua Gui & Jian-Yue Qiu leg.; SWU-B-BB100105 • 1 female; Hainan Prov., Diaoluoshan Mountain; 275 m; 25 May 2014; Xin-Ran Li, Shun-Hua Gui & Jian-Yue Qiu leg.; SWU-B-BB100106.

Differential diagnosis. The new species readily differs from all its congeners in the spination of hind tarsi. *Cyrtanotula epunctata* sp. nov. resembles *C. lata* Hanitsch, 1929 in testaceous body color and the length of hind metatarsus, but the new species can be distinguished from *C. lata* by the following characters: the coloration of facial part black, with clypeo-labral area yellowish brown, and vertex without visible lines (vs deep testaceous and vertex with three longitudinal dark lines in *C. lata*), and tegmina only reaching to the posterior margin of the third abdominal segment (vs reaching over the sixth abdominal tergite in *C. lata*).

Description. Measurements (mm). Overall length: male 20.7–21.0, female 28.9–39.5; pronotum length × width: male 6.3–6.5 × 9.3–9.5, female 8.5 × 11.3; tegmen length: male 9.3–9.6 × 5.6–5.9, female 13.0–18.6 × 8.0–11.9.

Male. Colouration testaceous. Surfaces smooth and glossy (Fig. 2A). Eyes black. Ocellar spots yellow white. Vertex, frons black; clypeus and labrum yellowish brown (Fig. 2B). Pronotum deep testaceous, without spots (Fig. 2E). Tegmina auburn, moderately punctured (Fig. 2G). Legs ferruginous. Abdomen and cerci dark brown (Fig. 2B).

Vertex concealed. Interocular space same as the width between the antennal sockets, slightly greater than ocellar distance. Pronotum nearly semicircular, anterior margin parabolic, posterior margin obtusely angled (Fig. 2E). Tegmina reduced, reaching up the 4th abdominal tergite only; apex rounded; venation distinct, all main veins (*Sc*, *R*, and *CuP*) present, *Sc* thickened (easily visible on ventral side of tegmen) (Fig. 2A, G). Wings vestigial, only reaching to the posterior margin of the 3rd abdominal segment, completely covered by tegmina. Front femur Type B₂ (Fig. 2F). Hind metatarsus depressed-cylindrical, nearly equal to the succeeding segments combined, with single complete row of spines along ventral margin and several additional spines on inner side; four proximal tarsomeres with pulvilli terminal, the one on the second tarsomere occupying practically the whole length of the segment; claws symmetrical and simple; arolium present (Fig. 5A). Abdominal tergites unspecialized; knobs along the posterior margin indistinct; weak spiracle-bearing outgrowths of tergite VIII with distinct spiracle. Supra-anal plate with the posterior margin widely rounded and a weak mesal incision. Cerci distinctly segmented, densely covered with bristles. Paraprocts of blaberid type, asymmetrical (Fig. 2H). Subgenital plate rounded, slightly asymmetrical; the base of the inner plate bifurcated. Styli cylindrical, apically rounded (Fig. 2I).

Male genitalia. Right phallomere with caudal part of sclerite R1T rectangular in shape; cranial part of R1T more or less straight; R2 curved; R3 long; R4 irregular plate-like; R5 large, fused with sclerite R3 in caudal part (Fig. 2J). “chaetae-bearing membranous area” absent. Sclerite L2D not divided into basal and apical parts, slender and rod-like, with basal end tapering and a bifurcated outgrowth born near the basal end (Fig. 2K). Sclerite L3 hooked, apex slightly rounded, with a small tooth on the inner margin less distinct; folded structure present, with bristles. Sclerite L4U distinct (Fig. 2L).

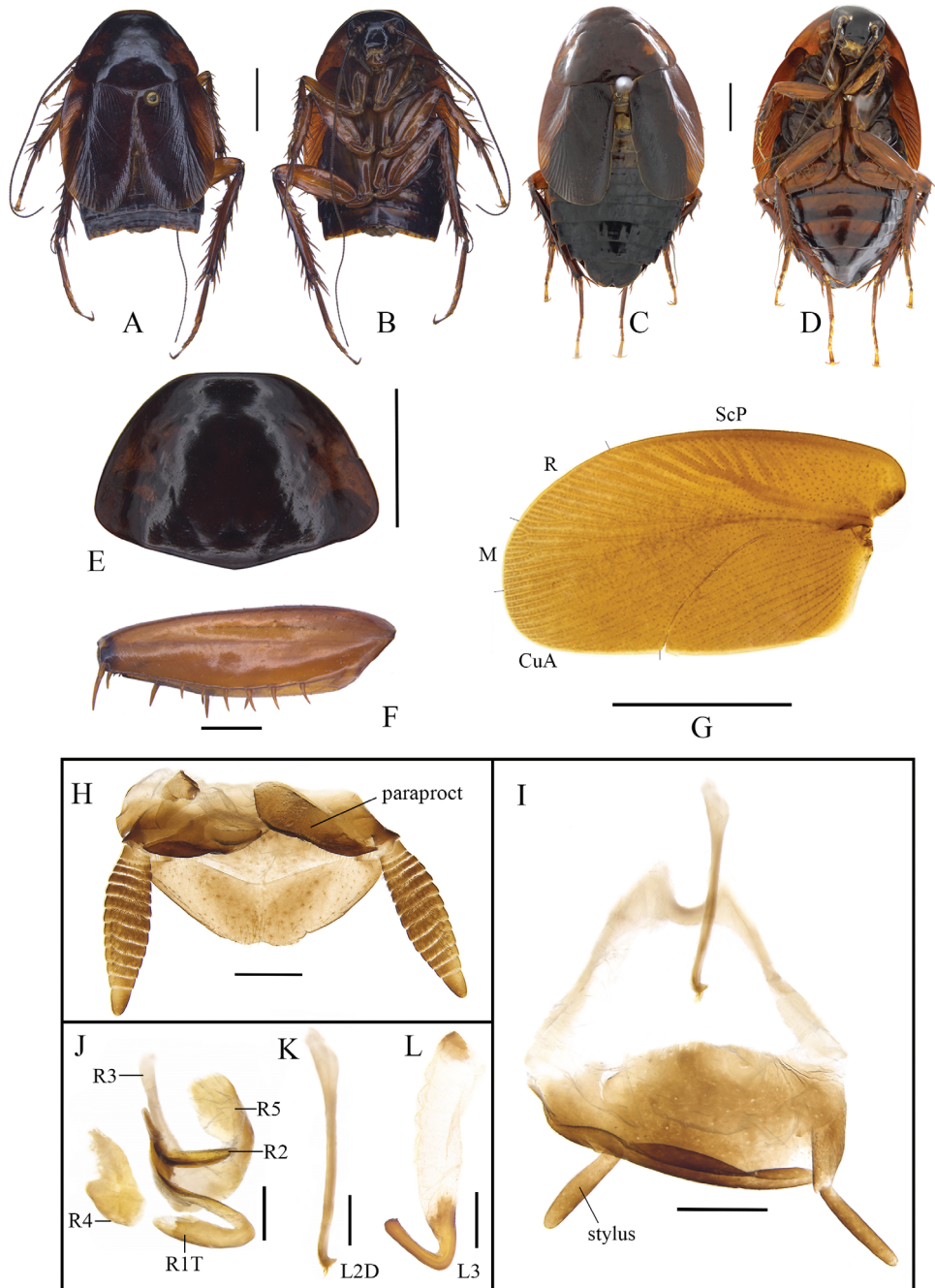


Figure 2. *Cyrronotula epunctata* Wang & Wang, sp. nov. **A, B, E–L** male **C, D** female **A** paratype, dorsal view **B** paratype, ventral view **C** paratype, dorsal view **D** paratype, ventral view **E** pronotum, dorsal view **F** front femur, ventral view **G** tegmen **H** supra-anal plate, ventral view **I** subgenital plate, dorsal view **J** right phallomere, dorsal view **K** median phallomere (sclerite L2D), dorsal view **L** left phallomere (sclerite L3), dorsal view. Scale bars: 1.0 cm (**C, D**); 5.0 mm (**A, B, E, G**); 1.0 mm (**F, H, I**); 0.5 mm (**J–L**).

Female. Similar to the male but body somewhat larger.

Etymology. Derived from the Latin word *epunctatus*, referring to the lack of visible spots on the body.

***Cyrtonotula maculosa* Wang & Wang, sp. nov.**

<http://zoobank.org/4DC34DE6-DFC6-4F5D-AE5C-B0A35CD8F97A>

Figs 3A–L, 5B, 6A

Type material. Holotype. CHINA • male; Hainan Prov., Yinggeling Nature Reserve, Nanfa Conservation Station; 650 m; 21 Apr. 2015; Lu Qiu & Qi-Kun Bai leg.; SWU-B-BB090101.

Paratypes. CHINA • 11 males & 11 females; same collection data as holotype; SWU-B-BB090102 to 090123.

Differential diagnosis. This new species is closely related to *C. tertia* Mavropulo, Anisyutkin, Zagoskin, Zagoskina, Lukyantsev & Mukha, 2015 in the shape of tegmina and body color, but the former can be distinguished from the latter by the specialized abdominal terga (vs unspecialized) and the shape of sclerite L3 of male genitalia, in which L3 hook is comparatively robust and posteriorly truncate distinctly (vs comparatively slender and rounded apically in *C. tertia*).

Description. Measurements (mm). Overall length: male 22.5–27.0, female 31.0; pronotum length × width: male 5.5–6.4 × 7.8–8.2, female 6.3 × 9.1; tegmen length: male 20.6–21.8 × 7.9–8.3, female 25.7 × 9.3.

Male. Body yellowish brown (Fig. 3A). Eyes black. Ocellar spots light yellow. Head black except for yellowish brown clypeo-labral area, facial part of head with weak transverse wrinkles (Fig. 3B). Pronotum yellow-brown, with densely scattered irregular brown spots (Fig. 3E). Tegmina dark yellow, punctured, with brown patches spreading along the veins (Fig. 3G). Coxa, trochanter, and femur yellowish brown; tibia and tarsomere light yellow. Abdomen and cerci blackish brown (Fig. 3B).

Vertex slightly exposed, with two longitudinal yellowish-brown bands. Distance between eyes approximately equal to the width between the antennal sockets and smaller than ocellar distance (Fig. 3B). Pronotum campaniform, widely rounded along anterolateral margins, posterior margin obtusely angled (Fig. 3E). Tegmina considerably shortened, reaching the third abdominal tergite, apex subtruncate; venation distinct, all main veins (*Sc*, *R* and *CuP*) present, *Sc* thickened (easily visible on ventral side of tegmen) (Fig. 3A, G). Wings vestigial, only reaching the first abdominal tergite. Anterior margin of fore femur Type B₂, with 6 or 7 spines (Fig. 3F). Hind metatarsus not quite as long as other segments combined with two rows of spines; well-developed pulvilli on all proximal tarsomeres; claws symmetrical and simple; arolium present (Fig. 5B). Abdominal tergite 1st specialized, lip-like (Fig. 6A); terga 3rd–7th with a few knobs (Fig. 3A); spiracles large, located on the posterolateral angles of tergite 8th. Supra-anal plate with the posterior margin widely rounded, a weak incision at middle. Cerci fusiform, traces of segmentation distinct. Paraprocts of blaberid type, asymmet-

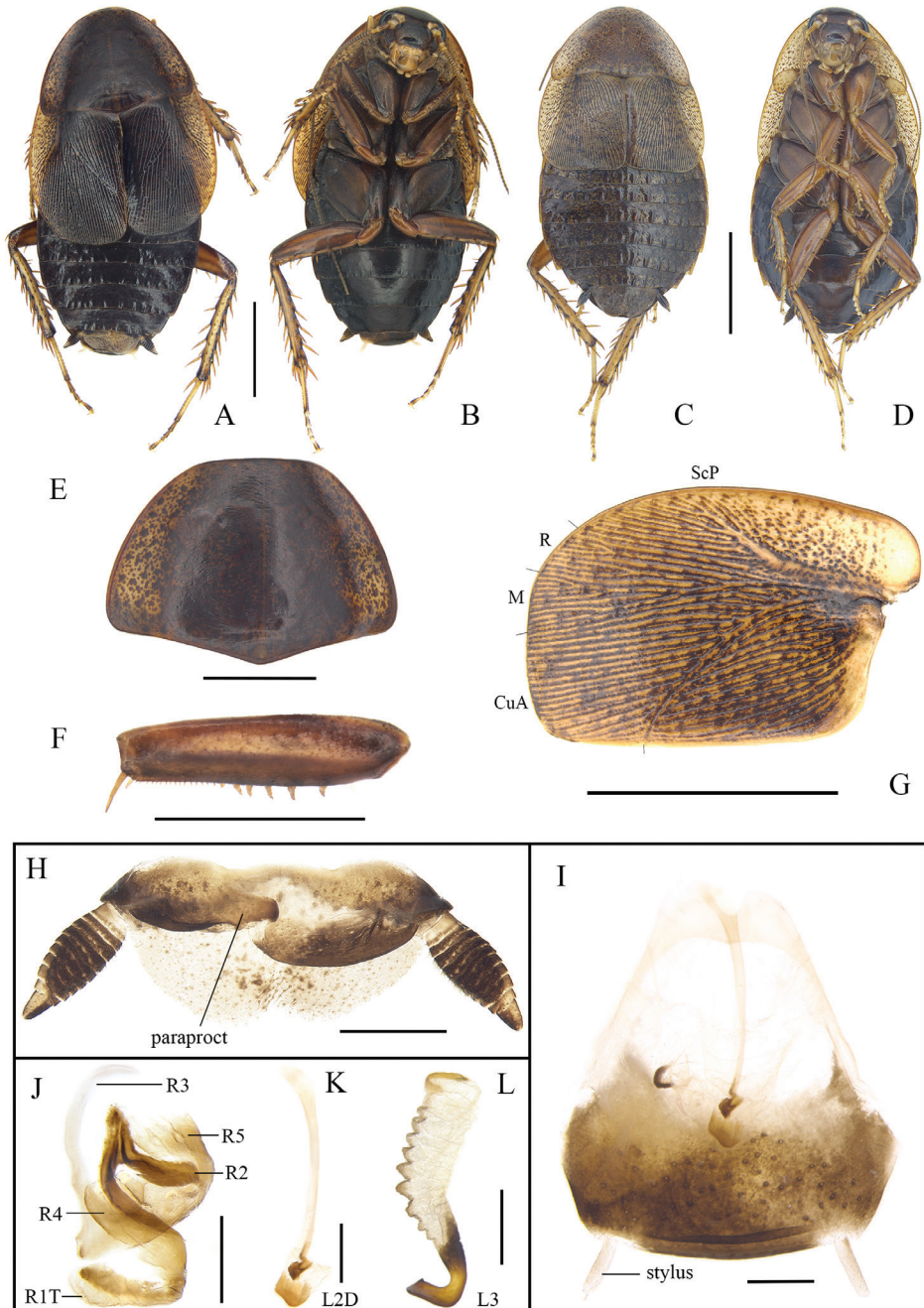


Figure 3. *Cyrtanotula maculosa* Wang & Wang, sp. nov. **A, B, E–L** male **C, D** female **A** holotype, dorsal view **B** holotype, ventral view **C** paratype, dorsal view **D** paratype, ventral view **E** pronotum, dorsal view **F** front femur, ventral view **G** tegmen **H** supra-anal plate, ventral view **I** subgenital plate, dorsal view **J** right phallomere, dorsal view **K** median phallomere (sclerite L2D), dorsal view **L** left phallomere (sclerite L3), dorsal view. Scale bars: 1.0 cm (**C, D**); 5.0 mm (**A, B, E–G**); 1.0 mm (**H–L**).

rical (Fig. 3H). Subgenital plate entire with hind margin rounded; base of the inner plate bifurcated. Styli cylindrical (Fig. 3I).

Male genitalia. Right phallomere with caudal part of sclerite R1T nearly rectangular in shape, cranial part of R1T curved; R2 rounded; R3 elongate apically, curved inward, fused with sclerite R5; R4 plate-like, separated. Sclerite L2D divided into basal and apical parts, basal part rod-like, widened apically, with irregular apical outgrowth; apical part with fine bristles; apical membrane covered with chaetae (Fig. 3K). Sclerite L3 hooked, apically subquadrate; inner margin with a tooth-shaped convexity at apex; folded structure distinct, with bristles; Sclerite L4U present, comparatively narrow (Fig. 3L).

Female. Similar to the male. Body color lighter. Tegmina only reaching the second abdominal tergite, with apex distinctly truncated. Abdominal tergites unspecialized.

Etymology. Derived from the Latin word *maculosus*, referring to the scattered with dense spots pronotum and tegmen.

***Cyrtototula longialata* Wang & Wang, sp. nov.**

<http://zoobank.org/164B8791-1167-4341-BACC-39F40F0B1A5C>

Figs 4A–K, 5C, 6B

Type material. Holotype. CHINA • male; Hainan Prov., Limuling Mountain; 18 Apr. 2015; Xin-Ran Li & Zhi-Wei Qiu leg.; SWU-B-BB090201.

Paratypes. CHINA • 3 males; same collection data as holotype; SWU-B-BB090202 to 090204 • 6 males & 2 females; Hainan Prov., Baoting County, Maogan Township; 549–776 m; 11–12 Apr. 2015; Xin-Ran Li, Lu Qiu, Zhi-Wei Qiu & Qi-Kun Bai leg.; SWU-B-BB090205 to 090212 • 1 male; Hainan Prov., Bawangling Mountain; 600–800 m; 29 Apr. 2015; Lu Qiu & Qi-Kun Bai leg.; SWU-B-BB090213 • 2 males; Hainan Prov., Diaoluoshan Mountain; 275m; 24 May 2014; Xin-Ran Li & Shun-Hua Gui leg.; SWU-B-BB090214 and 090215.

Differential diagnosis. The new species principally differs from all its congeners, except for *C. maculosa* sp. nov., in the presence of abdominal tergal glands. From *C. maculosa* sp. nov., *C. longialata* sp. nov. differs in having the completely developed tegmina and wings extending beyond the abdominal apex, the shape of tergal glands (see description below).

Description. Measurements (mm). Overall length: male 27.0–30.0, female 31.0; pronotum length × width: male 6.2–6.4 × 7.8–8.2, female 6.3 × 9.1; tegmen length: male 23.0–25.0 × 8.6–9.2, female 25.7 × 9.3.

Male. General colour brown (Fig. 4A). Eyes black. Ocellar spots yellow-white. Head black except for brown clypeo-labral area; facial part of head with weak transverse wrinkles and paired impressions under ocelli (Fig. 4B). Pronotum russet, reddish brown at center, speckled with small, brown patches (Fig. 4C). A few yellow spots present in tegmina (Fig. 4E); wings with costal field, radial field, mediocubital field fulvous, and anal field pale brown (Fig. 4F). Legs and abdomen dark yellowish brown. Cerci dark brown (Fig. 4B).

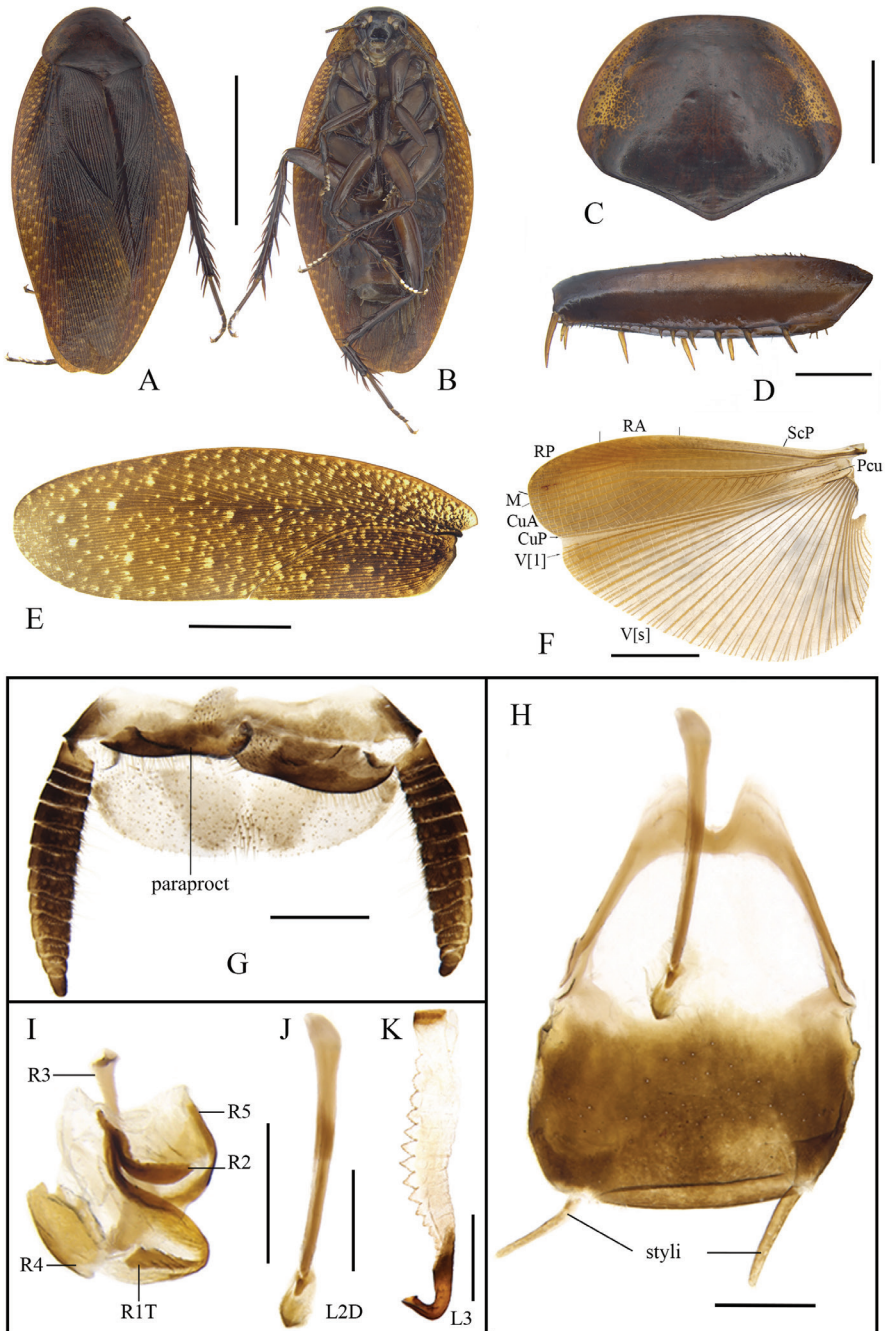


Figure 4. A–L *Cyronotula longialata* Wang & Wang, sp. nov., male **A** holotype, dorsal view **B** holotype, ventral view **C** pronotum, dorsal view **D** front femur, ventral view **E** tegmen **F** wings **G** supra-anal plate, ventral view **H** subgenital plate, dorsal view **I** right phallomere, dorsal view **J** median phallomere (sclerite L2D), dorsal view **K** left phallomere (sclerite L3), dorsal view. Scale bars: 1.0 cm (**A**, **B**); 5.0 mm (**C**, **E**, **F**); 1.0 mm (**D**, **G**–**K**).

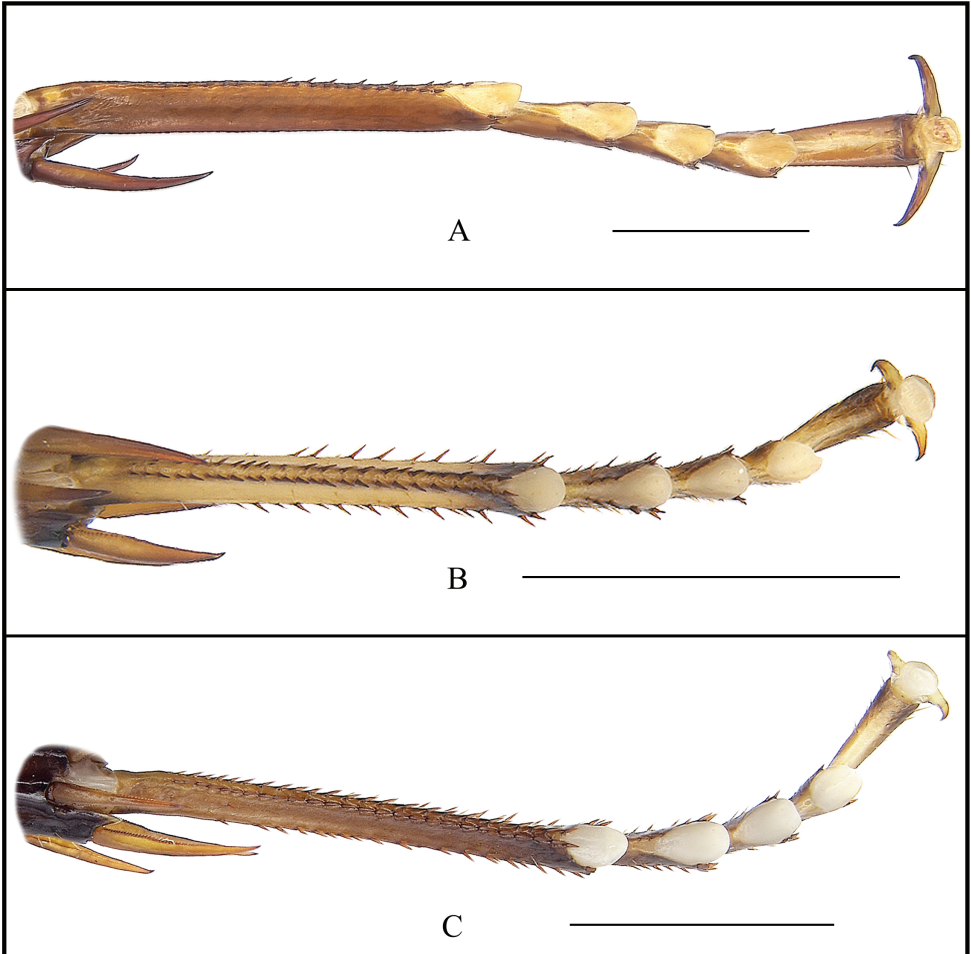


Figure 5. Hind tarsi **A** *Cyrtonotula epunctata* Wang & Wang, sp. nov., female, paratype **B** *Cyrtonotula maculosa* Wang & Wang, sp. nov., male, holotype **C** *Cyrtonotula longialata* Wang & Wang, sp. nov., male, holotype. Scale bars: 2.0 mm.

Vertex slightly exposed. Interocular distance as wide as inter-antennal distance, slightly greater than inter-ocellar distance. Pronotum flabellate, widely rounded along anterolateral margins, posterior margin obtusely angled (Fig. 4C). Tegmina and wings completely developed, exceeding abdominal apex; tegmina with rounded apex; venation distinct, all main veins (*Sc*, *R*, and *CuP*) present (Fig. 4E, F). Anterior margin of fore femur B_2 (Fig. 4D). Hind metatarsus distinctly longer than other segments combined, armed with two rows of spines; pulvilli large on all proximal tarsomeres; claws symmetrical and simple; arolium present (Fig. 5C). The first abdominal tergite specialized, cap-like (Fig. 6B); tergite VIII with posterolateral angles strongly expressed. Supra-anal plate with the caudal margin widely rounded and a weak median incision. Cerci robust, segmented. Paraprocts of blaberid type, asymmetrical (Fig. 4G). Subgenital plate

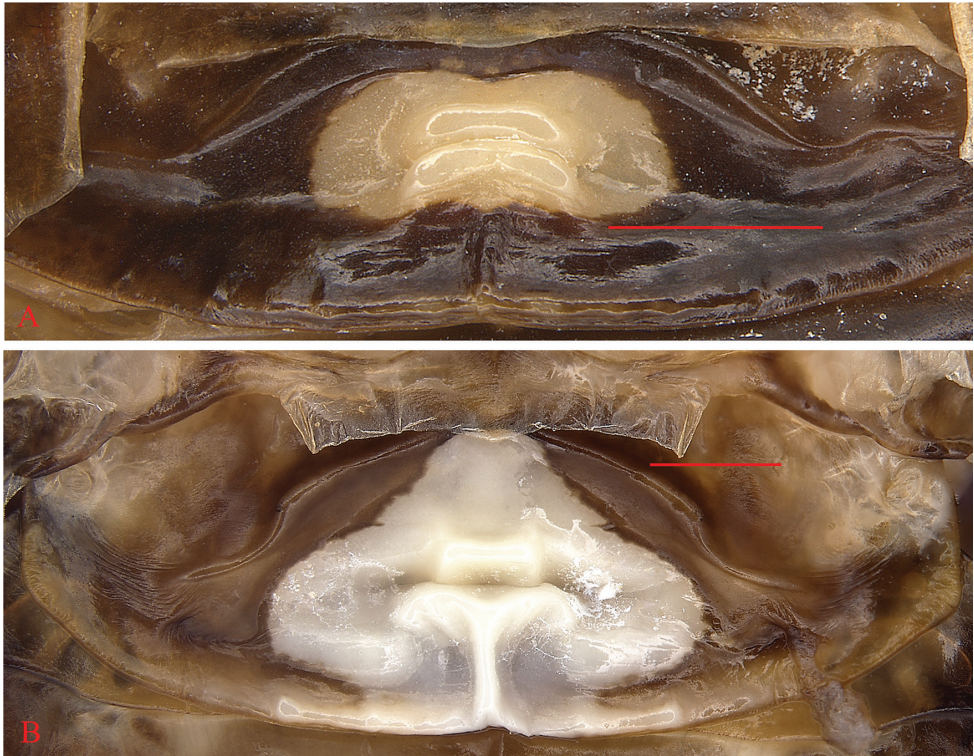


Figure 6. The first abdominal tergal gland **A** *Cyrtototula maculosa* Wang & Wang, sp. nov., male, paratype **B** *Cyrtototula longialata* Wang & Wang, sp. nov., male, holotype. Scale bars: 1.0 mm.

symmetrical, rounded. Base of inner plate bifurcated. Styli long, cylindrical, apically rounded (Fig. 4H).

Male genitalia. Right phallomere with caudal part of sclerite R1T nearly rectangular, cranial part of R1T curved; R2 arched; R3 elongate and widened apically, fused with sclerite R5 in caudal part; R4 irregular plate-like, separated (Fig. 4I). Sclerite L2D divided into basal and apical parts, basal part rod-like, widened cranially; apical part trifurcate; apical membrane covered with chaetae (Fig. 4J). Sclerite L3 hooked, apically subtruncate; inner margin with apex pointed; folded structure and bristles present; sclerite L4U distinct (Fig. 4K).

Female. Similar to the male. Abdominal tergites unspecialized.

Remarks. Currently, this is the only species of *Cyrtototula* with fully developed tegmina and wings. This species is placed in *Cyrtototula* because it closely resembles *C. maculosa* sp. nov. in having sclerite L3 hooked (apex nearly truncate and inner margin with a distinct point) and in the location of tergal gland.

Etymology. The species epithet is derived from the Latin adjective *longialatus*, which refers to the well-developed wings.



Figure 7. Living *Cyrtototula* species from Hainan, China **A** female *C. epunctata* sp. nov. (Diaoluoshan Mountain) **B** male *C. epunctata* sp. nov. (Diaoluoshan Mountain) **C** female *C. maculosa* sp. nov. (Yinggeling Mountain) **D** *Cyrtototula longialata* sp. nov. (Baoting County). Photos: **A–C** by Lu Qiu **D** by Xin-Ran Li.

Discussion

Flightless cockroaches are usually considered to persist in stable habitats, where food, shelter, and mates are easily accessible (Bell et al. 2007). All of previously known *Cyrtototula* species are brachypterous, but *C. longialata* sp. nov. is noteworthy for being the first macropterous in this genus. Brachypterous cockroaches, including *C. epunctata* sp. nov. and *C. maculosa* sp. nov., were observed on leaf litter and scree in areas with trickling water (Fig. 7A–C), while *C. longialata* sp. nov., maybe a canopy species, was collected in low vegetation (Fig. 7D). We speculate that habitats of *C. epunctata* sp. nov. and *C. maculosa* sp. nov. may be different from the habitat of *C. longialata* sp. nov., and habitat might be one of the determining factors in variations of the wings. This study is also the first to use COI DNA barcode to evaluate diversity of *Cyrtototula* species. Our results show that DNA-based species delimitation methods perform well and that individuals were correctly assigned to their corresponding species, although only 10 sequences of *Cyrtototula* were included here. Therefore, taking into consideration that there are only seven species of the genus found worldwide, we expect more species of *Cyrtototula*, especially macropterous ones, will be discovered and observed with further sampling, so that the knowledge of this genus *Cyrtototula* could be comprehensive and explored more deeply.

Acknowledgements

We express our sincere thanks to all the collectors of the type material. We especially thank Lu Qiu and Xin-Ran Li for providing the photos of living *Cytonotula* species, and we also thank John Richard Schrock for proofing the manuscript. This work was supported by the National Natural Sciences Foundation of China (no. 31872271) and the Fundamental Research Funds for the Central Universities, China (XDJK2020D040).

References

- Anisyutkin LN, Yushkova OV (2017) New data on cockroaches of the subfamily Epilamprinae (Dictyoptera: Blaberidae) from India and Sri Lanka, with descriptions of new species and the genital complex of *Aptera fusca* (Thunberg, 1784). *Zootaxa* 4236: 41–64. <https://doi.org/10.11646/zootaxa.4236.1.2>
- Bai QK, Wang LL, Wang ZQ, Lo N, Che YL (2018) Exploring the diversity of Asian *Cryptocercus* (Blattodea : Cryptocercidae): species delimitation based on chromosome numbers, morphology and molecular analysis. *Invertebrate Systematics* 32: 69–91. <https://doi.org/10.1071/IS17003>
- Beccaloni GW (2014) Cockroach Species File Online. Version 5.0/5.0. <http://cockroach.speciesfile.org/> [accessed 5 December 2020]
- Bell WJ, Roth LM, Nalepa CA (2007) *Cockroaches: Ecology, Behavior, and Natural History*. The Johns Hopkins University Press, Baltimore, 230 pp.
- Che YL, Gui SH, Lo N, Ritchie A, Wang ZQ (2017) Species delimitation and phylogenetic relationships in ectobiid cockroaches (Dictyoptera, Blattodea) from China. *PLoS ONE* 12: e0169006. <https://doi.org/10.1371/journal.pone.0169006>
- Djernæs M, Varadinová ZK, Koryk M, Eulitz U, Klass K-D (2020) Phylogeny and life history evolution of Blaberoidea (Blattodea). *Arthropod Systematics & Phylogeny* 78: 29–67.
- Hanitsch R (1929) Fauna Sumatrensis. (Beitrag No. 63). Blattidae. *Tijdschrift voor Entomologie* 72: 263–302.
- Kimura M (1980) A simple method for estimating evolutionary rates of base substitutions through comparative studies of nucleotide sequences. *Journal of Molecular Evolution* 16: 111–120. <https://doi.org/10.1007/BF01731581>
- Klass KD (1997) The external male genitalia and the phylogeny of Blattaria and Mantodea 42: 1–341.
- Kumar NP, Rajavel AR, Natarajan R, Jambulingam P (2007) DNA barcodes can distinguish species of Indian mosquitoes (Diptera: Culicidae). *Journal of Medical Entomology* 44: 1–7. <https://doi.org/10.1093/jmedent/41.5.01>
- Li M, Zhao QY, Chen R, He JJ, Peng T, Deng WB, Che YL, Wang ZQ (2020) Species diversity revealed in *Sigmella* Hebard, 1929 (Blattodea, ectobiidae) based on morphology and four molecular species delimitation methods. *PLoS ONE* 15: e0232821. <https://doi.org/10.1371/journal.pone.0232821>

- Li XR, Zheng YH, Wang CC, Wang ZQ (2018) Old method not old-fashioned: parallelism between wing venation and wing-pad tracheation of cockroaches and a revision of terminology. *Zoomorphology* 137: 519–533. <https://doi.org/10.1007/s00435-018-0419-6>
- Lucañas CC (2017) Some new brachypterous cockroaches (Blattodea: Blaberidae: Epilamprinae) from the Philippines. *Zootaxa* 4294: 130–136. <https://doi.org/10.11646/zootaxa.4294.1.9>
- Mavropulo VA, Anisyutkin LN, Zagoskin MV, Zagoskina AS, Lukyantsev SV, Mukha DV (2015) New data on the family Blaberidae (Dictyoptera) from Southeast Asia: new species, morphological diversity and phylogeny on the base of ribosomal DNA sequences. *Zoosystematica Rossica* 24: 14–30. <https://doi.org/10.31610/zsr/2015.24.1.14>
- Puillandre N, Lambert A, Brouillet S, Achaz G (2012) ABGD, Automatic Barcode Gap Discovery for primary species delimitation. *Molecular Ecology* 21: 1864–1877. <https://doi.org/10.1111/j.1365-294X.2011.05239.x>
- Roth LM (2003) Systematics and phylogeny of cockroaches (Dictyoptera: Blattaria). *Oriental Insects* 37: 1–186. <https://doi.org/10.1080/00305316.2003.10417344>
- Simon EL (1864) *Histoire naturelle des araignées (aranéides)*. Librairie encyclopédique de Roret, Paris, 556 pp. <https://doi.org/10.5962/bhl.title.47654>
- Uvarov BP (1939) Twenty-four new generic names in Orthoptera. *Annals and Magazine of Natural History (Series 11)* 3: 457–459. <https://doi.org/10.1080/03745481.1939.9723626>
- Wang LL, Liao SR, Liu ML, Deng WB, He JJ, Wang ZQ, Che YL (2019) Chromosome number diversity in Asian *Cryptocercus* (Blattodea, Cryptocercidae) and implications for karyotype evolution and geographic distribution on the Western Sichuan Plateau. *Systematics and Biodiversity* 17: 594–608. <https://doi.org/10.1080/14772000.2019.1659878>
- Wang ZZ, Zhao QY, Che YL, Wang ZQ (2018) Establishment of a new genus, *Brephallus* Wang et al., gen. nov. (Blattodea, Blaberidae, Epilamprinae) based on two species from *Pseudophoraspis*, with details of polymorphism in species of *Pseudophoraspis*. *ZooKeys* 785: 117–131. <https://doi.org/10.3897/zookeys.785.26565>

First record of the cimicomorphan family Plokiophilidae (Hemiptera, Heteroptera) from China, with description of a new species of *Plokiophiloides*

Jiuyang Luo¹, Yanqiong Peng², Qiang Xie¹

1 State Key Laboratory of Biocontrol, Sun Yat-sen University, 135 Xingangxi Road, Guangzhou 510275, Guangdong, China **2** Key Laboratory of Tropical Forest Ecology, Xishuangbanna Tropical Botanical Garden, Chinese Academy of Sciences, Kunming 650223, Yunnan, China

Corresponding author: Qiang Xie (xieq8@mail.sysu.edu.cn)

Academic editor: L. Livermore | Received 16 July 2020 | Accepted 8 February 2021 | Published 5 March 2021

<http://zoobank.org/B30951E8-B9E2-4FA3-9771-6BAD86F8AA17>

Citation: Luo J, Peng Y, Xie Q (2021) First record of the cimicomorphan family Plokiophilidae (Hemiptera, Heteroptera) from China, with description of a new species of *Plokiophiloides*. ZooKeys 1021: 145–157. <https://doi.org/10.3897/zookeys.1021.56599>

Abstract

Plokiophiloides bannaensis **sp. nov.**, is described from Xishuangbanna, Yunnan Province, representing the first record of the family Plokiophilidae from China. The new species also represents the first record of the genus *Plokiophiloides* in the Oriental Region, a second zoogeographical region besides the Afrotropical Region. Photographs of the live individuals inhabiting a spider web within natural habitats, male and female habitus, wings of adult, male genitalic structures, female abdomen structures and scanning electron micrographs of forewing, head, thorax and legs are provided. A key to all known species of *Plokiophiloides* is presented, with a distribution map.

Keywords

China, Cimicoidea, Cimicomorpha, new record, new species, Oriental Region, *Plokiophiloides*, taxonomy

Introduction

The family Plokiophilidae China, 1953 is a small group of true bugs, currently containing nine genera and 20 species (including one Baltic amber fossil genus and one fossil species). Their appearance is reminiscent of the Anthocoridae *sensu lato*, ranging in

length from 1.2 to 3.0 mm (Schuh and Slater 1995; Popov 2008; Schuh et al. 2015). Most of them were found to inhabit the webs of spiders or embiopterans, so they are also called web-lovers (Schuh and Weirauch 2020).

China and Myers (1929) described the first species of Plokiophilidae from Cuba, naming it *Arachnophila cubana* China & Myers, 1929 and placed it in the family Microphysidae. After more than two decades, China (1953) proposed the new name *Plokiophila* China, 1953 for *Arachnophila* China & Myers, 1929, which was preoccupied by *Arachnophila* Salvadori, 1874 (Aves) and described substitutive new genus and species from Trinidad, *Embiophila myersi* China, 1953 and also established Plokiophilinae as a subfamily of Microphysidae. Subsequently, Carayon (1961) upgraded Plokiophilinae to the family level, which was supported by Štys (1962); Štys (1967) described a new genus and species *Lipokophila chinai* Štys, 1967 from Brazil and provided a key to the Plokiophilidae. Carayon (1974) published a monograph of this family, describing a new genus and seven new species from continental Africa and Brazil. After the 1990s, a series of new genera and species were discovered by Štys (1991), Schuh (in Eberhard et al. 1993), Carpintero and Dellapé (2005), Schuh (2006) and Popov (2008). Recently, Schuh et al. (2015) published an influential monograph on the Plokiophilidae, in which two new genera and three new species were described and a revised higher classification for the family was offered. Mainly based on the male genitalic and female copulatory structures, a new subfamily Heissophilinae and a new tribe Lipokophilini were established by Schuh et al. (2015); in addition, the subfamily Embiophilinae was downgraded to the tribe level. In the present paper, we follow the taxonomic system of Schuh et al. (2015).

The genus *Plokiophiloides* Carayon, 1974 was established by discovery of five new species from the Afrotropical Region. After that, Štys (1991) described a new species *Plokiophiloides steineri* Štys, 1991 from Madagascar and he divided the genus into two species groups *P. asolen* group and *P. tubifer* group, based on the length of the male acus and existence of the external integumental paragenitalia of the female. Štys and Baňar (2016) reported a new free-living species and built a new genus *Neoplokioides* Štys and Baňar 2016, to hold the species; moreover, all the species of *Plokiophiloides tubifer* group were transferred into the genus *Neoplokioides*. At present, the genus *Plokiophiloides* s. str. includes four species, *P. asolen* Carayon, 1974, *P. balachowskyi* Carayon, 1974, *P. pilosus* Carayon, 1974 and *P. steineri* Štys, 1991.

In this work, the new species *Plokiophiloides bannaensis* sp. nov. is described. The family Plokiophilidae is a new record for the fauna of China and the first record of the genus *Plokiophiloides* beyond the Afrotropical Region.

Materials and methods

Specimens were collected from the webs of wolf spiders *Hippasa* sp. (Araneae: Lycosidae) in low herbaceous plants, in Xishuangbanna Tropical Botanical Garden (XTBG), Chinese Academy of Sciences. The collected specimens were preserved in 80% ethanol.

External structures and genitalic structures were examined by using a Zeiss Discovery V20 stereomicroscope. Measurements (in mm) were taken using the Zeiss Discovery V20 stereomicroscope with ZEN 2.5 pro software. Male genitalia and the female abdomen were macerated in warm 10% potassium hydroxide solution (KOH). Photographs of habitus, forewing, male genitalia and female abdomen were taken using a Canon EOS 7D Mark II camera, equipped with a tube lens and Mitutoyo M Plan Apo 10× objective lens. Scanning electron micrographs of forewing, head, thorax and legs were prepared using a Zeiss EVO MA 10 at the Instrumental Analysis & Research Center of Sun Yat-sen University. Maps were prepared using SimpleMappr (<http://www.simplemappr.net/>).

Morphological terminology follows Štys (1991), Schuh et al. (2015) and Štys and Baňář (2016). Depository: The type series of *Plokiophiloides bannaensis* sp. nov. is deposited in the Museum of Biology, Sun Yat-sen University, Guangzhou, China (SYSBM).

Abbreviations used in the text and figures are as follows:

a	acus	ph	phallosoma
ap	articulatory apparatus	py	pygophore
asg	abdominal scent gland orifice	R	radius
cf	costal fracture	rp	right paramere
cg	corial gland	Sc	subcostal
cgs	corial glands	sv	secondary vein
cp	corial process	ts1	first segment of tarsus
Cu	cubitus	ts2	second segment of tarsus
e	egg	t8	abdominal tergite 8
lp	left paramere	v8	abdominal ventrite 8
M	media	1An	first anal vein

Taxonomy

Family: Plokiophilidae China, 1953

Subfamily: Plokiophilinae China, 1953

Tribe: Plokiophilini China, 1953

Genus: *Plokiophiloides* Carayon, 1974

Plokiophiloides Carayon, 1974: 505.

Type species by original designation. *Plokiophiloides asolen* Carayon, 1974.

Comments. The genus *Plokiophiloides* currently includes four species and can be distinguished from other genera of Plokiophilidae by the following combined characteristics: a) tarsi 2-segmented, b) hemelytron with a distinct cuneus, c) male pygophore

tubular, erect, d) fore femora and middle femora without heavy spines on ventral surface, e) posterior margin of pronotum excavated and mesoscutum broadly exposed, f) male acus shorter than pygophore and its basis simple and g) females without paired external paragenitalia.

***Plokiophiloides bannaensis* sp. nov.**

<http://zoobank.org/738A74B1-4FC3-4DD1-983A-53A5B0CF59CA>

Figures 1–4

Material. Holotype: ♂, CHINA, Yunnan Province, Xishuangbanna, Mengla County, Menglun Town, XTBG: 21°54.965'N, 101°16.293'E; ca. 670 m elev.; leg. Qiang Xie & Jiuyang Luo; 2018-VI-27. **Paratypes:** 5♂♂, 5♀♀, and 2 nymphs, same data as holotype.

Diagnosis. The new species can be distinguished from the congeners by the combined characteristics: body with red pigment; exocorium with ca. 65 corial glands; whitish precuneal spot on forewing conspicuous; hypocostal lamina extending caudally as a short, pale whitish-yellow projection.

Description. Macropterous male: Small-sized (1.5–1.7 mm), elongate, relatively flat, forewing exceeding apex of abdomen (Fig. 1A–D). **Colouration:** Ground colour and head dark reddish-brown, ocelli and ventral surface of head paler. Antennal segment I dark reddish-brown; segment II light brown, distal 1/3 pale yellow, with reddish tinge; segment III brown, distal 1/4 paler, reddish; segment VI brown, distal 2/3 reddish. Labial segments I and II light reddish; segments III and IV yellowish-brown. Pronotum and propleura darker, dark brown to blackish-brown; middle of mesosternum with longitudinal suture, nearly black. Coxae dark reddish-brown; trochanters, femora and tibiae yellowish-brown, sometimes with reddish tinge; tibiae gradually darker to the apices; tarsi brown, basal and distal part paler (Fig. 1A–D). Corium and clavus light brown to brown, middle part of exocorium and outer part of cuneus dark reddish-brown; basal 2/5 of corium light whitish-yellow; the area around costal fracture and the area of membrane that is behind distal end of cuneus whitish. Membrane light brown, with two inconspicuous longitudinal veins; corial process brown (Fig. 2A). Posterior margin of abdominal sterna nearly red.

Surface and vestiture: Head, thorax, corium and clavus forewing and abdomen covered with relatively sparse and uniformly long semi-erect setae (Fig. 1A–D). Thorax (except for calli, mesoepleurae and metapleurae) and surface of forewing densely covered by microtrichia (Fig. 3B–G). Antennae and legs covered with dense, long, semi-erect setae.

Structure: Head porrect, cylindrical, length subequal to width. Eyes away from collar; minimum dorsal interocular distance greater than 2× the same distance ventrally. Ocelli large, widely separated from each other. Two pairs of strikingly-long setae placed on dorsal surface of head, one pair of setae located in inner part of eyes, at level of anterior margin of eyes, the other located in the posterolateral part of ocelli (Fig. 3E). Antennae thin, terete; segment I thicker than the others, segment II gradually thickening

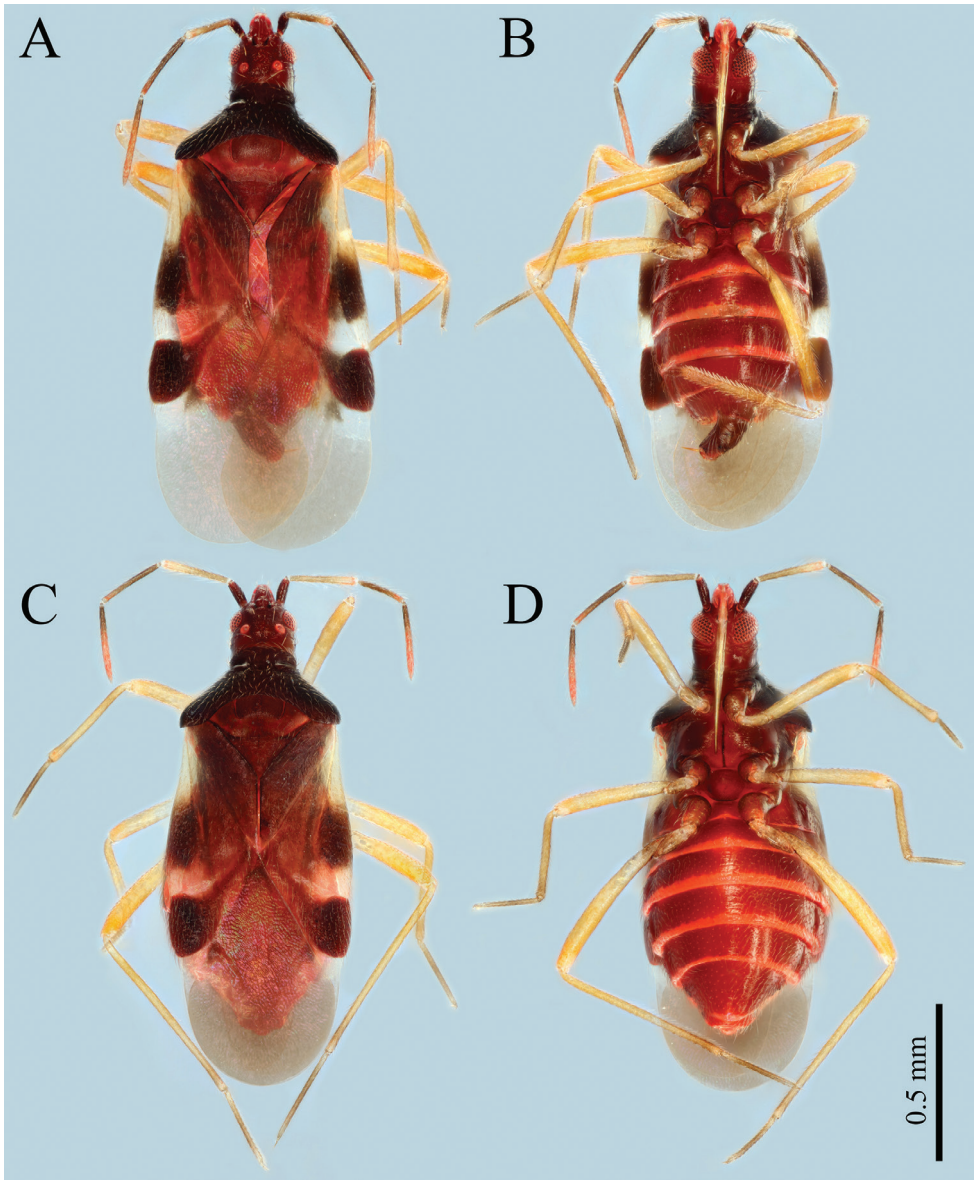


Figure 1. Habitus of *Plokiophiloides bannaensis* sp. nov. **A** male holotype in dorsal view **B** male holotype in ventral view **C** female paratype in dorsal view **D** female paratype in ventral view.

towards the apex, tip of segment IV fusiform; ratio of length of antennal segments I : II : III : IV = 3 : 7 : 7 : 9 (see Table 1). Labium slender, nearly reaching to posterior margin of mesosternum, segment I very short and wide; ratio of length of labial segments I : II : III : IV = 1 : 2.3 : 4 : 7. **Thorax:** pronotum trapezoidal, with distinct collar, one pair of extraordinarily-long setae placed in dorsal surface of collar; lateral margins of posterior

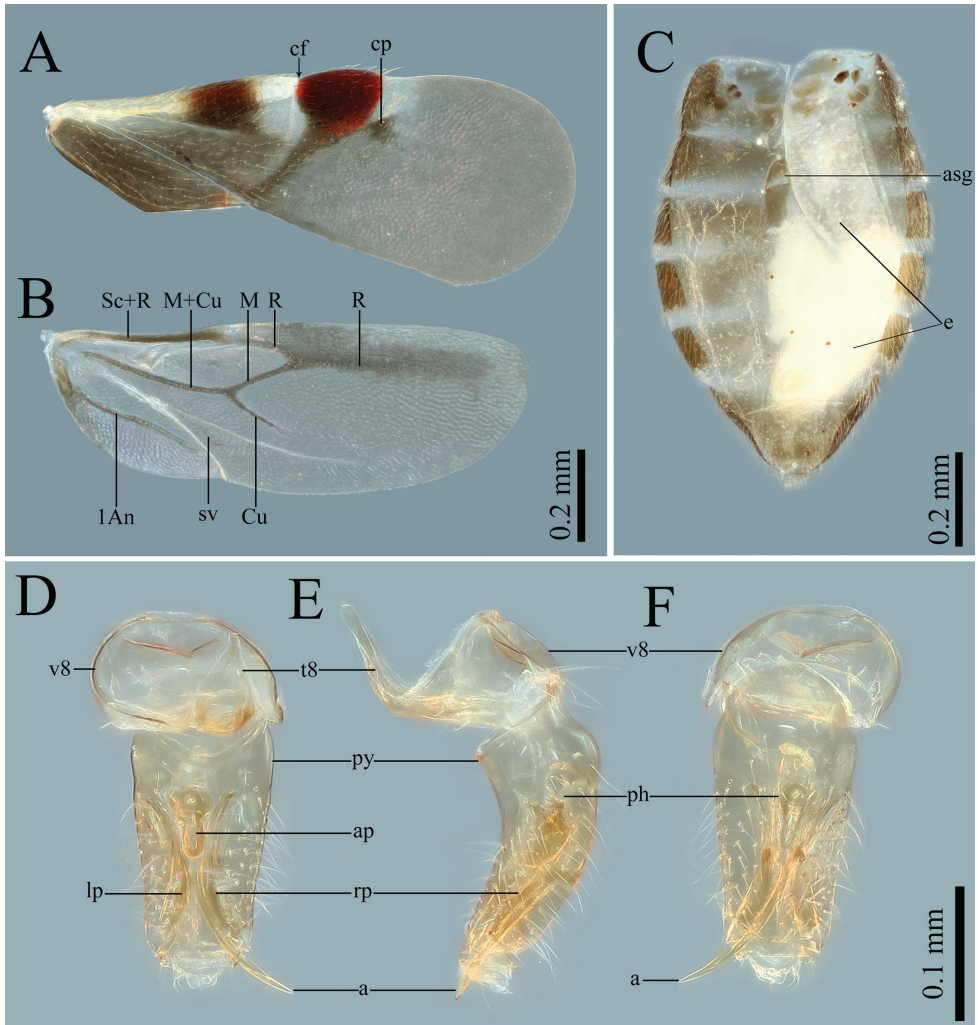


Figure 2. Morphology of *Plokiophiloides bannaensis* sp. nov. **A** male forewing in dorsal view **B** male hind-wing in dorsal view **C** female abdomen in dorsal view **D** male genitalia in dorsal view **E** male genitalia in lateral view **F** male genitalia in ventral view. Abbreviations: a = acus; ap = articular apparatus; asg = abdominal scent gland orifice; cf = costal fracture; cp = corial process; e = egg; lp = left paramere; ph = phallosoma; py = pygophore; rp = right paramere; t8 = abdominal tergite 8; v8 = abdominal ventrite 8.

lobe straight; posterior margin strongly excavated, broadly exposed mesoscutum; ratio of maximum length to maximum width = 1 : 2 (Fig. 3E–G). Costal margin of corium almost straight; hypocostal lamina extending caudally as a short, pale whitish-yellow end; costal fracture deep, almost reaching medial furrow, located ca. 3/4 from the base of corium (Fig. 3A, B). Venation of hind-wing as in Fig. 2B. Legs slender, femora and tibiae without heavy spines on distoventral surface, fore- and middle tibiae with a cleaning comb on apices of ventral surface; tarsi long and slender, 2-segmented, segment I very short, seg-

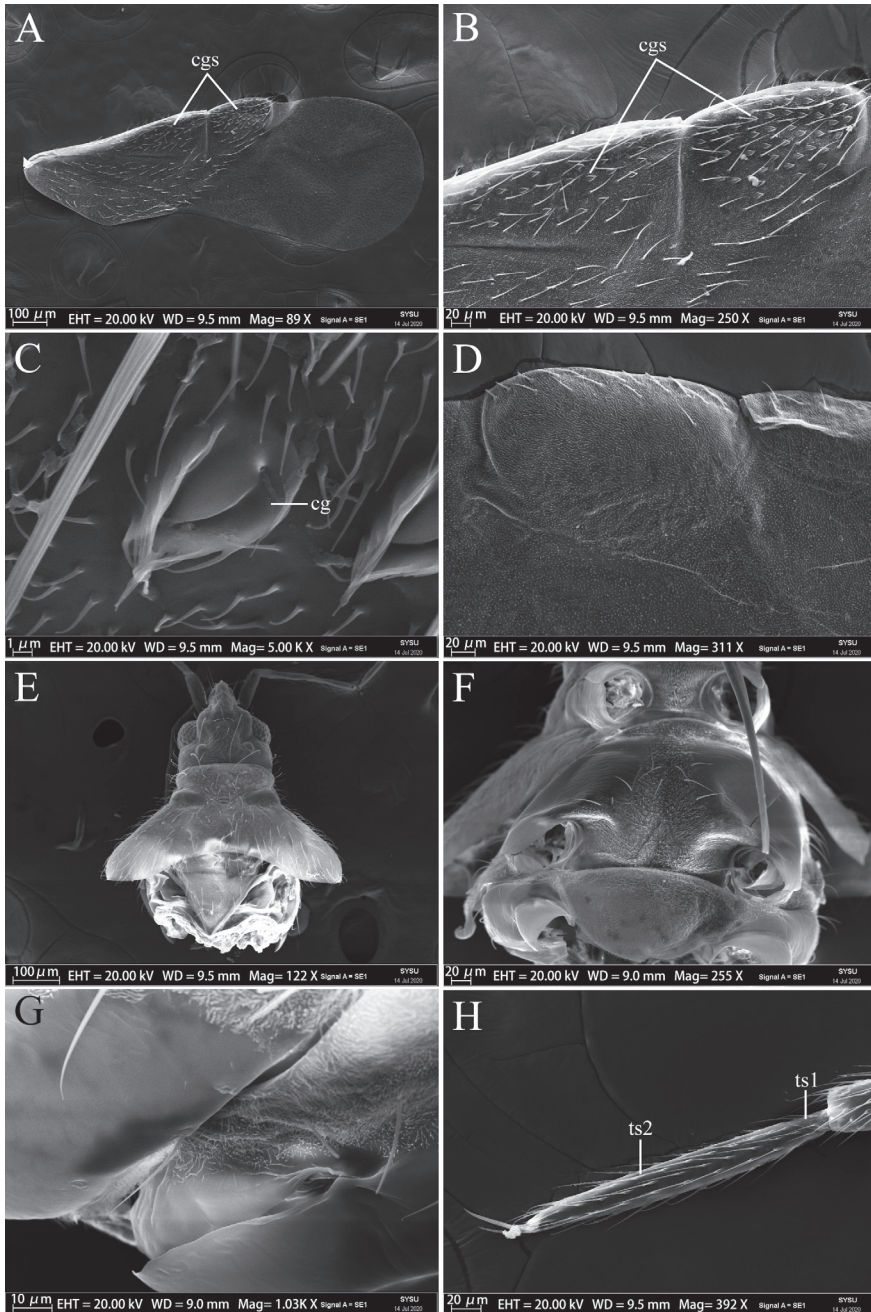


Figure 3. Scanning electron micrographs of *Plokiophiloides bannaensis* sp. nov. **A** male forewing in dorsal view **B** male forewing in dorsal view (with all corial glands) **C** detail of corial gland in dorsal view **D** male cuneus and costal fracture of forewing in ventral view **E** male head and thorax in lateral view (with all wings and legs removed) **F** male thorax in ventral view (with all wings and legs removed) **G** right lateral view of meso- and metathorax **H** male fore tibia anterior view. Abbreviations: cg = corial gland; cgs = corial glands; ts1 = first segment of tarsus; ts2 = second segment of tarsus.

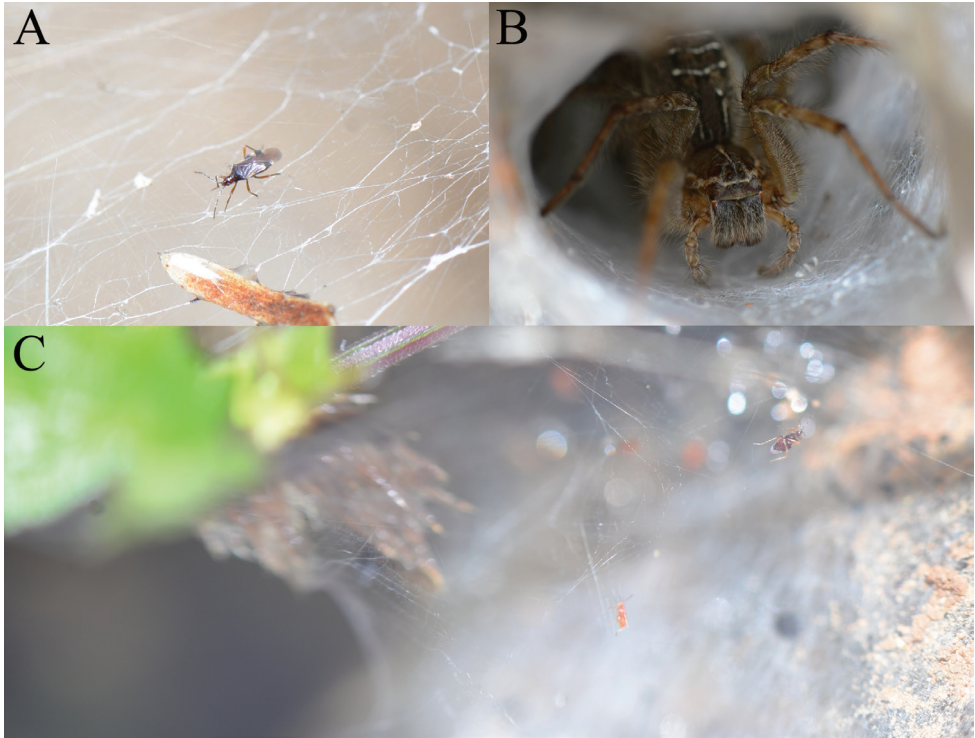


Figure 4. Habitus images of live individuals for *Plokiophiloides bannaensis* sp. nov. and spider host *Hippasa* sp. **A** an adult of *Plokiophiloides bannaensis* sp. nov. on web **B** an individual of *Hippasa* sp. in funnel of the web **C** an adult and a nymph of *Plokiophiloides bannaensis* sp. nov. near funnel of the web.

ment II elongate; claws long, inner claw longer than outer (Fig. 3H). **Abdomen:** Sterna entire, mediotergites membranous, except for segments I and II with discontinuous remnants of mediotergites and segment VII with a sclerotised medial plate. Abdominal scent gland orifice distinct. Segment VIII with a long, bell-shaped tergum and a U-shaped ventrite. **Male genitalia:** Pygophore tubular, symmetrical, slightly curved, ventral basal part moderately rounded and bulging. Parameres symmetrical. Phallosoma simple, long. Acus thin, shorter than pygophore, generally curving to the right (Fig. 2D–F).

Macropterous female: **Colouration, surface and vestiture and structures of head and thorax** as in male. **Abdomen:** Pregenital segments as in male, except for segment VII–IX with sclerotised, medial plates (Fig. 2C). **Female genitalia:** No paragenitalia present, boundary of ventrites VIII and IX are unidentified; proctiger simple.

Etymology. The specific name is derived from the abbreviated form of Xishuangbanna, the type locality of the new species.

Distribution. Known only from the type locality, XTBG, Xishuangbanna, Yunnan Province, China (Fig. 5).

Table 1. Measurements (in mm) of *Plokiophiloides bannaensis* sp. nov.

Body part	Male holotype	Male (n = 5)	Female (n = 5)	Last instar nymph (n = 2)
length of body	1.62	1.50–1.71	1.59–1.68	1.34–1.37
length of head	0.22	0.19–0.21	0.23–0.25	0.20
greatest width across eyes	0.21	0.19–0.23	0.19–0.22	0.20–0.21
minimum dorsal interocular distance	0.14	0.12–0.14	0.12	0.14–0.15
minimum ventral interocular distance	0.05	0.05	0.05	0.09–0.12
total length of antennae	0.76	0.72–0.83	0.74–0.80	0.67–0.70
length of antennal segment I	0.09	0.07–0.09	0.08–0.09	0.08–0.09
length of antennal segment II	0.2	0.20–0.23	0.19–0.22	0.17
length of antennal segment III	0.21	0.18–0.23	0.19–0.23	0.17–0.18
length of antennal segment IV	0.26	0.26–0.28	0.26–0.28	0.24–0.27
total length of labium	0.55	0.55–0.59	0.53–0.58	0.48–0.54
length of labial segment I	0.04	0.03–0.05	0.03–0.05	0.03
length of labial segment II	0.08	0.09–0.10	0.08–0.10	0.09–0.10
length of labial segment III	0.15	0.15–0.17	0.15–0.17	0.12–0.15
length of labial segment IV	0.28	0.26–0.28	0.25–0.28	0.24–0.26
greatest length of pronotum	0.26	0.23–0.27	0.24–0.26	0.18–0.19
width of pronotum	0.48	0.45–0.53	0.44–0.50	0.28–0.30
length of fore femur	0.34	0.31–0.38	0.31–0.33	0.29–0.30
length of fore tibia	0.34	0.33–0.40	0.34–0.35	0.31–0.33
length of middle femur	0.38	0.34–0.40	0.36–0.38	0.34–0.36
length of middle tibia	0.36	0.33–0.42	0.37–0.40	0.33–0.34
length of hind femur	0.49	0.49–0.55	0.50–0.53	0.45–0.47
length of hind tibia	0.56	0.56–0.64	0.56–0.60	0.51
length of forewing	1.08	1.05–1.24	1.07–1.19	
length of abdomen	0.59	0.54–0.76	0.73–0.91	0.63–0.65
width of abdomen	0.45	0.36–0.57	0.54–0.57	0.41–0.43

Key to the species of *Plokiophiloides* Carayon, 1974

Based partly on Carayon (1974), Štys (1991) and Štys and Baňar (2016)

- 1 Hypocostal lamina on ventral surface of forewing extending caudally as a long, dark carina **2**
- Hypocostal lamina on ventral surface of forewing not extending in a carina ... **3**
- 2 Proximal 1/2 of excorium devoid of corial glands; altogether 18–25 corial glands on forewing. Whitish precuneal spot inconspicuous. Body length 1.2–1.6 mm. (Tropical West Africa)..... ***P. balachowskyi* Carayon, 1974**
- Only proximal 1/3 of excorium lacking corial glands; altogether almost 50 corial glands on forewing. Whitish precuneal spot inconspicuous. Body length 2.0–2.6 mm. (Madagascar) ***P. steineri* Štys, 1991**
- 3 Body without red pigment. Large basal membrane cell distinct. Excorium with corial glands occurring almost up to its base; altogether ca. 60 corial glands on forewing. Body length 1.3–2.0 mm. (Tropical West and Central Africa)..... ***P. asolen* Carayon, 1974**
- Body with red pigment. Membrane cell indistinct or absent **4**

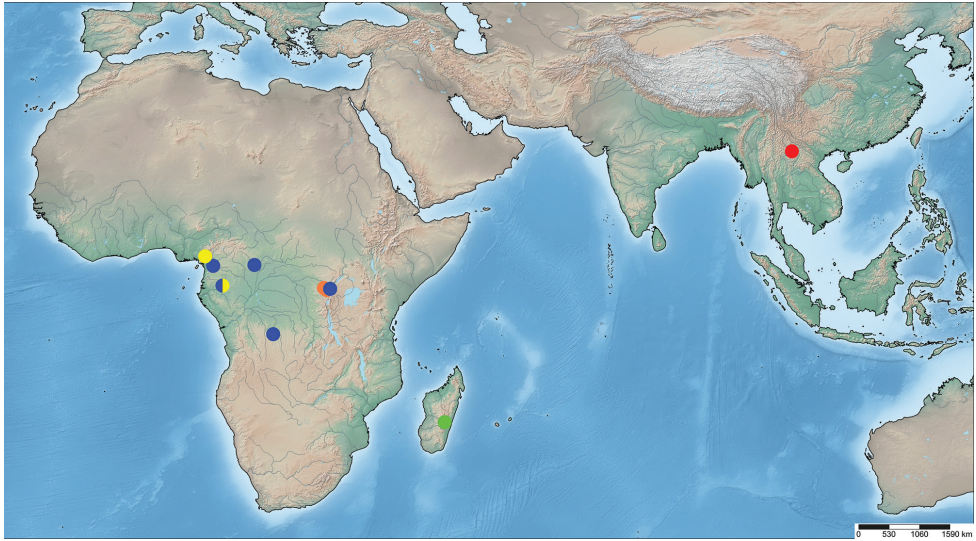


Figure 5. Distribution of all species of *Plokiophiloides* Carayon, 1974, red dot = type locality of *P. bannaensis* sp. nov.; blue dots = *P. asolen*; green dot = *P. steineri*, orange dots = *P. pilosus*, yellow dots = *P. balachowskyi*.

- 4 Membrane cell absent. Only the very distal part of exocorium with corial glands; altogether ca. 30 corial glands. Macropterous or brachypterous. Body length 1.3–1.6 mm (Tropical Central Africa)..... ***P. pilosus* Carayon, 1974**
- Membrane cell indistinct. The distal 1/4 and middle part of exocorium with two groups of corial glands; altogether ca. 65 corial glands. Macropterous. Body length 1.5–1.7 mm (Tropical Asia: China) ***P. bannaensis* sp. nov.**

Discussion

Lifestyle of all species of Plokiophilidae is reviewed in Table 2. Amongst them, only two species of the genus *Embiophila* were directly discovered in symbiosis with Embiodea. In addition to *Plokiophiloides bannaensis* sp. nov. (Fig. 4A–C), another eleven species belonging to seven genera were directly discovered in symbiosis with Araneae. Only one species *Neoplokiodes raunoi* was confirmed to be not associated with webs of spiders or embiids by observations during several expeditions (Štys and Baňář 2016). According to our field observation, individuals of *Plokiophiloides bannaensis* sp. nov. were found on five spider webs and there were about 5–8 individuals of them on each web. We examined about 30 specimens, including adults and last-instar nymphs, but other instar nymphs and eggs were not found. Adults and last-instar nymphs of web-lovers like to gather near the entrance of the funnel part of webs, which may be convenient for feeding on the remains of the prey of spiders. The new species of Plokiophilidae and its host spider *Hippasa* sp. are currently only found in tropical China.

Table 2. Distribution (using 2-letter country codes) of all known species of Plokiophilidae, lifestyle and symbiotic relationships amongst them and their hosts.

Species of plokiophilids	Distribution	Lifestyle	Species of host	Reference
<i>Embiophila africana</i> Carayon, 1974	CG	symbiosis	Embiodea: Embiidae: “ <i>Dihyboercus femorata</i> (Navas)”	Carayon 1974
<i>Embiophila maesi</i> Carpintero & Dellapé, 2005	NI	unknown	unknown, the specimens were collected with Malaise traps	Carpintero and Dellapé 2005
<i>Embiophila myersi</i> China, 1953	TT	symbiosis	Embiodea: an unidentified embiid species	China 1953
<i>Heisophilina macrotheleae</i> Schuh, 2006	TH, ID	symbiosis	Araneae: Hexathelidae: <i>Macrothele</i> sp.	Schuh 2006; Schuh et al. 2015
<i>Lipokophila chinai</i> Štys, 1967	BR	unknown	unknown, the specimens were collected in litter	Štys 1967
<i>Lipokophila eberhardi</i> Schuh, 1993	CR, PA	symbiosis	Araneae: Zoropsidae: <i>Tengella radiata</i> (Kulczyński, 1909)	Eberhard et al. 1993; Cambra et al. 2014
<i>Lipokophila stysi</i> Carayon, 1974	BR	unknown	unknown	Carayon 1974
<i>Lipokophila tengella</i> Schuh, 1993	CR	symbiosis	Araneae: Zoropsidae: <i>Tengella radiata</i> (Kulczyński, 1909)	Eberhard et al. 1993
<i>Monteithophila fijiensis</i> Schuh et al., 2015	FJ	unknown	unknown	Schuh et al. 2015
<i>Monteithophila queenslandana</i> Schuh et al., 2015	AU	symbiosis	Araneae: an unidentified spider species	Schuh et al. 2015
<i>Neoplokioides biforis</i> (Carayon, 1974)	GA	symbiosis	Araneae: Dipluridae: <i>Lathrothele catamita</i> (Simon, 1907)	Carayon 1974; Štys and Baňaf 2016
<i>Neoplokioides raunoi</i> Štys & Baňaf, 2016	MG	free living	unknown, the specimens were collected in leaf litters	Štys and Baňaf 2016
<i>Neoplokioides tubifer</i> (Carayon, 1974)	KE	symbiosis	Araneae: an unidentified spider species	Carayon 1974
<i>Paraplokiophiloides schwendingeri</i> Schuh et al., 2015	TH	symbiosis	Araneae: Hexathelidae: <i>Macrothele</i> sp.	Schuh et al. 2015
† <i>Pavlostysia wunderlichi</i> Popov, 2008	Baltic amber.	unknown	Unknown, no possible hosts were reported in the same amber	Popov 2008
<i>Plokiophila cubana</i> (China & Myers, 1929)	CU	symbiosis	Araneae: Dipluridae: <i>Diplura macrura</i> (Koch, 1841)	China and Myers 1929
<i>Plokiophiloides asolen</i> Carayon, 1974	AO, CF, CG, CM, GA,	symbiosis	Araneae: Agelenidae: <i>Agelena consociata</i> Denis, 1965	Carayon 1974
<i>Plokiophiloides balachowskyi</i> Carayon, 1974	CM, GA	symbiosis	Araneae: Agelenidae: <i>Agelena republicana</i> Darchen, 1967	Carayon 1974
<i>Plokiophiloides bannaensis</i> sp. nov.	CN	symbiosis	Araneae: Lycosidae: <i>Hippasa</i> sp.	present paper
<i>Plokiophiloides pilosus</i> Carayon, 1974	CG	unknown	unknown, the specimens were collected in soil samples	Carayon 1974
<i>Plokiophiloides steineri</i> Štys, 1991	MG	unknown	unknown, the specimens were collected in flight interception traps	Štys 1991

Notes. Country codes of countries: AO = Angola, AU = Australia, BR = Brazil, CF = Central African Republic, CG = Congo, CM = Cameroon, CN = China, CR = Costa Rica, CU = Cuba, FJ = Fiji, GA = Gabon, ID = Indonesia, KE = Kenya, MG = Madagascar, NI = Nicaragua, TH = Thailand, TT = Trinidad and Tobago. The symbol † indicates fossil species.

The geographic distribution pattern of *Plokiophiloides* is shown in Fig. 5. *Plokiophiloides bannaensis* sp. nov. was found in the Oriental Region and the remaining four species in the Afrotropical Region. Such an unusual intermittent distribution of *Plokiophiloides* reminds us that tropical regions between the Afrotropical and Oriental Regions may contain a high diversity of hidden species in this genus. Similarly, three species of *Embiophila* are separately distributed in the Neotropical and Afrotropical Regions. Therefore, more investigation is needed to clarify the species diversity and thus the distribution pattern of Plokiophilidae in pantropical regions.

Acknowledgements

We sincerely thank Prof. Zhisheng Zhang (Southwest University, Chongqing, China), Ms. Yu Men (Sun Yat-sen University, Guangzhou, China) and Mr. Quanyu Ji (Jiangsu University, Nanjing, China) for identification of the spider host. We also thank Mr. Laurence Livermore (Natural History Museum, London, UK), Dr. Tomohide Yasunaga (AMNH, New York, USA) and Dr. Catarina Lopes (Instituto Oswaldo Cruz, Rio de Janeiro, Brazil) for reviewing the manuscript and providing valuable comments and constructive suggestions. This project was supported by the National Science Foundation of China (grant number: 31222051).

References

- Cambra R, Quintero D, Santos A (2014) Primer registro para Panamá de la familia Plokiophilidae y de la especie *Lipokophila eberhardi* Schuh, 1993 (Hemiptera: Heteroptera). *Tecnociencia* 16(2): 5–8.
- Carpintero DL, Dellapé PM (2005) A new species and first record of *Embiophila* (Heteroptera: Plokiophilidae) from Nicaragua. *Studies on Neotropical Fauna and Environment* 40(1): 65–68. <https://doi.org/10.1080/01650520400007322>
- Carayon J (1961) La viviparité chez les Hétéroptères. *Verhandlungen: XI. Internationaler Kongress für Entomologie, Wien* 1: 711–714.
- China WE (1953) A new subfamily of Microphysidae (Hemiptera-Heteroptera). *Annals and Magazine of Natural History, Series 12*, 6: 67–74. <https://doi.org/10.1080/00222935308654396>
- China WE, Myers JG (1929) A reconsideration of the classification of the cimicoid families (Heteroptera), with the description of two new spider-web bugs. *Annals and Magazine of Natural History, Series 10*, 3: 97–125. <https://doi.org/10.1080/00222932908672943>
- Eberhard WG, Platnick NI, Schuh RT (1993) Natural history and systematics of arthropod symbionts (Araneae; Hemiptera; Diptera) inhabiting webs of the spider *Tengella radiata* (Araneae, Tengellidae). *American Museum Novitates* 3065: 1–17.
- Popov YA (2008) *Pavlostysia wunderlichi* gen. nov. and sp. nov., the first fossil spider-web bug (Hemiptera: Heteroptera: Cimicomorpha: Plokiophilidae) from the Baltic Eocene Amber. *Acta Entomologica Musei Nationalis Pragae* 48: 497–502. https://www.aemnp.eu/data/article-1194/1175-48_2_497.pdf
- Schuh RT (2006) *Heissophila macrotheleae*, a new genus and new species of Plokiophilidae from Thailand (Hemiptera, Heteroptera), with comments on the family diagnosis. *Denisia* 19: 637–645. https://www.zobodat.at/pdf/DENISIA_0019_0637-0645.pdf
- Schuh RT, Slater JA (1995) *True Bugs of the World (Hemiptera: Heteroptera)*, Classification and Natural History. Cornell University Press, Ithaca, New York, 336 pp.
- Schuh RT, Štys P, Cassis G, Lehnert M, Swanson D, Bruce TF (2015) New genera and species of Plokiophilidae from Australia, Fiji, and Southeast Asia, with a revised classification of the family (Insecta: Heteroptera: Cimicoidea). *American Museum Novitates* 3825: 1–24. <https://doi.org/10.1206/3825.1>

- Schuh RT, Weirauch C (2020) True Bugs of the World (Hemiptera: Heteroptera): Classification and Natural History (2nd Edn). Siri Scientific Press. Manchester, 800 pp.
- Štys P (1962) Venation of metathoracic wings and notes on the relationships of Microphysidae (Heteroptera). *Acta Societatis Entomologicae Čechosloveniae* 59(3): 234–239.
- Štys P, Baňář P (2016) A new Afrotropical genus of Plokiophilidae with a new free-living species from Madagascar (Hemiptera: Heteroptera). *Entomologica Americana* 122: 220–229. <https://doi.org/10.1664/15-RA-036>

